WHOLE MILK FOULING OF HEATED SURFACES

A thesis presented in partial fulfilment of the requirements for the degree of Master of Technology in Food Engineering at Massey University

HAYDEN ALBERT EDWARD BENNETT

2000

TO KAREN

ABSTRACT

Whole milk fouling of surfaces within dairy products processing plants, especially that which occurs on heat treatment equipment, is an important operating problem, threatening the quality of product and reducing thermal and mechanical efficiency of equipment.

A fouling monitoring system was developed using a commercial heat flux probe and temperature sensor. The fouling monitor was installed in two unit operations of a custom built milk powder pilot plant. The unit operations replicated heat treatments found in plate heat exchangers and falling film evaporators. The research plate heat exchanger consisted of six miniature plate heat exchangers or modules in series. Individual modules could be isolated at any point during a run allowing access to the fouling deposit. The research falling film evaporator was a flat plate attached to a steam chamber and milk weir box. The onset and build-up of whole milk fouling on the evaporator plate was viewed through a sight window installed in the evaporator casing.

Trials conducted with the research plate heat exchanger showed that the monitoring system could detect whole milk fouling in terms of a reduction in the overall heat transfer coefficient. This reduction was shown to directly correspond to an increase in fouling deposit thickness.

For the same bulk milk temperature, the fouling rate decreased significantly when the surface was unheated compared with heated surfaces. This observation lead to a set of experiments that manipulated the start up procedure on both the milk and heating medium side of the research plate heat exchanger. More fouling was observed on plates after air start up (on the milk side) than on plates after water start up. Similarly, Surface Conditioning by Operational Protocol (SCOP) extended the fouling induction period. The SCOP trials compared steady state heating with unsteady state heating during start-up. Similar amounts of fouling were observed on plates removed from the steady state heated modules after 30 minutes and on plates removed from the unsteady state modules after 9 hours. These results indicate that the state of the stainless steel surface when the milk first makes contact has an important effect on the

subsequent rate of fouling. It is recommended that future work aims to identify which milk components deposit first onto the surface and what influence they have on inhibiting or facilitating fouling.

The fouling monitoring system successfully estimated the extent of fouling for all of the trials. Industry trials for the fouling monitoring system, particularly on heated surfaces are recommended. The system will allow local areas of intense fouling to be mapped within the processing plants. A number of recommendations are presented concerning future work associated with start up procedure manipulation, evaporator trials and seasonal variation trials.

ACKNOWLEDGEMENTS

During my study towards a Masters Degree in Food Engineering I made friendships that I will cherish for the rest of my life.

Firstly, I would like to thank my chief supervisor, Dr. K. Tuoc Trinh for his guidance throughout my study. I appreciate the hard work Tuoc put into providing an excellent study environment with impeccable resources. The knowledge and experience I gained from this exercise was invaluable for which I am indebted to him. My second supervisor Dr. Graham Manderson, for his kind, gentle and down-to-earth approach to supervision. I will not forget the support, humour and kindness both of you brought to my study.

I would like to thank my sponsor Dr. Dave Woodhams – Project Manager of the Milk Powder Plant Availability Project, New Zealand Dairy Board – Manufacturing Consistency and Efficiency Committee. Without their financial support, this study would not have been possible.

Special thanks must be given to technicians Mr. Byron McKillop and Mr. Mark Dorsey who worked closely with me during the design and construction of the pilot plant. Their technical knowledge and experience made the construction of the pilot plant a success. Technical support from Mr. Garry Radford, Mr. Don McClean, Mr. Binh Trinh, Mr Bryden Zaloum and Mr. Steve Glasgow was also appreciated.

Fellow students Mr. Richard Croy, Mr. Andrew Hinton, Miss Carol Ma, and Mr. Mark Downey provided a happy and supportive group environment. I wish success to you all for your future studies.

Finally, I would like to thank extended family and friends. Particular thanks to my partner Karen for her patience, encouragement and advice. I dedicate this thesis to Karen for her hard work throughout my studies.

TABLE OF CONTENTS

LIST OF FIGURES

LIST OF TABLES

LIST OF UNIT ABBREVIATIONS

Unit Abbreviation	Definition
°	degrees
°C	degrees Celsius
h	hour
Hz	hertz
K	Kelvin
kPa	kiloPascal
kW	kilowatt
l	litre
m	metre
mm	millimetre
mV	millivolt
s	second
V	volt
W	watt
w/w	weight/weight

LIST OF ABBREVIATIONS

Abbreviation	Definition
β-lg	beta-lactoglobulin
BSP	British standard pipe
CIP	clean in place
COD	chemical oxygen demand
CPU	central processing unit
DSI	direct steam injection
DTHE	double tube heat exchanger
HSSS	hot side steady state
HSUSS	hot side unsteady state
HTC	non-silicone heat transfer paste
HTS	silicone heat transfer paste
MPHE	miniature plate heat exchanger
NOHTC	normalised overall heat transfer coefficient
NZF	New Zealand Fasteners
OD	outer diameter
OHTC	overall heat transfer coefficient
PLC	programmable logic controller
PHE	plate heat exchanger
RFC	heated radial flow cell
RFFE	research falling film evaporator
RTD	resistance thermal device
TC	thermocouple
UHT	ultra-high-temperature

LIST OF SYMBOLS

Symbol	Definition	Units
λ	thermal conductivity	W/mK
χ	thickness of resistance layer	m
$\Delta\theta$	temperature difference	K
θ_0	temperature of process fluid	°C
θ_{100}	temperature of process fluid	°C
θ_c	calibrated temperature	°C
θ_p	temperature of process fluid	°C
θ_r	read temperature	°C
θ_s	temperature of heat flux sensor surface exposed to heating medium	°C
a	regression coefficient	
b	regression coefficient	
F	voltage multiplication factor (heat flux)	W/m^2
q	heat flux	W/m^2
R_a	heat transfer resistance of air	m^2K/W
R_c	heat transfer resistance of cement	m^2K/W
R_f	heat transfer resistance of fouling layer	m^2K/W
R_m	heat transfer resistance of milk	m^2K/W
R_p	heat transfer resistance of heat flux sensor	m^2K/W

LIST OF SYMBOLS (Cont)

Symbol	Definition	Units
R_{ss}	heat transfer resistance of stainless steel plate	m^2K/W
R_t	total heat transfer resistance	m^2K/W
U	overall heat transfer coefficient	W/m^2K
U_n	normalised overall heat transfer coefficient	
U_o	initial overall heat transfer coefficient	W/m^2K

1 INTRODUCTION

New Zealand milk production in 1998/99 totalled just over 10.5 billion litres. Of this 10.2 billion litres was used for manufacturing purposes, the rest being used for the domestic liquid milk market. This equated to an annual turnover of NZ$ 7.4 billion as at 31 May 1999. Therefore the dairy industry is very important to the New Zealand economy (New Zealand Dairy Board, 2000).

At present, half of the milk solids produced in New Zealand each year are made into milk powder which is sold in markets throughout the world. A major constraint of milk powder plant run times is the build-up of fouling on processing surfaces. Milk fouling (deposition of solidified milk components) lowers the efficiency of heat transfer, increases pressure drop through the plant, endangers plant and process sterility and ultimately necessitates daily cleaning of the plant. The estimated cost of fouling to the New Zealand Dairy Industry is NZ$ 141 million per year (Steinhagen *et al.*, 1990). Potential gains obtained from better control of fouling are expected to run into millions of dollars.

Over the last ten years, important progress has been made in the area of heat exchanger fouling by dairy products. However, a solution to this type of fouling problem has not yet been achieved. Furthermore, investigations of fouling within other heat treatment equipment used in milk processing plants such as evaporators have received little attention.

Fouling of heat exchangers is classically observed during experiments through pressure drop and overall heat transfer coefficient measurements. At the end of fouling experiments, dry weights of the deposit can be measured on the heat transfer area giving the distribution of deposit quantities in the heat exchanger. These methods give an overall measure of fouling and do not address the issue of local areas of strong fouling. Similarly the tools used to monitor fouling in industry are substandard with run times simply decided from past experience.

A wall heat flux probe has been used to measure the extent of local fouling of unheated pipes in two commercial plants (Truong *et al.*, 1998). A similar method was used by Jones *et al.* (1994) to study the fouling of a small heated cell by whey protein solutions.

The objectives of this work were to:

- Design and construct a fully computerised pilot plant that simulates the preheating section of a milk powder processing plant.
- Design and construct heated surfaces that simulate a plate heat exchanger and evaporator, both with accessible fouling surfaces.
- Refine the technique of local fouling monitoring on heated surfaces using a wall heat flux sensor.
- Use the probe to investigate the effect of operating conditions on the extent of fouling on heat exchanger and evaporator surfaces.
- Establish the correlation between probe output and fouling layer thickness.

2 LITERATURE REVIEW

2.1 Introduction

Fouling, the formation of unwanted solid deposits within process plants, is a common and severe problem in the food industry, and can be a limiting factor in the operation of continuous food processing plants. Fouling leads to both an increase in the pressure drop through the food processing equipment and a decrease in the heat transfer efficiency. The deposits that are formed can also represent a hazard to quality and sterility, and they therefore have to be removed at frequent intervals (Fryer and Pritchard, 1989).

Fouling is of considerable importance in the dairy industry (Tissier and Lalande, 1986). Milk fouling results from the deposition of solidified milk components, proteins and minerals, on the inner surface of the processing plant. These deposits ultimately limit the operational time of the plant. The most troublesome fouling deposits occur in heat treatment equipment in milk processing plants such as heat-exchangers, holding tubes and evaporators. The deposit build-up on heat treatment equipment surfaces is so severe that cleaning of the plant is required at least once a day. The costs of cleaning and of temporarily halting a process are very high.

A survey undertaken by Steinhagen *et al.* (1990) estimated the costs of fouling to the New Zealand dairy industry to be approximately NZ$141 million per year. These costs can be divided into:

1. increased capital costs due to:
    - oversizing of the heat transfer equipment
    - installation of parallel units as an alternative processing route during cleaning
    - early replacement of equipment because of the shortening of technical life-time
    - special design and use of special construction materials
    - installation of clean-in-place (CIP) equipment

2. increased energy (fuel) costs, due to:
   - a decreasing heat transfer coefficient during operation
   - an increasing pressure drop during operation
   - cleaning at elevated temperature to remove deposit
3. high maintenance costs, due to:
   - use of cleaning chemicals and water
   - treatment of cleaning effluent before disposal
4. costs for production losses, due to:
   - product which remains on the wall of the heat exchanger
   - product losses during plant shut-down for cleaning and start-up procedures
   - down-time for cleaning, during which no production can take place

Obviously, the problem of fouling is very costly not only in terms of money but also in terms of environmental load. Hence, the reduction of fouling has always been considered to be a very important topic of research.

The design and operation of heat treatment equipment that minimises the effects of fouling, necessitates an understanding of the mechanism of formation, the rate and the extent of deposition and the location of worst fouling within the equipment (Truong *et al.*, 1996). This literature survey initially discusses the mechanisms of formation reported in dairy literature followed by models proposed by researchers based on knowledge of the physical and chemical background of these fouling mechanisms. A review of the major research equipment used by these researchers and potential commercial local fouling monitors is also provided.

2.2 Fouling Composition

A commonly quoted classification of the major types of fouling by milk in heat exchangers used by many authors was developed by Burton (1968). Burton distinguished two different types of deposit, "A" and "B", depending on the intensity of heating, each with its own specific character (see Table 2.1). Other authors (Yoon and Lund, 1989; Grandison, 1996; Lalande *et al.*, 1984) have reported slightly different temperature ranges for these fouling types. Table 2.1 shows a list of fouling

type temperature ranges including the appearance and composition of fouling at each range.

Table 2.1 Summary of reported fouling types

Type	Temperature	Appearance and Composition (% dry matter)	Author
A	70-90°C	spongy, creamy white, wet, 50-60% protein, 30-35% minerals, 4-8% fat	Burton (1968).
B	110-140°C	Compact, crystalline, glassy, 15-20% protein, 70% minerals, 4-8% fat	
A	85-100°C	Soft, voluminous material, 50-70% protein, 30-40% minerals	Grandison (1996).
B	100°C upwards	Brittle, hard, 10-20% protein, 70-80% minerals	
A	90-100°C	Soft, creamy white, 50-60% protein, 30-35% minerals, small amounts of fat	Yoon and Lund (1989).
B	120-140°C	Brittle, grey compact, 15-20% protein, 70% minerals, small amounts of fat	
Preheating section	90-110°C	50-60% protein, 30-35% minerals, 4-8% fat	Lalande *et al.* (1994).
Heating section	120-140°C	15-20% protein, 70% minerals, 4-8% fat	

Type "A" is commonly referred to protein fouling owing to its high protein content while type "B" with its high mineral content is known as mineral fouling. Despite the temperature discrepancies, most authors agree that protein and minerals are the main components of milk fouling. β-lactoglobulin (β-lg) has been found to represent nearly half of the protein content of deposits while casein (molecular and micellar) is the other major protein type (Belmar-Beiny and Fryer, 1993; Yoon and Lund, 1989). Calcium and phosphate are the major minerals present in milk deposits. Jeurnink *et al.* (1988) state that more than 80% of the ash consists of calcium and phosphate, most likely in the form of $Ca_3(PO_4)_2$. Lactose is found infrequently in milk deposits because it is water-soluble (Jeurnink *et al.*, 1996).

Table 2.1 show that authors report relatively low fat contents of fouling deposits. Some authors (Visser *et al.*, 1997; Jeurnink *et al.*, 1996; Burton, 1968) state that fat does not play an important role in the process of fouling. However, there have been

reports of unusually high fat content. Jeurnink (1995a) found that recombined milk made from skim milk powder and anhydrous milk fat homogenised at 130 bar produced a deposit of which 60% (w/w dry basis) was fat. Burton (1968) stated that the deposit on the unheated holding tube surface after direct heating in an ultra-high-temperature (UHT) treatment process contained 34% (w/w dry basis) fat. Skudder *et al.* (1986) reported that deposits located in the sections of the heater where the temperature was between 100-105°C consisted of approximately 15-20% (w/w dry basis) fat.

Fung (1998) investigated milk fouling deposits of damaged and undamaged whole milk which produced fouling layers with fat contents of greater than 45% on a dry weight basis. Fung (1998) stated that other fouling investigations made in New Zealand have produced similar results.

The composition of milk deposit in an evaporator is not known in detail (Jeurnink and Brinkman, 1994). Brinkman and van Voskuilen (1992) reported figures for the chemical oxygen demand (COD) of cleaning solutions used in evaporators which indicated the presence of organic material. These researchers assumed that the fouling layer in an evaporator consists of a protein matrix with trapped calcium phosphate and fat.

2.3 Possible Fouling Mechanisms

2.3.1 Phases of Fouling

Bott (1989) presented an idealised fouling resistance curve. Fouling resistance refers to the resistance to heat transfer due to the build-up of the fouling deposit. The curve shows the development of fouling resistance in three distinct phases.

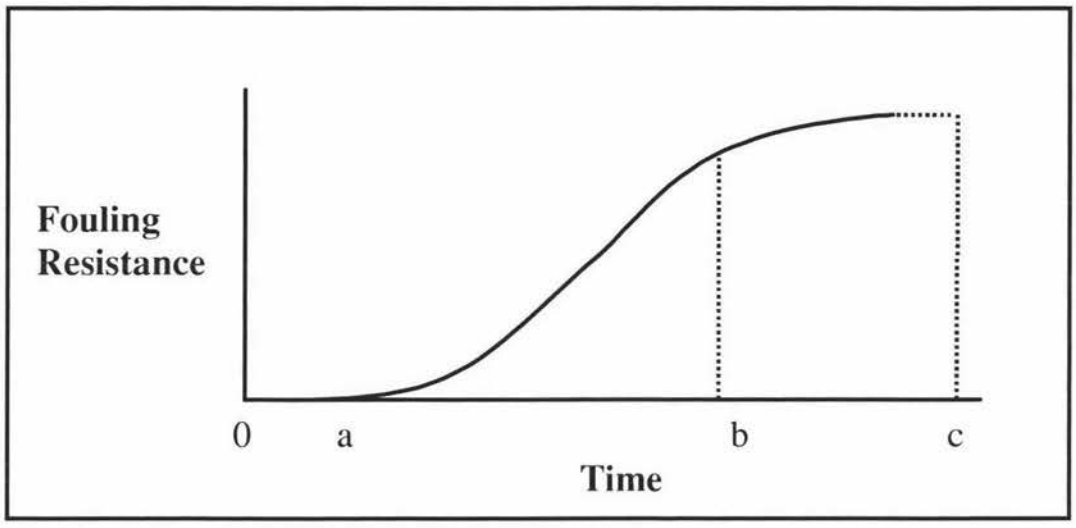

Figure 2.1 Idealised fouling curve (Bott, 1989)

From the graph the region 0-a indicates low fouling resistance. This period represents a conditioning or initiation period during which the heat transfer surface is modified so that eventually fouling can take place. The region a-b represents a period of steady growth of deposit on the surface. During the last phase (b-c) fouling resistance remains constant and this phase is often referred to the plateau or asymptotic fouling resistance value (Bott, 1989).

The evolution of fouling resistance in heat exchangers fouled with milk and milk based fluids show a similar trend to the ideal curve proposed by Bott (1989). Delplace *et al.* (1994) plotted the change of the overall heat transfer coefficient values with time for a plate heat exchanger fouled with whey protein solutions. Figure 2.2 gives the plot showing the three distinctive phases of fouling described by Bott (1989).

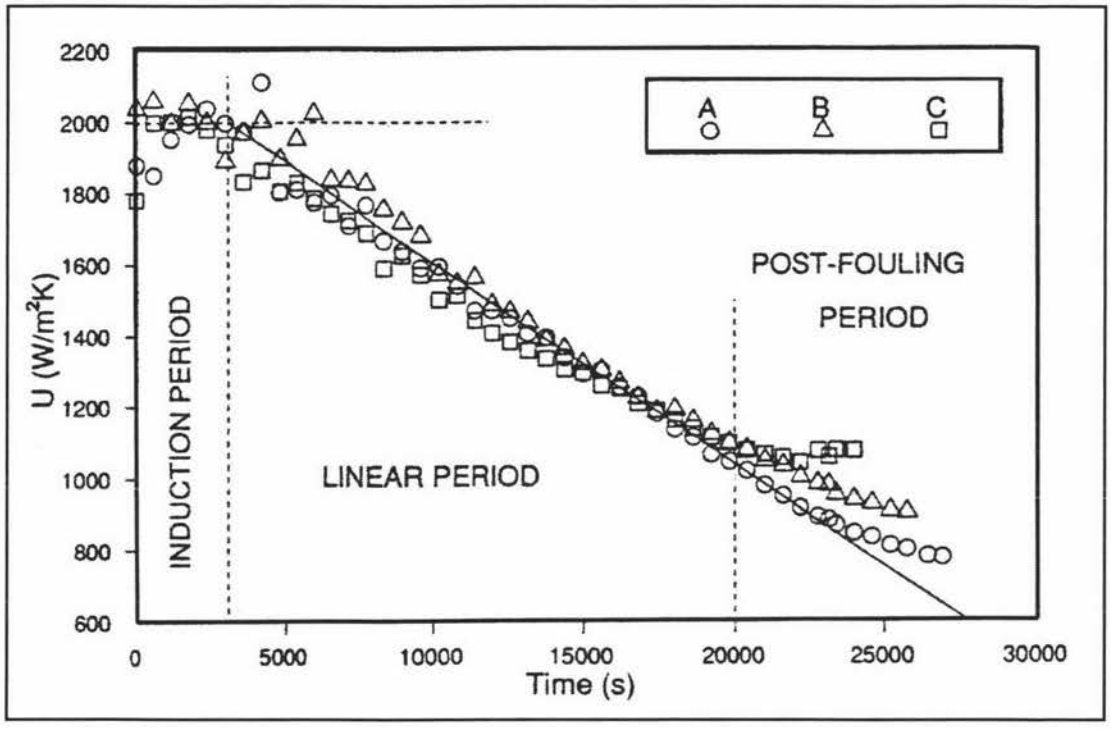

Figure 2.2 Evolution of overall heat transfer coefficient for a plate heat exchanger fouled with whey protein solutions (Delplace *et al.*, 1994)

These phases have been described as follows:

- Initially, an induction phase was observed in which the overall heat transfer coefficient remained relatively constant. The fouling deposit was very thin and there was negligible resistance to heat transfer. The thin fouling deposit enhanced surface roughness which actually increased heat transfer coefficient slightly (de Jong, 1997).
- The induction phase was followed by a fouling phase in which overall heat transfer coefficient values decreased linearly with time. This period represented a steady growth of deposition on the surface during which the rate of fouling is controlled primarily by surface bond formation which is governed by protein-protein interactions (Belmar-Beiny and Fryer, 1993; Fryer and Pritchard, 1989; Fryer, 1989).
- The final phase was described as the post-fouling period where constant fouling resistance values were observed (Delplace *et al.*, 1994). The rate of decrease of overall heat transfer coefficient became smaller in this phase.

2.3.2 Fouling Mechanisms

2.3.2.1 Overview of fouling mechanism

Jeurnink *et al.* (1996) provided a schematic representation of the fouling mechanisms during the heating of whey and milk in heat exchangers as shown in Figure 2.3.

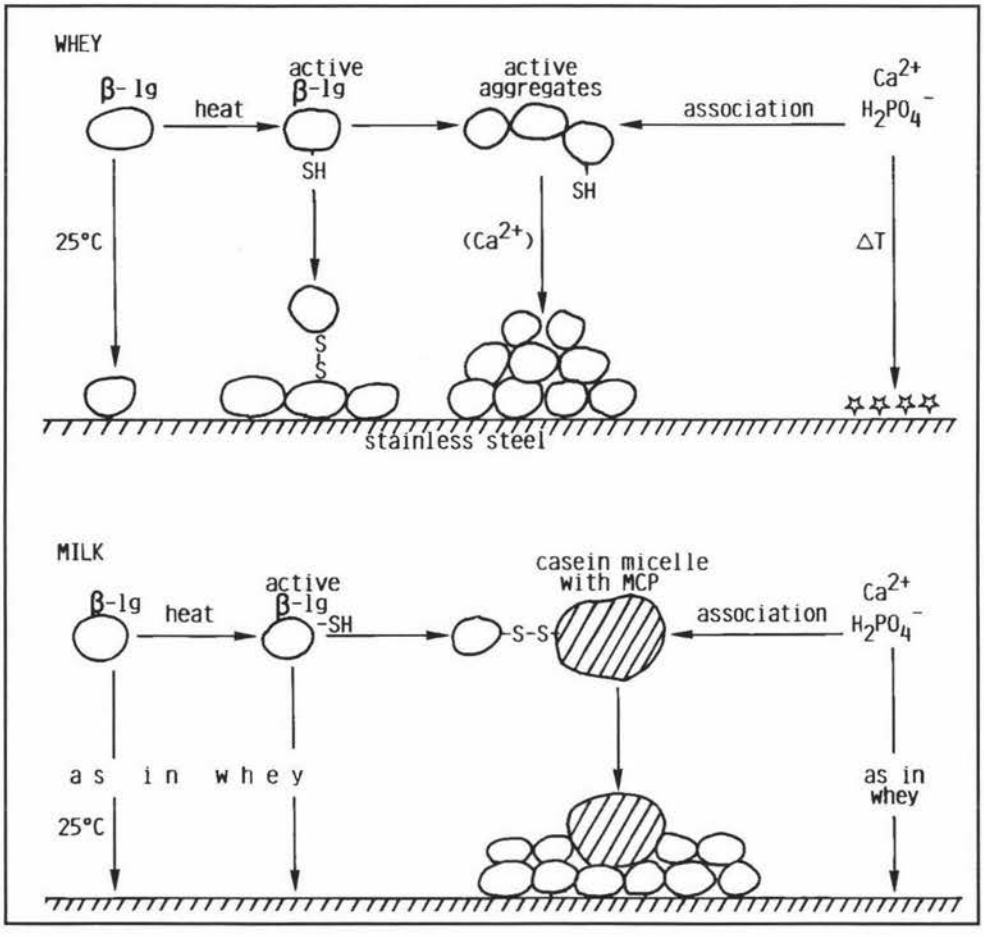

Figure 2.3 Schematic representation of the fouling mechanisms during the heating of whey and milk (Jeurnink *et al.*, 1996)

Jeurnink *et al.*, (1996) state that as soon as a stainless steel surface comes into contact with a serum protein solution, an induction layer adsorbs to the surface. Further deposits will adsorb onto this induction layer. The deposition process occurring on the surface of the induction layer can be described as follows:

1. formation of a fouling intermediate in the bulk of the solution. The fouling intermediate refers to the activated β-lg molecules which have become partly unfolded due to heating (β-lg denaturation).

2. transport of this intermediate to the metal surface.
3. deposition of the intermediate.

The deposition of the fouling intermediate may be enhanced in the presence of calcium. Calcium phosphate may precipitate directly onto stainless steel wall, promoted by a large temperature difference. Calcium phosphate may also associate with β-lg aggregates or with micellar calcium phosphate if casein micelles are present (Figure 2.3). In milk the active β-lg molecules may associate with the κ-casein at the surface of the casein micelle and may entrap the micelles in the deposit (Jeurnink *et al.*, 1996).

The fouling mechanism is discussed further in Sections 2.3.2.2-2.3.2.5.

2.3.2.2 Induction Layer

Fouling of equipment surfaces may begin with a thin induction layer. A number of studies have attempted to determine which milk components deposit onto the heated surface first (Delsing and Hiddink, 1983; Fryer, 1989; Foster and Green, 1990; Foster *et al.*, 1989; Belmar-Beiny and Fryer, 1993). However, there has been no agreement between researchers. Delsing and Hiddink (1983) concluded that a conditioning film of proteinaceous material is most likely to be the first fouling layer to form. They also found that further growth of the fouling layer only appeared possible if calcium was present.

Fryer (1989) suggested that the presence of a layer of mineral salts adjacent to the heated surface shows that this layer was the first to be deposited. However, Foster and Green (1990) argued that the proteinaceous layer was so diffuse and irregular and that it seems very probable that salts could pass through it thus allowing the salts and protein layers to be built up simultaneously.

Belmar-Beiny and Fryer (1993) summarise recent theories on the subject: "The surface analysis results obtained indicated that proteins were most likely to be the first species to adhere to the stainless steel surface. Proteins are very surface active and a clean metal surface has a large free surface energy gradient. Proteins will therefore be adsorbed to the surface reducing this free surface energy."

2.3.2.3 Protein Denaturation and Aggregation

A direct link exists between fouling and the heat denaturation of whey proteins when dairy fluids are processed at temperatures above 65°C (Visser *et al.*, 1997). Whey proteins start to unfold during heating at temperatures above 65°C. For β-lactoglobulin, a free thiol- or SH-group is then exposed and the molecules come into an activated state. This denaturation of whey proteins makes possible adhesion to the already bound induction layer. Deposition of whey proteins will occur if activated groups are present in the vicinity of the heating surface (Visser *et al.*, 1997).

Skudder *et al.* (1981) found that the addition of potassium iodate, a sulphydryl oxidising agent, reduced the amount of deposit formed during milk processing thus demonstrating that disulphide exchange reactions and protein aggregation are important in fouling. Jeurnink (1995b) found that if serum proteins were almost totally absent in milk, there was a large decrease in fouling compared to normal milk.

As previously mentioned, Jeurnink *et al.* (1996) describe the deposition process occurring on the surface of the induction layer as follows:

1. Formation of some fouling intermediate in the bulk of the solution
2. Transport of this intermediate to the surface
3. Deposition of the intermediate

The fouling intermediate described by Jeurnink *et al.* (1996) refers to a component of a model constructed by Roefs and de Kruif (1994). The partly unfolded and therefore activated β-lg molecules are defined as the fouling intermediates. This model describes the aggregation of β-lg in analogy to a radical chain reaction; upon raising the temperature a thiol group of β-lg is exposed and becomes accessible to disulfide-thiol exchange reactions. This activated molecule acts like a radical. The rate of deposition is proportional to the concentration of these activated β-lg molecules, as calculated on the basis of the model. This model is discussed in detail in Section 2.4.2.

Transport to the surface is determined by the flowrate and the geometry of the apparatus. During this transport an activated molecule of β-lg can be inactivated

through a reaction with another activated β-lg molecule in the bulk or with the κ-casein at the surface of the casein micelles (Jeurnink *et al.*, 1996).

For protein deposition to occur it is necessary that the free exposed SH-group is oriented towards the surface thus enabling it to react with a disulphide bond of an already adsorbed protein molecule in such a way that a new disulphide bond can be formed. Not every collision with the surface will lead to deposition because the reaction depends on the orientations of both the approaching molecule and the already deposited molecules (Visser *et al.*, 1997).

2.3.2.4 Mineral Precipitation

The second major contribution to fouling is mineral components of milk. There is an inverse relationship between calcium phosphate solubility and temperature. In milk, the main calcium salts are present in several forms of calcium phosphate and calcium citrate. The first precipitating form of calcium phosphate is usually dicalcium phosphate dihydrate which may be converted into the more stable calcium phosphate afterwards (Jeurnink *et al.*, 1996). Calcium phosphate may precipitate in the solution or it may deposit onto the casein micellar surface and/or onto β-lg molecules in the serum phase (Visser *et al.*, 1997).

The presence of positively charged calcium ions leads to a reduction in the electrostatic repulsion between β-lg molecules thus enabling the formation of larger aggregates upon the heating of serum protein. In the presence of calcium ions the deposition of proteins may also occur through formation of non-covalent bonds, in which the specific orientation of the approaching protein molecule is no longer needed and therefore the sticking probability of serum proteins to the stainless steel surface will increase (Jeurnink *et al.*, 1996).

2.3.2.5 Minor Components

2.3.2.5.1 Casein

Casein micelles can be entrapped in a deposit through surface bound β-lg or, when the colloidal stability is low, through aggregation near or at the heating surface due to the high temperature (Jeurnink *et al.*, 1996). At room temperature almost all the casein molecules in milk are associated into casein micelles. Upon heating to 80-90 °C both the size and the mutual interactions of these micelles increase through association with β-lg. Since β-lg is reactive towards casein micelles and to stainless steel, this molecule may act as a sticking agent between the micelles and the stainless steel surface (Visser *et al.*, 1997).

If the colloidal stability of casein micelles in milk is decreased, the deposition process may no longer be controlled by denaturing serum proteins but directly by coagulation of casein micelles at the stainless steel wall (highest temperature). Furthermore, under these conditions (decreased colloidal stability) a decrease in the heat stability of the milk may also be observed. This parallel in behaviour suggests a link between these two processes. Hence the mechanism for deposition of casein micelles upon heating milk may be similar to that of the heat coagulation of milk (Jeurnink *et al.*, 1996).

2.3.2.5.2 Lactose

Lactose is scarcely found in milk deposits because it is water soluble. Only at high temperatures (>100°C) when caramelisation or intense Maillard reactions may take place will lactose contribute to a deposit. Kessler and Schraml (1996) found that upon heating whey protein concentrates containing 25% dry matter, spongy layers of protein aggregates were formed, entrapping some of the heated fluid. As a result these deposits contained up to 50% (dry matter basis) lactose.

2.3.2.5.3 Fat

Some authors (Burton, 1968; Visser *et al.*, 1997; Lalande *et al.*, 1984) state that fat plays a minor role in the process of milk fouling. Although there is evidence of fat being located within the fouling deposit, these authors maintain that milk fat has little effect on deposition process. Furthermore, Maas *et al.* (1985) found that in spite of the high fat content of whipping cream (85% of the total solids) the fouling behaviour of this cream resembled that of whole milk. However, high amounts of fat have been found in fouling deposits suggesting fat may play an important role (Jeurnink *et al.*, 1996; Fung, 1998; Skudder *et al.*, 1986; Jeurnink, 1995). Jeurnink *et al.* (1996) found that homogenised at 130 bar, recombined milk made of skim milk powder and anhydrous milk fat fouled rapidly and the deposit contained up to 60% (w/w dry matter basis) fat, present as fat globules. Jeurnink *et al.* (1996) concluded that this observation suggests active deposition of emulsion particles possibly due to an enhanced activity of the proteinaceous membrane.

Similarly high fat contents have been reported in New Zealand fouling investigations. Fung (1998) investigated the effect of milk fat globule membrane damage on fouling in heat exchangers. The fouling deposits had a relatively high fat content (>45% on a dry weight basis). It was hypothesised that large globules formed by the coalescence of native globules whose membrane have been damaged could migrate more easily to the stainless steel heating surface. There, they could act as anchor points for the build-up of a fouling layer with a continuous protein phase. However further investigation was warranted.

2.3.3 Rate Controlling Processes

If deposit formation results only from a combination of mass transfer and chemical reactions then the slowest of these processes will be the rate controlling step. Belmar-Beiny *et al.* (1993) considered the following two cases:

1. If fouling is mass transfer controlled then the slowest process will be the transfer of reacted protein to the wall. In this case, the rate of deposit formation will not be a strong function of temperature.

2. If the fouling process is reaction controlled, deposit formation will be a function of temperature where the controlling reaction takes place. Reactions in a number of different places could control the process:
    a. *Surface reaction.* If only surface processes control fouling, deposition will occur wherever the wall temperature is hot enough for protein denaturation and aggregation to occur, regardless of the bulk milk temperature. The process will be a function of the wall temperature, not the bulk milk temperature.
    b. *Bulk reaction.* If the controlling reaction for fouling takes place in the bulk, then two conditions can be envisaged:
        i. If the wall temperature is such that protein denaturation and aggregation will occur and the bulk temperature is such that native protein is thermally stable then fouling will result from deposition of protein which has be denatured and aggregated in the thermal boundary layer adjacent to the wall.
        ii. If both the boundary layer and the turbulent core are hot enough for protein denaturation and aggregation then protein denatured and aggregated in both regions will contribute to deposit formation.

If a surface reaction is responsible for fouling, the amount of fouling should depend only on the wall temperature. If the bulk processes contribute to fouling, then the amount of fouling should increase when the fluid bulk becomes hot enough to produce denatured and aggregated protein and thus be a function of bulk temperature and fluid velocity.

Belmar-Beiny *et al.* (1993) used a tubular heat exchanger fouled with whey protein concentrate to study the bulk and surface effects. They found that a simple model in which fouling was correlated with the volume of fluid hot enough to produce denatured and aggregated protein produced reasonable agreement between theory and experiment, indicating the possible importance of bulk reactions.

2.4 Fouling Models

The main aim of studying fouling is to develop operating procedures which minimise it, with the ultimate goal to design fouling resistant heat exchangers which are less expensive than those currently available. To do this, the processes which occur during fouling should be quantified and then modelled (Fryer, 1989).

Visser *et al.* (1997) give a summary of the major models and equations developed for describing the process of fouling by dairy products:

1. Models based on fouling resistance (R_f). These are useful for engineers in charge of sizing heat transfer equipment.
2. Models providing the amount of deposit formed in heat exchanger ducts after a given processing time. These models could help heat exchanger manufacturers to compare the efficiency of different types of heat exchangers in terms of fouling mitigation, and could help designers find new heat exchangers which are less prone to fouling.
3. The interpretation of the equations found for fouling rates. The activation energy for fouling by milk of heat exchangers found by Lalande and Corrieu (1981) was a good example of the use of fouling models to develop a better understanding of the process of fouling.

The two major approaches taken by researchers in the modelling of fouling of heat exchangers by dairy products are:

1. To consider only the chemical phenomena governing fouling rather than all the heat induced phenomena which are difficult to identify. In this context, the key role of β-lg in fouling has been identified, and fouling models have been developed on the basis of this idea.
2. The classical chemical engineering approach where the system undergoing fouling by a dairy liquid is considered as a reactor. Velocity coefficients and their variations with operating conditions can be obtained in this way (Visser *et al.*, 1997).

Modelling is of great interest for engineering purposes and the expanding use of software for equipment sizing and design of heat exchangers will make the development of efficient fouling models more necessary (Visser *et al.*, 1997).

2.4.1 The Role of β-lactoglobulin.

Studies on the heat denaturation of milk soluble proteins and a possible relation with fouling of heat transfer equipment by dairy products have been carried out by many authors over the last 10 years. Similarly the model of a heat activated β-lactoglobulin molecule being able to adhere to a heat transfer surface has been well established (Visser *et al.*, 1997).

According to Jeurnink *et al.* (1996), the deposition of β-lactoglobulin is determined by three steps:

1. Formation of an activated molecule in the bulk of the solution upon heating.
2. Transport of this molecule to the heating surface. During this transport, however, an activated β-lactoglobulin molecule can be inactivated through reaction with another molecule in the bulk of the fluid.
3. Deposition of the activated molecule through an interaction with an already deposited molecule, for example through the formation of a disulphide bridge.

Although β-lactoglobulin plays a key role in the process of fouling, researchers do not agree on the reaction order of β-lactoglobulin heat denaturation. Lyster (1970) suggests the denaturation of β-lactoglobulin is second order with respect to time:

$$\frac{dC}{dt} = -kC^2 \qquad \textbf{(2.1)}$$

where, for $343 \leq T \leq 363$ K

$$\log k = 37.95 - 14.51\frac{10^3}{T} \qquad \textbf{(2.2)}$$

and for $T \geq 363$ K

$$\log k = 5.98 - 2.86\frac{10^3}{T} \qquad \textbf{(2.3)}$$

Lyster's denaturation kinetics were successfully used by Delplace *et al.* (1994) and Delplace and Leuliet (1995) to calculate the total amount of β-lactoglobulin denatured in a plate heat exchanger during fouling trials using a whey protein solution.

Jeurnink *et al.* (1996) related fouling to a model for the denaturation and aggregation of β-lg developed by Roefs and de Kruif (1994). Similarly de Jong *et al.* (1992) presented a fouling model based on denaturation kinetics of β-lg as published by Dannenberg and Kessler (1988) and de Wit (1990). Both models identified the denaturation reaction as first order.

2.4.2 Denaturation and Aggregation Model

Roefs and de Kruif (1994) describe the denaturation of β-lg as an ordinary radical addition polymerisation reaction in which the thiol groups play the role of "radical". The reaction scheme contains an initiation, a propagation and a termination step.

initiation: $$B \xrightarrow{k_1} B^* \quad \textbf{(2.4)}$$

propagation: $$B + B_i^* \xrightarrow{k_2} B_{i+1}^* \quad \textbf{(2.5)}$$

termination: $$B_i^* + B_j^* \xrightarrow{k_3} B_{i+j} \quad \textbf{(2.6)}$$

where B = native whey protein molecules

B_i^*, B_j^*, B_{i+1}^* = activated protein molecules or polymers

B_{i+j} = aggregated polymers

k_1 = reaction rate constant (initiation)

k_2 = reaction rate constant (propagation)

k_3 = reaction rate constant (termination)

In the first step, native whey protein molecules (B) are partially unfolded, whereby the thiol group becomes activated (B^*). In the second step these activated molecules can react with another native molecule to form an activated dimer (B_{i+j}^*) which can react in turn with other native protein molecules to form larger activated polymers. The polymerisation process stops when two activated polymers react with each other to form a non-activated polymer (B_{i+j}).

Jeurnink *et al.* (1996) assumed that the initiation rate was much slower than the propagation rate and that steady state was reached. Therefore their model predicted a reaction order of 1½ for the decrease of native β-lg, and the overall reaction rate constant k':

$$k' = k_2 \left(\frac{k_1}{2k_3} \right)^{0.5} \qquad \textbf{(2.7)}$$

The general fouling model proposed by de Jong *et al.* (1992) was based on denaturation kinetics published by Dannenberg and Kessler (1988) and de Wit (1990). Their model of denaturation is as follows:

Upon heating β-lg begins to unfold; this involves the breakdown of hydrogen and hydrophobic bonds and exposure of the sulphydryl group, which is able to react with other proteins:

$$B \leftrightarrow B^* \qquad \textbf{(2.8)}$$

where B = native β-lg monomer

B^* = activated monomer with exposed sulphydryl group.

It has been postulated that i activated monomers polymerise with each other to form B^*_i. The second denaturation step is aggregation with other proteins:

$$B_i^* + B_j^* \rightarrow T_{i+j} \qquad \textbf{(2.9)}$$

where T_{i+j} = an aggregate of denatured proteins.

The active β-lactoglobulin is also able to aggregate with components that are attached to the heat exchanger surface, resulting in a deposition rate:

$$B_i^* \xrightarrow{+M} F \qquad \textbf{(2.10)}$$

where M = milk constituents

F = deposited material.

Assuming that the amount of deposited material is negligible compared with the bulk concentration of β-lactoglobulin, the following reaction rate equations are valid:

$$r_B = -k_{unfolding}[B] \tag{2.11}$$

$$r_{B*} = k_{unfolding}[B] - k_{aggregation}[B*]^2 \tag{2.12}$$

$$r_T = k_{aggregation}[B*]^2 \tag{2.13}$$

where r = the reaction rate in the bulk

$[B]$ = concentration of native β-lg

$[B*]$ = concentration of activated β-lg

The reaction rate constants (k) are described by the Arrhenius relationship:

$$k = k_0 \exp\left(-\frac{E_a}{RT_s}\right) \tag{2.14}$$

where E_a = activation energy

R = gas constant

T_s = absolute wall temperature

2.4.3 Deposit Formation Kinetics

Lalande and Corrieu (1981) attempted to model the fouling by milk of heat treatment equipment. Experimental results obtained with a plate heat exchanger could be described by an autocatalytic reaction given by Equation (2.15).

$$\frac{dm_d}{dt} = bm_d^{0.5} \tag{2.15}$$

where m_d = mass deposited

b = rate constant

Integrating Equation (2.15) shows that the mass deposited is proportional to the time squared as shown by Equation (2.16).

$$m_d = \frac{b^2}{4}t^2 \tag{2.16}$$

The experimental fouling rate constant (b) could be correlated to the ammonia concentration of the milk which depends, for example on aging and the temperature of the depositing surface:

$$b = 3.62\times10^{9}\exp\frac{-96.14}{8.36\times10^{-3}T_d} + 0.84\times10^{-5}\left(C_{NH_3} - 5.3\right) \qquad \textbf{(2.17)}$$

where T_d = temperature of the depositing surface

C_{NH3} = ammonia concentration of the milk

(Visser *et al.*, 1997)

The fouling model for heat exchangers operating at temperatures up to 100°C proposed by de Jong *et al.* (1992) was based on the assumption that the local fouling process can be considered as a heterogeneous adsorption reaction of milk constituents at the surface with mass transfer and reaction in series: transport at the boundary layer and the reaction process at the surface. Figure 2.4 shows the concentration profile describing the fouling process proposed by de Jong *et al.* (1992).

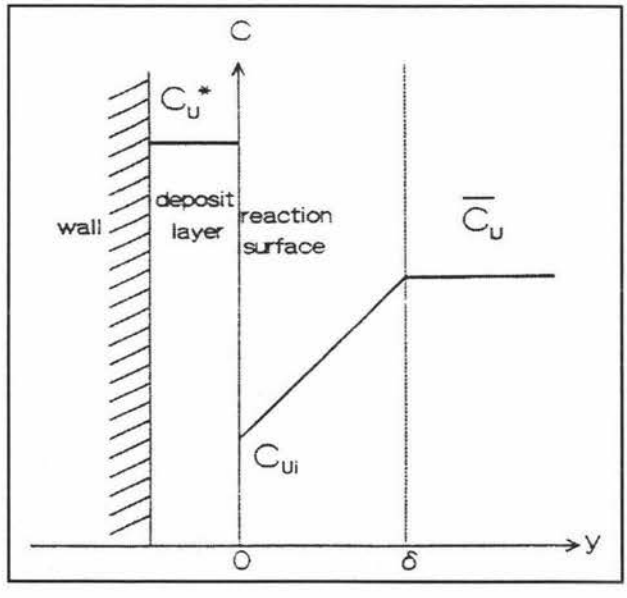

Figure 2.4 Proposed concentration profile for deposit formation (de Jong *et al.*, 1992). See text for explanation of symbols

The model used to describe the fouling rate in heat exchangers was given by Equations (2.18 – 2.27).

Mass transfer equation:

$$J_F = \frac{D_F}{x\delta}\left(\overline{C_U} - C_{Ui}\right) \qquad \textbf{(2.18)}$$

where J_F = mass flux

D_F = diffusion coefficient

x = fraction of β-lg in the deposit

δ = thickness of the thermal boundary layer

U = unfolded β-lg

C_{Ui} = local concentration of U near the surface

$\overline{C_U}$ = bulk concentration of U

C_U^* = concentration of U in the deposit layer

Reaction rate equation:

$$R_F'' = -k'' C_{Ui}^n \qquad \textbf{(2.19)}$$

where R_F'' = production rate

k'' = reaction rate constant of surface reaction

Mass balance:

$$J_F = -R_F'' \qquad \textbf{(2.20)}$$

Using the above three equations the unknown concentration C_{Ui} can be eliminated:

$$J_F = \frac{D_F}{x\delta}\left(\overline{C_U} - \left(\frac{J_F}{k''}\right)^{\frac{1}{n}}\right) \qquad \textbf{(2.21)}$$

Whether fouling is controlled by chemical reaction or mass transfer follows from the Hatta number. The square of the Hatta number is equal to the ratio of the maximum reaction rate of the adsorption and the maximum diffusional transport:

$$Ha^2 = \frac{k''\overline{C_U}^n}{\frac{D_F}{x\delta}\overline{C_U}} \qquad \textbf{(2.22)}$$

When $Ha < 0.3$: the kinetic reaction rate completely limits the adsorption rate

$Ha > 0.2$: the rate of mass transfer limits the adsorption rate.

The diffusion coefficient (D_F) of the adsorbed milk constituents and the film thickness are unknown and therefore these values must be estimated. For example, when the

diameter of the particles are known, the diffusion coefficient can be estimated by the Wilke-Chang equation:

$$D_F = 1.3\times10^{-17}\frac{T}{\eta_L V_F^{0.6}} \qquad \textbf{(2.23)}$$

where η_L = viscosity of the liquid phase

T = absolute temperature

V_F = molecular volume of the adsorbed particles is given by Equation (2.24):

$$V_F = N_{Av}\frac{1}{6}\pi d_F^3 \qquad \textbf{(2.24)}$$

where N_{Av} = Avogadro constant

d_F = particle diameter

The thickness of the boundary layer can be estimated from the Sherwood number:

$$Sh = \frac{k_L d}{D_F}$$

$$k_L = \frac{D_F}{\delta} \qquad \textbf{(2.25)}$$

$$\delta = \frac{d}{Sh}$$

where k_L = mass transfer coefficient

d = characteristic diameter

Sh = Sherwood number

In the range $2000 < \mathrm{Re} < 10^5$ and $\mathrm{Sc} > 0.7$ a relation for mass transfer between a wall and a turbulent flow is given by:

$$Sh = 0.027\,\mathrm{Re}^{0.8}\,Sc^{0.33} \qquad \textbf{(2.26)}$$

De Jong *et al.* (1992) used experimental data to determine the fouling kinetics. The fouling model was given by substituting Equation (2.14) into Equation (2.21):

$$\ln J_F = \ln k_0'' - \frac{E_a}{R}\frac{1}{T} + n\ln\left(\overline{C_U} - \frac{x\delta J_F}{D_F}\right) \qquad \textbf{(2.27)}$$

De Jong *et al.* (1992) state that the model provides for the design of heating equipment and the determination of the optimum holding temperature and time required to reduce fouling in heat exchangers.

Jeurnink *et al.* (1996) state that transport to the surface is determined by the flowrate and the geometry of the apparatus. During this transport an activated molecule of β-lg can be inactivated through a reaction with another activated β-lg molecule in the bulk or with the κ-casein at the surface of the casein micelles.

Near the stainless steel wall there is a hypothetical layer where an activated β-lg molecule has an equal chance of colliding with the wall or with a casein micelle. The thickness of this layer can be estimated by making it equal to the mean free distance between micelles as shown in Equation (2.28):

$$z = 0.225 d_{vs}\left(\frac{0.74}{\phi} - 1\right) \qquad \textbf{(2.28)}$$

where z = mean free distance between micelles

d_{vs} = volume/surface average diameter

ϕ = volume fraction

Jeurnink *et al.* (1996) proposed that the deposition process could be represented by Equation (2.29). This equation was derived assuming that the removal of deposited material during the fouling process can be neglected.

$$\frac{d\Gamma}{dt} = \frac{\omega.k}{x.B^{*}(t)} \qquad \textbf{(2.29)}$$

where $d\Gamma/dt$ = deposition rate

ω = sticking probability of the protein

k = transport coefficient

x = fraction of β-lg in the deposit

$B^*(t)$ = bulk concentration of activated β-lg molecules at time t as calculated from the denaturation model.

Note that the transport coefficient would be constant for a given geometry of heat exchanger which comprises both the diffusion coefficient of the protein and the flowrate of the liquid.

2.4.4 Modelling the Overall Heat Transfer Coefficient

Fryer (1989) used a dimensionless fouling Biot number (Bi) to describe the decrease in the overall heat transfer coefficient (U) with time for tubular geometries undergoing fouling.

$$Bi = \left(\frac{U_o}{U}\right) - 1 = R_f U_o \qquad \textbf{(2.30)}$$

where R_f = thermal fouling resistance

U_o = initial overall heat transfer coefficient

U = overall heat transfer coefficient

The final overall heat transfer model (Equation 2.32) was based on ideas of Kern and Seaton (1959), in which fouling is regarded as a balance between deposition and removal:

$$\frac{dR_f}{dt} = \phi_d - \phi_r \qquad \textbf{(2.31)}$$

where R_f = thermal fouling resistance

ϕ_d = flux of material deposited

ϕ_r = flux of material removed

Fryer (1989) developed a simplified Kern-Seaton model using a classical chemical engineering approach shown as Equation (2.32):

$$\frac{dBi}{dt} = \frac{k_d}{\mathrm{Re}} \exp\left(-\frac{E}{R} \cdot \frac{1+Bi}{T_w + T_b Bi}\right) - k_r Bi \qquad \textbf{(2.32)}$$

where k_d = rate constant of deposition

k_r = rate constant of removal

T_w = wall temperature

T_b = bulk temperature

E = activation energy

R = gas constant

Re = Reynolds number

Fitting of experimental data gave the values $k_d = 4.85 \times 10^{13}$ s^{-1} and $k_r = 1.3 \times 10^{-3}$ s^{-1}. The value for the activation energy, E, was found to be 89 ± 6 kJ/mol which was very close to the value obtained by Lalande and Corrieu (1981).

Delplace and Leuliet (1995) modelled the overall heat transfer coefficient evolution with time for fouling of a plate heat exchanger by reconstituted whey protein concentrates. Figure 2.5 shows a close fit was found between the model and experimental data.

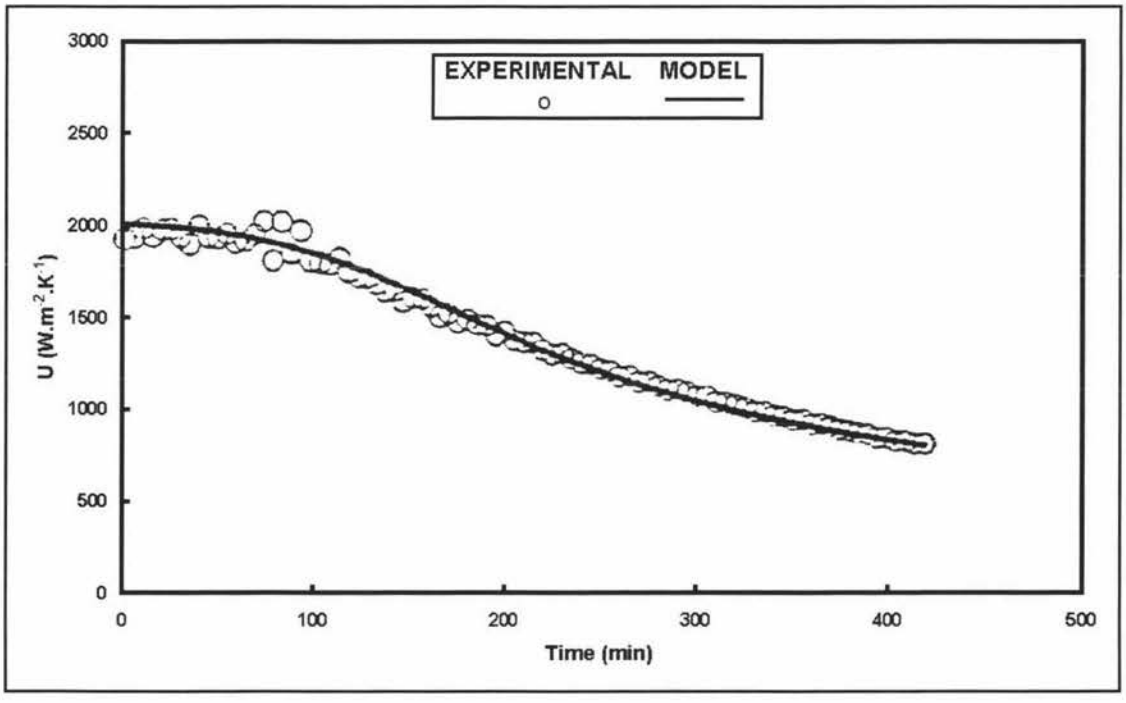

Figure 2.5 Modelling overall heat transfer coefficient values with time for fouling of a plate heat exchanger by reconstituted whey protein concentrates (Delplace and Leuliet, 1995)

A total of five fouling runs were conducted by Delplace and Leuliet (1995) who found that the evolution of overall heat transfer coefficient with time took the form of Equation (2.33):

$$U(t) = \frac{U_o \lambda(t)}{U_o \sigma t + \lambda(t)} \qquad \textbf{(2.33)}$$

where the parameter σ is related to both the heat denaturation of β-lactoglobulin and the fouling behaviour of the heat exchanger through Equation (2.34):

$$\sigma = \frac{0.12733}{\rho_d N} \sum_{i=1}^{N} Q_i \Delta C_i^{0.5} \qquad \textbf{(2.34)}$$

where ρ_d = density of deposit

N = number of PHE channels

Q_i = volumetric flowrate in channel i

ΔC_i = difference between inlet and outlet native β-lactoglobulin concentration in channel i

The deposit's thermal conductivity, λ, was found to be a function of processing time. From experimental measurements of both overall heat transfer coefficient and the deposit quantities, Delplace and Leuliet (1995) proposed the following empirical model for λ:

$$\lambda(t) = 3.73e^{-2.5\times10^{-4}t} + 0.27 \qquad \textbf{(2.35)}$$

the asymptotic value of 0.27 is close to the classical values deduced from thermal diffusivity measurements of proteins.

The form of the overall heat transfer coefficient equation (Equation 2.33) was deduced by relating the classical relationship:

$$R_f = \frac{x}{\lambda} \qquad \textbf{(2.36)}$$

with the equation for dry mass deposition as calculated on the basis of the heat denaturation of β-lactoglobulin:

$$\frac{md_i}{SV_i} = 0.127\Delta C_i^{0.5} \qquad \textbf{(2.37)}$$

where md_i = dry mass of deposit in channel i

ΔC_i = difference between inlet and outlet native β-lactoglobulin concentration in channel i

S = surface area

V_i = volume of fluid in channel i

2.4.5 Modelling Pressure Drop

Visser *et al.* (1997) state that changes in the friction factor versus Reynolds number as a result of the changes in heat exchanger duct geometry by a deposit are not easy to take into account. For this reason, accurate modelling of pressure drop with time will often be quite difficult to achieve, especially when deposit quantities are important. Furthermore, random local blockages that result in increases in pressure drop are difficult to predict with any continuous model.

2.5 Fouling Measurement

There have been a number of studies conducted on fouling of heat treatment equipment by milk based fluids. Research equipment employed by these studies vary from simple stainless steel particles (<100 mesh) to fully instrumented pilot scale heat exchangers. However, most of this research work was concentrated on tubular or plate heat exchangers and ultra-high-temperature (UHT) plants. Fouling composition and mechanisms in evaporators have received little attention.

Although various experimental equipment have been used, all studies use one or more of the following methods to measure fouling:

- Monitoring pressure drop.
- Monitoring heat transfer (temperature change).
- Physical measurement (thickness of fouling deposit and/or weight of fouling deposit).

These methods will be discussed in Section 2.5.1.4 which follows a section discussing common experimental apparatus that have been used for fouling studies (Section 2.5.1.3).

2.5.1 Experimental Measurement

Before discussing experimental apparatus in detail, a generic overview of model surfaces and fluids commonly used by researchers to study fouling will be presented.

2.5.1.1 Test fluid

Although fresh milk or skim milk are obvious choices for the test fluid used during fouling experiments, researchers have used other fluids to study the phenomenon of fouling for a variety of reasons. Many authors (Delplace *et al.*, 1994; Delplace and Leuliet, 1995; Belmar-Beiny and Fryer, 1993; Belmar-Beiny and Fryer, 1992; Gotham *et al.*, 1992; Fryer *et al.*, 1996; Fryer and Bird, 1994; Schreier *et al.*, 1994; Belmar-Beiny *et al.*, 1993) have used whey protein solutions to study fouling because studies have linked the thermal stability of β-lactoglobulin with the formation of fouling deposits (Gotham *et al.*, 1992). Some researchers argue that whey protein solutions improve repeatability of fouling experiments by reducing seasonal effects associated with milk (Delplace and Leuliet, 1995). However it has also been noted that extension of the results to milk fouling is not straightforward owing to the influence of other milk constituents (Davies *et al.*, 1997).

Jeurnink (1995a) investigated the use of reconstituted milk as a model fluid. It was found that reconstituted milk gave much less fouling than fresh milk because, in part, denatured serum proteins are less active in the fouling reaction. The process of powder making also affected the fouling behaviour by decreasing the calcium concentration and the calcium ion activity. Even though reconstituted milk produced less fouling, it is still used as a model fluid as seasonal variations are eliminated as a parameter in fouling.

2.5.1.2 Model Surface

The most obvious model surface is that used most frequently within the industry experiencing fouling. For the case of milk fouling within the dairy industry, stainless steel would be the most appropriate test surface.

Fouling studies have been conducted with other surfaces to determine the effect each surface has on the amount of deposit formed. Yoon and Lund (1989) found that the fouling rate was slowest with electropolished 304 S.S., followed by standard No. 4 finish S.S., Teflon-coated S.S., titanium and S.S. coated with sulfonated polyurethane monomer. Although Yoon and Lund (1989) found a difference between initial

deposits formed on each surface, chemical analysis of the final deposits proved that this difference did not influence subsequent deposition.

Britten *et al.* (1988) used various polymer-coated stainless steel discs to investigate the effect interfacial properties had on deposit formation. The study showed the different coatings did not affect the amount of deposit formed but did affect the strength of the adhesion. Thus, it appears that coatings may enhance the cleaning rate but not reduce the fouling rate.

2.5.1.3 Experimental Apparatus

2.5.1.3.1 U-Tube

Burton (1961) described an apparatus and procedure for the laboratory investigation of various factors that control milk deposits on heat exchange surfaces. Figure 2.6 gives an isometric drawing of the apparatus.

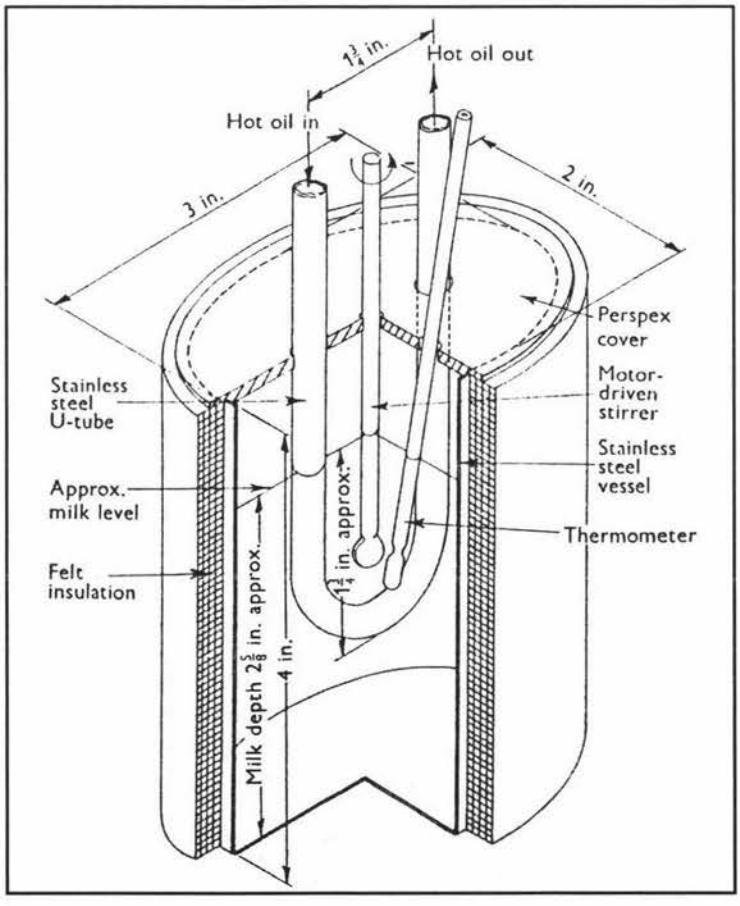

Figure 2.6 Isometric drawing of U-tube apparatus (Burton, 1961)

Milk was contained in the stainless steel vessel that was elliptical in section and thermally insulated with felt. The heating surface was a stainless steel U-tube fitted with a threaded brass union at each end. The U-tube was connected by the unions to lagged pipes through which oil was pumped at a constant flowrate from a thermostatically controlled oil bath.

In operation, the stainless steel vessel was supported around the U-tube so that the tube was immersed in the milk. The vessel had a Perspex cover to prevent excessive evaporation from the milk surface. Small holes in the cover gave entry for the heating coil, a motor-driven stirrer and a thermometer.

The apparatus had the advantage of using small volumes of milk during trials that could be repeated from a common bulk. However, the U-tube method was very sensitive to variations in the amount of dissolved air in the milk. This made it unsuitable for comparing samples that were likely to contain different amounts of dissolved air. In particular, it made it impossible to determine the effect of forewarming processes which have been used in practice to reduce the amount of deposition from milk during heat treatment.

2.5.1.3.2 Platinum Wire

Burton (1965) developed another method for studying the formation of deposits from milk on a heated surface under controlled heat transfer conditions. The method used an electrically heated platinum wire as the surface on which deposits are formed. Figure 2.7 gives a schematic representation of the apparatus.

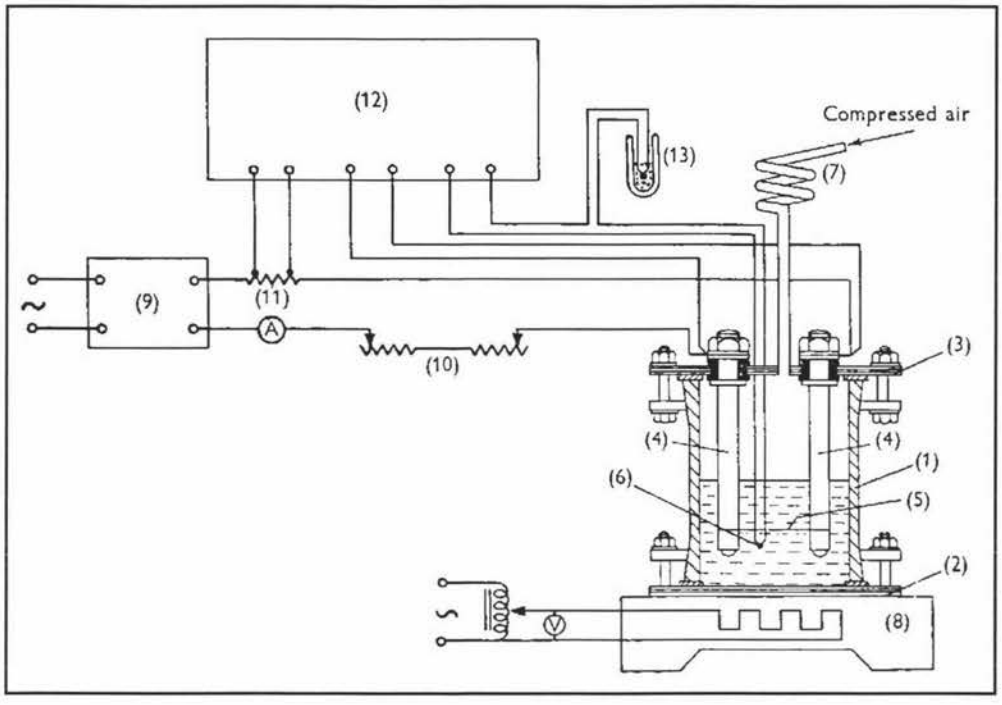

Figure 2.7 Heated platinum wire apparatus (1) milk vessel (2) machined base (3) machined lid (4) stainless steel pillars (5) platinum wire (6) thermojunction (7) condenser coil (8) hot plate (9) stabilised power unit (10) current control resistors (11) standard resistor (12) vernier potentiometer (13) cold junction (Burton, 1965).

The milk vessel (1) was made from a length of glass pipeline. Both the base (2) and lid (3) were machined stainless steel plates and each was held in position by a backing flange with a rubber gasket. The lid supported 2 stainless steel pillars (4), insulated from the lid by rubber grommets and projecting down in to the vessel. The lower ends of the pillars formed screwed terminal blocks in which the ends of the platinum wire (5) were clamped between flat surfaces.

A copper-constantan thermocouple, sheathed in stainless steel, passed through the lid in a bushing and was placed so that the thermojunction (6) was below the centre of the platinum wire. Compressed air was supplied to the inside of the vessel through the coil to prevent boiling of the milk at the heating wire surface. The vessel and its contents were maintained at a constant temperature with a hot plate supplied through a variable auto-transformer by which its temperature can be controlled. A new piece of platinum wire was used for each trial. Each piece of wire was annealed before use at orange heat for approximately 10 minutes by passing a low voltage alternating current through it.

This apparatus was suitable for studying the differences in deposit formation resulting from changes in milk composition or changes in pre-treatment. However, it was not suitable for studying the relation between the deposit and the surface on which it is formed because the deposition surface was made of platinum rather than stainless steel, which is almost universal in practice.

2.5.1.3.3 Stainless Steel Discs

Britten (1988) described a laboratory apparatus in which deposits formed on preheated or coated stainless steel discs under controlled conditions. The amount of fouling material deposited and its strength of adhesion were related to the surface properties of the disc. Figure 2.8 gives a schematic representation of the stainless steel disc apparatus.

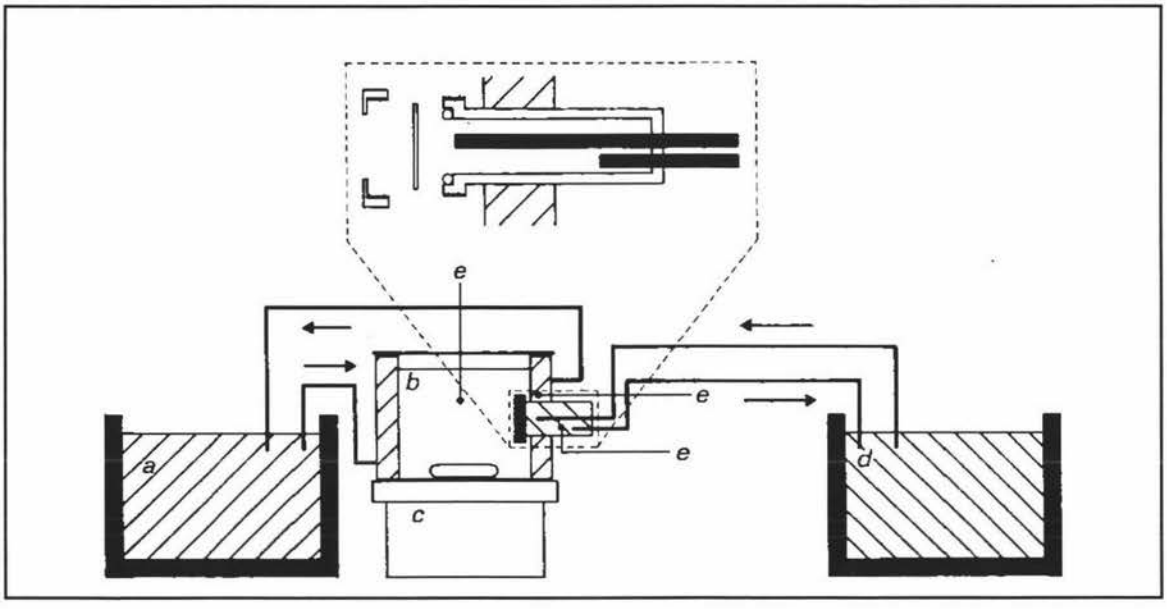

Figure 2.8 Laboratory apparatus for milk deposit formation (a) water bath at 60°C (b) milk container (c) magnetic stirrer (d) oil bath at 100°C (e) thermocouples (Britten *et al.*, 1988)

The apparatus consisted of a chamber filled with hot oil at 100°C which was sealed by the fouling surface. This chamber was inserted in the milk container so that the fouling surface was completely immersed in the milk. The milk container was a jacketed vessel placed on a magnetic stirrer. The temperature of the jacket was kept constant at 60°C while the stirring rate was set at 200 rev/min to ensure renewal of milk material close to the surface without inducing severe shear stress at the surface.

The duration of a trial was 60 minutes using approximately 200 ml of raw whole aged milk.

The apparatus was useful for determining the adhesion strength of deposits formed on various polymer coated surfaces. However, flow conditions in a milk processing plant cannot be fully reproduced by laboratory-scale apparatus. Therefore, true fouling kinetics cannot be obtained because the recycle nature of the system.

2.5.1.3.4 Plate Heat Exchangers

Many researchers (Sandu *et al.*, 1984; Jeurnink and de Kruif, 1995; Schreier *et al.*, 1994; Fryer *et al.*, 1996; Delplace and Leuliet, 1995; Delplace *et al.*, 1994; Jeurnink, 1995; Lalande *et al.*, 1984; Skudder *et al.*, 1981; Skudder *et al.*, 1985; Yoon and Lund, 1989; Calvo and de Rafael, 1995; Yoon and Lund, 1994) have used plate heat exchangers to study fouling. Often the pilot scale equipment was designed to simulate conditions found in commercial plants. Plate heat exchangers allow deposit distribution and composition to be determined with relative ease because the heat exchanger can be disassembled readily. However the operating pressures are limited by the plate gasket characteristics and the small hydraulic cross-section of plate heat exchanger makes this apparatus particularly prone to blocking by deposits.

Belmar-Beiny *et al.* (1993) state that conventional plate heat exchangers are hydrodynamically complex equipment where fluid flows between a series of corrugated plates in channels of varying width. Fluid travelling through such equipment experiences a range of shear rates and temperatures, both of which affect the rate of fouling. Although these kinds of heat exchangers are widely used in the food industry, and thermal models for some types of exchanger are available, their complex and poorly defined temperature, flow and shear fields mean that fouling results are difficult to use for understanding either kinetics or mechanism of deposition.

Figure 2.9 gives a schematic representation of a typical pilot scale plate heat exchanger.

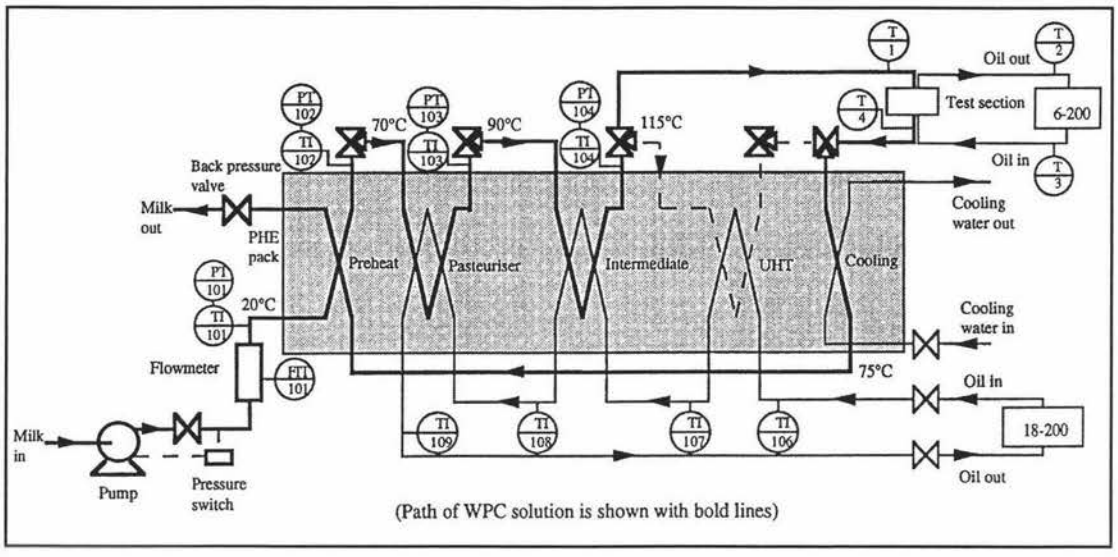

Figure 2.9 Schematic representation of a pilot scale plate heat exchanger (Schreier *et al.*, 1994)

The PHE incorporates four sections: preheater, pasteuriser, intermediate and UHT. A series of three-way valves connect the sections. The apparatus is designed to use up to 300 litres of fouling fluid at flowrates of up to 150 litres per hour. The PHE is usually operated at least 6 bar (gauge) pressure to prevent nucleate boiling.

2.5.1.3.5 Tubular Heat Exchanger

Another common apparatus used by researchers (Davies *et al.*, 1997; Swartzel, 1983; Burton, 1968; Lund and Bixby, 1975; Jeurnink, 1995; Fung, 1998; Fryer and Bird, 1997; Belmar-Beiny *et al.*, 1993; Jeurnink, 1990) to study fouling is the tubular heat exchanger. Figure 2.10 shows a tubular heat exchanger used by the Netherlands Institute for Dairy Research (Jeurnink, 1990) to study the process of fouling.

Owing to the robust structure of conventional tubular heat exchangers, the fouling deposit is usually inaccessible and therefore the deposit's distribution and composition cannot be determined. Generally, the fouling material is removed by rinsing techniques which can be chemically analysed, although fouling experiments have been carried out using model tubular heat exchangers in which tubes can be removed thus eliminating this disadvantage (Belmar-Beiny *et al.*, 1993; Fung, 1998).

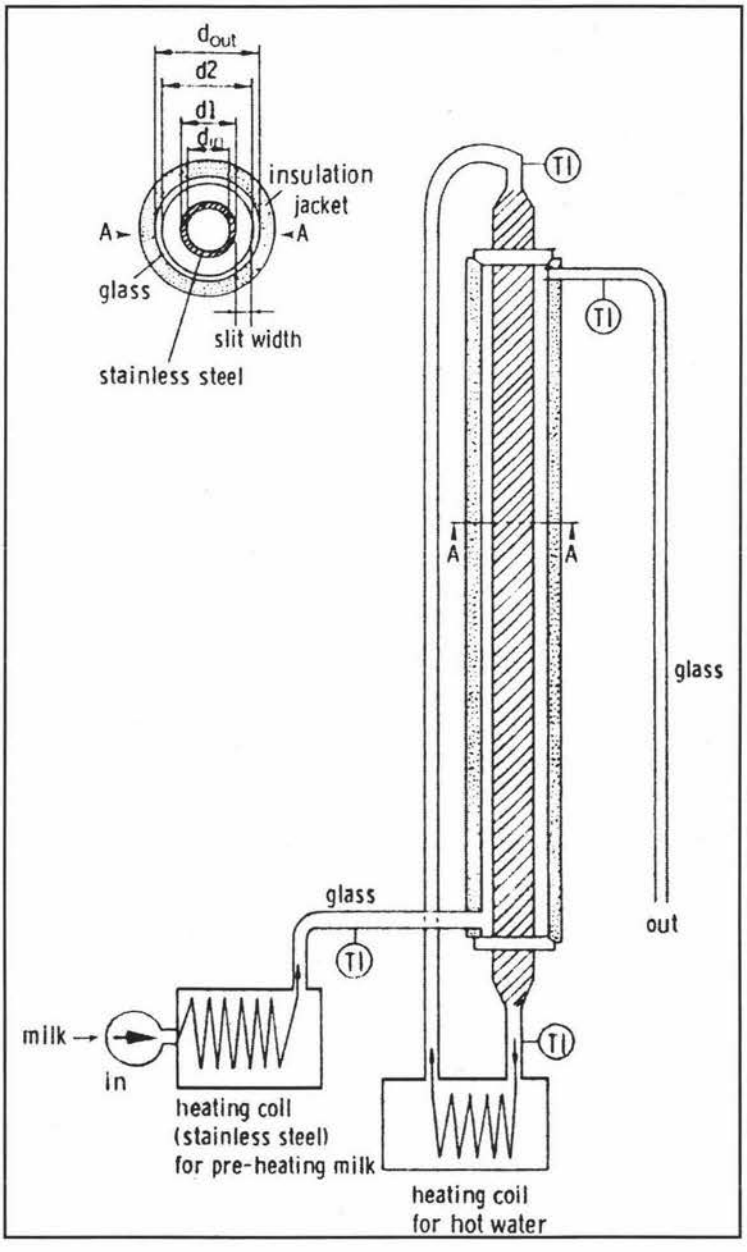

Figure 2.10 Experimental set-up of the heat exchanger consisting of two concentric tubes (Jeurnink, 1990)

The advantage of using a tubular heat exchanger for fouling studies is that the equations for predicting heat transfer and friction factors are well known.

2.5.1.3.6 Evaporator

Little research has been conducted on fouling deposits in evaporators (Fryer, 1995). Chen *et al.* (1996) studied fouling caused by sweet cheese whey and reconstituted whey powder solutions in a Centritherm evaporator. Using this apparatus, it was only possible to study the initial stages of fouling from whey solutions on rotating surfaces.

2.5.1.4 Methods of Measurement

2.5.1.4.1 Heat Transfer

The basic heat transfer equation relating the heat flux across a surface (q), to the temperature driving force ($\Delta\theta$), between a hot and cold fluid can be given by Equation (2.38):

$$q = U\Delta\theta \qquad \textbf{(2.38)}$$

where U = heat transfer coefficient

As fouling proceeds, the overall heat transfer coefficient, U, decreases. This process can be described by introducing the concept of a thermal fouling resistance, R_f (m^2K/W), defined as:

$$\frac{1}{U} = \frac{1}{U_o} + R_f \qquad \textbf{(2.39)}$$

where U_o = heat transfer coefficient of the clean surface (Visser *et al.*, 1997)

In a heat exchanger, heat is transferred from a fluid on one side of a dividing wall to a fluid on the other side. At any point in the heat exchanger the heat transfer is defined by:

Rate of heat flow = driving force / resistance

The driving force is the temperature difference between the two fluids. For the whole heat exchanger the rate equation is:

$$\phi = UA\Delta\theta_m \qquad \textbf{(2.40)}$$

where ϕ = rate of heat transfer

A = heat transfer area

θ_m = mean temperature difference between fluid (driving force) which can be shown to be logarithmic mean temperature difference for pure counter-current or parallel flow heat exchangers.

Figure 2.11 gives a schematic representation of a simple heat exchanger. The hot and cold fluids are referred to as A and B respectively, the two ends of the heat exchanger

1 and 2. Fluid A has a heat capacity of c_a and a flowrate of m_a. Fluid B has a heat capacity of c_b and a flowrate of m_b.

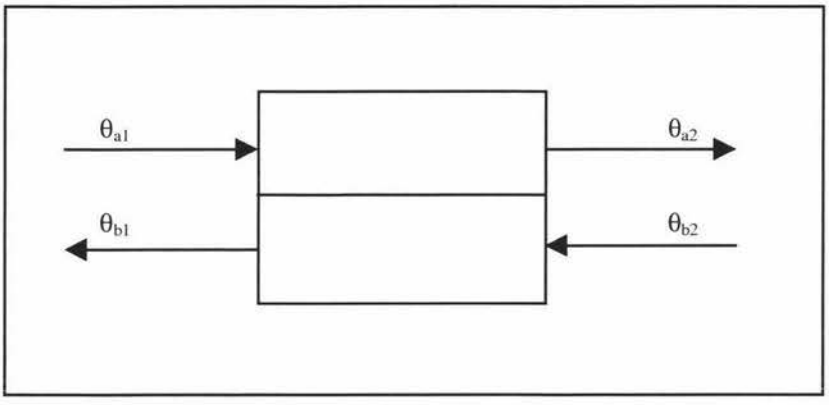

Figure 2.11 Schematic representation of a pure counter current heat exchanger (Paterson *et al.*, 1996)

The heat loss by one fluid should be taken up by the other fluid assuming that the heat losses to the environment are negligible. This can be expressed in a heat balance equation:

$$\phi_a = \phi_b \tag{2.41}$$

$$m_a c_a (\theta_{a2} - \theta_{a1}) = m_b c_b (\theta_{b2} - \theta_{b1}) \tag{2.42}$$

For a pure counter-current heat exchanger the mean temperature difference is a logarithmic mean:

$$\Delta\theta_m = \Delta\theta_{lm} \tag{2.43}$$

The log mean temperature difference can be calculated using Equation (2.44):

$$\Delta\theta_{lm} = \frac{\Delta\theta_1 - \Delta\theta_2}{\ln\left(\frac{\Delta\theta_1}{\Delta\theta_2}\right)} \tag{2.44}$$

where $\Delta\theta_1 = \theta_{b1} - \theta_{a1}$

$\Delta\theta_2 = \theta_{b2} - \theta_{a2}$

The overheat transfer coefficient can be calculated using the following equation:

$$U = \frac{\phi}{A\Delta\theta_m} \tag{2.45}$$

Therefore the fouling resistance (R_f) as a function of time can be calculated explicitly by monitoring temperature and flow. This method is an overall method requiring extensive instrumentation.

2.5.1.4.2 Pressure Drop

Another well-known consequence of the formation of a deposit layer on a heat exchange surface is the increase in pressure drop over the heat exchanger with time. This process can easily be monitored with reasonable accuracy by using differential pressure sensors (Visser *et al.*, 1997).

The increasing pressure drop is due to the decrease in hydraulic diameter during fouling of heat exchanger ducts. Pressure drop measurements are useful for characterisation of the geometry changes within flow channels when fouling takes place. For example, rapid increase of pressure drop can be observed in a PHE when channels are blocked by deposit. Because the change in pressure drop with time can be completely different for trials performed under the same conditions, the conclusion reached by Burton (1966) that "Pressure drop measurements should never be used as a means to determine deposit quantities..." is confirmed.

2.5.1.4.3 Physical Measurement

Researchers often measure the amount of fouling simply by physical methods such as mass or thickness of deposit. Obviously these methods are intrusive and often require the system to be shutdown and therefore would not be appropriate for commercial monitoring of fouling.

Fouling deposit-weight measurements cannot take place with conventional shell and tube heat exchangers. Therefore this method is generally only applicable to plate heat exchangers and model tubular heat exchangers with removal tubes. Deposit thickness measurements are difficult to obtain on plate heat exchanger plates that are corrugated. Similarly, thickness measurements can usually only be obtained at the ends of the tubes of a tubular heat exchanger.

The methodology for weighing fouling deposits varies slightly among researchers (Skudder *et al.*, 1981; Skudder *et al.*, 1985; Yoon and Lund, 1994; Fryer *et al.*, 1996; Delplace and Leuliet, 1995). The generic procedure is as follows:

- Fouled plates from the heat exchanger are flushed with a minimum amount of water.
- Plates are dried – in ambient air or oven.
- Drying duration varies from 6 hours to overnight.
- Plates weighed directly.

Thickness measurements are usually made with conventional measuring devices such as micrometers or verniers (Jeurnink *et al.*, 1989; Truong *et al.*, 1998).

2.5.2 Industrial Fouling Monitor

As mentioned previously, the build-up of fouling on heat transfer surfaces requires daily cleaning of milk processing plants during which time the production process is stopped. This approach leads to considerable periods of plant down-time and the use of significant quantities of cleaning materials, resulting in the loss of plant efficiency and the accompanying significant economic penalties.

Clearly, some form of sensor that is capable of monitoring the onset and build-up of fouling would be beneficial in determining the optimum point at which to stop production and begin the cleaning operation, thus minimising plant down-time and maximising process efficiency. The use of sensing techniques in other industries has already demonstrated that it is feasible to monitor the build-up of fouling on-line, thus enabling the optimum point at which to begin cleaning to be determined (Withers, 1996).

Jones *et al.* (1994) outline four criteria for a fouling sensor:

- Size. The monitor should be of modest size so that it can be easily installed, serviced and replaced. Although large units are likely to provide closer simulation of the heat transfer and flow conditions found in the plant, their capital and running costs are likely to be too high for general use.

- Cost. It is likely to be some time before the value of using an on-line monitor to measure fouling becomes widely accepted, and therefore the capital cost should be as low as possible.
- Reliability. The monitor should be robustly constructed, require the minimum of maintenance, and provide reproducible data that are easy to interpret.
- Relevance. It is important that, within these restrictions, heat transfer and fluid flow conditions in the monitor can be related to those in the plant. It would also be useful if samples of the deposits formed in the monitor could be easily removed for examination.

Withers (1996) proposed an additional criterion; any sensor should not influence to any significant degree the process or the phenomenon that it is monitoring and more specifically, the presence of the sensor in the system should not promote atypical fouling.

Although a fouling sensor has not been used commercially to date to monitor fouling, a number of workers (Withers, 1996; Truong *et al.*, 1998; Jones *et al.*, 1994; Fryer and Pritchard, 1989; Davies *et al.*, 1997) have reported potential sensors. These devices are generally of local nature opposed to an overall fouling measure like pressure drop and deposit weight. Sections 2.5.2.1-2.5.2.6 describes these potential fouling sensors and monitors.

2.5.2.1 Heat Radial Flow Cell

Fryer and Pritchard (1989) discussed the use of a heated radial flow cell (RFC) to monitor the build-up of fouling. Originally the device was unheated and was used for the study of the adhesion of micro-organisms under a range of flow conditions. Both the heated and unheated versions have the advantage that the effects of different surface compositions and finishes can readily be studied by using discs of appropriate material.

Figure 2.12 gives a schematic representation of the heated radial cell device. The device consisted of a pair of flat parallel discs, through the centre of one disc the fluid entered and flowed radially outwards, its velocity and therefore the surface shear

stress on the discs decreases from the centre outwards. The changes in temperature at the various thermocouples across the plate gave a measure of the progress of fouling under different conditions of flow temperature.

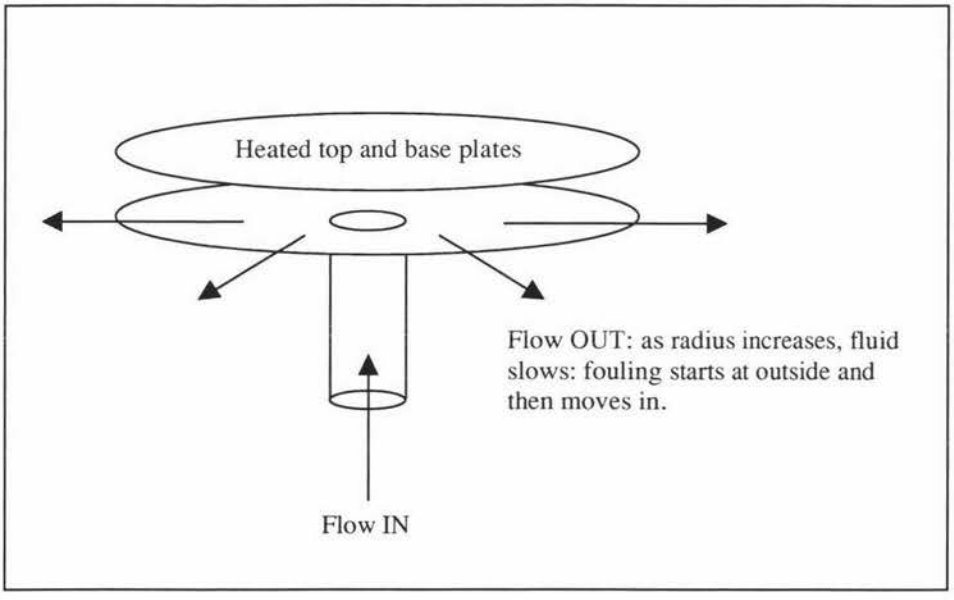

Figure 2.12 Schematic representation of heated radial flow cell (Fryer and Pritchard, 1989)

The advantage of this fouling monitor was that the progress of fouling under different conditions of flow and temperature could be obtained. Therefore, several data points could be generated simultaneously which was the most valuable type of information obtained by this monitoring device.

However there was one major drawback to this technique – the gap between the plates required to be very narrow if the desired range of surface shear stresses were to be reproduced. Thus the presence of even a small amount of deposit significantly lowers the cross-sectional area and diverts the flow rapidly away from the fouled area, increasing the surface temperature and thus allowing rapid fouling to take place. The end result of this process was a distorted fouling pattern. Therefore, the RFC is only suitable for studying the earliest stages of deposition.

2.5.2.2 Tapered Tube

Fryer and Pritchard (1989) compared the RFC to another device called the tapered tube. This device consisted of a tapered tube, 400 mm in length, varying in internal

diameter from 19.0 mm at the inlet to 12.7 mm at the outlet. Figure 2.13 gives a schematic representation of the device.

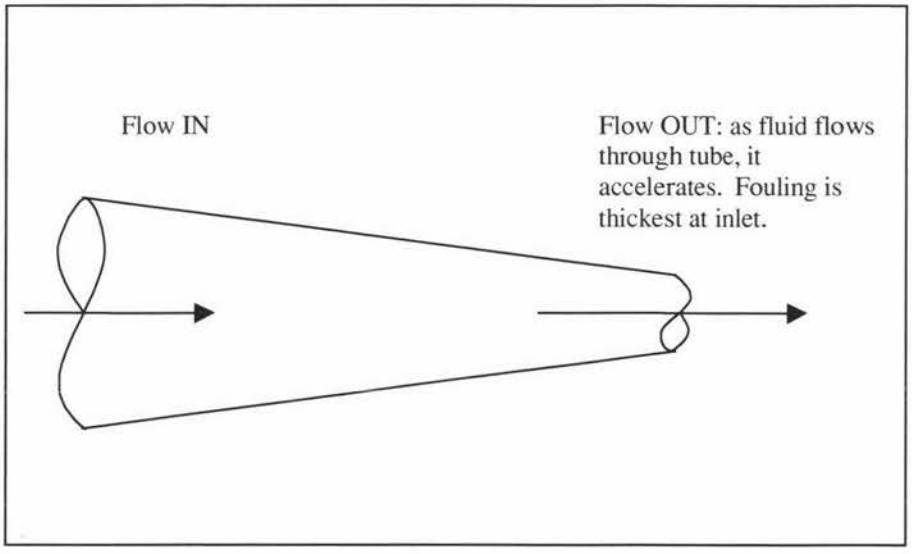

Figure 2.13 Schematic representation of heated tapered tube (Fryer and Pritchard, 1989)

Formation of a deposit of a given thickness on its walls therefore has much less effect on the flow than the RFC. Similar to the RFC, a range of shear stresses is produced simultaneously, but the converging flow is more stable than the diverging flow of the RFC.

Fryer and Pritchard (1989) concluded that the tapered tube is more likely to be suitable for further development as a fouling monitor, as it is unlikely to be prone to blocking by deposit in the same way as the radial flow cell. However, there is considerable amount of further work to be done, both in the laboratory to examine the build-up of deposits, and in industry so that the measurements from the monitor can be correlated with plant performance. A disadvantage of this monitor was the expense of its fabrication. However, Fryer and Pritchard (1989) suggest that other much cheaper manufacturing processes may remove this disadvantage.

Both the tapered tube and the radial flow cell would need to be installed in a side stream in a commercial processing plant. Therefore it would be difficult to simulate the same type of treatment in the side stream as found in the rest of the plant. In addition, after these monitors have been installed, they would be difficult to re-install

in other locations of the plant. This would be a severe disadvantage if the initial location of the installation was not prone to fouling.

2.5.2.3 Optical Sensor

Withers (1996) described the use of an optical sensor for detection of fouling. Although this technique does not appear to be an obvious choice (due to the opaque stainless steel pipes and fittings), it may be possible to install 'sight glasses' or inspection ports into the process plant. The underlying assumption associated with this sensor was that the sight glass should exhibit fouling characteristics similar to the stainless steel pipe. This assumption may not always hold. This technique can be considered to be non-invasive because there is no disruption to the flow.

The principle of operation relies on the fact that the light-reflectance characteristics of the boundary between the transparent sight glass and the product will change in the presence of a fouling film. Withers (1996) claims that despite the fact that the fouling characteristics of the sight glass are likely to be different from that of the stainless steel, provided it can be shown that the glass surface fouls in a repeatable fashion, the fouling on the glass can be related to that on the stainless steel.

The Danish Biotechnological Institute has developed an optical sensor as part of the European Union – FLAIR project (Mikkelsen, 1994). Initial trials showed that the technique could be made to work using a simple white-light source and photosensor fitted to a glass insert mounted in the flow system. Through further experimental work, it was found that the sensor output was dependent on processing conditions, including flowrate and temperature.

Development and refinement of the sensor has led to a complex design in which the product was forced to flow along a specially designed channel within the sensor so that fouling produced there matches that produced in other parts of the plant, such as in heat exchangers. The lower limit of sensitivity in terms of film thickness was in the order of 0.01mm. A range of detection was not given.

This sensor will require appropriate configuration and calibration before it could be used to predict fouling at locations within a plant. This may also be a difficult task.

Figure 2.14 gives a typical output from the optical sensor. The process fluid used during these experiments was skim milk.

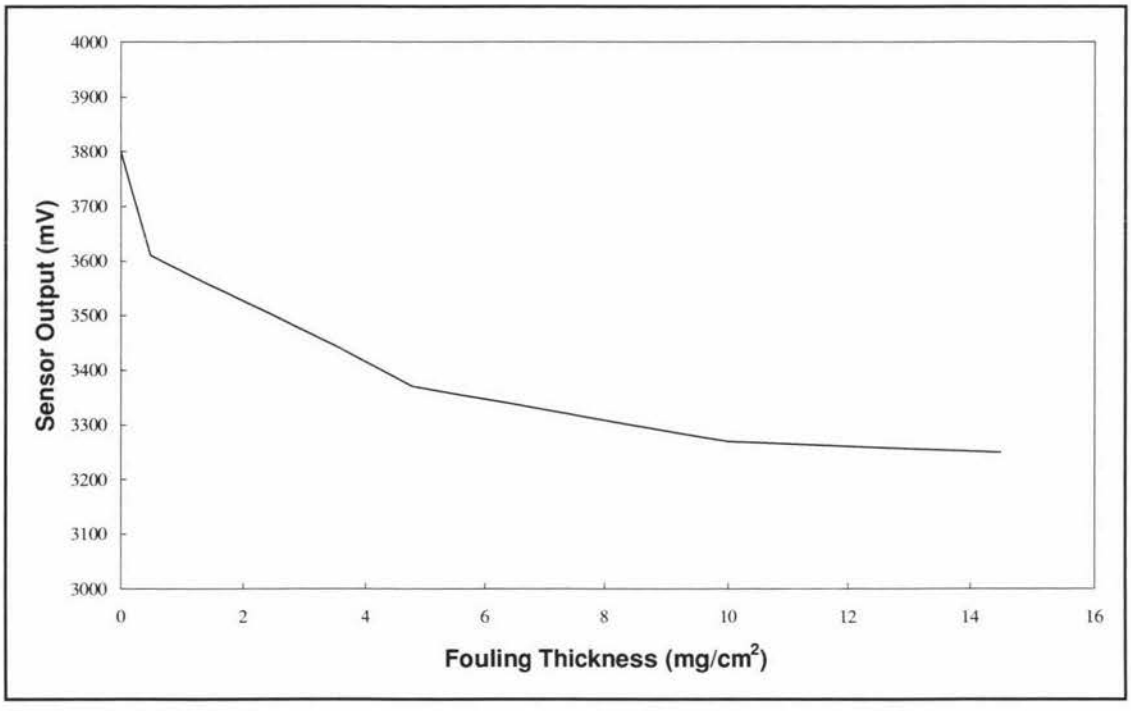

Figure 2.14 Plot of optical sensor output against fouling film thickness (Withers, 1996)

2.5.2.4 Acoustics: the vibration sensor

A sensor that operates on the principles of acoustic emission was developed by the Danish Technological Institute (Dam Madsen, 1994). Withers (1996) describes acoustic emission monitoring in detail. Most processes generate some form of 'noise'. This noise may be used to determine the condition of the process or of the machines performing that process. The noise can be quantified in terms of its relative level at different frequency bands. If the frequency spectrum of a machine or process is compared with a previously recorded spectrum of a 'healthy' machine or process, any deviations will be visible and will point to potential problems or faults long before they can be detected by more obvious signs.

A modification of this technique may be used in which some form of excitation signal is applied to the system under examination and the response to this recorded. Analysis of this response and comparison with a response obtained under known conditions will give some indication of the unknown condition.

This sensor was especially designed for use in plate heat exchangers. The developed sensor was a small transducer bonded to the surface of a plate on the process fluid side of the plate pack. The transducer was located such that it would be directly affected by the build up of a fouling film on its surface. The transducer, a piezo-electric crystal-based device was made to vibrate over a range of frequencies that encompasses its own natural frequency. The presence of a fouling film on the sensor has two effects: first, it damps down the amplitude of the vibrations; second; it shifts the natural frequency slightly. Both of these effects can be measured and related to the degree of fouling.

An obvious disadvantage to this technique was the intrusive nature of the sensor. However, Withers (1996) argues that the sensor occupies a small volume within the plate pack and if the design of the sensor can be optimised, the transducer should foul in the same way as the rest of the plate pack. The sensor would be cleaned by normal clean-in-place operations.

Another disadvantage of this sensor was the ability to detect relatively small masses of fouling. The equivalent film thickness detection range of the prototype sensor was found to be 0.1mm to 0.4mm. This range would need to be extended if this sensor was to be introduced into industry.

The sensor was also found to be sensitive to temperature but this could be reliably compensated for at the signal processing stage. Although the sensor was temperature sensitive, it was able to operate under realistic processing conditions, these being 100-200 kPa, 5-140°C and 0-30 l/min.

Figure 2.15 shows the frequency response of the acoustic sensor for both a clean and a fouled heat exchanger. The layers referred to on the graph are consecutive layers of

fouling deposited on top of each other during a series of trials using pasteurised milk as the bulk product.

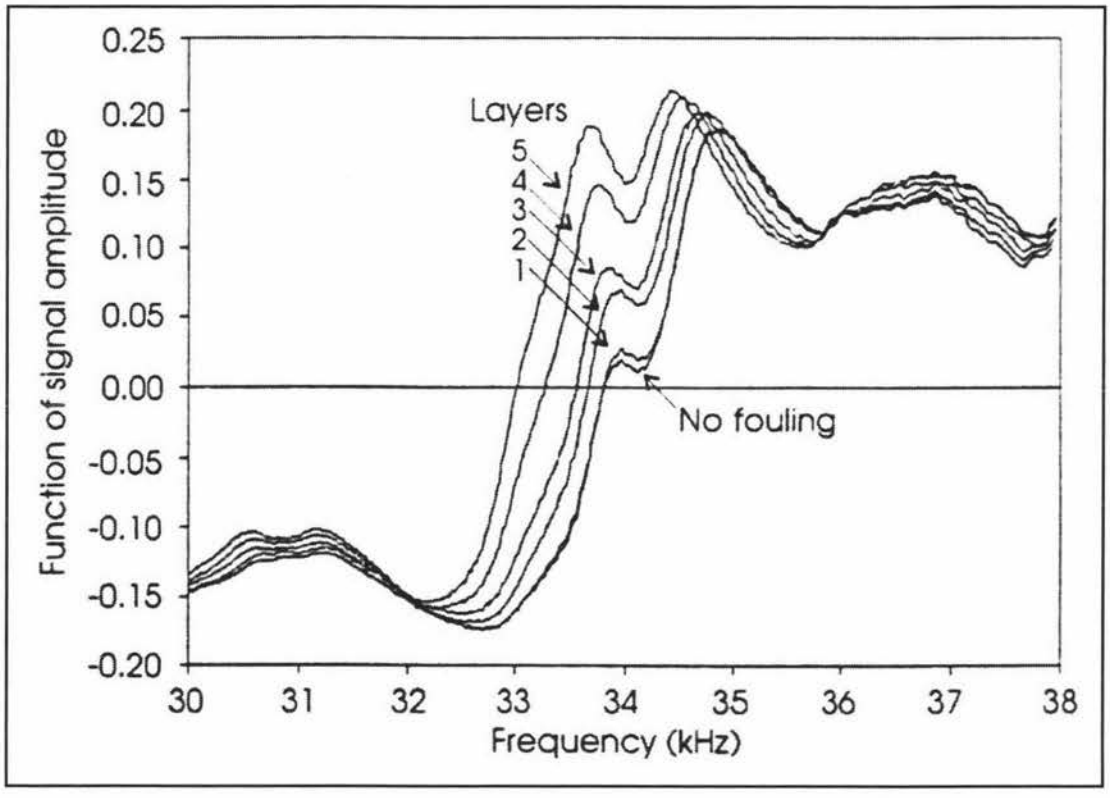

Figure 2.15 Frequency response of the vibration sensor plotted against a function of amplitude for cleaned and fouled surfaces (Dam Madsen, 1994)

2.5.2.5 Heat flux

The thermal resistance of the piping system is increased by fouling deposits and the overall heat transfer coefficient, hence the thermal resistance of the fouling layer, can be calculated from the measured heat flux (Jones *et al.*, 1994).

Local heat flux sensors which measure the temperature across a thin wafer of known thermal conductivity have been used to monitor fouling (Jones *et al.*, 1994; Truong *et al.*, 1998; Truong *et al.*, 1996; Davies *et al.*, 1997). A thermopile across the two faces of the wafer generates a voltage which can be measured. Figure 2.16 shows the principle operation of a heat flux sensor.

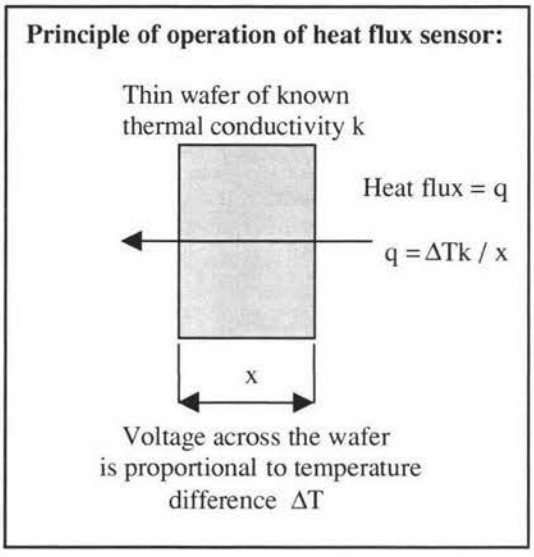

Figure 2.16 Operation of a heat flux sensor (Visser *et al.*, 1997)

Jones *et al.* (1994) used such a device to successfully monitor milk fouling in a small heated cell. The sensor was a Microfoil Heat Flux Sensor, supplied by Rhopoint Ltd, Oxford, UK. Preheated protein solution flowed across the sensor, which was mounted on a heated copper block that maintained the sensor at a known surface temperature. The change in heat flux was recorded by a change in voltage output to a nanovoltmeter. The nanovoltmeter reading was recorded on a microcomputer along with the temperature of the heated block surface and the temperature of the protein solution. However the device was only a prototype that needed development before it could be used within commercial process plants.

Truong *et al.* (1998) describe the use of a sensing device, similar to the one used by Jones *et al.* (1994), to measure locally the rate of fouling on unheated surfaces in two commercial plants. The heat transfer resistance (R_f) contribution to fouling was estimated from experimental measurements using the Equation (2.46):

$$R_f = \frac{1}{U} - \frac{1}{U_o} \qquad \textbf{(2.46)}$$

where: U = overall heat transfer coefficient

U_o = initial overall heat transfer coefficient

There were assumptions associated with the use of this equation of which the three most important are:

- The flowrate and temperature of the milk are steady throughout the run.
- The reduction in cross-sectional area available to flow as fouling progresses is negligible.
- The heat transfer coefficient outside the pipe is constant throughout the run. For unheated pipes this side represents ambient conditions in the plant.

Truong *et al.* (1998) found in practice that assumption (3) was almost always violated as random variations in ambient conditions near the heat flux sensor are difficult to avoid. To solve this problem, the temperature of the external pipe wall was also monitored which allowed calculation of the internal overall heat transfer coefficient U_i. This coefficient was normalised with its initial value U_o which collapsed into a much more reproducible pattern data from disturbed and undisturbed ambient condition trials. The heat flux probe was found to detect fouling deposit thickness up to 3 mm in pilot plant trial conducted by Truong (1998).

The relatively small size and simplicity of the sensor would allow the device to be easily adapted to monitor fouling at different locations in the plant. This ability is particularly important for a local sensor because the worse case location of fouling build-up may not always be the first point of installation.

2.5.2.6 Ultrasonic

Withers (1994) analysed an ultrasonic signal in the time domain i.e. in terms of change in time of flight of the signal, as a means of detecting and measuring the thickness of fouling deposits in the pipe-work of continuous high-temperature processing plants. Ultrasound is sound energy with a frequency range that covers the region from the upper limit of human hearing, which is generally considered to be 20 kHz to beyond hundreds of MHz.

Initially Withers (1994) considered two techniques for the sensor: pulse-echo and transmission. Pulse-echo involves the use of a single transducer on the outer surface of the piping transmitting a pulse of ultrasound into the piping. The same transducer

is then used to receive any echoed signals. The echoes, or reflections, are produced when the pulse of ultrasound meets boundaries, or interfaces, between different materials or voids within the materials. The time taken for the reflections to return to the transducer can be measured and the resultant data used to deduce the thickness of the various materials. This technique was abandoned by Withers (1994) for a number of reasons. The surface of the film and hence the boundary between the film and the product will not be regular. Thus, the ultrasound pulse will be scattered and very little signal will be directly reflected back to the transducer. The mismatch between the acoustic properties of the material of the pipe wall and those of the materials of the product and fouling layer will result in a large reflection from the pipe-product boundary which will tend to drown the much smaller reflection from the film surface.

The alternative approach used by Withers (1994) was transmission (two transducers - transmitter and receiver). In the case of a pipe, the transducers are mounted on opposite sides of the pipe and the ultrasound would pass through the pipe walls, the product and any fouling that may be present. A disadvantage of this approach is that the ultrasound has to pass through the product, which may be flowing at high velocity and/or contain particulates or gas bubbles, all of which can result in signal loss.

Two techniques can be used to analyse the signals obtained from the receiving transducer. The signal can be considered in terms of changes either in its amplitude or in its time of flight through the system. Both approaches rely on the assumption that the fouling film and the product will have different acoustic properties (Withers, 1996).

The amplitude of the signal depends on several factors including attenuation owing to the nature of the product and the mismatch in acoustic properties of the various materials. If this approach is to be successful then none of the properties of the pipe walls, product or transducers must change. Unfortunately, this is unlikely to be the case (Withers, 1996).

The second approach, that of monitoring the time of flight of the signal, attempts to overcome the problems inherent to the analysis of signal amplitude by considering a function of the ultrasonic signal that is independent of its amplitude. Withers (1994)

monitored the time of flight of the signal because of disadvantages associated with analysing the amplitude of the signal

The principle of operation of the sensor was as follows: the ultrasonic pulse from the transmitter will take a finite time to travel through the pipe wall, the product and the opposite pipe wall, determined by the velocities of the sound in those materials. This time will remain constant (providing all other factors are constant) until a fouling film forms. Assuming that the velocity of sound in the fouling film is different to that of the product and as the film has replaced some of the product, then the time taken for the sound to travel through the system, known as the time of flight, will change. If the change in time of flight is measured and the sound velocity in the fouling film is known, then the thickness of the film can be determined (Withers, 1994).

One major disadvantage to the transmission technique is particles in suspension will scatter the signal e.g. very small amounts of entrained air in milk could result in the signal being lost entirely.

A prototype sensor (refer to Figure 2.17) was able to detect the presence of deposits with a minimum thickness of 0.1 mm and measure the thickness of films over the range 0.5 to 6.0mm. This sensor can be considered to be a non-invasive technique. The compensation for temperature effects was applied to the transmission technique for both milk and water products over the temperature range 20-130°C. Flowrates up to 10 l/min and processing pressures up to 3×10^5 Pa did not affect the sensor (Withers, 1994).

Equation (2.47) was used to calculate the thickness of the fouling layer.

$$T = \frac{D - x}{V_p} + \frac{x}{V_f} \qquad \textbf{(2.47)}$$

where T = time of flight measured by ultrasound

V_p = velocity of sound in product

V_f = velocity of sound in fouling

D = diameter of pipe

x = unknown thickness of film

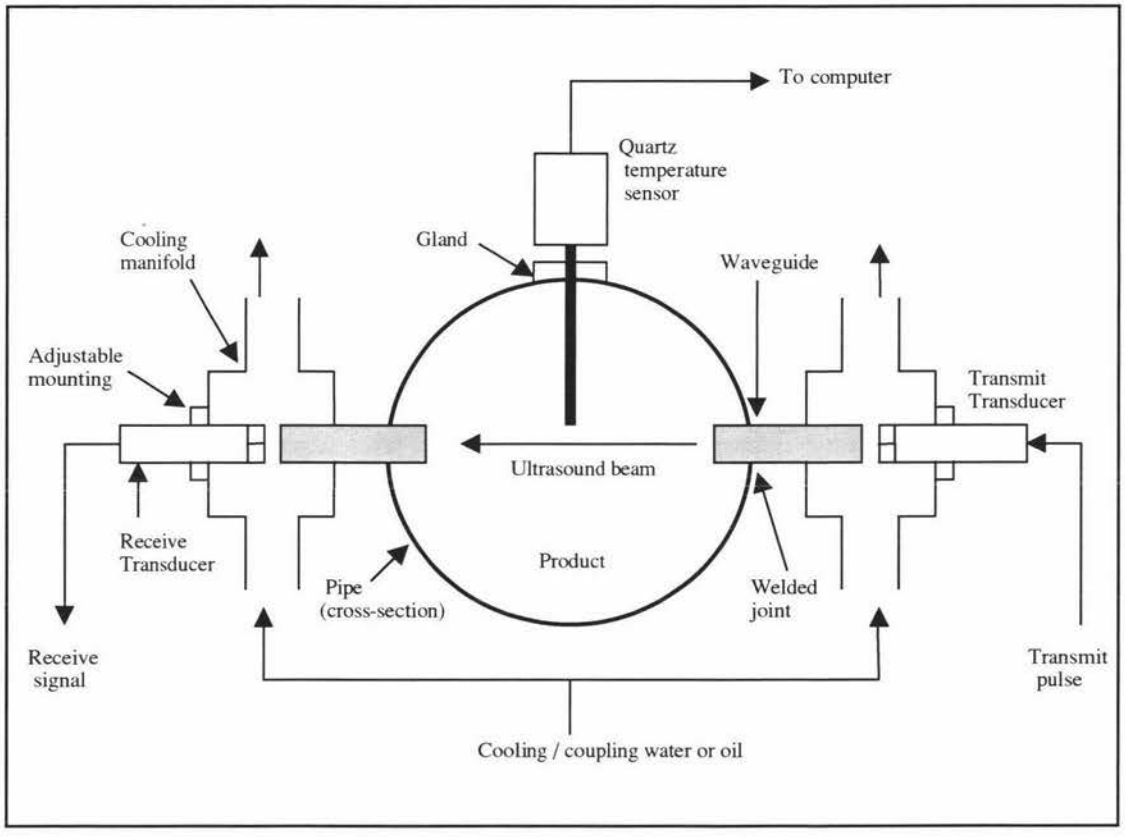

Figure 2.17 Schematic representation of ultrasonic sensor system layout (Withers, 1994)

2.6 Conclusion

This literature survey has discussed previous studies made by researchers in the area of milk fouling on heat treatment equipment. The results, conclusions and experimental techniques used by these researchers have been discussed. Most studies concentrated on the role of protein and minerals in ultra high temperature conditions. Little attention has been paid to fouling in evaporators.

Considerable progress had been made in the area of modelling the fouling of heat exchangers by dairy products. Modelling has lead to a better understanding of the process of fouling however, a complete model has not been published.

Traditionally researchers have measured fouling using overall measurements of temperature and pressure or by physical methods such as fouling deposit mass or

thickness. Transferring these techniques to industry is not easy. Therefore, it would seem possible that a local fouling monitor operating in real-time would be beneficial in determining the optimum time to begin cleaning. A number of techniques and possible sensing devices have been reviewed and of these, it appears that the heat flux sensor has the most potential as a possible industrial fouling monitor. The heat flux sensor is small, cheap, and simple and can be easily reinstalled in milk processing plants, particularly at the "worse case" fouling sites. Recently, the sensor has been used to monitor fouling on unheated surfaces in two commercial plants (Truong *et al.*, 1998). Further refinement of this technique is required.

3 THEORY

3.1 Introduction

The use of a heat flux probe appeared to be the technique with the greatest potential to monitor milk fouling on heated surfaces in industry and therefore was adopted in this research project. The technique has been used to study fouling on unheated surfaces in commercial plants (Truong *et al.*, 1998) and study fouling of whey protein solutions in a small heated cell (Jones *et al.*, 1994). There has been no detailed investigation into practical problems associated with this device. Furthermore, the sensor has not been tested with realistic heated surfaces found in industry, for example, plates with fluid flow on both sides. Before the technique could be used successfully, an investigation was required into the stability of resistances of the system into which the probe was introduced. The operating principle and explanation of system resistances are given in this chapter.

3.2 Operating Principle

The heat flux probe operates on the following principle. The heat transfer equation relating the heat flux across a surface to the temperature driving force between a hot and cold fluid is given by:

$$q = U\Delta\theta \qquad \textbf{(3.1)}$$

where: q = heat flux (W/m²)

U = overall heat transfer coefficient (W/m²K)

$\Delta\theta$ = temperature difference (K)

For the experimental apparatus used in this research project the temperature difference was defined as:

$$\Delta\theta = \theta_s - \theta_p \qquad \textbf{(3.2)}$$

where: θ_s = temperature of the heat flux sensor surface exposed to the heating medium (°C)

θ_p = temperature of the milk (°C)

Substituting Equation (3.2) into (3.1) and rearranging making U the subject:

$$U = \frac{q}{\theta_s - \theta_p} \qquad \textbf{(3.3)}$$

Therefore, the overall heat transfer coefficient (a measure of fouling), could be calculated for a system where these three variables were known. For the experimental apparatuses used in this research project (miniature plate heat exchanger and research falling film evaporator), the heat flux passing through the heated surface was measured by a thin-foil heat flux sensor (refer Section 4.4.1). The temperature of the heat flux sensor surface in direct contact with the heating medium was measured by an on-board Type T thermocouple. The process fluid temperature in the miniature plate heat exchanger was initially measured by a Resistance Temperature Device (RTD) but was replaced by a Type T thermocouple due to the RTD's performance inadequacies. Two RTDs installed in the research falling film evaporator measured the process fluid temperature.

3.3 System Resistances

As fouling proceeds, the overall heat transfer coefficient (OHTC) decreases because the thermal resistance of the surface has increased (Visser *et al.*, 1997). The total resistance to heat transfer, R_t, between the milk and the side of the heat flux sensor not in contact with the heated surface can be expressed as the inverse of the OHTC as shown in Equation (3.4):

$$R_t = \frac{1}{U} \tag{3.4}$$

The total thermal resistance is made up of several terms as shown by Equation (3.5):

$$R_t = R_{ss} + R_p + R_c + R_m + R_f \tag{3.5}$$

where: R_{ss} = heat transfer resistance contributed by stainless steel plate (m²K/W)

R_p = heat transfer resistance contributed by probe (m²K/W)

R_c = heat transfer resistance contributed by cement (m²K/W)

R_m = heat transfer resistance contributed by milk (m²K/W)

R_f = heat transfer resistance contributed by fouling (m²K/W)

Figure 3.1 gives a schematic representation of the resistances found in the experimental apparatus used in this research project.

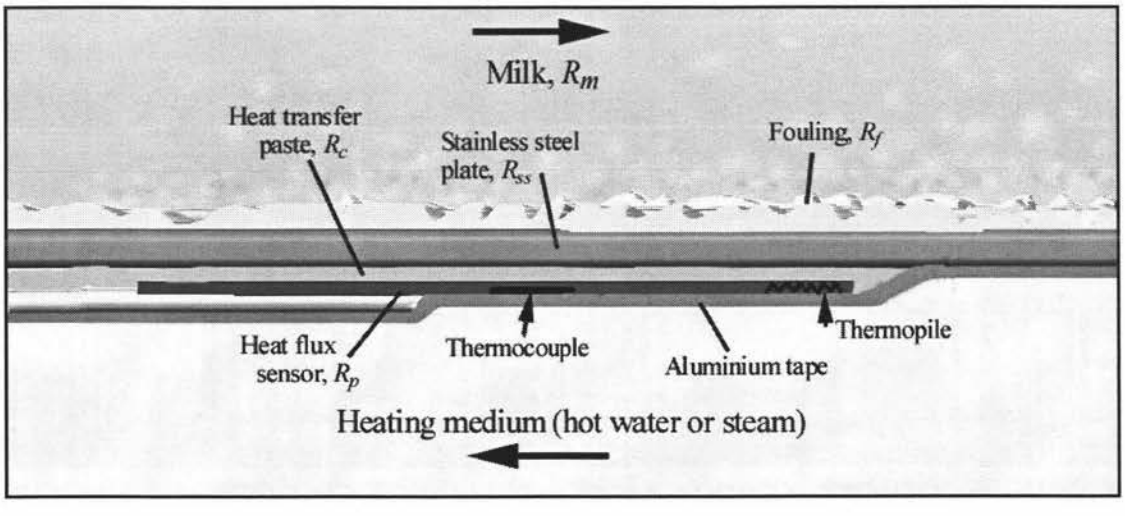

Figure 3.1 Schematic representation of system resistances found in the miniature plate heat exchangers and the research falling film evaporator (drawn by R. Croy)

Assuming that resistances R_{ss}, R_p, R_c, and R_m remain constant during a run, any decrease in OHTC will be due to an increase in R_f. The sum of resistances, R_{ss}, R_p, R_c and R_m may be approximated by the inverse of the initial overall heat transfer coefficient, U_o, measured at the beginning of the run when the surface is clean (Truong *et al.*, 1998):

$$\frac{1}{U_o} = R_{ss} + R_p + R_c + R_m \qquad \textbf{(3.6)}$$

Then the fouling resistance can be estimated from experimental measurements:

$$R_f = \frac{1}{U} - \frac{1}{U_o} \qquad \textbf{(3.7)}$$

The assumption that all initial resistances (R_{ss}, R_p, R_c, and R_m) remain constant throughout the run may not always hold. A series of experiments was designed to investigate the stability of each individual resistance. Based on the results of these experiments, compensation may be required before the probe could be successfully used as a fouling monitor in industry.

4 MATERIALS AND METHODS

4.1 Introduction

An outline of materials used during this study is presented, followed by an overview of the custom built Pilot Plant with detailed descriptions of the two equipment assemblies (fouling rig and research falling film evaporator) used to study milk fouling on heated surfaces. A generic pilot plant operating procedure is presented followed by specific details of experiments performed during this research project.

4.2 Materials

4.2.1 Milk

Standardised, homogenised and pasteurised full cream milk (3.2% protein, 3.3% fat) manufactured by Kiwi Dairies Limited, Longburn N.Z. was used in the present fouling study.

4.2.2 Steam

Laboratory steam (condensate removed) was supplied from the Riddet Building boiler at 2 bar pressure and was used as a heating medium.

4.2.3 Water

Tap water supplied from the Massey University high pressure water circuit was used as a cooling medium and during Clean-In-Place rinses. Availability and low cost were advantages of using tap water.

4.2.4 Vacuum

Vacuum was supplied from the Riddet Building vacuum pump at pressures in the range of –0.6 to –0.8 bar.

4.2.5 Clean-In-Place Chemicals

- Caustic solution: sodium hydroxide, made up to a strength of 1.0% w/w strength from 50% w/w concentrated caustic (765 g/l).
- Acid solution: nitric acid, made up to a strength of 0.5% w/w from 68% w/w concentrated nitric (970 g/l).

Both chemicals supplied by Orica Chemnet Ltd., Tauranga, N.Z.

4.2.6 Adhesive Tape

Aluminium adhesive tape (3M Scotch, No. 425, General Machinery, Palmerston North, N.Z.) was used to temporarily attach the heat flux sensors to the stainless steel test plates.

4.2.7 Heat Transfer Paste

To ensure high thermal conductivity, a layer of heat transfer paste was placed between the heat flux sensor and heated surface during the attachment process (refer to Section 4.4.1). The following two heat transfer pastes were used during trials:

- Non-silicone heat transfer compound (Electrolube, Product No. HTC103)
- Silicone heat transfer compound (Electrolube, Product No. HTS35SL)

Both pastes were supplied from Spectron Electronics, Palmerston North, N.Z.

4.3 Pilot Plant

4.3.1 Introduction

The study was carried out along side three other research projects. All projects made use of a custom built pilot plant (see Figure 4.1) that was designed and built by the postgraduate students involved in the projects and Food, Nutrition and Human Health Institute technicians.

Table 4.1 lists the members of the design and construction group with details of individual tasks performed by each member.

Table 4.1 Pilot Plant design and construction group with division of labour

Name	Position	Responsibility
Hayden Bennett	MTech student	Fouling rig, research falling film evaporator, junction boxes and sensor wiring conduit.
Richard Croy	MTech student	CIP system, milk vat and plate heat exchanger.
Andrew Hinton	PhD student	Direct steam injection systems, concentric double tube heat exchanger and heating medium circuit.
Byron McKillop	Senior Technician	Mechanical construction and structural modifications.
Mark Dorsey	Technician	Control cabinet, control systems including programming of PLC and microcomputer.
Tuoc Trinh	Supervisor	Project leader.

Each individual project had specific objectives which had to be catered for during the design of the pilot plant. These objectives were as follows:

- To design a pilot plant that would replicate unit operations found in a milk powder processing plant.
- To design unit operations that allowed easy access to fouled surfaces.
- To provide measurement of important process variables including temperature, flowrate and pressure.
- To allow control of process variables including flowrate, temperature and pressure.
- To allow direct conveyance of milk into the pilot plant.
- To incorporate a Clean-In-Place system into the pilot plant similar to that used in industry.
- To allow control of thermophilic bacterial populations on targeted areas of the plant.
- To allow ease of process fluid sampling throughout the plant.
- To provide refrigerated storage of a bulk supply of milk.
- To allow straightforward removal of certain sensors from main sensor conduit.

Based on the above objectives the first stages of a milk powder pilot plant were designed and constructed. The pilot plant included all unit operations up to and including an evaporator. In the future additional units including a three-effect evaporator and spray drier are to be incorporated into the pilot plant.

Figure 4.1 Pilot plant

4.3.2 Overview

The constructed pilot plant had two major circuits; milk and CIP. A process flow diagram of each circuit is given as Figure 4.2 and Figure 4.3. The two circuits are essentially the same except for the origin of the process fluid.

The Process and Instrumentation Diagram of the pilot plant is shown as Figure 4.4. All control loops are shown as dashed lines. The pilot plant consists of 10 major units:

1. milk vat
2. plate heat exchanger
3. direct steam injection (DSI 1)
4. fouling rig
5. flowmeters
6. double tube heat exchanger
7. direct steam injection (DSI 2)
8. holding tubes
9. research falling film evaporator
10. clean in place system

All of the units will be described individually in the following sections. A detailed description is made of the fouling rig and research falling film evaporator because these two unit operations were used extensively in this research project.

Figure 4.2 Pilot plant milk flow diagram

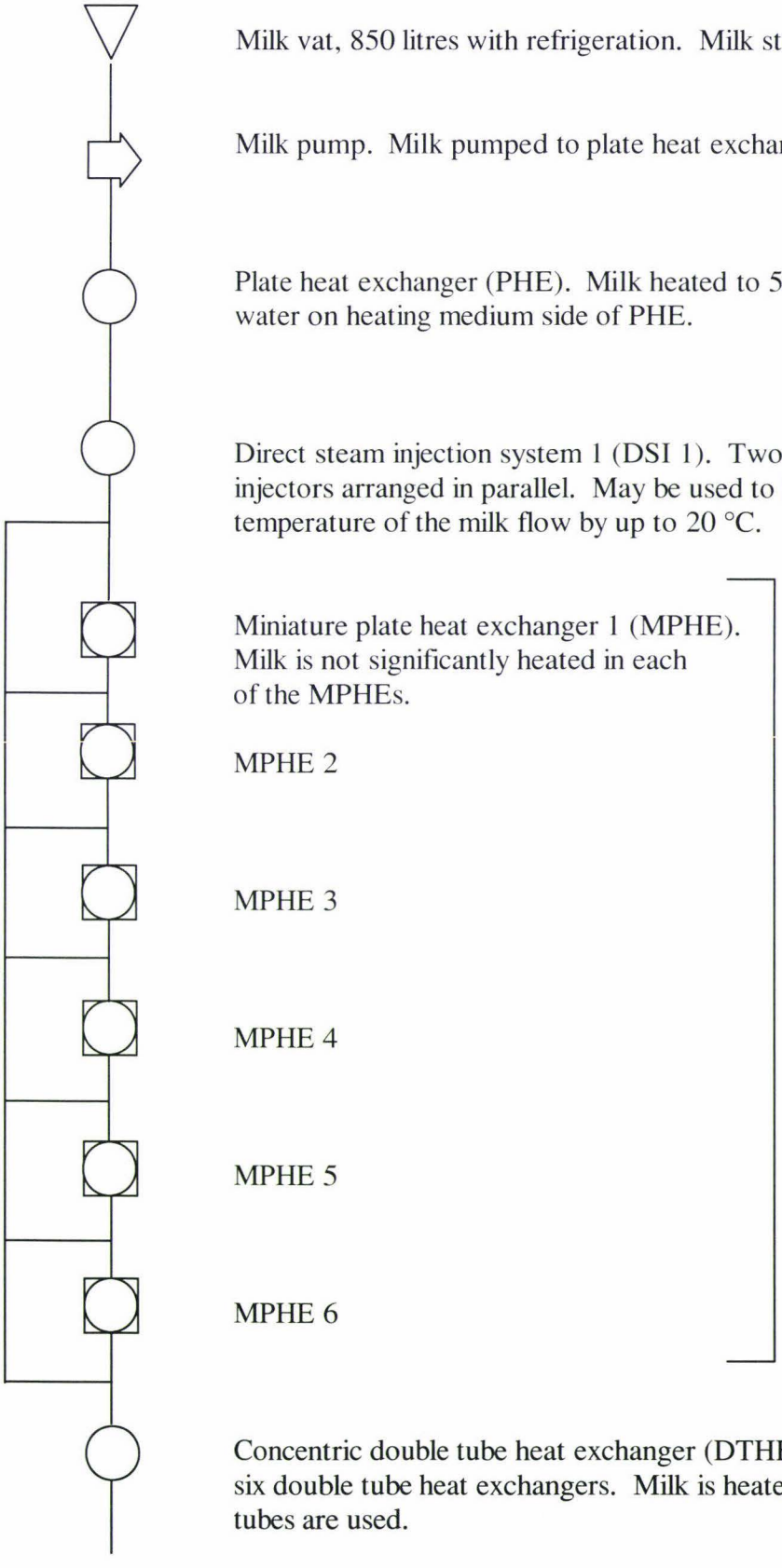

Figure 4.2 Pilot plant milk flow diagram (cont.)

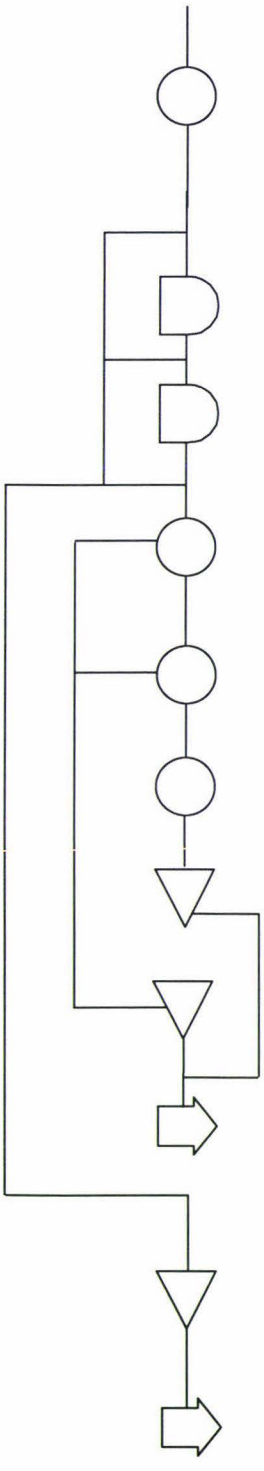

Direct steam injection system 2 (DSI2). Two direct steam injectors arranged in parallel. May be used to increase the temperature of the milk flow by up to 20°C.

Holding tube. Holding time: 50 seconds at 45 l/h

Holding tube. Holding time: 25 seconds at 45 l/h.

Research falling film evaporator (RFFE). Single evaporative plate.

Separator.

Condenser.

Condensate collection vessel.

Product collection vessel.

Monopump. Fluids discharged to drain.

CIP tank 1, 500 l.

CIP pump. Water diluted milk discharged to drain at the end of the run.

Figure 4.3 Pilot plant clean-in-place (CIP) fluids flow diagram

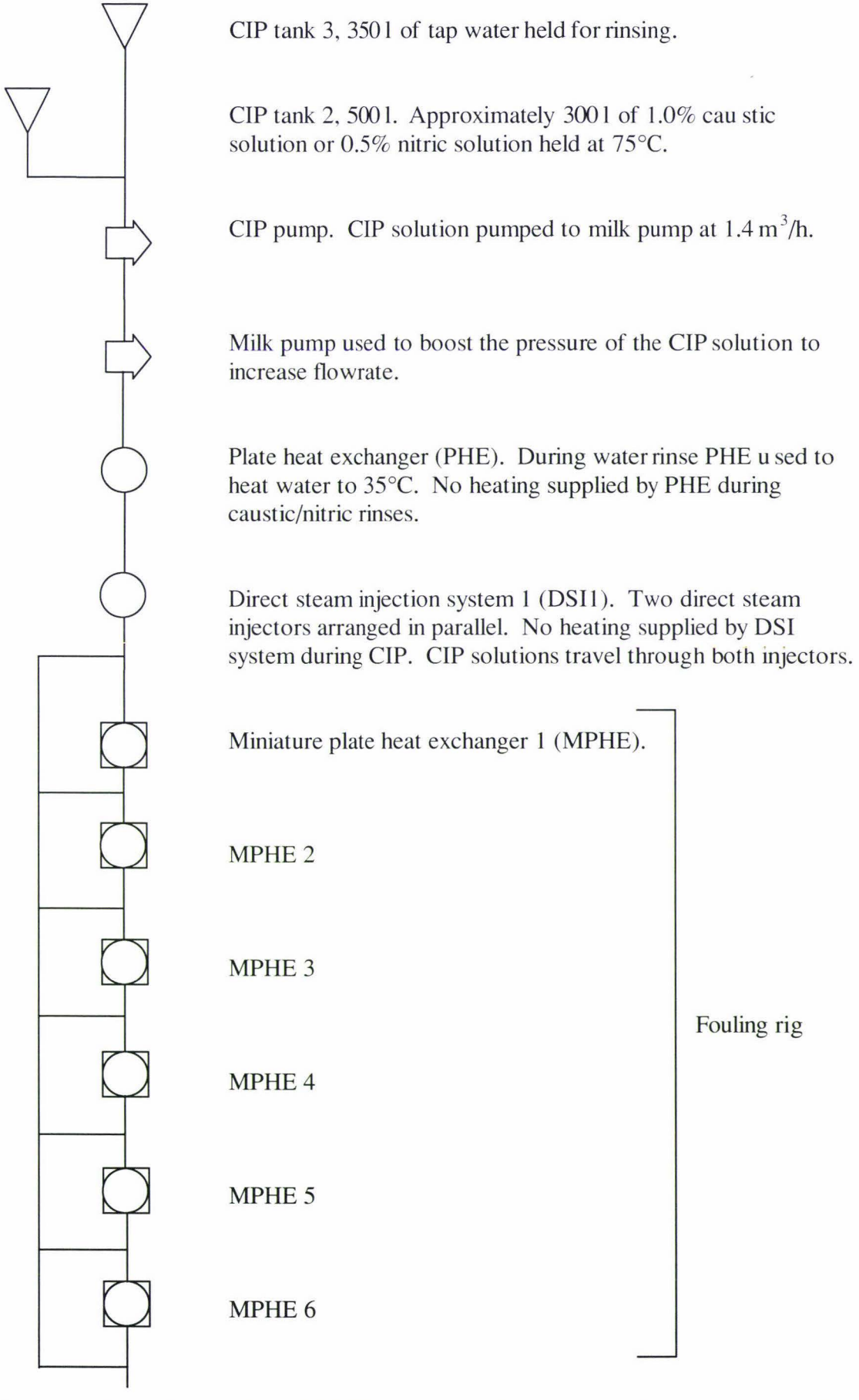

Figure 4.3 Pilot plant clean-in-place (CIP) fluids flow diagram (cont.)

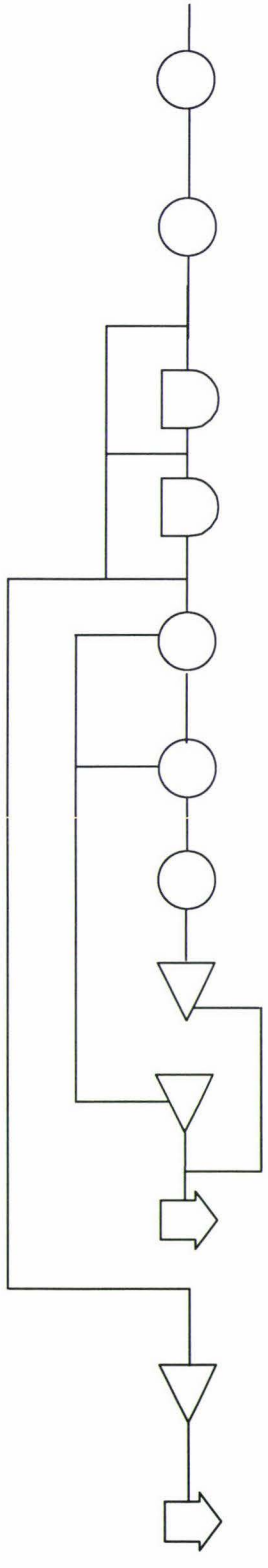

Concentric double tube heat exchanger (DTHE). Either two or six double tube heat exchangers.

Direct steam injection system 2 (DSI2). Two direct steam injectors arranged in parallel.

Holding tube.

Holding tube.

Research falling film evaporator (RFFE). Single evaporative plate.

Separator.

Condenser.

Condensate collection vessel.

Product collection vessel.

Monopump. CIP fluids discharged to drain.

CIP tank 1, 500 l.

CIP pump. CIP solution pumped to drain at the end of the run.

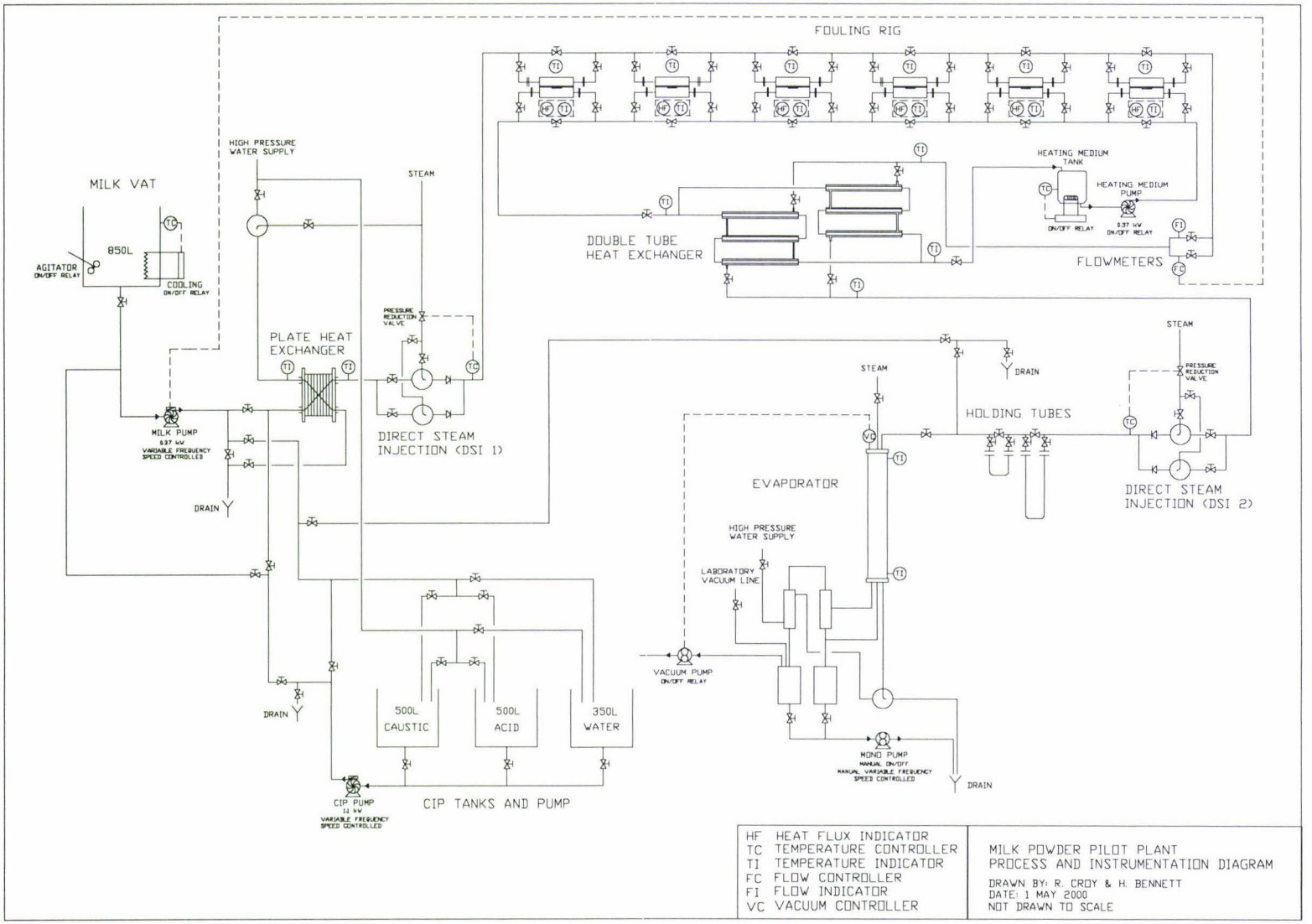

Figure 4.4 Process and Instrumentation Diagram for pilot plant

4.3.3 Milk Vat

A reservoir of milk was required that could sustain 16 hours of pilot plant operation at a flowrate of 45 l/h. To avoid spoilage, the milk required refrigeration, which necessitated agitation. Straightforward transport of the milk from outside the plant building to the milk reservoir was also required.

An 850 l stainless steel tank (Berry Ltd., Model No. 1R1309L, Palmerston North, N.Z.) was sourced from Massey University that met all of the above requirements. Figure 4.5 shows the interior of the tank used as the milk vat.

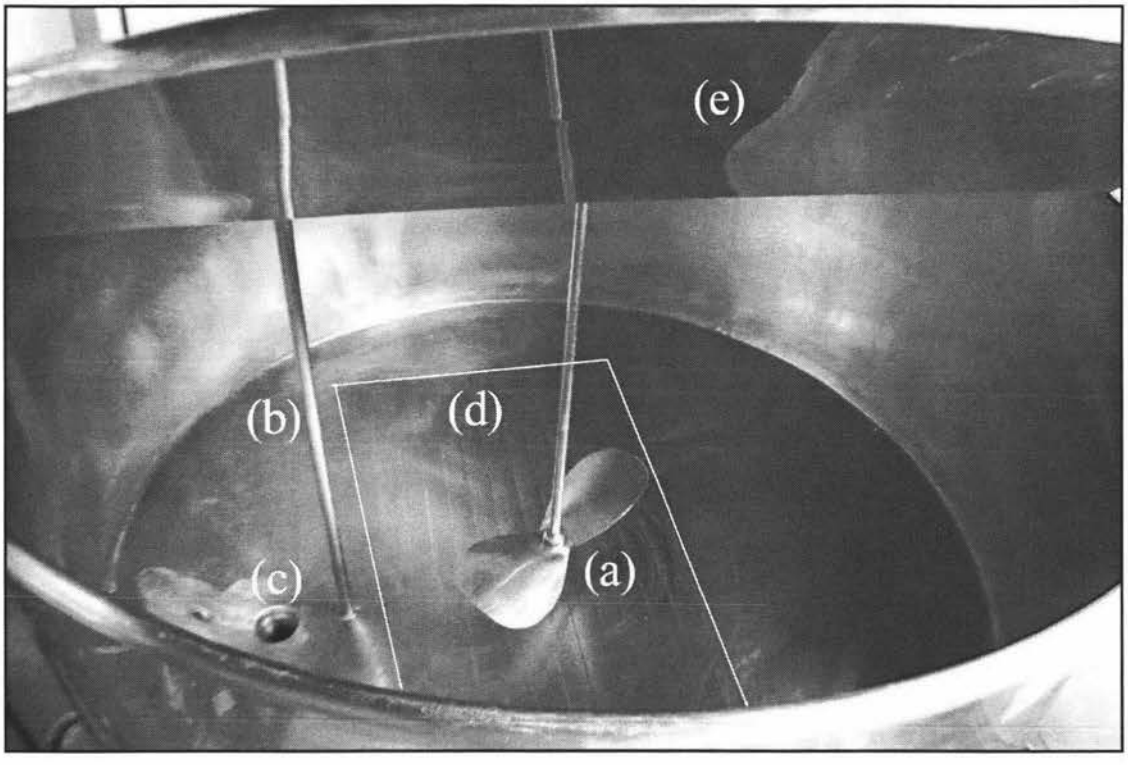

Figure 4.5 Interior of milk tank (a) agitator (b) well (c) fluid drain (d) outline of plate above refrigeration coil (e) tank cover

A refrigeration unit (Ellis, Hardie and Syminton Limited, Model No. ERJ 0200 TAD, 1.1 kW, Auckland, N.Z.) was mounted outside the pilot plant building as shown by Figure 4.6, (a). The unit was protected by a galvanised iron shroud manufactured by Judd Refrigeration Ltd., Palmerston North, N.Z. The refrigeration pipes entered the pilot plant room through a circular slot in the exterior wall and the refrigeration unit

was located outside the building to reduce the noise within the pilot plant and to save valuable floor area.

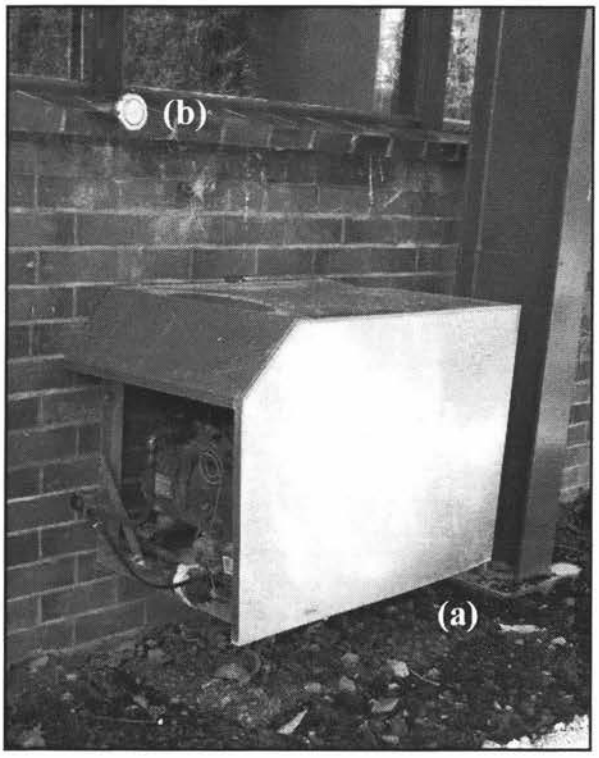

Figure 4.6 Exterior wall of pilot plant (a) refrigeration unit and (b) bulk milk inlet pipe

The bulk milk inlet pipe (64 mm diameter) was located above the refrigeration unit as shown in Figure 4.6, (b). The pipe was used to transfer the milk through the exterior wall to the milk vat. Flexible tubing (Rubicon, Model No. 9102, Australia) and a mono-pump (Mono Pump Ltd., Model No. CP25, Auckland, N.Z.) were used to transport the milk from the delivery truck to the bulk milk inlet pipe. A detailed discussion of milk reception and transfer is given in Section 4.7.1.

An agitator paddle was installed within the milk vat to ensure the milk would not freeze on the stainless steel surface directly above the refrigeration coil. An agitator paddle motor (Leroy Somer, IEC44-1, Longburn, N.Z.) was installed on top of the vat that was engaged by a simple on/off relay.

A Resistance Temperature Detector (RTD) installed within the well measured the temperature of the milk within the vat (see Figure 4.5). The well was filled with heat transfer oil (Mobiltherm 603, Product No. 988688, Wellington, N.Z.) to increase the

thermal conductivity between the RTD and the milk. The temperature was used as the controlled variable in the refrigeration control loop.

A centrifugal pump (Ebara, Model No. CDX70/05, 0.37kW, Keith R. Norling Ltd., Palmerston North, N.Z.) was used to pump milk and CIP fluids through the plant. The pump was controlled by a variable frequency speed drive (Allen-Bradley, Model No. 60-BA04NSF1, Rockwell Automation, Palmerston North, N.Z.). A centrifugal pump was chosen instead of a positive displacement pump because of the following reasons:

- Most common pump used in dairy industry
- Low cost – the centrifugal pump was relatively cheap compared with the positive displacement pumps investigated
- Safety – centrifugal pumps can operate safely for short periods of time during flow blockage upstream from pump. Positive displacement pumps do not possess this characteristic.

4.3.4 Plate Heat Exchanger

The milk was required to be heated to 70°C before entering the fouling rig. This was achieved using a plate heat exchanger (APV, Model No. U 265 R, Denmark) and a direct steam injection system. A photograph of the plate heat exchanger (PHE) used to heat the milk up to 55°C is shown as Figure 4.7. Hot water was used as the heating medium for the PHE. A simple brass DSI was used to produce the hot water for the PHE by mixing laboratory line steam and cold water from the Massey University high pressure water circuit. After the hot water passed through the PHE, the cooled water discharged to drain.

The simple brass DSI was also used to generate hot water for the CIP cycles. When hot water was required for CIP, the DSI pipe connected to the PHE would be disconnected and attached to a high temperature hose (Rubicon, Model No. 9102, Australia) by a stainless steel union (NZF Stainless Ltd., Palmerston North, N.Z.). The hose could then be placed in any of the three CIP tanks (refer to Section 4.3.12.).

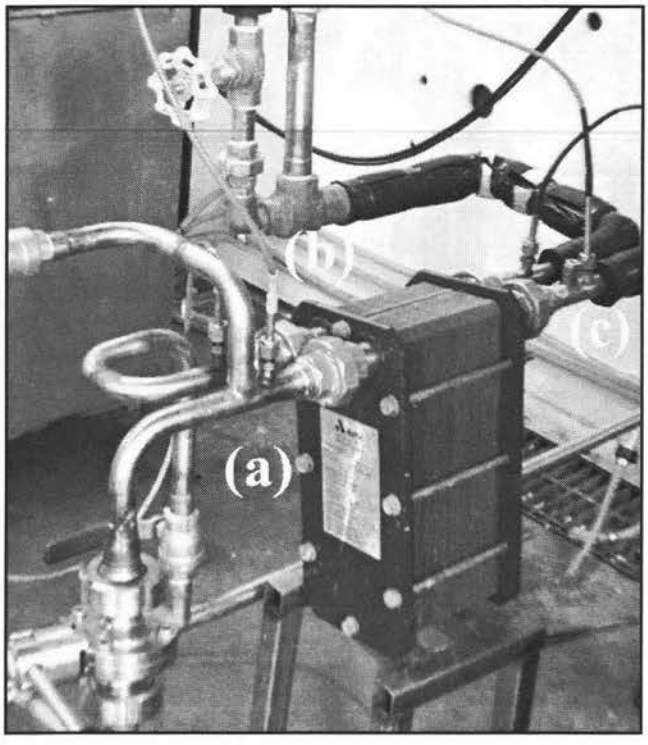

Figure 4.7 Plate heat exchanger and surrounding piping system (a) PHE (b) DSI that heated water used as heating medium for PHE (c) RTDs for heating medium inlet and process fluid outlet

Two RTDs were used to measure the inlet hot water temperature and the milk outlet temperature from the PHE. These variables were not part of a control loop but were indicative of important process variables. After experiments were completed for this research project, two RTDs were installed on the milk inlet and heating medium outlet streams.

4.3.5 Direct Steam Injection System 1

A direct steam injection system was designed and assembled to heat the milk from 55°C to 70°C. Figure 4.8 gives a schematic representation of the DSI system assembly. The DSI consists of the following items:

- 2 x steam injector
- 1 x pneumatic control valve (W. Arthur Fisher Limited, Model No. V201 BUE, Auckland, N.Z.)
- 2 x 3.2 mm ball valve BSP (NZF Stainless Ltd., Palmerston North, N.Z.)
- 4 x 12.7 mm two-piece body ball valve BSP (NZF Stainless Ltd., Palmerston North, N.Z.)

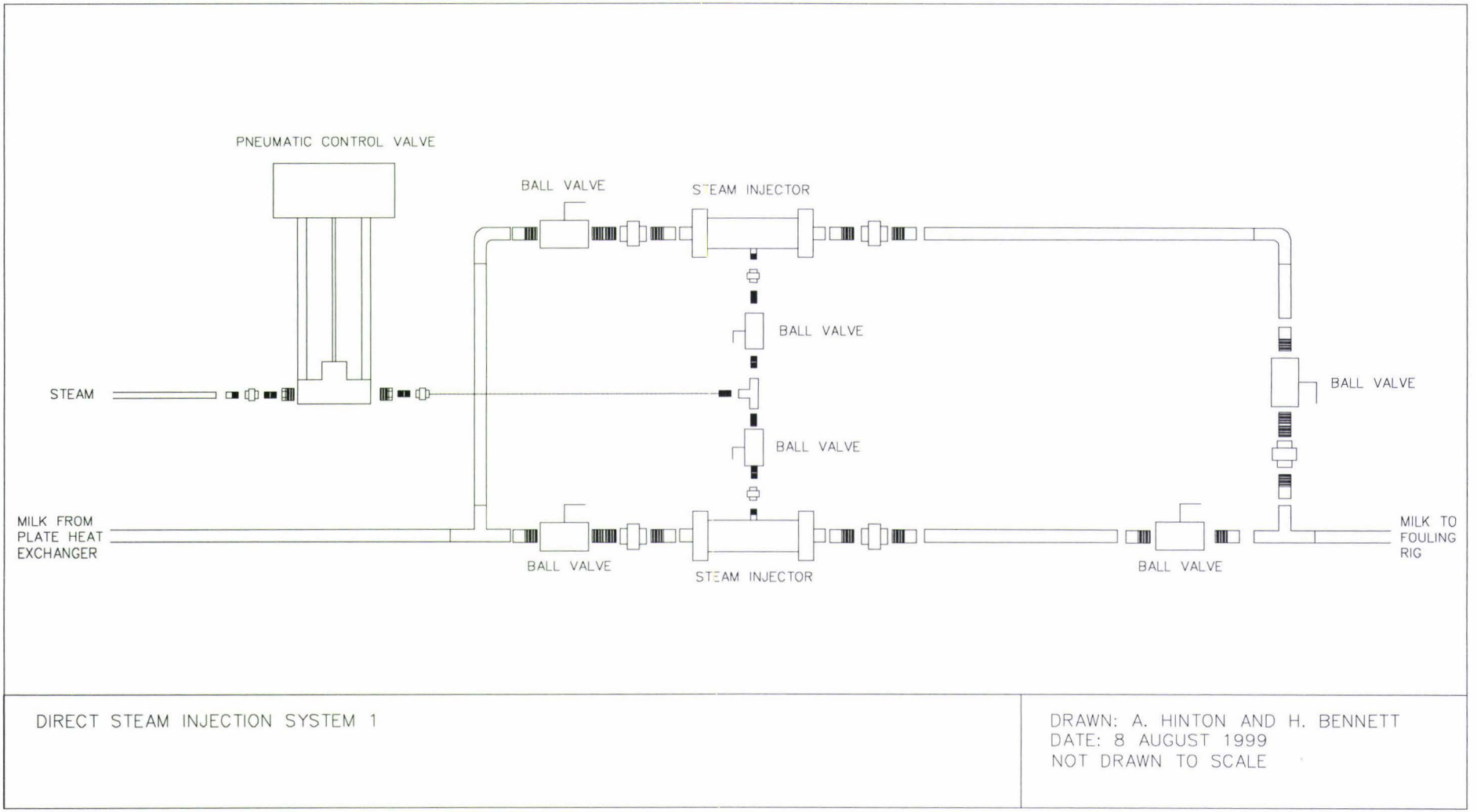

Figure 4.8 Schematic representation of direct steam injection system 1

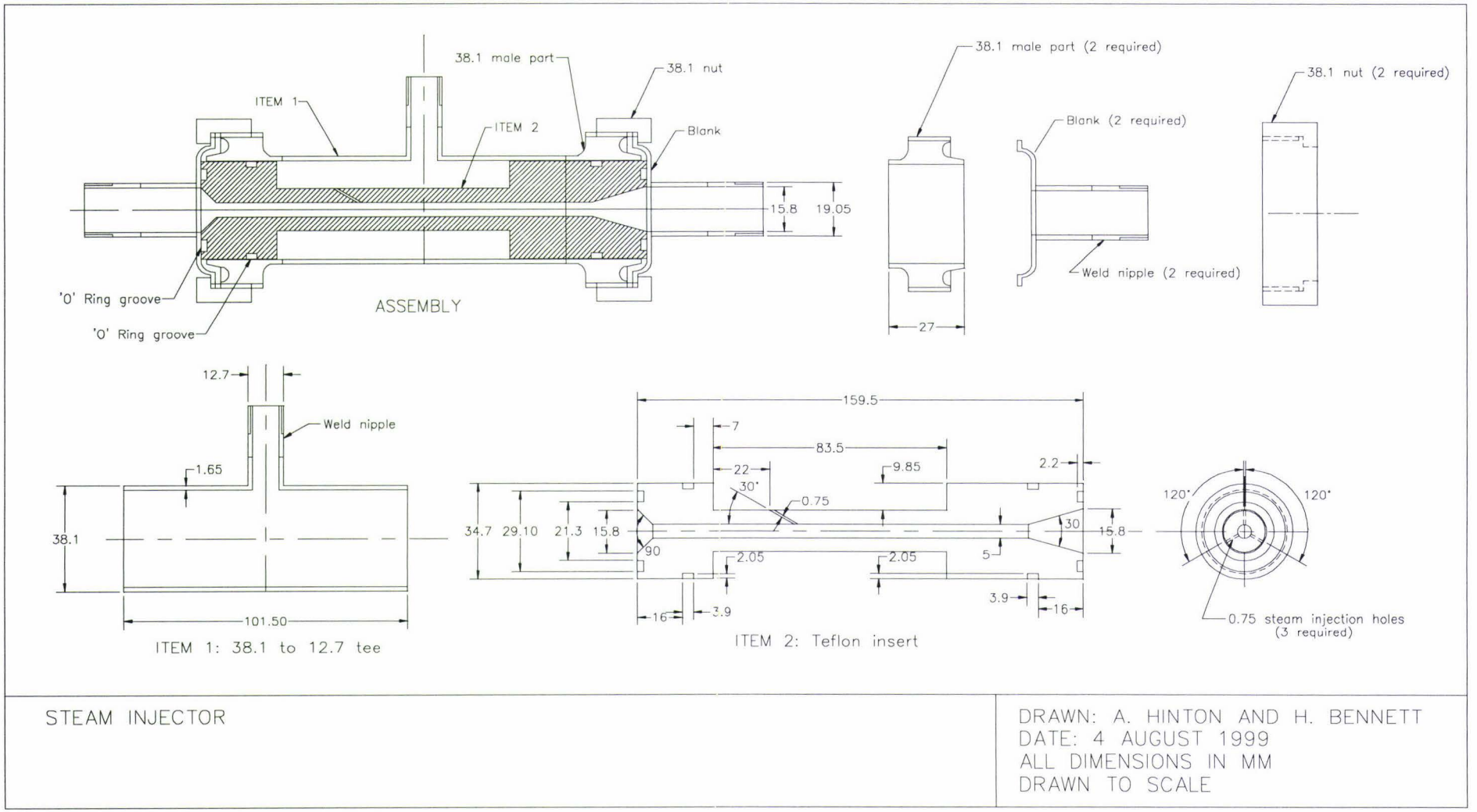

Figure 4.9 Detail and assembly drawing of steam injector

The DSI system consists of two steam injectors in parallel. Milk flows through one of the steam injectors at any one time. When one steam injector has fouled extensively, milk is re-routed through the second. A steam injector typically takes 8 hours to foul, therefore the plant can run up to 16 hours, before the DSI system is dismantled for cleaning.

Figure 4.9 gives a detail and assembly drawing of a steam injector. A steam injector contains the following components:

- 1 x 38.1 mm to 12.7 mm tee (NZF Stainless Ltd., Palmerston North, N.Z.)
- 2 x Kleanflow 38.1 mm male part (NZF Stainless Ltd., Palmerston North, N.Z.)
- 2 x Kleanflow 38.1 mm blank (NZF Stainless Ltd., Palmerston North, N.Z.)
- 2 x Kleanflow 38.1 mm slotted nut (NZF Stainless Ltd., Palmerston North, N.Z.)
- 1 x Teflon insert (Engineering Plastics Ltd., Palmerston North, N.Z.)
- 4 x "o" ring (Engineering Plastics Ltd., Palmerston North, N.Z.)

Two male parts were welded onto the 38.1 mm ends of the 38.1 mm to 12.7 mm tee to make the casing of the steam injector. The Teflon insert with appropriate o-rings was placed inside the casing. Two 38.1 mm blanks were then secured onto both ends of the casing by tightening the slotted nut onto the male parts.

Milk flows through a 5 mm chamber in the centre of the Teflon insert. Steam enters the steam injector via the 12.7 mm tee section where it collects between the Teflon insert and steam injector casing. When the pressure of steam reaches the correct level, steam passes through the three 0.75 mm holes drilled in the Teflon insert, into the milk chamber.

A pneumatic control valve controlled the flow of steam into the injectors. Two 3.2 mm BSP ball valves were installed between the control valve and the two steam injectors so that steam could be directed into one, the other or both steam injectors.

The DSI system was found to destabilise the milk flowrate during fouling experiments. Therefore, the entire preheating duty (4 – 70°C) was provided by the PHE during most of the fouling trials. During micro-organism trials (conducted by

other members of the design team), where the control of milk flowrate was not crucial, the DSI system was used without problems.

4.3.6 Fouling Rig

The next unit operation of the pilot plant after the first DSI was a fouling rig consisting of six Miniature Plate Heat Exchangers (MPHE) in series. The design of the fouling rig was based on the following objectives:

- To provide a series of heated surfaces similar to the surfaces found in plate heat exchangers.
- To allow isolation of the surface at any point during a run without interference to the other surfaces.
- To provide removal surfaces that can be physically inspected.
- To allow the study of fouling on different heated surfaces.
- To allow sampling of milk throughout the apparatus.
- To provide a surface that allows the installation and study of a heat flux sensor under controlled conditions.
- To allow the study of fouling on surfaces of different orientations.

Based on the above objectives a fouling rig consisting of six MPHEs was designed and constructed. A photograph of a MPHE is shown as Figure 4.10.

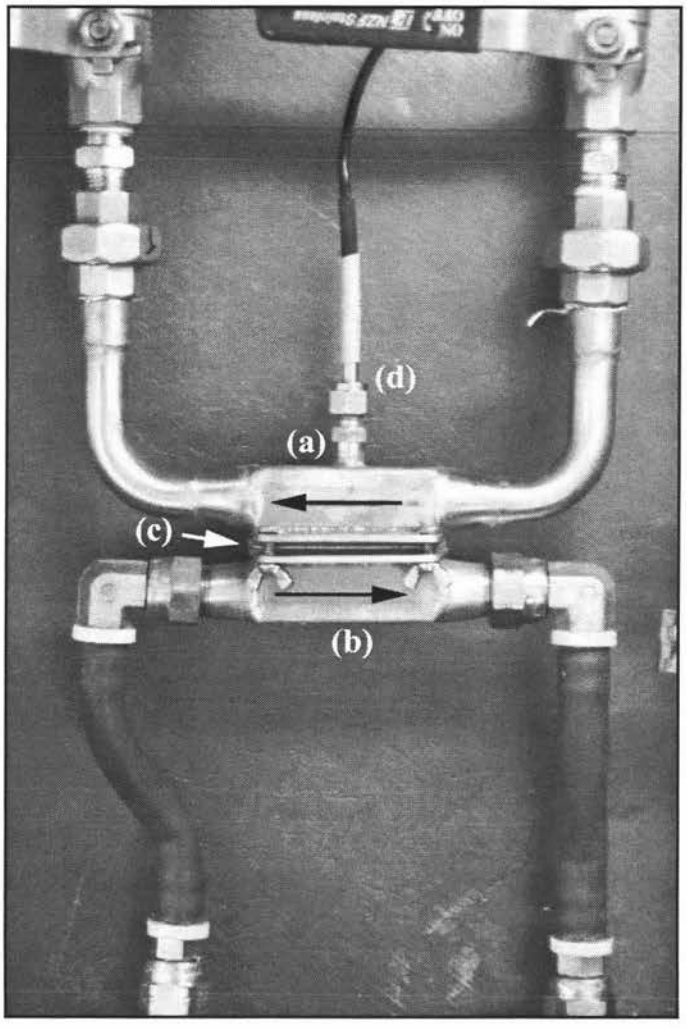

Figure 4.10 Photograph of miniature plate heat exchanger (a) process fluid chamber (b) heating medium chamber (c) test plate (d) temperature sensor well (RTD shown here). Black arrows indicate direction of flow.

The major components of the MPHE are:

- process fluid chamber (refer to Figure 4.12 for details)
- heating medium chamber (refer to Figure 4.13 for details)
- test plate

A chamber was a square section of pipe with one side removed to which a flange was attached. The section removed left a window with dimensions of 53 x 22mm. The two chambers were manufactured by Mike Christie Sheetmetals Ltd. (Palmerston North, N.Z.) and were made of stainless steel (T304, NZF Stainless Ltd., Palmerston North, N.Z.). The test plates used for the majority of fouling experiments were 0.6 mm thick stainless steel plates (T304, NZF Stainless Ltd., Palmerston North, N.Z.)

with dimensions of 73 x 46mm. The three parts of the MPHE were closed and sealed by a flange system using 4 bolts (M5, NZF Stainless Ltd., Palmerston North, N.Z.), 4 wing nuts (M5, NZF Stainless Ltd., Palmerston North, N.Z.) and two silicone gaskets (Engineering Plastics Ltd., SRS2.36FDA, 2.36mm, Palmerston North, N.Z.). The bolts were welded to the four corners of the milk chamber flange that lined up with corresponding holes drilled in the heating medium chamber flange. Therefore the two "windows" of the chambers line up consistently each time the MPHE was assembled. The silicone gaskets were rectangles of dimensions 73 x 46 mm with a rectangular window cut out of the centre of dimensions 53 x 22 mm. These dimensions correspond to the size of the test plates and chamber windows.

The assembly procedure of the MPHE was as follows:

1. Place a gasket on each side of the test plate ensuring all sides are flush.
2. Place the test plate and gaskets between the four bolts of the process fluid chamber ensuring all sides are flush.
3. Position the heating medium chamber over the test plate and gaskets ensuring that the bolts are inserted into appropriate holes on heating medium chamber flange.
4. Fasten wing nuts on bolts using pliers.

A heat flux sensor (RdF Corporation, Model No. 27036-3, New Hampshire, U.S.A.) was attached to the test plate within the chamber window area. The installation and description of the heat flux sensor is discussed in detail in Section 4.4.1.

A temperature sensor was also installed within the process fluid chamber. Initially, a RTD was installed in the MPHE using a tube socket weld union (Swagelok, Model No. SS-400-6-4W, Auckland, N.Z.) as shown in Figure 4.10. RTD manufacture will discussed in detail in Section 4.4.2.

A 3-dimensional representation of the MPHE including gaskets and test plate is shown as Figure 4.11.

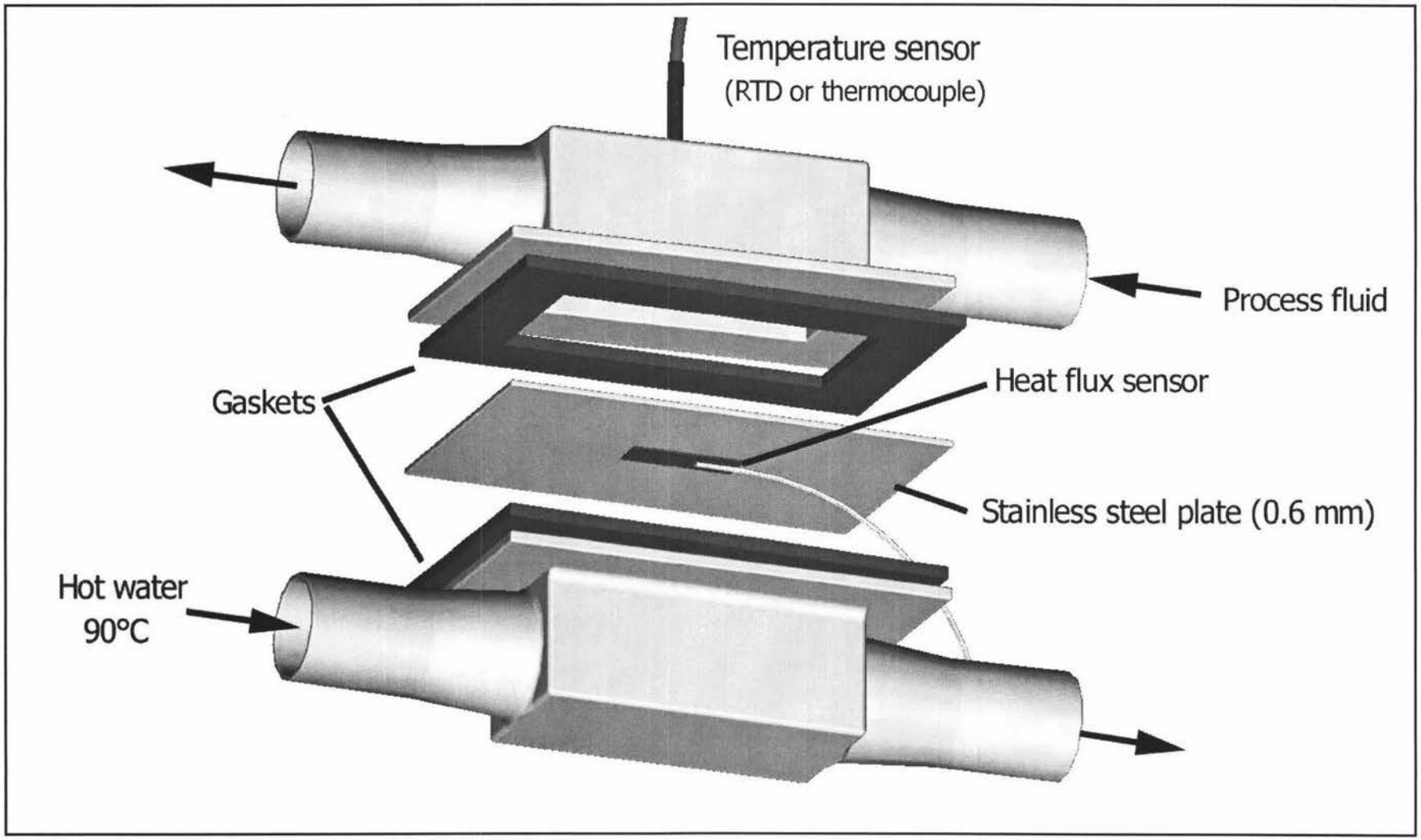

Figure 4.11 Schematic representation of miniature plate heat exchanger assembly (Drawn by R. Croy)

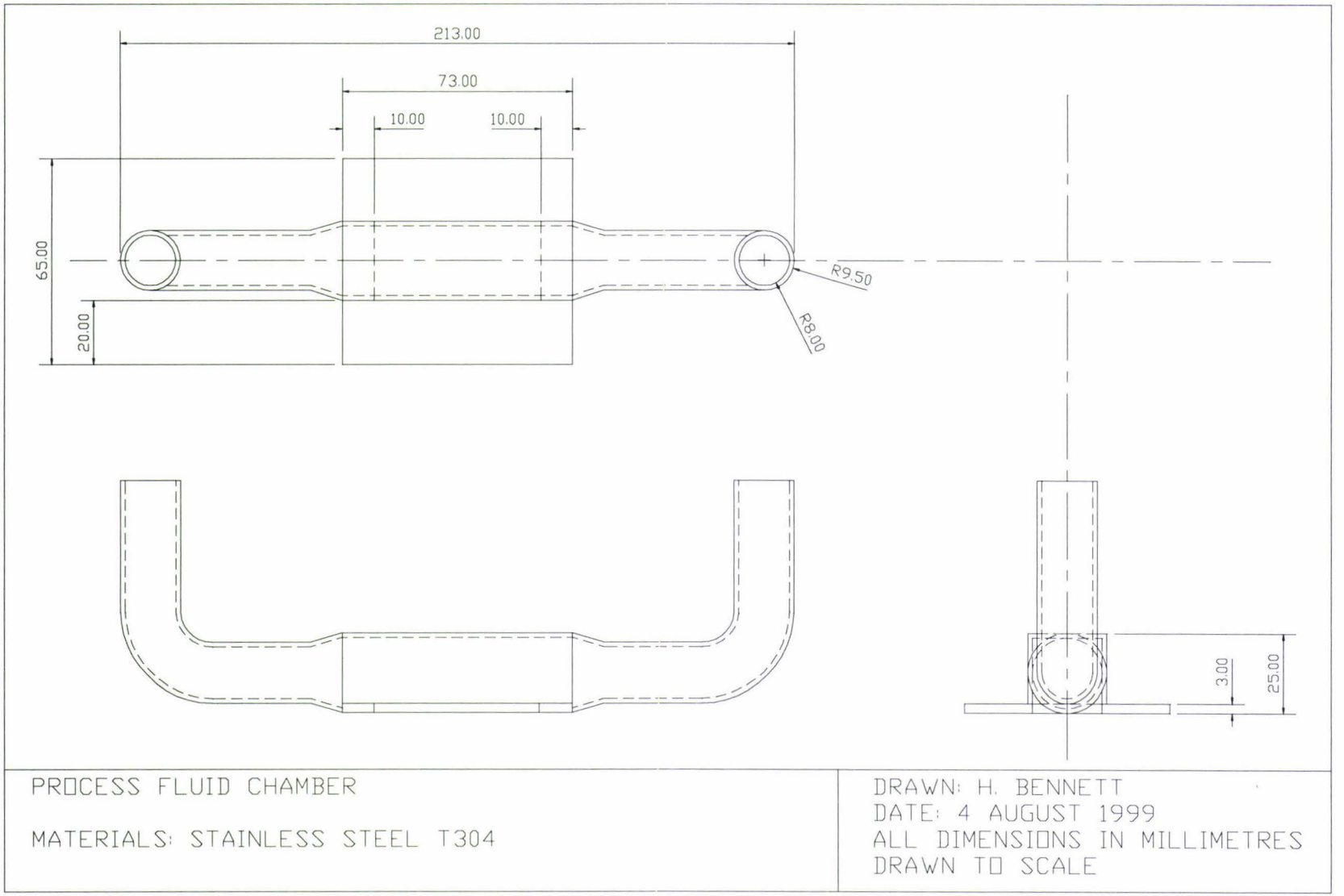

Figure 4.12 Orthogonal projection of process fluid chamber of miniature plate heat exchanger

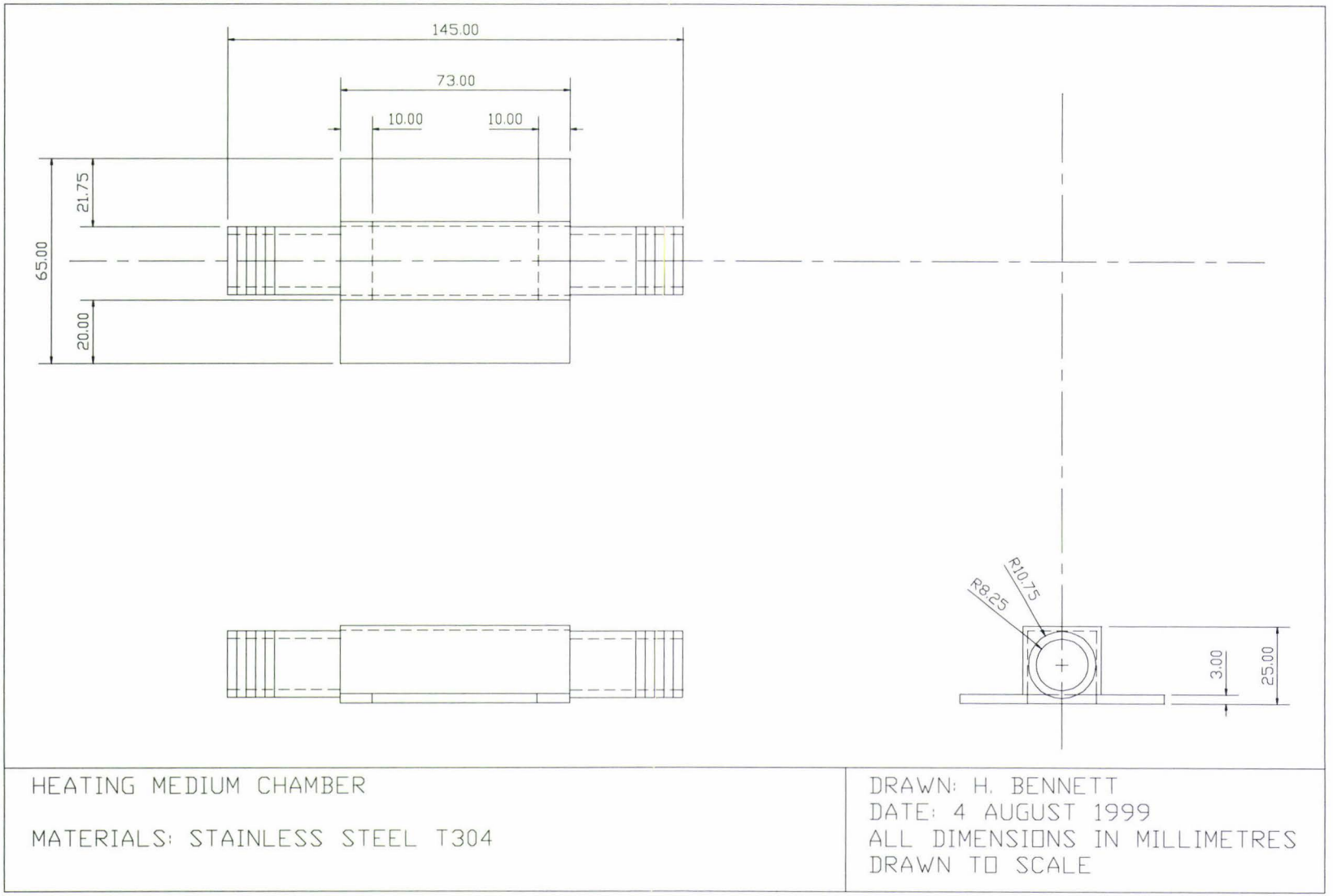

Figure 4.13 Orthogonal projection of heating medium chamber of miniature plate heat exchanger

Figure 4.14 shows the final configuration of the fouling rig with heating medium below the test plate and process fluid above. All piping, unions, valves, hexagon nipples and welding nipples of the process side were made of stainless steel (T304, NZF Stainless Ltd., Palmerston North, N.Z.). The valves used were two-piece body ball BSP supplied by NZF Stainless Ltd., Palmerston North, N.Z.

The heating medium chamber side was constructed from a variety of materials:

- One-piece topic ball valves (Harold Pierard Ltd., Palmerston North, N.Z.)
- Hi Temperature Push-Lok flexible hose (The General Machinery Co. Ltd., Palmerston North, N.Z.)
- 19 mm T304 stainless steel welding nipples (NZF Stainless Ltd., Palmerston North, N.Z.)
- T304 stainless steel pipe (NZF Stainless Ltd., Palmerston North, N.Z.)

Each MPHE had a system of 6 valves (3 stainless steel, 3 topic) that enabled the MPHE to be isolated from the two fluid streams at any point during a trial allowing the run to continue uninterrupted. After isolation, the MPHE could be unpacked allowing the test plate to be inspected and physical measurements such as fouling deposit thickness to be made.

The configuration of the fouling rig could be changed to study the effects of orientation on fouling. Figure 4.15 shows the fouling rig configuration used to study the effect of orientation on fouling deposits. The first three MPHE circuits were disassembled from the main array and moved to the appropriate position. Additional piping was installed between the three circuits.

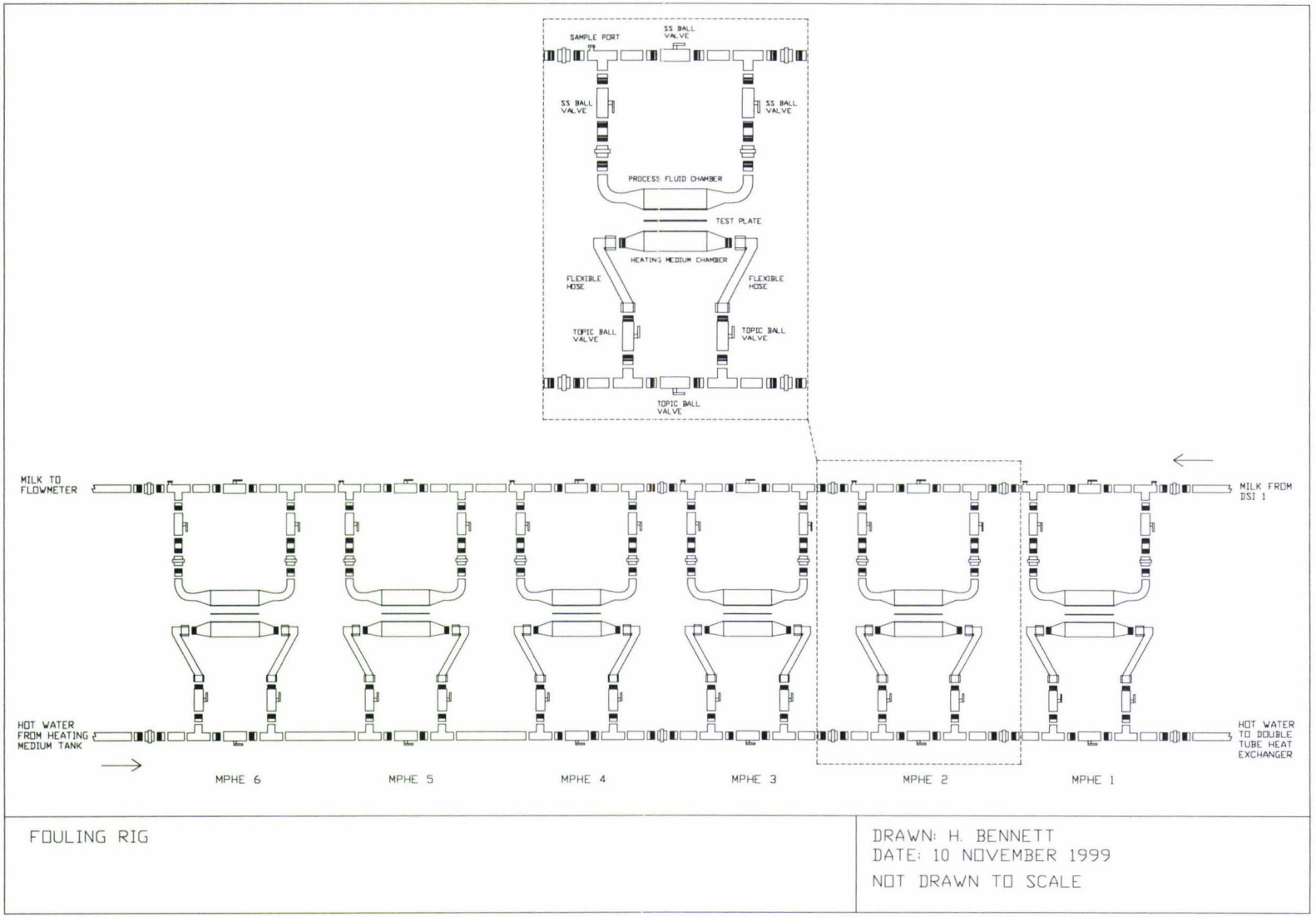

Figure 4.14 Schematic representation of fouling rig

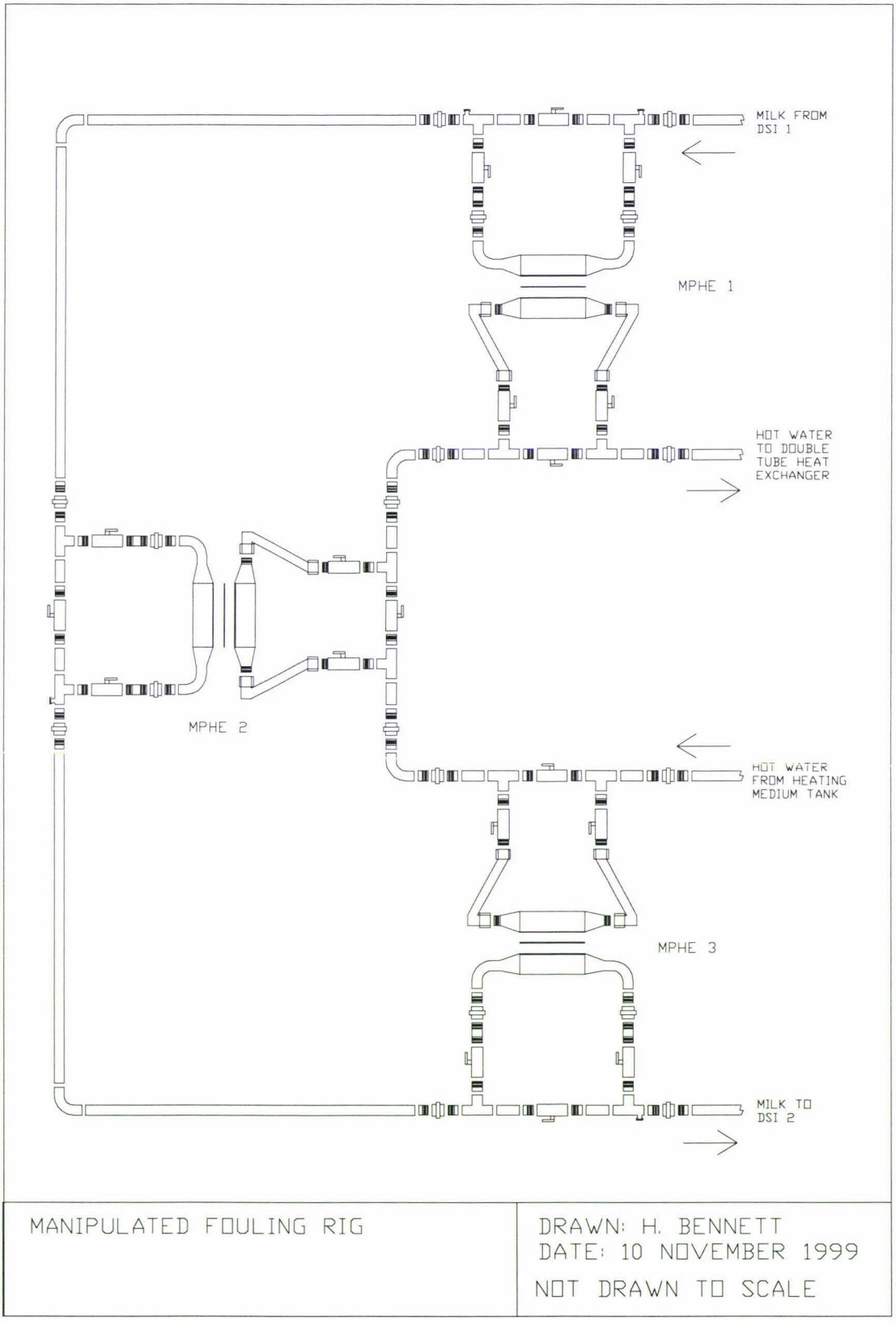

Figure 4.15 Schematic representation of fouling rig configuration used to study fouling deposits on different plate orientations

The heating medium used in the current research was hot water generated by an electric element (Eutro, 3kW, Stewards Ltd., Palmerston North, N.Z.) installed in a 130 litre stainless steel tank. The water was recycled through a circuit that provided heating to both the fouling rig and double tube heat exchanger as shown in Figure 4.16. The double tube heat exchanger will be discussed in Section 4.3.8. The hot water was circulated by a centrifugal pump (Ebara, Model No. CDX70/05, 0.37kW, Keith R. Norling Ltd., Palmerston North, N.Z). The pump was controlled by a simple on-off relay set at 50Hz.

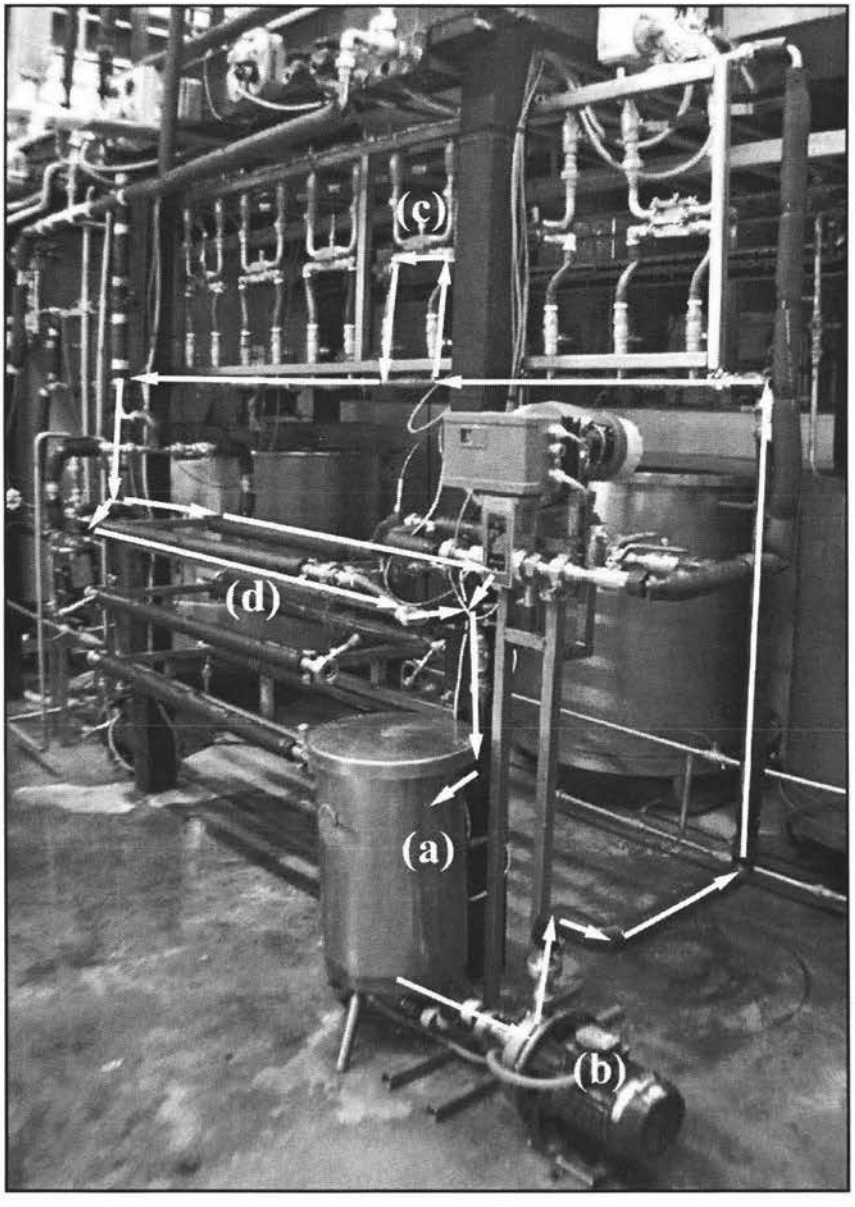

Figure 4.16 Heating medium circuit for fouling rig and double tube heat exchanger. (a) heating medium tank (b) heating medium centrifugal pump (c) miniature plate heat exchanger (d) double tube heat exchanger

4.3.7 Flowmeters

After exiting the fouling rig, the milk passed through an electromagnetic flowmeter (Endress-Hauser Picomag, Model No. 11 PM 165333, EMC Industrial Instrumentation, Auckland, N.Z.). The flowmeter provided the controlled variable in the PID control loop that manipulated the speed of the milk pump. The flowmeter was required to measure flowrates between 30 – 60 l/h.

A second electromagnetic flowmeter (Endress-Hauser Promag, Model No. 30FT25-AA1AA11A21B, EMC Industrial Instrumentation, Auckland, N.Z.) was installed in parallel with the milk flowmeter to measure the flow of CIP fluids. Two flowmeters were required because the milk flowmeter was not capable of measuring relatively high CIP flowrates of 1400 l/h. A two-piece body ball valve was placed in front of each flowmeter that allowed the process fluid to be diverted to the appropriate flowmeter depending on what type of fluid was passing through the plant at that time.

4.3.8 Double Tube Heat Exchanger

The milk enters the double tube heat exchanger (DTHE) after passing through the flowmeter. This heat exchanger consists of an inner (12.7 mm OD, NZF Stainless Ltd., Palmerston North, N.Z.) and outer tube (25.4 mm OD, NZF Stainless Ltd., Palmerston North, N.Z.) Hot water flows through the inner tube and milk in the annular channel between the inner and outer tube. Fouling develops on the outer surface of the inner tube which can be removed from the heat exchanger for visual inspections and fouling sample collection at the end of a run.

The entire heat exchanger was 6 meters long, made up of 6 one-metre lengths. The configuration of the heat exchanger can be regarded as 2 stacks of three-metre long heat exchangers in parallel. However during fouling runs completed for this research project, only 2 one-metre long heat exchangers in parallel were used.

4.3.9 Direct Steam Injection System 2

The second direct steam injection system was required to heat the milk from 70 to 95°C. The design of the second DSI was the same as the first, except that dairy standard unions and valves were used as shown in Figure 4.17.

The second DSI system consists of the following items:

- 2 x steam injector
- 1 x pneumatic control valve (W. Arthur Fisher Limited, Model No. V201 BUE, Auckland, N.Z.)
- 2 x 3.2 mm ball valve BSP (NZF Stainless Ltd., Palmerston North, N.Z.)
- 4 x 25.4 mm Kleanflow heavy duty butterfly valve (NZF Stainless Ltd., Palmerston North, N.Z.)

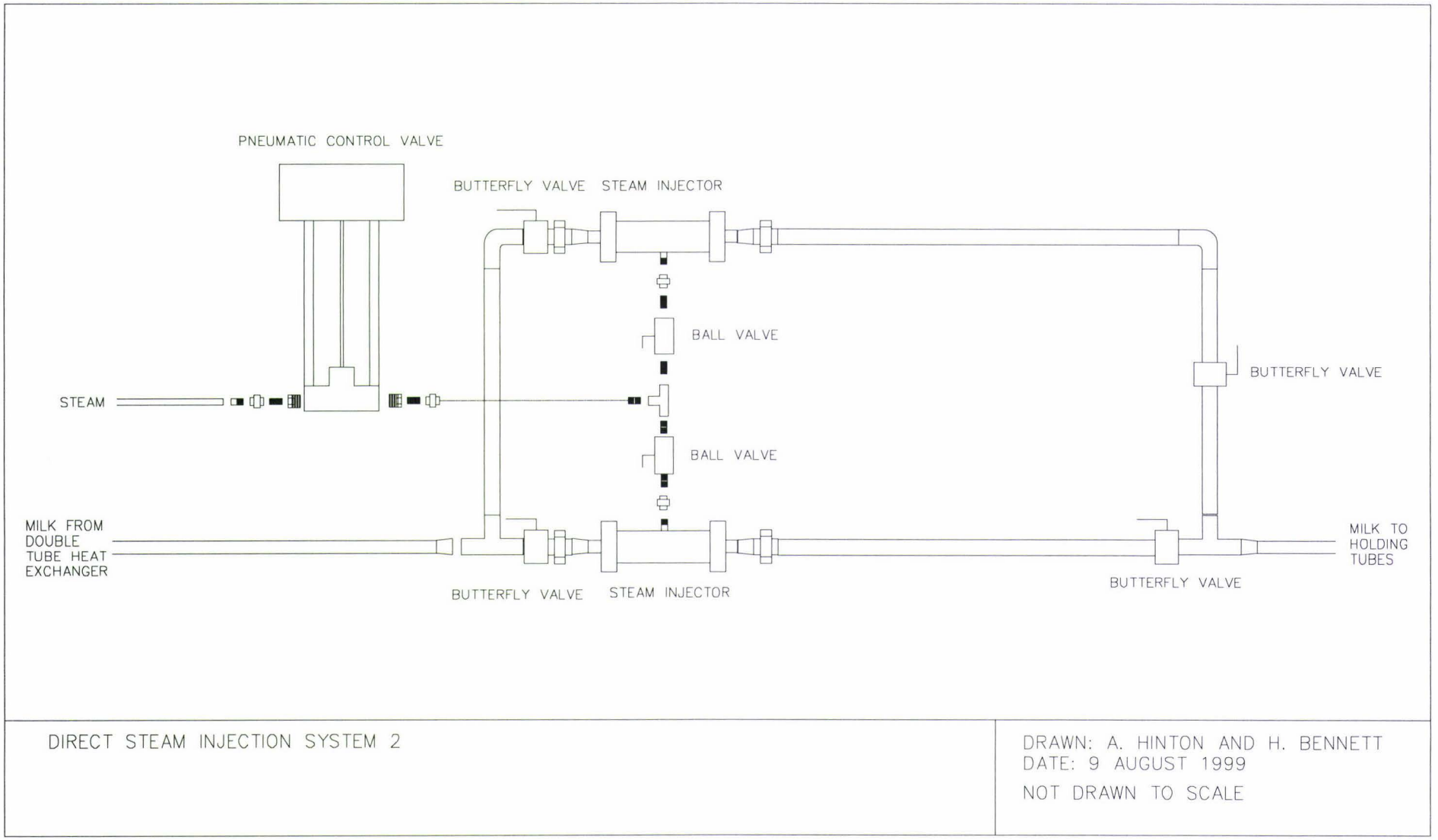

Figure 4.17 Schematic representation of direct steam injection system 2

4.3.10 Holding Tubes

Two sets of tubes known as holding tubes were installed directly after the second DSI system. These holding tubes were designed to precondition the whey proteins of the milk before entering the evaporator in a similar manner to the preheating unit operation typically found in the dairy industry. Figure 4.18 shows the two sets of holding tubes.

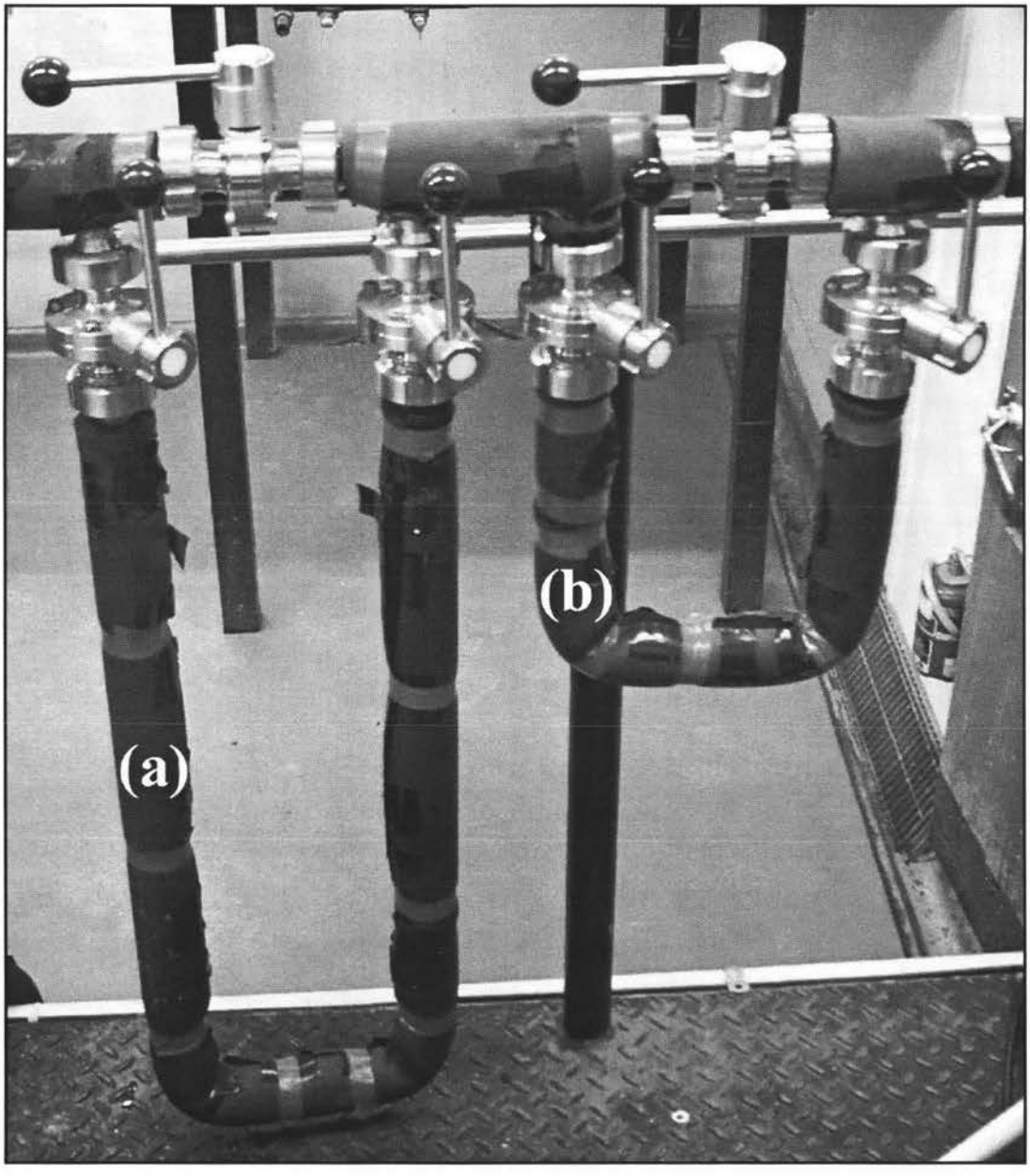

Figure 4.18 Holding tubes (a) holding tube 1, 50s at 45 l/h (b) holding tube 2, 25s at 45 l/h

The holding tubes were constructed from 25.4 mm stainless steel tube (NZF Stainless Ltd., Palmerston North, N.Z.). Six dairy standard valves (Kleanflow heavy duty butterfly, NZF Stainless Ltd., Palmerston North, N.Z.) controlled the flow of milk to the tubes.

The holding tubes were designed so that the milk could be held at one temperature for different periods of time. Assuming a constant flowrate, three holding times could be achieved, for example, at a flowrate of 45 l/h holding times of 25, 50 and 75s could be achieved. The holding tubes were by-passed during the fouling experiments conducted in this research project.

4.3.11 Research Falling Film Evaporator

The last unit operation in the pilot plant was a research falling film evaporator (RFFE). The design of the RFFE was based on the following objectives:

- To provide an evaporative fouling surface similar to that of a falling film evaporator.
- To allow observations of the surface during the evaporation process.
- To allow the installation and study of a heat flux probe under controlled evaporative conditions.
- To allow the surface to be removed at any point during a run.

Based on the above objectives a RFFE was designed and constructed that is shown schematically as Figure 4.19. The RFFE can be broken into four major sections:

1. evaporator surface and casing
2. separator
3. condenser
4. collection vessels and pumps

Each will be described in the following sections.

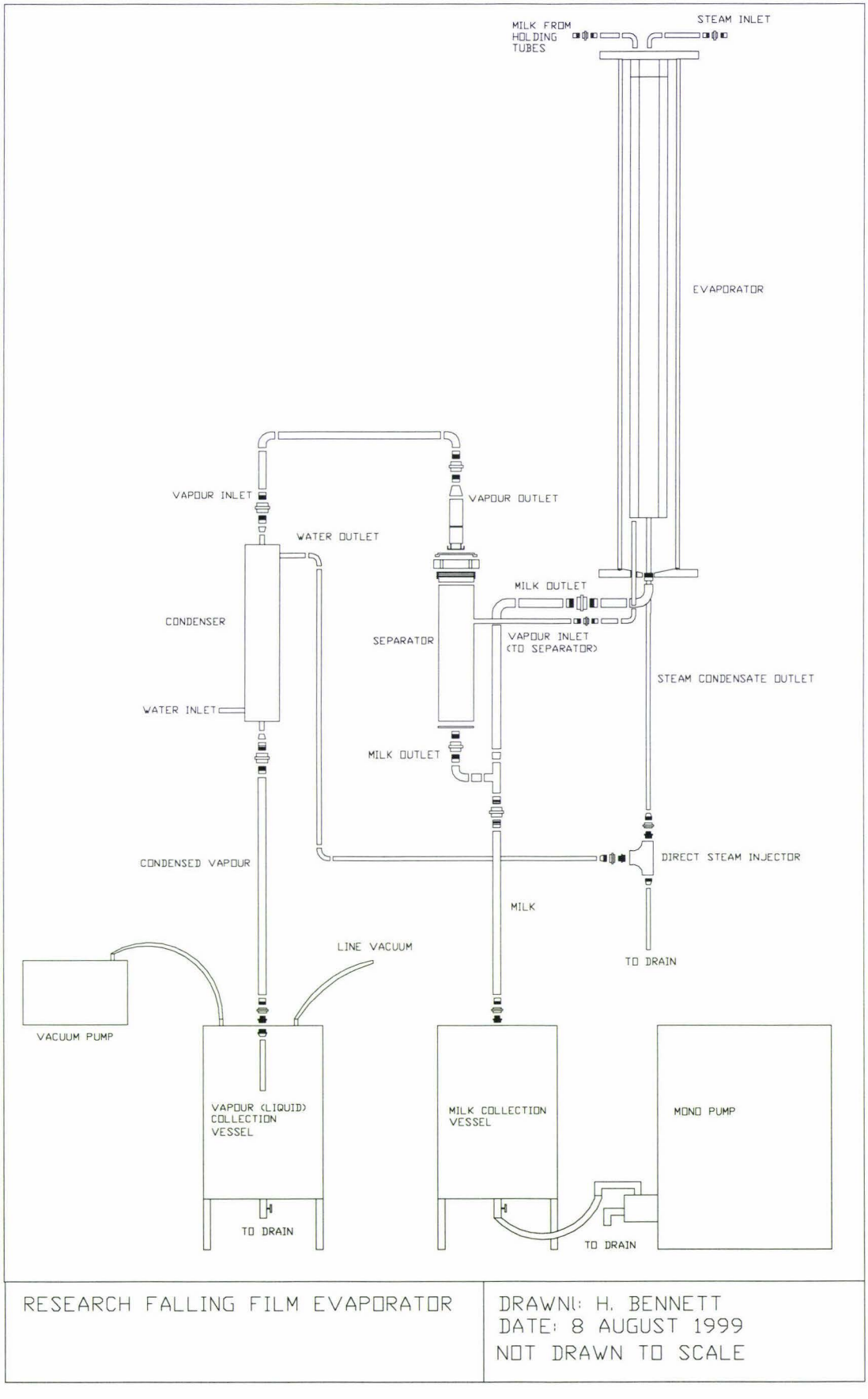

Figure 4.19 Schematic representation of research falling film evaporator

4.3.11.1 Evaporator surface and casing

A schematic representation of the evaporator surface assembly is shown as Figure 4.19. The evaporator surface consists of a flat stainless steel plate (T306, NZF Stainless Ltd., Palmerston North, N.Z.) with a weir box and steam chamber attached to one side. Both the weir box and steam chamber had a flange which was used to secure each component to the evaporator plate. Milk enters near the bottom of the weir box (Figure 4.21, (a)) where the liquid level rises until the milk on reaching the top of the evaporator plate flows over forming a thin film. Guide bars on both the weir box and evaporator plate ensured that milk flow was restricted to the evaporator plate. The guide bars and weir box were made of stainless steel (T316, NZF Stainless Ltd., Palmerston North, N.Z.).

The evaporator plate, steam chamber, weir box, and guide plates were held together by a series of M4 bolts (NZF Stainless Ltd., Palmerston North, N.Z.) installed down the length of the guide bars. The bolts lined up with holes drilled through the flanges of the weir box and steam chamber and holes drilled in the evaporator plate. Wing nuts (M4, NZF Stainless Ltd., Palmerston North, N.Z.) wound onto the bolts secured all the components together.

Steam housed in the steam chamber provides the heating medium for the evaporator surface. The steam enters the chamber approximately 400 mm from the top of the steam chamber. This location corresponded to approximately a third of the length of the steam chamber as shown by Figure 4.21, (b). Steam entered at this point so that an even distribution of steam was obtained within the steam chamber. Since the steam chamber does not cover the entire evaporator plate area, the milk starts to evaporate 120 mm from the top of the evaporator plate. Steam condensate was removed at the bottom of the steam chamber as shown by Figure 4.21, (b).

Heat flux sensors were installed on the steam chamber side of the evaporator surface. The sensor wires passed through a port (Swagelok, Model No. SS-8MO-1-4RT, Auckland, N.Z.) installed in the back of the steam chamber as shown by Figure 4.21, (b). The sensor installation method was similar to the method used for the test plates of the MPHE. Sensor installation is presented in Section 4.4.1.

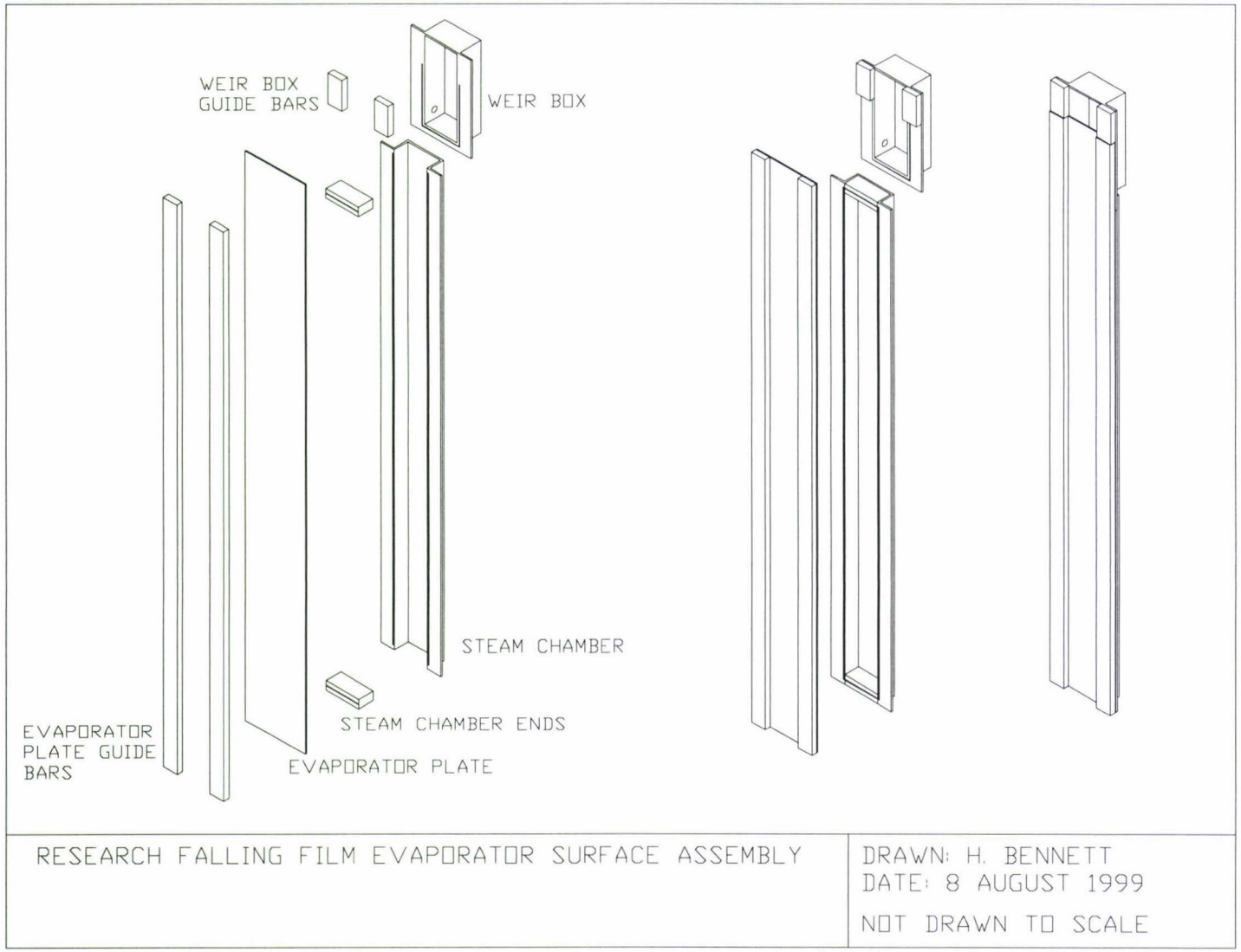

Figure 4.20 Schematic representation of evaporator surface assembly

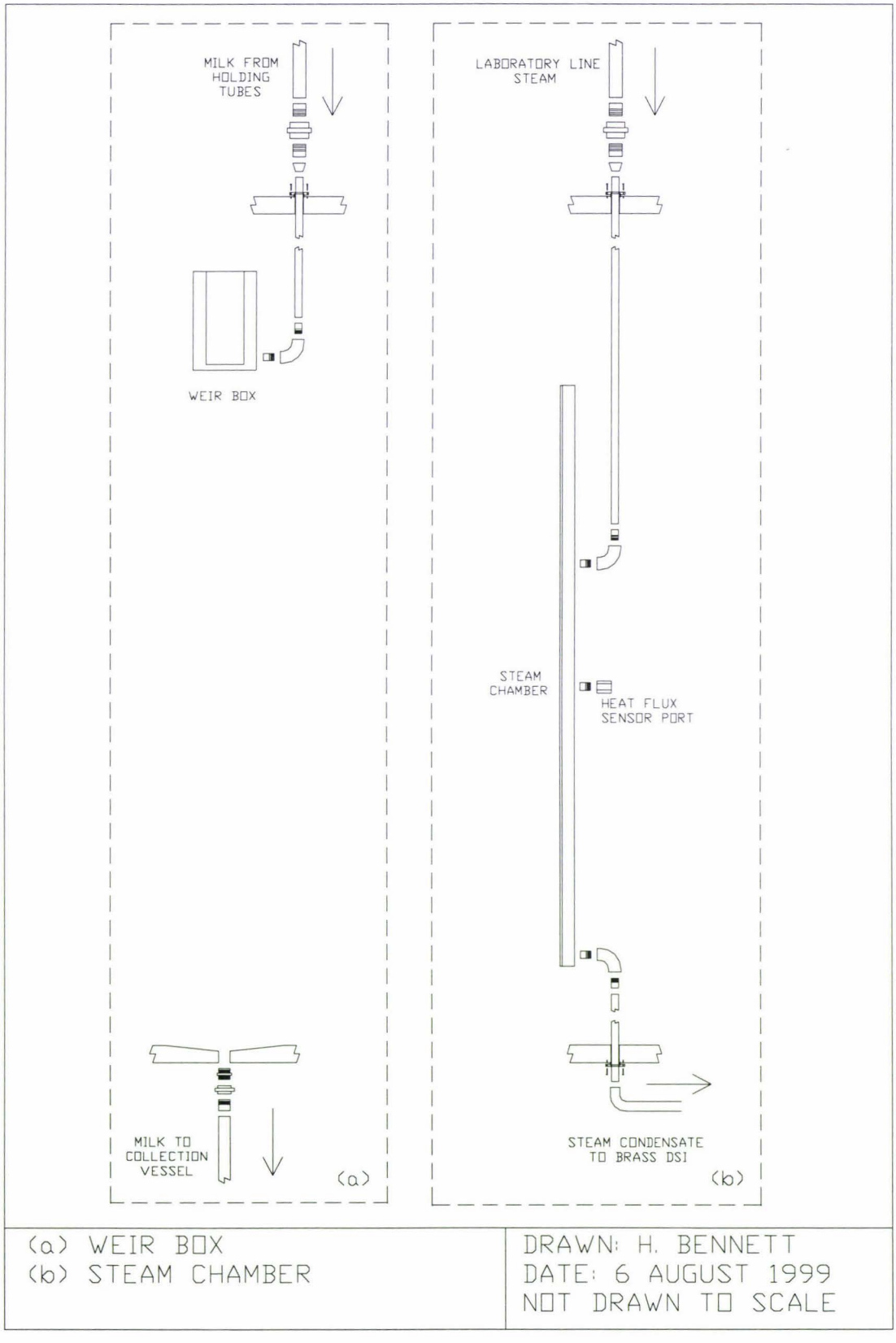

Figure 4.21 Schematic representation of (a) front view detail of milk inlet to weir box and milk outlet from evaporator (b) side view detail of steam inlet to steam chamber and steam condensate outlet from evaporator

The evaporator surface was installed within a stainless steel cylinder casing (T304, Mike Christie Sheetmetals Ltd., Palmerston North, N.Z.). An orthogonal projection of the casing is shown as Figure 4.22. Flanges where attached to both ends of the cylinder so that the casing could be sealed by bolting acetal plastic discs, with o-rings, to the flanges. A slot (1300 x 80 mm) was cut from the side of the casing so that the milk film on the evaporator plate could be observed during trials. A flange was welded to the edges of the slot and a transparent polycarbonate sheet (Ceelon Ltd. Product No. PCS006, Wellington, N.Z.) was bolted to this flange. The polycarbonate sheet was sealed to the flange by a silicone gasket (Engineering Plastics Ltd., SRS2.36FDA, 2.36 mm, Palmerston North, N.Z.). The milk weir and therefore evaporator surface was bolted to the top acetal end. The evaporator surface was removed from the casing by unbolting the top acetal end from the casing flange.

A number of ports were installed in the acetal ends to allow for pipe inlets and outlets, sensor installation and light windows. A photograph of the top acetal end is shown as Figure 4.23. There were six ports in the top acetal end:

1. milk inlet
2. steam inlet
3. RTD
4. heat flux
5. vacuum sensor
6. light window

There were four ports in the bottom acetal end:

1. milk outlet
2. condensate outlet
3. vapour outlet
4. RTD

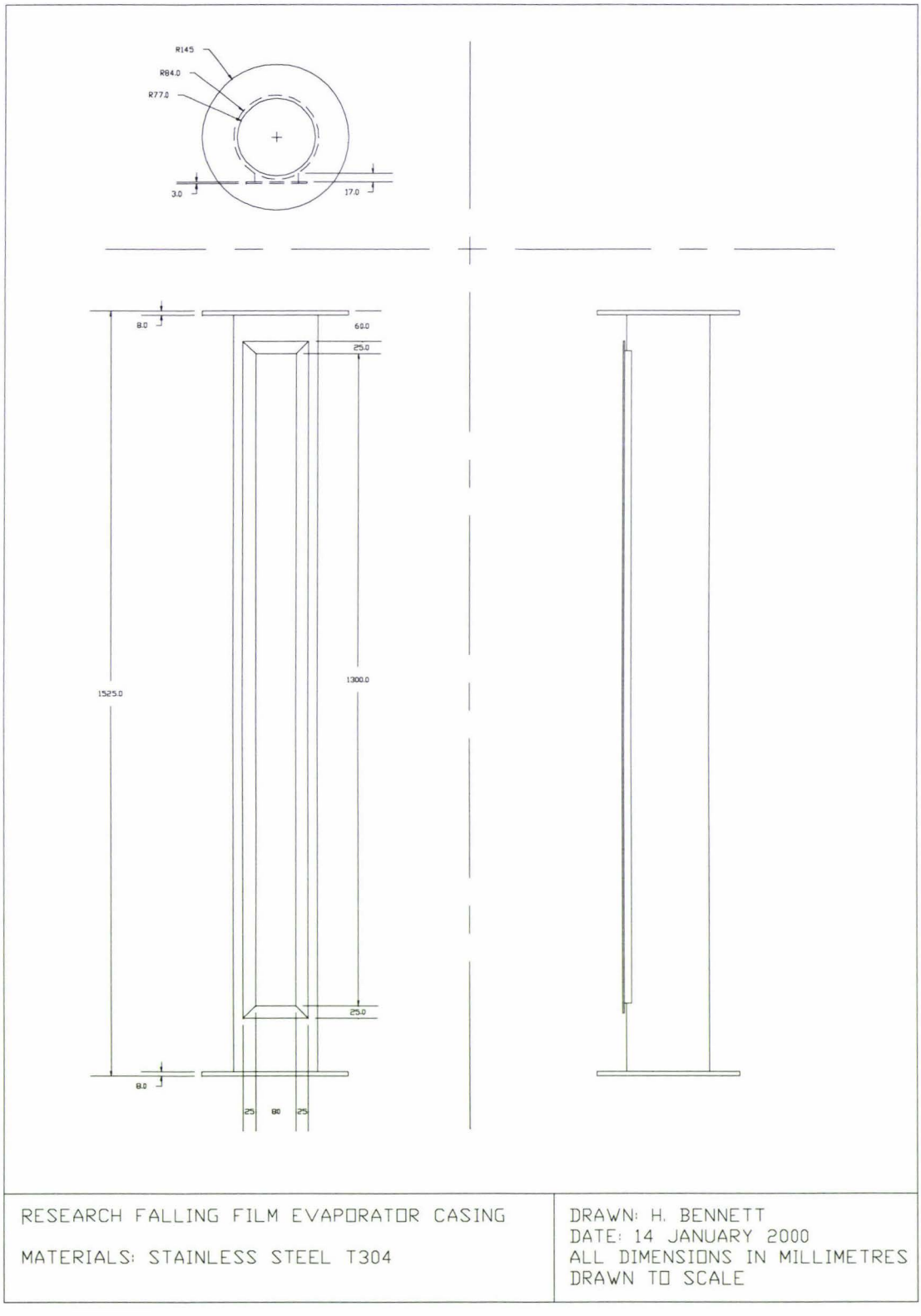

Figure 4.22 Orthogonal projection of evaporator casing

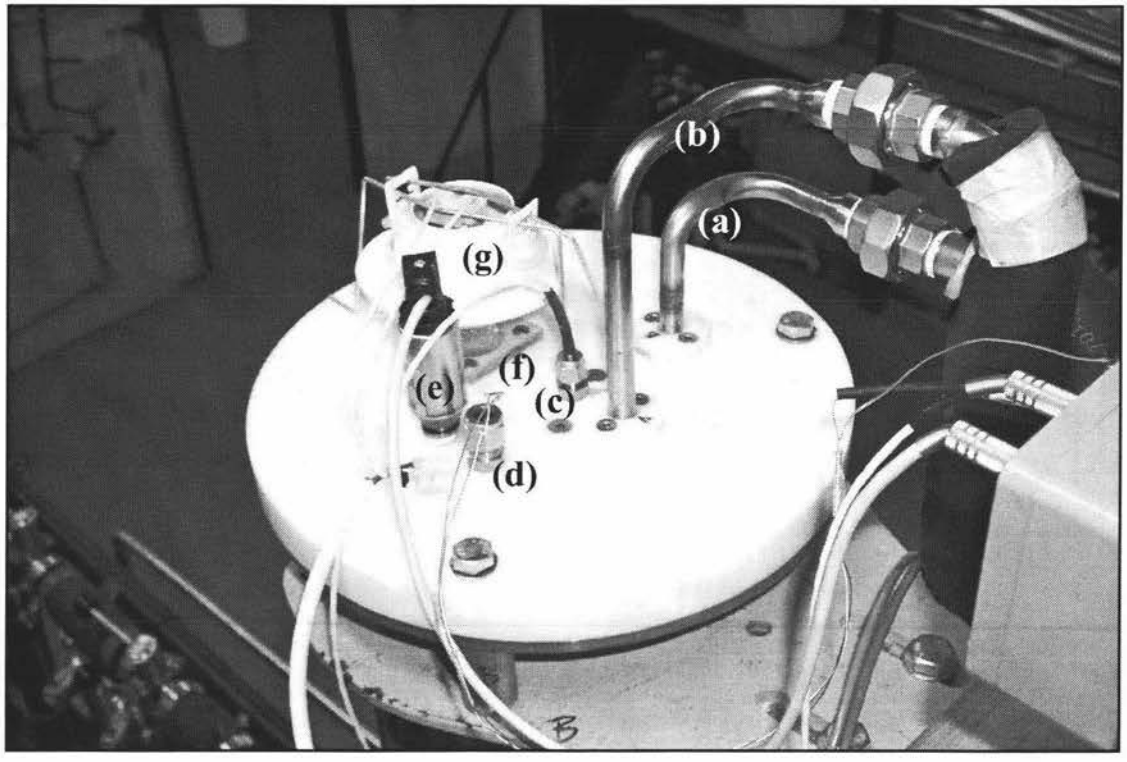

Figure 4.23 Photograph of acetal top (a) milk inlet (b) steam inlet (c) RTD port (d) heat flux probe port (e) vacuum sensor (f) light window (g) 12V light

A 12V light (Osram, Model No. 46870 SP, Lumen-Famco Lighting Ltd., Palmerston North, N.Z.) positioned above a transparent port in the top acetal end was used to illuminate the interior of evaporator. The illumination enhanced the quality of photographs and videotape footage taken of the evaporator surface. A vacuum sensor (Gems Sensors Ltd., Model No. 560550-0064, Hampshire, U.K.) monitored the pressure of the evaporator system and this measurement was used as the controlled variable in the RFFE pressure control loop. This control loop was linked to a vacuum pump (Javac Ltd., Model No. JDX220, Auckland, N.Z.) as discussed in Section 4.3.11.4.

4.3.11.2 Separator

The vapour formed during the evaporation process entered a cyclone-type separator where milk droplets in the vapour stream could be removed. A schematic representation of the separator is shown as Figure 4.24. The water vapour was vented from the top of the separator while the milk droplets collected at the bottom and drained to the milk collection tank. The separator had a removable top so that cleaning could take place with relative ease.

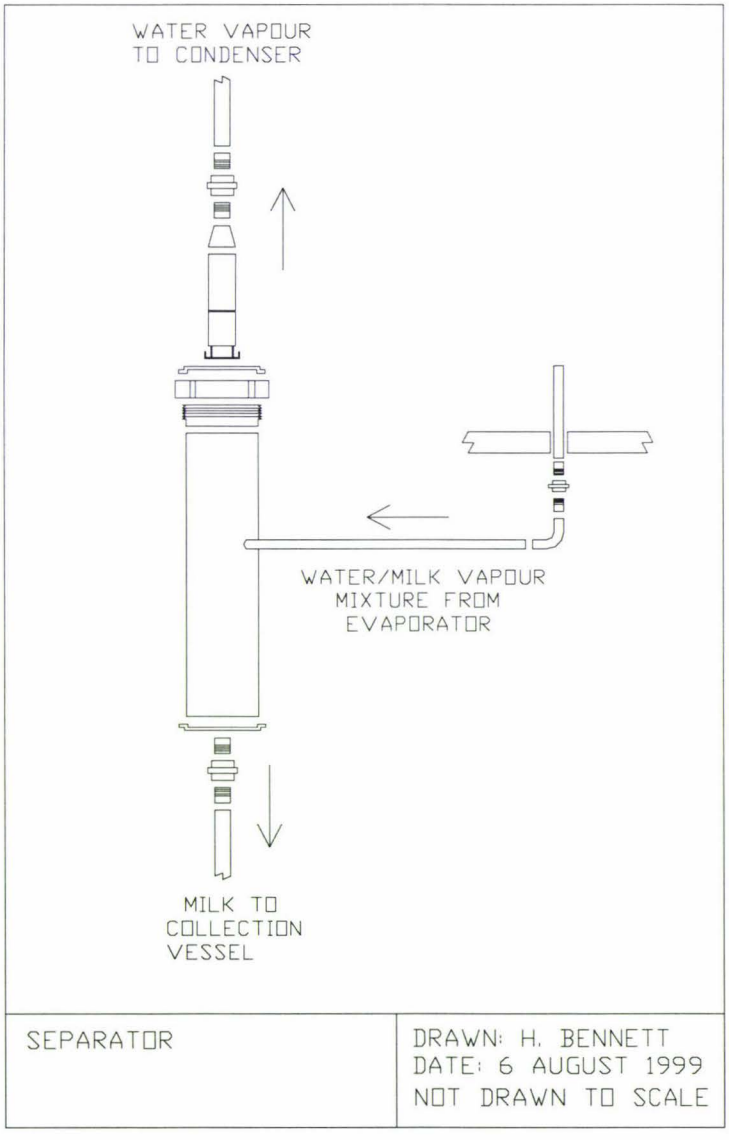

Figure 4.24 Schematic representation of cyclone separator showing assembly detail

4.3.11.3 Condenser

The vented water vapour from the cyclone-type separator entered a condenser. A schematic representation of the condenser is shown as Figure 4.25. The condenser was a stainless steel coil surrounded by a cylinder filled with a coolant. Tap water supplied from the Massey University high pressure water circuit was used as the condenser coolant. The condensed vapour drained to a collection vessel.

The cooling water exiting the condenser cylinder discharged to a brass DSI similar to the one used to heat the water for the PHE. The steam condensate from the steam chamber also entered this brass DSI producing hot water which was discharged to drain. The purpose the brass DSI was to cool the steam condensate so that hot steam was not released into the pilot plant.

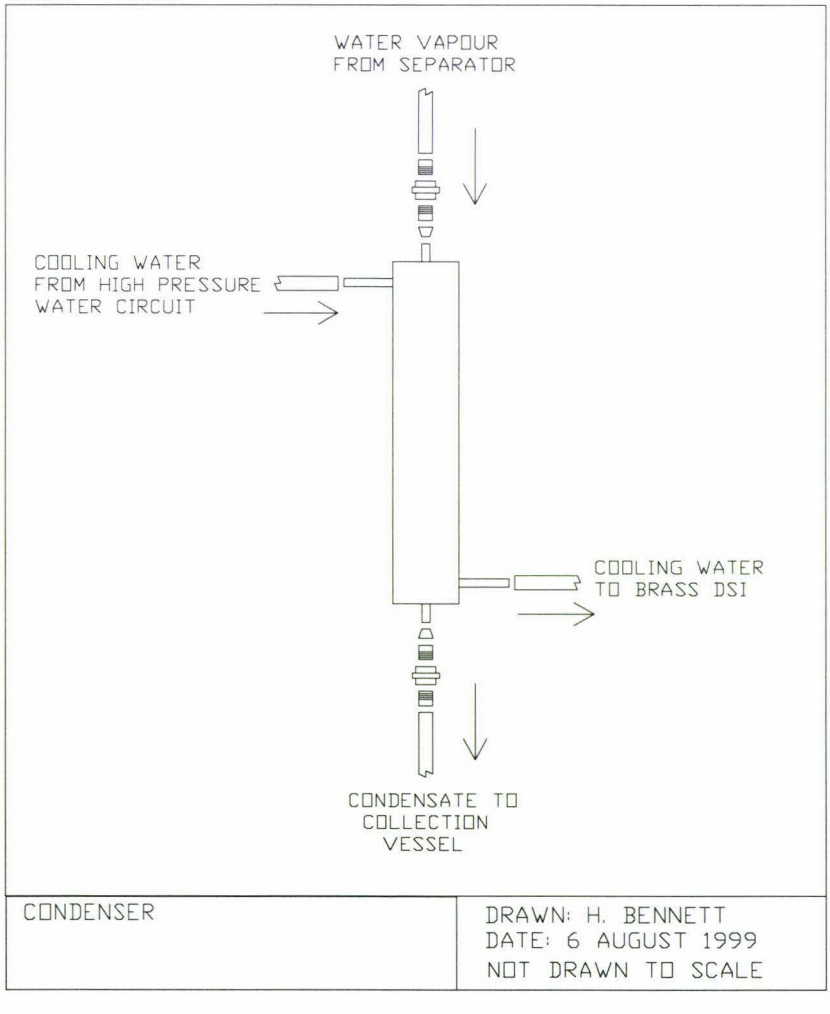

Figure 4.25 Schematic representation of condenser showing assembly detail

4.3.11.4 Collection Tanks and Pumps

Two 40 l sealed vessels were used to collect the milk and vapour condensate and were drained via an outlet at the bottom of each vessel. A mono-pump (Mono Pumps Ltd., Model No. B14, Auckland, N.Z.) emptied both vessels to drain when required. A mono-pump was chosen because vacuum pressure could be retained at a constant level when pumping fluids from the collection tanks using this type of pump. This was important because the vacuum pressure was required to be constant throughout the evaporator trials.

The condensate vessel was connected to both the laboratory vacuum line and a vacuum pump (Javac Ltd., Model No. JDX220, Auckland, N.Z.). Locating the condenser before the milk condensate collection vessel ensured that no vapour entered the vacuum lines. The vacuum acted on the entire evaporator system, therefore each component of the system needed to be well sealed. A photograph of the collection vessels and pumps is shown as Figure 4.26.

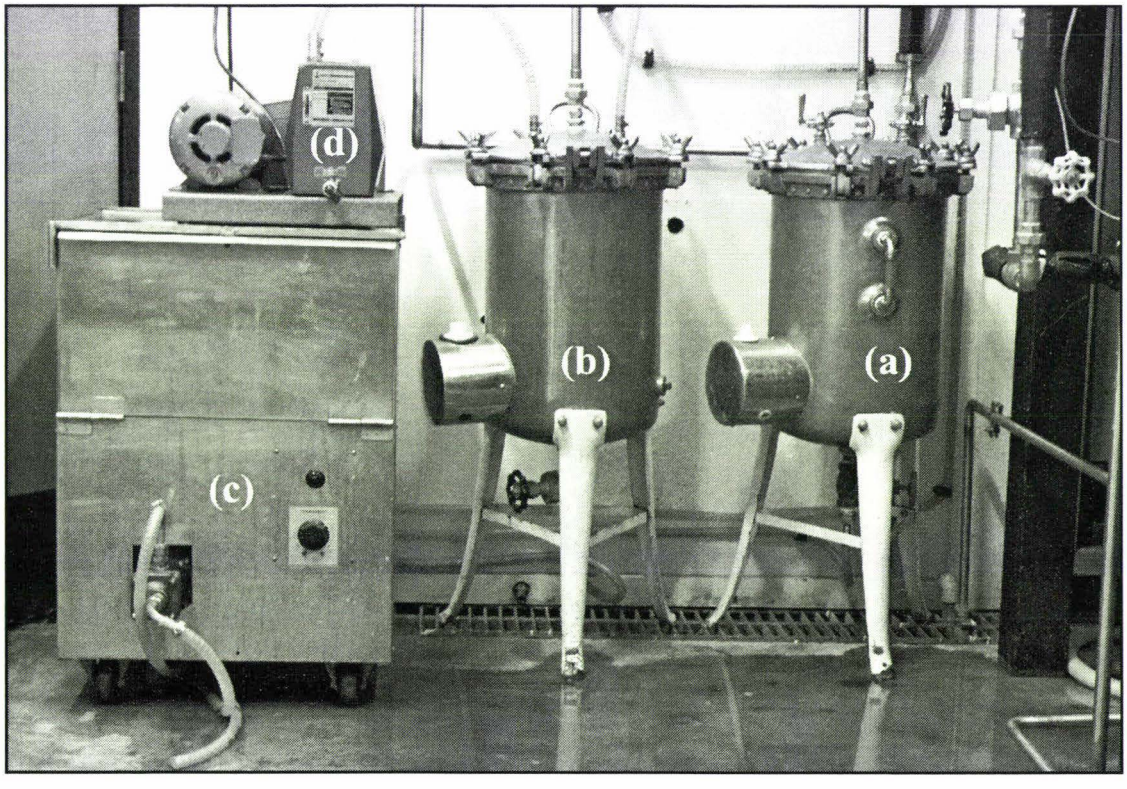

Figure 4.26 Photograph of collection vessels and pumps (a) milk collection vessel (b) condensate collection vessel (c) mono pump (d) vacuum pump

4.3.12 Clean In Place System

The CIP system consists of three stainless steel tanks (MacDonalds Machinery Ltd., Auckland, N.Z.) and a centrifugal pump (Fristam, Model No. FP712KF, 1.1kW, Auckland, N.Z.). The CIP tanks were used to hold the following solutions:

- Tank: 1 (500 l) spent caustic, nitric, rinsing water and processed milk.
- Tank: 2 (500 l) dilute nitric (0.5% w/w) and dilute caustic (1.0% w/w).
- Tank: 3 (350 l) rinsing water.

The contents of the tanks were discharged through an outlet located at the bottom of each tank. Baffles were installed in each tank to minimise the effect of vortices during pumping of fluids from the tanks. For safety reasons the tanks were covered with stainless steel lids manufactured by Mike Christie Sheetmetals Ltd. (Palmerston North, N.Z.) Each tank had a high pressure water inlet and CIP return inlet.

A centrifugal pump circulated the CIP fluids from all three tanks through the plant. The milk pump was also employed to boost the flow of CIP solutions through the pilot plant. The CIP pump was used to empty the CIP tanks to drain.

4.4 Instrumentation

4.4.1 Heat Flux Sensor

Six heat flux sensors (RdF Corporation, Model No. 27036-3, New Hampshire, U.S.A.) were used to measure the heat flux through the test plates installed in the MPHE and evaporator plate installed in the RFFE. A photograph of the sensor is shown as Figure 4.27.

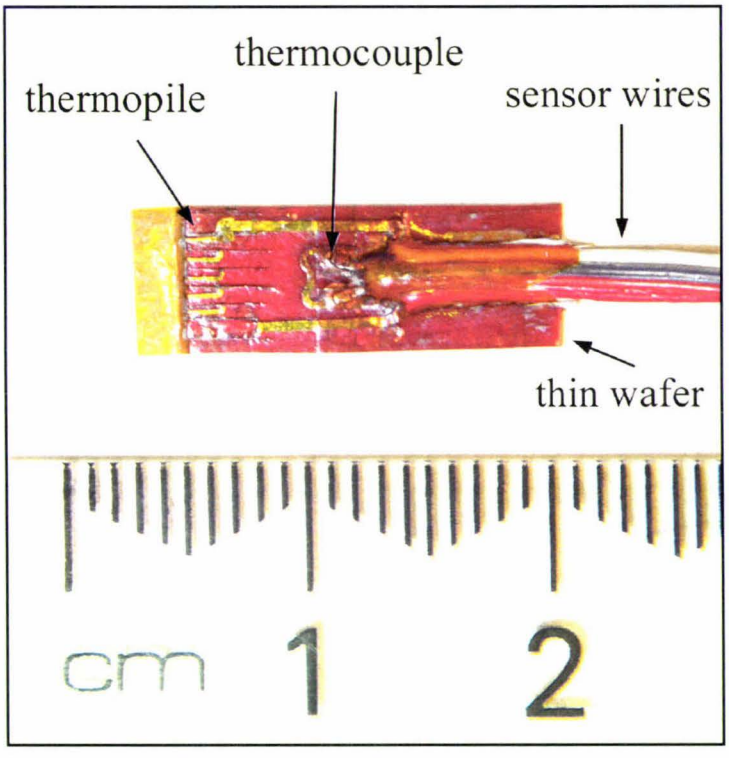

Figure 4.27 Photograph of heat flux sensor

The sensor was a thin polyimide wafer (6 x 18 x 0.2mm) with four 3 m long signal wires leading from one end. The heat flux sensor had a thermopile bonded to both sides of a thermal insulating material (thin wafer) of known conductivity. The difference in temperature across the wafer is proportional to heat flow through the sensor. Thermoelectric junctions are formed from two materials (e.g. Chromel and Alumel) on the upper surfaces of the wafer. In series with these are corresponding junctions mirror imaged on the lower surface. When heat flows through the sensor, thermal energy at the upper junction generates a small voltage while a differential

voltage is generated at the lower junction. Since the temperature differential is proportional to the voltage differential, the heat transfer rate can be directly read out as a function of voltage.

A Type T thermocouple was located on-board the thin wafer that measured the temperature of heating medium in contact with the heat flux sensor. The thermocouple was located near the centre of the thin wafer on the surface closest to the heating medium (i.e. the non-contact surface of the probe). Calibration of the heat flux sensors' thermocouples is presented in Section 4.4.2.

Since the sensors where installed in both the fouling rig and research falling film evaporator, they needed to be portable and only temporarily attached to the heat exchange surfaces. To overcome the first requirement, junction boxes were constructed that allowed removal of the heat flux sensor wires from the main sensor conduit. The pilot plant had two junction boxes, one was placed above the fouling rig and the other above the RFFE. Table 4.2 gives details of ports installed in the junction boxes.

Table 4.2 Number and type of ports in sensor junction boxes

Junction Box	RTD Ports	Heat Flux Sensor Ports	Thermocouple Ports	Vacuum Sensor Ports
Fouling Rig	6	6	6	-
Research Falling Film Evaporator	2	6	6	1

Preferably heat flux sensors should be permanently attached to surfaces with a cement of known thermal conductivity. This method would result in a consistent and uniform attachment between the sensor and the surface which ensures that reliable measures of heat flux are obtained. Since a permanent attachment was not desirable, a temporary method of attachment was developed that used aluminium tape (3M Scotch, No. 425, General Machinery Ltd., Palmerston North, N.Z.) and heat transfer paste compound (Electrolube, Product No. HTC103 and No. HTS35SL, Spectron Electronics Ltd., Palmerston North, N.Z.).

The final technique of sensor attachment for the test plates of the fouling rig was as follows:

- Aluminium tape was cut into a rectangle larger than test plate.
- Desired attachment position of probe was marked on adhesive side of tape with scribe using one corner of the tape as a reference point. This desired attachment position was generally the centre of the test plate.
- Probe was placed on adhesive side of tape as indicated by scribed lines.
- Uniform layer of heat transfer paste was applied to exposed surface of probe.
- Tape with attached probe was placed on the plate so the reference corner of the tape was set flush with one corner of the plate. This would result in the probe being located in the centre of the plate.
- Aluminium tape was pressed down ensuring no air bubbles were caught between tape and plate.
- Excess tape was trimmed from plate.

Figure 4.28 shows a test plate with probe installed.

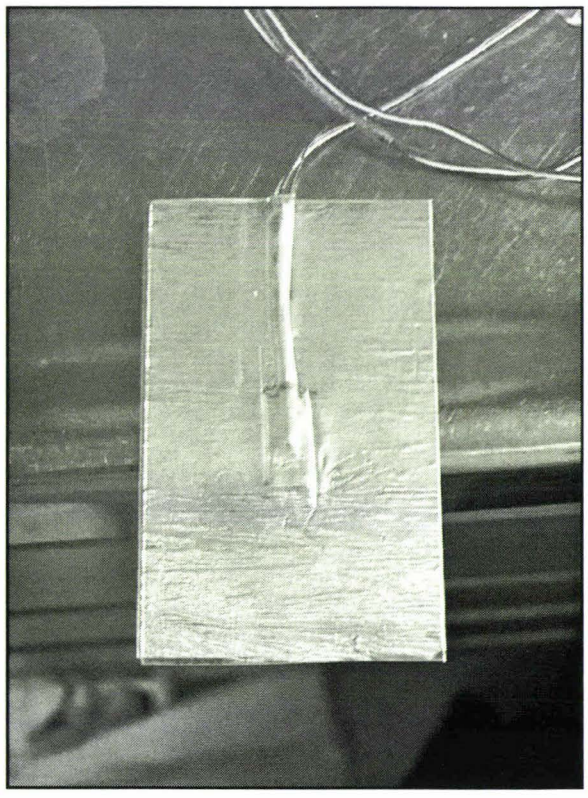

Figure 4.28 Heating medium side of test plate with probe attached

Installing the heat flux sensor on the steam chamber side of the evaporator plate used the same materials but a different method:

- A uniform layer of heat transfer paste was applied to contact surface of probe.
- Probe was placed on evaporator plate at desired location ensuring sensor wires were orientated towards the sensor wire port installed in the steam chamber.
- Length of aluminium tape was cut longer than width of evaporator plate.
- Tape was placed over probe and pressed down ensuring no air bubbles were caught between tape and plate.
- Excess tape was trimmed from plate.

Calibration:

Each individual heat flux sensor was supplied with a calibration certificate stating the sensor output at 21°C. For the current project, calibration of the sensor was made using the supplied manufacturer's values (Table 4.3). In the future, however, new on-site calibration will be required to enhance the accuracy and reliability of the data.

Table 4.3 Sensor output at 21°C as supplied by RdF Corporation

Heat flux sensor No.	**1**	**2**	**3**	**4**	**5**	**6**
Output at 21°C ($\mu V/W/m^2$)	0.4184	0.4089	0.4153	0.4089	0.4153	0.4089

The sensors were connected to thermocouple/mV modules within an Allen Bradley Programmable Logic Controller (refer to Section 4.5.2). The thermocouple modules were programmed to measure the voltage across the sensors within the range ±50mV and digitise the voltages to an integer between –32767 and 32768. These digital values were converted to heat flux values in SI units using FIX DMACS software installed on the pilot plant's control computer (refer to Section 4.5.3).

A heat flux value that corresponded to a voltage of 50mV was calculated for each sensor using the manufacturer's calibration data. For sensor No. 1:

$$q_{50mV} = \frac{50000\mu V}{output(\mu V/W/m^2)} = \frac{50000}{0.4184} = 119502.87 W/m^2 \qquad \textbf{(4.1)}$$

A factor (F) for converting the integer (± 32767) to a heat flux value in SI units was then calculated:

$$F = \frac{q_{50mV}}{32767} = \frac{119502.87}{32767} = 3.64705 W/m^2 \qquad \textbf{(4.2)}$$

Table 4.4 gives all the corresponding heat flux voltage values and multiplication factors.

Table 4.4 Heat flux value at 50 mV and conversion factors for the six heat flux sensors

Heat flux sensor No.	1	2	3	4	5	6
q_{50mV} (W/m^2)	119502.87	122279.29	120394.90	122279.29	120394.90	122279.29
F (W/m^2)	3.64705	3.73178	3.67427	3.73178	3.67427	3.73178

Real-time calculations and conversions were performed by the FIX DMACS software and logged to disk automatically as described in Section 4.5.3.

4.4.2 Temperature Sensors

Figure 4.4 shows the location of the temperature sensors in the pilot plant where 24 temperature sensors were installed (Table 4.5).

Table 4.5 Location and type of temperature sensor installed in pilot plant

No.	Location	Type of sensor
1	Milk vat	RTD
2	PHE – process fluid outlet	RTD
3	PHE – heating medium inlet	RTD
4	DSI 1 – process fluid outlet	RTD
5	MPHE 1 – process fluid	RTD*
6	MPHE 1 – heat flux surface (heating medium) RFFE 1 – heat flux surface (heating medium)	Thermocouple
7	MPHE 2 – process fluid	RTD*
8	MPHE 2 – heat flux surface (heating medium) RFFE 2 – heat flux surface (heating medium)	Thermocouple
9	MPHE 3 – process fluid	RTD*
10	MPHE 3 – heat flux surface (heating medium) RFFE 3 – heat flux surface (heating medium)	Thermocouple
11	MPHE 4 – process fluid	RTD*
12	MPHE 4 – heat flux surface (heating medium) RFFE 4 – heat flux surface (heating medium)	Thermocouple
13	MPHE 5 – process fluid	RTD*
14	MPHE 5 – heat flux surface (heating medium) RFFE 5 – heat flux surface (heating medium)	Thermocouple
15	MPHE 6 – process fluid	RTD*
16	MPHE 6 – heat flux surface (heating medium) RFFE 6 – heat flux surface (heating medium)	Thermocouple
17	DTHE – process fluid inlet	RTD
18	DTHE – process fluid outlet	RTD
19	DTHE – heating medium inlet	RTD
20	DTHE – heating medium outlet	RTD
21	Heating medium vessel	RTD
22	DSI 2 – process fluid	RTD
23	RFFE – process fluid inlet	RTD
24	RFFE – process fluid outlet	RTD

Note:

- RTD* - originally installed with RTD however replaced later with Type T thermocouple (see below).

- Since the heat flux sensor could be moved between the fouling rig and RFFE, the on-board Type T thermocouple of the heat flux sensor measured temperatures in both the fouling rig and RFFE.

The RTDs were PT100 electronic components (Farnell Electronic Components Ltd, Model No. DM503, Auckland, N.Z.) shielded in a stainless steel sheath. The sheath was a stainless steel tube (6 mm OD, NZF Stainless Ltd., Palmerston North, N.Z.) with one sealed end. Initially the RTDs were manufactured in-house using the following method:

- Both PT100 leads were soldered to three signal wires.
- Soldered connections were insulated using heat shrink plastic tube.
- PT100 inserted in a 70 mm long stainless steel sheath ensuring that the PT100 made contact with the sealed end of the stainless steel sheath.
- Sheath filled with heat transfer oil (Mobiltherm 603, Product Name 988688, Wellington, N.Z.) .
- Polymer adhesive (Super Strength Araldite Epoxy Resin, Shelleys Chemical Company Pty. Ltd., Auckland, N.Z.) applied to open end of sheath.
- Open end of sheath sealed with heat shrink plastic tube.

All RTDs were installed through ports of tube socket weld unions (Swagelok, Model No. SS-400-6-4W, Auckland, N.Z.) that had been welded to the pipes of the pilot plant. The two RTDs installed in the RFFE where installed through ports that had been tapped into the acetal ends.

The performance of the on-site manufactured RTDs deviated between probes. It was possible that the contact between the PT100 and the stainless steel sheath was inconsistent leading to errors in measured temperature. Therefore, all the probes where replaced by commercially manufactured RTDs (Wrights Ltd., Model No.NR.3-2550E/000, Lower Hutt, N.Z.). The commercial RTDs were installed in the pilot plant using the same method used for the on-site manufactured probes. Although the accuracy of data reported by the commercial probes was greatly improved they still introduced significant errors. Since a precise measurement of process fluid temperature was required in the MPHEs, the RTDs of the MPHEs were replaced by

Type T thermocouples. A detailed discussion of the reasons for this change is given in Section 5.2.5. The thermocouples were installed in the existing tube socket weld unions and sealed with a small rubber bung. A SCADA (Supervisory Control and Data Acquisition) Station (Section 4.6.3) was used to log data from these thermocouples because the Pilot Plant's PLC (Section 4.5.2) thermocouple input capacity had been reached.

Calibration:

The RTDs and thermocouples were calibrated with ice/water (distilled) and boiling water (distilled). The RTDs, thermocouples and heat flux sensors (note: calibration of on-board thermocouple – not heat flux) were placed in a flask containing an ice/water slurry. The temperature was recorded every second for a period of 5 minutes. The data obtained were averaged and this value was used as the temperature reading of the probes for the ice point (0°C). The temperature sensors were then immersed in a kettle of boiling water which remained boiling throughout the calibration exercise (temperature errors arising from the effects on apparent boiling point of the barometric pressure or superheating in the boiling kettle were insignificant in comparison with other experimental errors). The process of data collection and analysis was repeated resulting in the probe readings for boiling point (100°C). Two simultaneous equations were solved for each sensor to derive a linear relationship between the read and calibrated temperatures.

Assuming:

$$\theta_c = a\theta_r + b \qquad \textbf{(4.3)}$$

Where: θ_c = calibrated temperature reading (°C)

θ_r = read temperature (°C)

a = regression coefficient

b = regression coefficient

Then a calibrated reading could be obtained by substituting the read temperature of the sensors into Equation (4.3). Regression coefficients a and b were calculated using the following equations:

$$a = \frac{100}{\theta_{100} - \theta_0} \quad \textbf{(4.4)}$$

$$b = -a\theta_0 \quad \textbf{(4.5)}$$

Where: θ_{100} = reported temperature at boiling point

θ_0 = reported temperature at ice point

Calibration data for a selection of temperature sensors is given in Table 9.1 of the Appendix.

4.4.3 Vacuum Sensor

A vacuum sensor (Gems Sensors Ltd., Model No. 560550-0064, Hampshire, U.K.) was used to measure the pressure inside the RFFE system. The sensor reading was used as the controlled variable in a control loop that was linked to the vacuum pump.

4.4.4 Flowmeters

Two flowmeters were used to measure the flow of fluids through the plant. The milk flowmeter provided the controlled variable of the PID circuit that manipulated the speed of the milk pump. The CIP flowmeter provided a measure of CIP solutions flowrates through the plant. A description of the flowmeters is given in Section 4.3.7

4.5 Process Control

4.5.1 Process Control Computers

A microcomputer running Windows NT 4.0 (Intel Celeron, Advantage Computers Ltd., Palmerston North, N.Z.) and a Programmable Logic Controller (Allen-Bradley SLC 500, Rockwell Automation Ltd., Palmerston North, N.Z.) were used to control the pilot plant and provide a user interface. The microcomputer displayed experimental data in real-time which were automatically logged to disk.

4.5.2 Programmable Logic Controller

The Programmable Logic Controller (PLC) was a 13-slot modular chassis containing a Central Processing Unit (CPU) and 12 input/output modules. Table 4.6 gives the type of module in each chassis slot of the PLC.

Table 4.6 Modules within 13-Slot Modular Chassis

Chassis Module Slot	Module Type	No. of channels	Catalogue No.
0	CPU – 12K user memory	-	1747-L532
1	Thermocouple/mV input	4	1746-NT4
2	Thermocouple/mV input	4	1746-NT4
3	Thermocouple/mV input	4	1746-NT4
4	RTD/Resistance input	4	1746-NR4
5	RTD/Resistance input	4	1746-NR4
6	RTD/Resistance input	4	1746-NR4
7	Analog input	4	1746-NI4
8	RTD/Resistance input	4	1746-NR4
9	Analog current output	4	1746-NO4I
10	Digital input	16	1746-IB16
11	RTD/Resistance input	4	1746-NR4
12	Isolated relay output	8	1746-OX8

The PLC receives all of the sensor inputs and delivers all the control outputs to the pilot plant. Although the PLC was capable of PID control calculations, these calculations were carried out by the microcomputer allowing quick reprogramming of the control loops.

4.5.3 Microcomputer

The microcomputer was used to display and log data from the PLC and also provide PID feed back control to the pilot plant via the PLC. FIX DMACS Version 7.0 (Intellution Inc., Industrial Interface Ltd., Auckland, N.Z.) software package was used to display and log the plant data as well as provide a user interface that allowed manipulation of controlled variables. Table 4.7 shows a list of the variables controlled using the FIX DMACS software. The variables that could be controlled automatically could also be controlled manually if required.

Table 4.7 Variables controlled using the FIX DMACS software

Plant Item	Control Type	Automatic Control Ability	Automatic Control Controlled Variable
Milk vat agitator	On/off	No	
Refrigeration unit	On/off	Yes	Temperature sensor No. 1
Milk pump	Speed control	Yes	Milk flowmeter
DSI 1	% open	Yes	Temperature sensor No. 4
Heating medium Pump	On/off	No	
Heating medium Heater	On/off	Yes	Temperature sensor No. 22
DSI 2	% open	Yes	Temperature sensor No. 23
Vacuum pump	On/off	Yes	Vacuum sensor
CIP pump	Speed control	Yes	CIP flowmeter

Three control screens were set up for the pilot plant using the FIX DMACS software that provided real-time sensor measurement display and control of plant variables. Figure 4.29 shows a screen shot of the preheating control screen. A real time plot of variable measurements could be viewed using the Historical Display program of the FIX DMACS software. The Historical Display program could display any of the plant variables on a user defined time scale. Figure 4.30 shows a screen shot of a Historical Display plot.

The micro-computer logged all variable data to disk automatically. A sample of each sensor measurement was logged to disk every 1 second. Control variables such as pump speeds were logged to disk every 30 seconds. Variable data required for further analysis could be exported from the FIX DMACS software using the Historical Report program. Data were exported into comma-delimited text files which could be easily manipulated by spreadsheet programs such as Microsoft Excel.

The FIX DMACS software was used to perform simple calculations in real-time. All sensor calibration calculations were performed in real time and logged to disc automatically. Calculations of important analytical data such as overall heat transfer coefficient were performed and could be displayed in real-time using the Historical Display program.

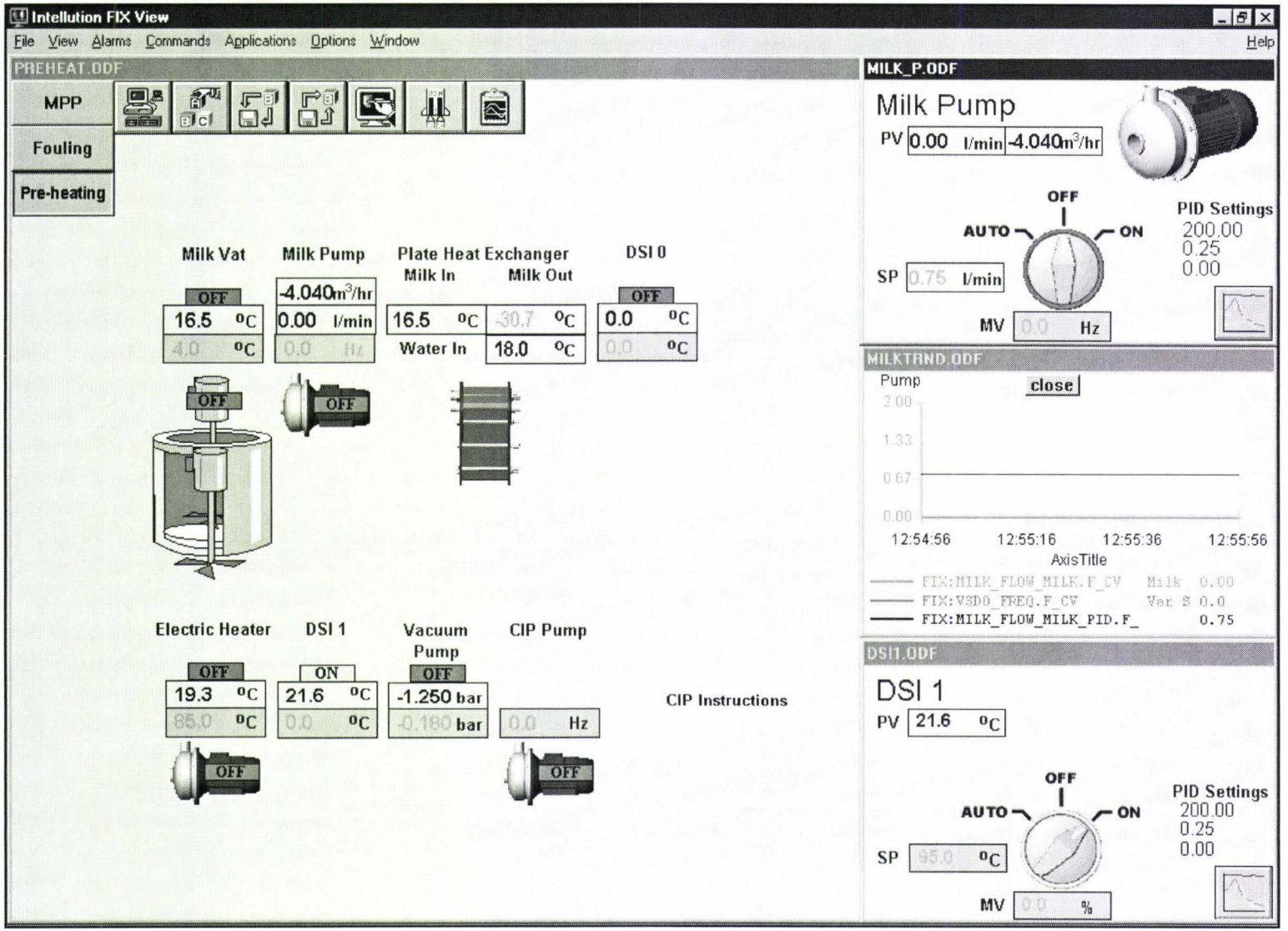

Figure 4.29 Screen shot of preheating control screen

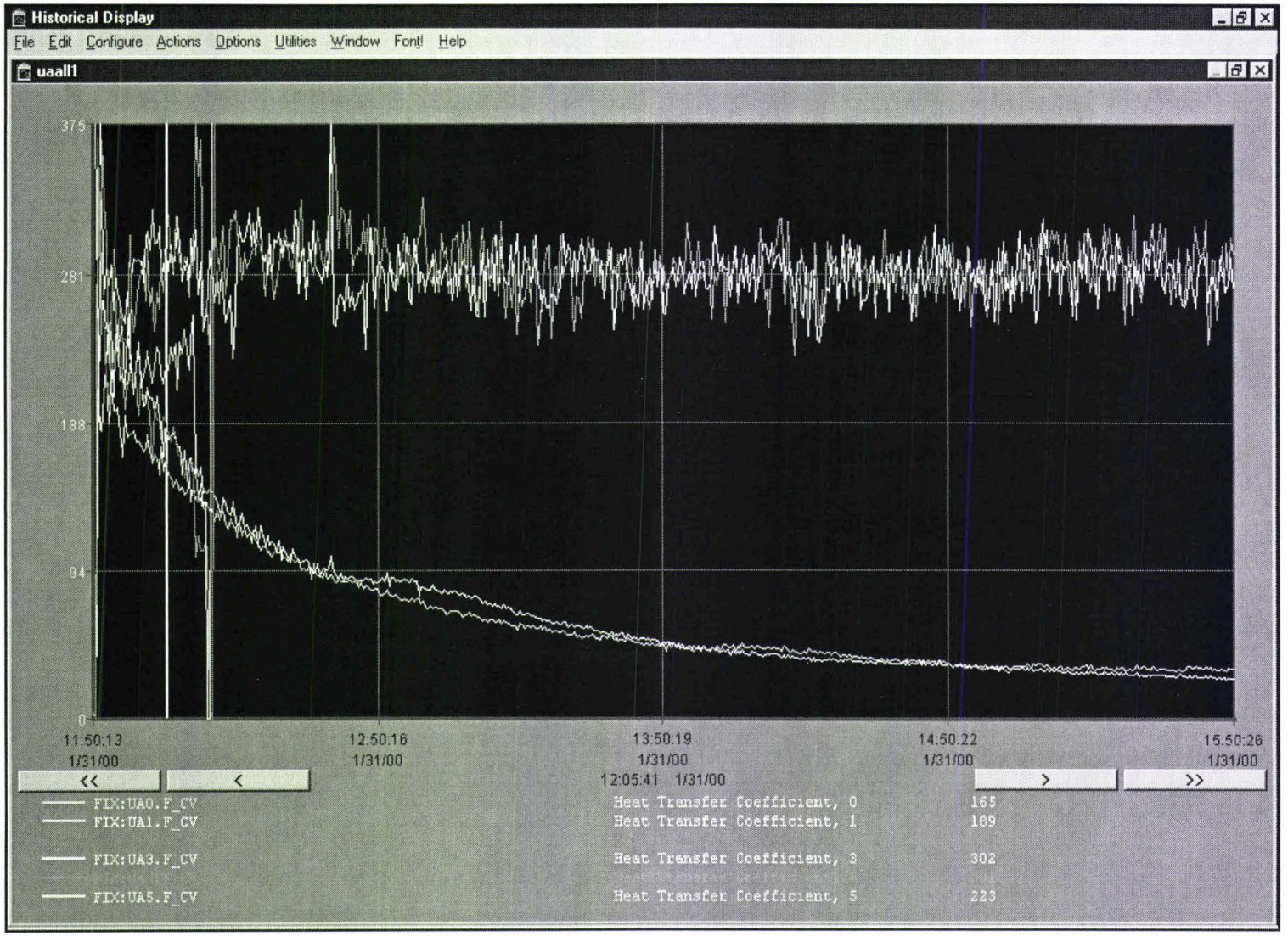

Figure 4.30 Screen shot of historical data display

4.6 Additional Equipment

4.6.1 Electronic Dial Depth Gauge

The thickness of the fouling deposits on test plates removed from the fouling rig were measured by a digital dial depth gauge (Mitutoyo Corporation, Model No. 1DC-112E, Aurora, U.S.A.) attached to an arm (primary) that could be raised or lowered as shown in Figure 4.31. The dial gauge had an accuracy of ± 0.001 mm and a range of 0-12.7 mm. The spindle head of the dial gauge was replaced by a shaft with a pointed head so that pin-point measurements could be obtained. The spindle lifting lever for raising and lowering the spindle was maintained under spring pressure and controlled via a screw tapped in a secondary arm attached to the primary arm.

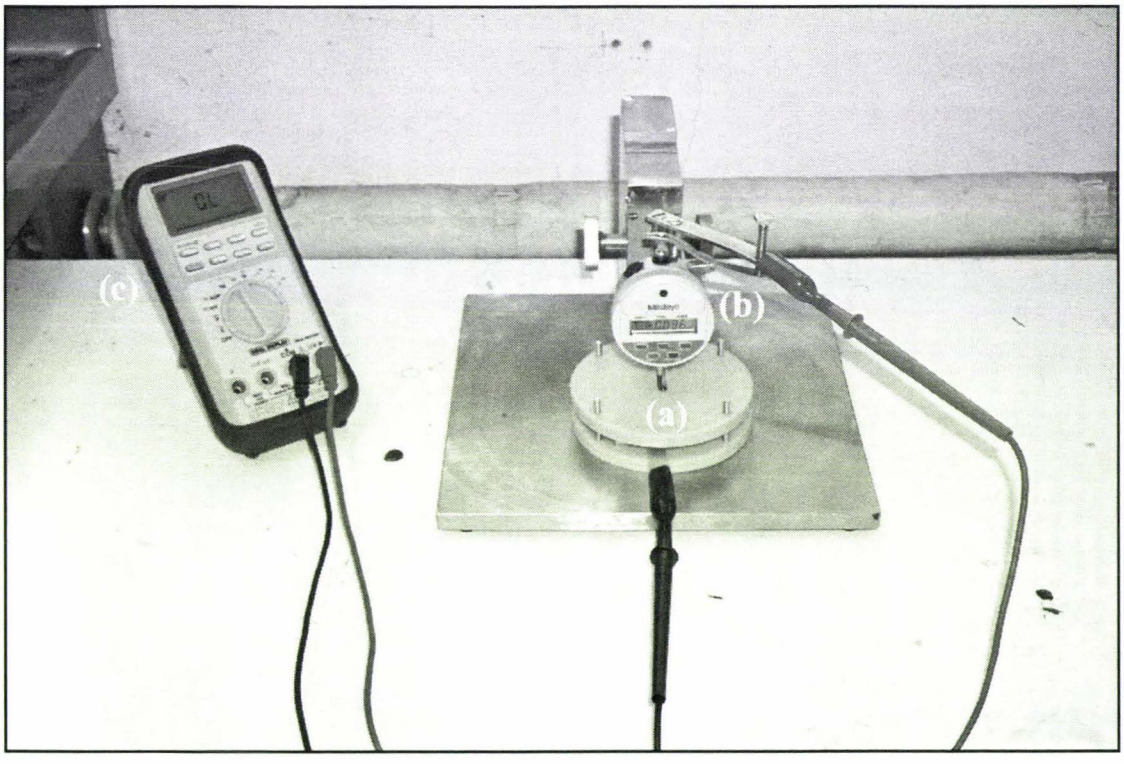

Figure 4.31 Photograph of fouling electronic dial gauge (a) test plate brace (b) dial gauge (c) multimeter

The thermal resistance due to the fouling deposits was only measured for fouling deposits directly above the probe. Therefore, only the thickness of fouling deposits above the probe could be compared with the output of the probe. It was therefore

crucial to accurately locate the corresponding position of the probe on the fouled side of the test plate. A brace constructed from two acetal plastic discs, an aluminium sheet and four M4 screws was used to locate the position of the probe. Figure 4.32 gives a schematic representation of the test plate brace components.

The aluminium component was used to hold the test plates between the two acetal discs and had the same dimensions as a MPHE gasket. The acetal discs had identical slots cut from the centre that had the same dimensions as heat flux probe (6 x 18mm). After fouling experiments the aluminium component (holder) was placed over a fouled test plate ensuring that the fouling deposit window of the test plate lined up with the window of the holder. The probe was removed from the test plate which left an outline of the probe in the remaining heat transfer paste. Aluminium tape secured the test plate to the holder which was then placed between the acetal discs. The arm of the holder was used to manoeuvre the test plate into the correct position where the outline of the probe could be seen through the slot of the bottom acetal disc. The four M4 screws were tightened and the brace was placed on the base directly below the dial depth gauge. The brace was manoeuvred until the spindle shaft was directly above the slot of the top acetal disc. The screw used to control the spindle lever was turned which made the spindle lower onto the fouling layer through the top acetal disc slot. Contact between the spindle head and fouling deposit was indicated by a multi-meter (Brymen Model No. BM727, Dick Smith Electronics, Palmerston North, N.Z.) measuring ohms. The leads of the multi-meter were attached to the arm of the aluminium holder and secondary arm of the dial depth gauge and therefore when the spindle head made contact with the fouling deposit, the circuit would be complete and a reading would be displayed on the multi-meter. The digital reading of the dial depth gauge was recorded. The spindle lever was used to force the spindle head through the fouling deposit until making contact with the metal test plate. Another dial gauge reading was taken at this point. The thickness of the fouling deposit was calculated by subtracting the second reading away from the first.

The brace was moved so that other points in the top acetal slot could be measured. Five random measurements were made that were averaged to give a relative thickness measurement of fouling directly above the probe.

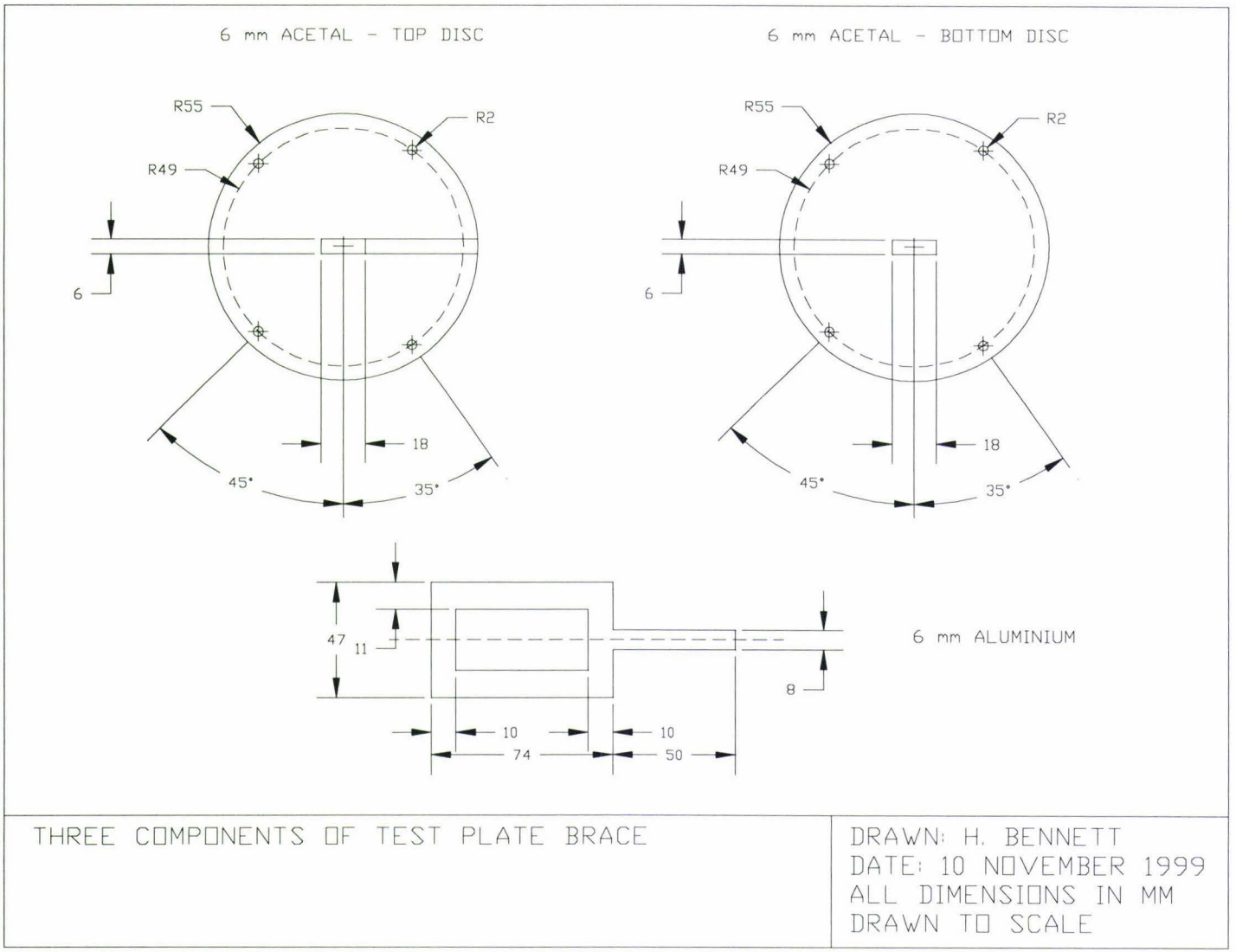

Figure 4.32 Schematic representation of test plate brace components

4.6.2 Digital Camera

Photographic images were captured using a digital camera (Kodak Model No. DC290, New York, U.S.) placed on a tripod. Test plates removed from the fouling rig were photographed in a small room with light provided by two lamps. The lamps could be manoeuvred to provide appropriate lighting for each plate. Obtaining focused images was aided by the use of a television monitor which provided a magnified preview of the image.

Evaporator plate images were captured while the plate was still installed in the RFFE. The sight window installed in the evaporator casing made in-line photography possible. Light was provided from the 12 V light installed above the top acetal end of the evaporator casing. The television monitor was also used to aid the capture of focused images of the evaporator plate.

4.6.3 SCADA Station

A mobile SCADA (Supervisory Control and Data Acquisition) station (Intel Pentium, Advantage Computers Ltd., Palmerston North, N.Z.) running Windows 3.1 was used to log data from the replacement thermocouples installed in the fouling rig (refer to Section 4.4.2). FIX DMACS Version 5.5 (Intellution Inc., Industrial Interface Ltd., Auckland, N.Z.) software was used to log and export the thermocouple data. The thermocouples were calibrated while connected to the SCADA Station using the method outlined in Section 4.4.2. Calibration data is given in Table 9.1 of the Appendix.

4.7 Experimental Methods

The study of whole milk fouling on heated surfaces was conducted with the custom-built fouling rig and research falling film evaporator. Each apparatus had heated surfaces on to which heat flux probes were attached. The probes were used to monitor, in real-time, the onset and build-up of deposits on the heated surfaces. After commissioning experiments had taken place i.e. investigating the stability of various

system resistances (refer to Section 3.3), detailed experiments investigating the effect of operating conditions on fouling deposits were performed.

A generic operating procedure for the fouling rig and RFFE is presented followed by a detailed description of commissioning and fouling experiments conducted.

4.7.1 Reception of Milk

Batches of fresh whole milk (850 l) were purchased from Kiwi Dairies Ltd. (Longburn, N.Z.) and shipped in 1000 litre containers. The container was transported from the Kiwi Dairies processing plant to the pilot plant. On receipt, milk was pumped (Mono Pump Ltd., Model No. CP25, Auckland, N.Z.) from the 1000 litre container through the bulk milk inlet pipe (refer Figure 4.6) into the milk vat for storage at 4 °C. The milk vat held enough milk for approximately 5 days of fouling experiments.

4.7.2 Generic Pilot Plant Operation

4.7.2.1 Fouling Rig

4.7.2.1.1 Start Up

The generic pilot plant start up procedure used for commissioning and fouling trials conducted with the fouling rig was as follows:

1. Inspect control computer ensuring:
   - Milk vat agitator is on.
   - Refrigeration automatic control loop is on with set point of 4°C.
   - Temperature sensors are functioning correctly.
2. Remove clean test plates from solution of caustic (in which the plates had been submerged overnight).
3. Rinse test plates with water.
4. Let plates dry in ambient air.
5. Attach heat flux probe to test plates using procedure described in Section 4.4.1.
6. Install test plates in MPHEs using procedure described in Section 4.3.6.

7. Connect heat flux sensors to junction box above fouling rig.
8. Inspect control computer to determine if the heat flux sensors in the MPHEs are functioning correctly.
9. Fill fouling rig heating medium tank with water and adjust set point of heating element to 90°C on PC interface.
10. Manipulate heating medium chamber valves of fouling rig so that the heating medium is able to flow through the heating medium chambers of the MPHEs.
11. Ensure heating medium circuit valves of double tube heat exchanger are turned on.
12. Initiate heating medium pump allowing temperature of RTD temperature sensor No. 21 to reach steady state.
13. Manipulate plate heat exchanger hot side valves so that heating medium is able to pass through PHE proceeding to drain.
14. Fully open laboratory steam valve to heating equipment (PHE, DSI 1, DSI 2).
15. Half open plate heat exchanger direct steam injector water valve.
16. Fully open plate heat exchanger direct steam injector steam valve.
17. Manually adjust plate heat exchanger direct steam injector water valve until RTD temperature sensor No. 3 reads 60°C on control computer.
18. Manipulate valves on the milk circuit so that milk passes through the pilot plant in following sequence:
    - Milk vat
    - Milk pump
    - PHE
    - DSI 1
    - Fouling rig main line not MPHE laterals
    - Flowmeter
    - DTHE
    - DSI 2
    - CIP Tank 1
19. Turn milk pump on manual control using a frequency set point of 30 Hz.
20. Inspect control computer for a positive flowmeter reading.
21. Adjust DSI 1 system valves so milk and steam are able to flow through one steam injector.

22. Adjust DSI 1 RTD temperature sensor No. 4 set point to 70°C.
23. Initiate automatic control on DSI 1.
24. After RTD temperature sensor No. 4 reaches set point, initiate automatic control on milk pump set to 45 l/h.
25. After milk flowrate reaches set point, manipulate valves on process fluid chamber side so that milk flows through the chamber.

Typically trials ran for 4 hours during which time individual MPHE modules could be isolated without interruption to the rest of the pilot plant system.

4.7.2.1.2 Shut-Down

The generic pilot plant shut-down procedure for commissioning and fouling trials conducted with the miniature plate heat exchangers was as follows:

1. Isolate any remaining MPHE modules not already isolated.
2. Close laboratory steam valve to heating equipment.
3. Set value of DSI 1 control valve to 0%.
4. Close DSI 1 system steam injector valve.
5. Close PHE direct steam injector steam valve.
6. Close PHE direct steam injector water valve.
7. Stop heating medium pump.
8. Stop milk pump.
9. If milk still present in the milk vat, ensure agitator paddle motor is turned on and refrigeration control loop set to automatically control milk temperature to 4°C.

4.7.2.1.3 Cleaning Procedure

The generic procedure used to clean the pilot plant after fouling and commissioning trials conducted with the fouling rig was as follows:

1. Disconnect DSI pipe from plate heat exchanger.
2. Attach high temperature hose to DSI pipe using union and place end of hose in drain.
3. Fully open laboratory steam valve to heating equipment.
4. Half open plate heat exchanger DSI water valve.

5. Fully open plate heat exchanger DSI steam valve.
6. Manually adjust plate heat exchanger DSI water valve until RTD temperature sensor No. 3 reads 85°C on control computer.
7. Place high temperature hose end in Tank 2 and fill until tank contains approximately 300 l.
8. Remove hose from Tank 2 and measure depth of water.
9. Calculate exact volume of hot water in Tank 2.
10. Based on this volume, calculate quantity of concentrated caustic required to make solution 1.0% (w/w) caustic.
11. Add required quantity of concentrated caustic to Tank 2.
12. Close plate heat exchanger DSI steam valve.
13. Close plate heat exchanger DSI water valve.
14. Disconnect high temperature hose from DSI pipe.
15. Reconnect DSI pipe to plate heat exchanger.
16. Install test plates in MPHEs using procedure discussed in Section 4.3.6.
17. Fill Tank 3 until it contains approximately 350 l of water by opening water inlet valve.
18. Manipulate valves on the milk/CIP circuit so that CIP fluids can pass through the pilot plant in following sequence:
    - CIP Tank 3
    - CIP pump
    - Milk pump
    - PHE
    - DSI 1
    - Fouling rig
    - Milk and CIP flowmeters
    - DTHE
    - DSI 2
    - CIP Tank 1
19. Repeat steps 4-6 except setting RTD temperature sensor No. 3 to 50°C.
20. Turn on both CIP and milk pump using a set point of 50 Hz for both pumps.
21. Inspect control computer for positive flowmeter readings.

22. Turn off CIP and milk pump when approximately 200 l of fluid has flowed through the pilot plant.
23. Close plate heat exchanger direct steam injector steam valve.
24. Close plate heat exchanger direct steam injector water valve.
25. Manipulate valves so that contents of Tank 1 can be discharged to drain.
26. Turn on CIP pump to a set point of 50 Hz.
27. Turn off CIP pump when Tank 1 is empty.
28. Manipulate valves on milk/CIP circuit so that hot caustic solution flows from Tank 2 through the plant returning to Tank 2 in a recycle manner.
29. Turn on both CIP and milk pump using a set point of 50 Hz for both pumps.
30. Inspect control computer for positive flowmeter readings.
31. After approximately 15 minutes of recycle, turn off CIP and milk pump.
32. Add cold water to Tank 2 supplied from the tank water inlet.
33. Manipulate valves so that contents of Tank 2 discharges to drain.
34. Turn on CIP pump to a set point of 50 Hz.
35. Turn off CIP pump when Tank 2 is empty.
36. Repeat steps 17-27.
37. Repeat steps 1-9.
38. Based on this volume, calculate quantity of concentrated nitric acid required to make solution 0.5% nitric acid.
39. Add required quantity of concentrated nitric acid to Tank 2.
40. Repeat steps 12-15.
41. Manipulate valves on milk/CIP circuit so that hot nitric acid solution flows from Tank 2 through the plant returning to Tank 2 in a recycle manner.
42. Repeat steps 29-36.

4.7.2.2 Research Falling Film Evaporator

4.7.2.2.1 Start Up

The generic pilot plant start up procedure used for commissioning trials conducted with the research falling film evaporator was as follows:

1. Inspect control computer ensuring:
    - Milk vat agitator is on.

- Refrigeration automatic control loop is on with set point of 4°C.
- Temperature sensors are functioning correctly.

2. Remove clean evaporator plate from solution of caustic (in which the plate had been submerged overnight).
3. Rinse plate with water.
4. Let plate dry in ambient air.
5. Attach heat flux probes to plate using procedure discussed in Section 4.4.1.
6. Assemble evaporator surface as described in Section 4.3.11.1.
7. Install evaporator surface in casing and tighten flange bolts.
8. Connect flexible hosing to steam condensate pipe from steam chamber.
9. Connect steam and milk inlet pipes.
10. Connect heat flux sensors, RTDs and vacuum sensor wires to junction box above RFFE.
11. Inspect control computer to determine if the sensors in the RFFE are functioning correctly.
12. Fully open laboratory vacuum valve.
13. Initiate automatic control on vacuum pump at a set point of -0.5 bar.
14. Fully open laboratory steam valve to steam chamber.
15. Inspect steam condensate line until flow seen.
16. Half open condenser water inlet valve.
17. Inspect steam condensate/condenser water outlet DSI for flow.
18. Manipulate plate heat exchanger hot side valves so that heating medium is able to pass through PHE proceeding to drain.
19. Fully open laboratory steam valve to heating equipment.
20. Half open plate heat exchanger direct steam injector water valve.
21. Fully open plate heat exchanger direct steam injector steam valve.
22. Manually adjust plate heat exchanger direct steam injector water valve until RTD temperature sensor No. 3 reads 60°C on control computer.
23. Manipulate valves on the milk circuit so that milk passes through the pilot plant in following sequence:
    - Milk vat
    - Milk pump
    - PHE

- DSI 1
- Fouling rig
- Flowmeter
- DTHE
- DSI 2
- CIP Tank 1

24. Turn milk pump on manual control using a frequency set point of 30 Hz.
25. Inspect control computer for a positive flowmeter reading.
26. Adjust DSI 1 system valves so milk and steam are able to flow through one steam injector.
27. Adjust DSI 1 RTD temperature sensor No. 4 set point to 70°C.
28. Initiate automatic control on DSI 1.
29. Adjust DSI 2 system valves so milk and steam are able to flow through one steam injector.
30. Adjust DSI 2 RTD temperature sensor No. 22 set point to 95°C.
31. Initiate automatic control on DSI 2.
32. After RTD temperature sensor No. 22 reaches set point, initiate automatic control on milk pump set to 45 l/h.
33. After milk flowrate reaches set point, open milk inlet valve to evaporator and close milk valve to CIP Tank 1.

Typically trials ran for 30 minutes during which time the development of fouling could be observed on the evaporator plate.

4.7.2.2.2 Shut-down

The generic pilot plant shut-down procedure for commissioning trials conducted with the research falling film evaporator was as follows:

1. Fully open milk valve to CIP Tank 1.
2. Close milk inlet valve to evaporator.
3. Close laboratory steam valve to steam chamber.
4. Close laboratory steam valve to heating.
5. Set value of DSI 1 control valve to 0%.
6. Close DSI 1 system steam injector valve.

7. Set value of DSI 1 control valve to 0%.
8. Close DSI 1 system steam injector valve.
9. Close PHE direct steam injector steam valve.
10. Close PHE direct steam injector water valve.
11. Turn off vacuum pump automatic control.
12. Close laboratory vacuum valve.
13. Close condenser water inlet valve.
14. Stop milk pump.
15. Connect flexible hose from milk collection vessel outlet to mono-pump inlet.
16. Open outlet valve of milk collection vessel.
17. Initiate mono-pump.
18. Turn off mono-pump when vessel empty.
19. Close outlet valve of milk collection vessel.
20. Disconnect flexible hose from mono-pump inlet.
21. Connect flexible hose from condensate collection vessel outlet to mono-pump inlet.
22. Open outlet valve of condensate collection vessel.
23. Initiate mono-pump.
24. Turn off mono-pump when vessel empty.
25. Close outlet valve of condensate collection vessel.
26. If milk still present in the milk vat, ensure agitator paddle motor is turned on and refrigeration control loop set to automatically control milk temperature to 4°C.

4.7.2.2.3 Cleaning Procedure

The generic procedure used to clean the pilot plant after commissioning trials conducted with the research falling film evaporator was as follows:

1. Disconnect DSI pipe from plate heat exchanger.
2. Attach high temperature hose to DSI pipe using union and place end of hose in drain.
3. Fully open laboratory steam valve to heating equipment.
4. Half open plate heat exchanger DSI water valve.
5. Fully open plate heat exchanger DSI steam valve.

6. Manually adjust plate heat exchanger DSI water valve until RTD temperature sensor No. 3 reads 85°C on control computer.
7. Place high temperature hose end in Tank 2 and fill until tank contains approximately 100 l.
8. Remove hose from Tank 2 and measure depth of water.
9. Calculate exact volume of hot water in Tank 2.
10. Based on this volume, calculate quantity of concentrated caustic required to make solution 1.0% caustic.
11. Add required quantity of concentrated caustic to Tank 2.
12. Close plate heat exchanger DSI steam valve.
13. Close plate heat exchanger DSI water valve.
14. Disconnect high temperature hose from DSI pipe.
15. Reconnect DSI pipe to plate heat exchanger.
16. Fill Tank 3 until it contains approximately 350 l of water by opening water valve.
17. Manipulate valves on the milk/CIP circuit so that CIP fluids can pass through the pilot plant in following sequence:
    - CIP Tank 3
    - CIP pump
    - Milk pump
    - PHE
    - DSI 1
    - Fouling rig
    - Milk and CIP flowmeters
    - DTHE
    - DSI 2
    - Evaporator with plate installed
    - Milk collection vessel
    - Condensate collection vessel
18. Repeat steps 4-6 except setting RTD temperature sensor No. 3 to 50°C.
19. Turn on both CIP and milk pump using a set point of 50 Hz for both pumps.
20. Inspect control computer for positive flowmeter readings.

21. Turn off CIP and milk pump when both milk and condensate collection vessels are full.
22. Close plate heat exchanger direct steam injector steam valve.
23. Close plate heat exchanger direct steam injector water valve.
27. Connect flexible hose from milk collection vessel outlet to mono-pump inlet.
28. Open outlet valve of milk collection vessel.
29. Initiate mono-pump.
30. Turn off mono-pump when vessel empty.
31. Close outlet valve of milk collection vessel.
32. Disconnect flexible hose from mono-pump inlet.
33. Connect flexible hose from condensate collection vessel outlet to mono-pump inlet.
34. Open outlet valve of condensate collection vessel.
35. Initiate mono-pump.
36. Turn off mono-pump when vessel empty.
37. Close outlet valve of condensate collection vessel.
38. Manipulate valves on milk/CIP circuit so that hot caustic solution flows from Tank 2 through the plant collecting in evaporator collection vessels.
39. Turn on both CIP and milk pumps using a set point of 50 Hz for both pumps.
40. Inspect control computer for positive flowmeter readings.
41. Turn off CIP and milk pumps when both milk and condensate collection vessels are full.
42. Repeat steps 27-37.
43. Repeat steps 16-37
44. Repeat steps 1-9.
45. Based on this volume, calculate quantity of concentrated nitric acid required to make solution 0.5% nitric acid.
46. Add required quantity of concentrated nitric acid to Tank 2.
47. Repeat steps 12-15.
48. Manipulate valves on milk/CIP circuit so that hot nitric acid solution flows from Tank 2 through the plant collecting in evaporator collection vessels.
49. Repeat steps 39-43.

4.7.3 Commissioning Studies

Table 9.2 of the Appendix gives a summary of all the trials conducted during this research project. The table gives a description of the trials conducted with important process variables listed. Details of all process variables of the trials are given in Microsoft Excel workbooks located in corresponding trial numbered folders of the CD-ROM included in the Appendix.

4.7.3.1 Miniature Plate Heat Exchanger

4.7.3.1.1 Effect of air (Section 5.2.1-5.2.2)

(Run 8) A preliminary run with original fouling rig configuration (milk flowing below test plate) and air bleed installed in all MPHEs.

(Run 16) RTDs were installed in the Swagelok fitting of all MPHEs. The RTD traces were inspected for the effect of air released from heated milk.

4.7.3.1.2 Effect of Probe (Section 5.2.3)

(Runs 1-6) A series of sighter trials were conducted early on in the research program with a single MPHE installed in a simple recycle system. Since these trials were not conducted with the pilot plant, details of experimental set-up and operating conditions are given in the results and discussion section (Section 5.2.3).

4.7.3.1.3 Effect of Aluminium Tape (Section 5.2.4)

(Run 14) A strip (74 x 25 mm) of aluminium tape was placed over the centre of a test plate. The plate was installed in MPHE 3 and photographed after 4 hours of plant operation. No heat flux sensor was installed on the test plate for this trial.

4.7.3.1.4 Effect of Temperature Sensor Design (Section 5.2.5)

(Run 16) A damp cloth was placed on nearby piping, downstream from the RTD on MPHE 1 and MPHE 3. The cloth was removed several minutes later and the RTD trace for each MPHE inspected.

(Run 17) All six MPHEs had two temperature sensors installed. The RTD was installed in the Swagelok fitting while a Type T thermocouple was installed through the flange system of the MPHE which was sealed using 2 silicone gaskets.

4.7.3.1.5 Fouling Deposit Thickness versus Probe Trace (Section 5.2.7)

(Run 9) MPHEs were isolated at irregular intervals in the following order: MPHE 6 – 10 mins, MPHE 5 – 30 mins, MPHE 4 – 68 mins, MPHE 3 – 130 mins, MPHE 2 – 180 mins, MPHE 1 – 253 mins. The thickness of fouling deposit above the probe was measured using the method discussed in Section 4.6.1.

4.7.3.2 Research Falling Film Evaporator

4.7.3.2.1 Control (Section 5.3.1)

(Run 14) A control trial was conducted with the absence of installed heat flux probes. The purpose of this trial was to refine lighting and camera techniques and to establish how readily the evaporator plate fouls.

4.7.3.2.2 Evaporator Trials (Sections 5.3.2-5.3.4)

(Runs 18-20) Three heat flux probes were installed on the steam chamber side of the evaporator plate. The effects of probe attachment and probe interference on evaporator fouling were investigated with these trials.

4.7.4 Fouling Studies

Table 9.2 of the Appendix gives a summary of all the trials conducted during this research project. The table gives a description of the trials conducted with important process variables listed. Details of all process variables of the trials are given in Microsoft Excel workbooks located in corresponding trial numbered folders of the CD-ROM included in the Appendix. Fouling studies were only conducted with the fouling rig.

4.7.4.1 Heated and Unheated Surfaces (Section 6.1)

(Run 10) Milk flowed through the fouling rig with the heating medium flowing through MPHE 1, 5 and 6 (heated surfaces). The heating medium did not flow through the remaining MPHEs (unheated surfaces).

4.7.4.2 Air and Water Start Up (Section 6.2)

(Run 22) MPHEs 1 and 3 filled with water before start up (water start up). The remaining MPHEs were absent of water during start up (air start up).

4.7.4.3 Surface Conditioning by Operational Protocol (Section 6.3)

(Run 13) The heating medium was not flowing through MPHEs 4-6 when the milk flow was initiated. The heating medium flow was initiated in these MPHEs after 7 minutes of plant operation. The heating medium was flowing through MPHEs 1-3 when the milk flow was initiated. The test plates were removed from MPHEs 3 and 6 after 30 minutes of plant operation. Air start up mode was used in this trial.

4.7.4.4 Orientation of Test Plate (Section 6.4)

(Run 21) The fouling rig configuration was manipulated as described in Section 4.3.6. The manipulated rig provided three plate orientations: MPHE 1: horizontal and above the heating medium, MPHE 2: vertical to the heating medium, MPHE 3: horizontal and below the heating medium. Air start up mode was used in this trial.

5 COMMISSIONING STUDIES

5.1 Introduction

This chapter will present results from commissioning trials conducted with the fouling rig and research falling film evaporator.

5.2 Fouling Rig

A number of commissioning trials were conducted with the fouling rig. These included an investigation into the stability of thermal resistances of the MPHE system discussed in Section 3.3. Trials in this series were designed with the aim of determining the effect of each thermal resistance on the heat flux probe measurement (refer to Section 4.7.3.1). Other commissioning trials investigated the effect of operational problems of the fouling rig on the fouling deposit pattern. The following sections will discuss the problems faced and the solutions employed to minimise their effects.

5.2.1 Trapped Air

Air trapped in the fouling rig caused a number of problems. There were two major sources of trapped air; the air present in the rig during start up and the dissolved air released from the heated milk. The first source of air will be discussed in this section while the problem of released air during a trial will be discussed in the following section.

In the initial design of the fouling rig, the milk flowed below the plate as shown in Figure 5.1.

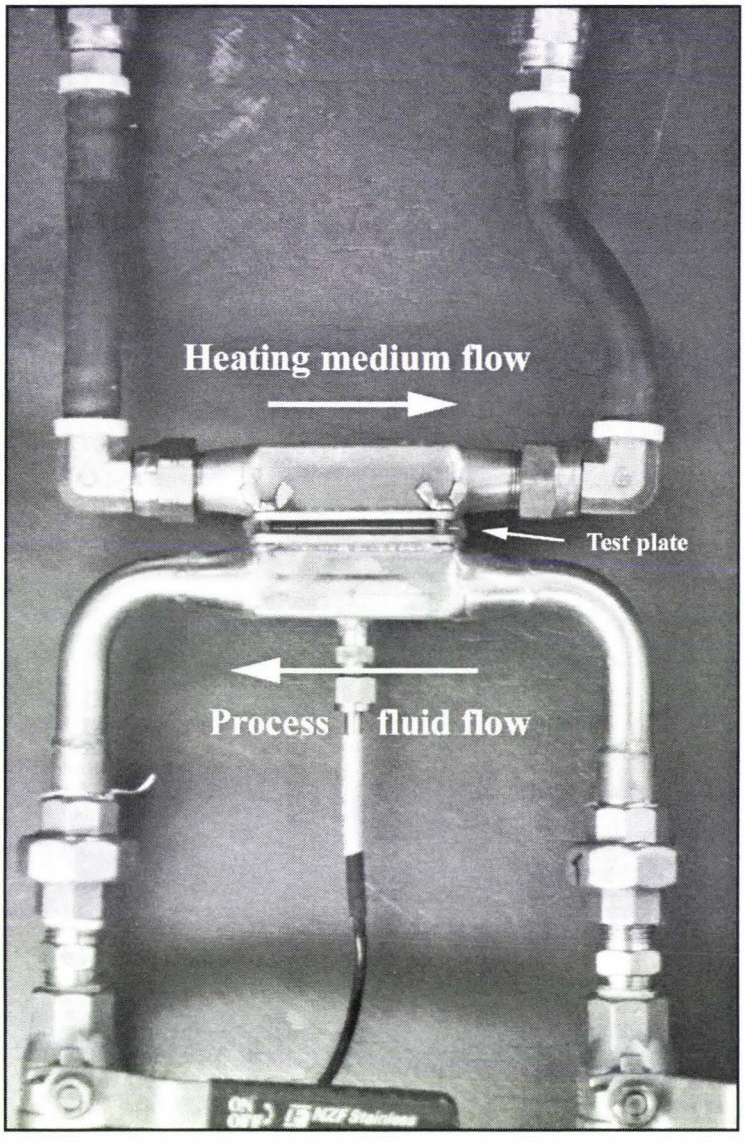

Figure 5.1 Initial configuration of miniature plate heat exchanger

This geometry was adopted because it had been reported that more fouling occurred if the heated surface was situated above the milk stream (Ma and Trinh, 1999). However, in this configuration the fouling modules were higher than the connecting piping legs and therefore the highest point in the milk line was directly underneath the test plate. Since air tends to become trapped at high points in the rig, an air layer between the milk stream and test plate was trapped during start up.

Figure 5.2 shows a trapped air bubble in a module with the test plate replaced by a transparent polycarbonate sheet. Water entered the module at 45 l/h. After 5 minutes, the water was photographed. The photograph clearly shows an air bubble covering a large proportion of the fouling window.

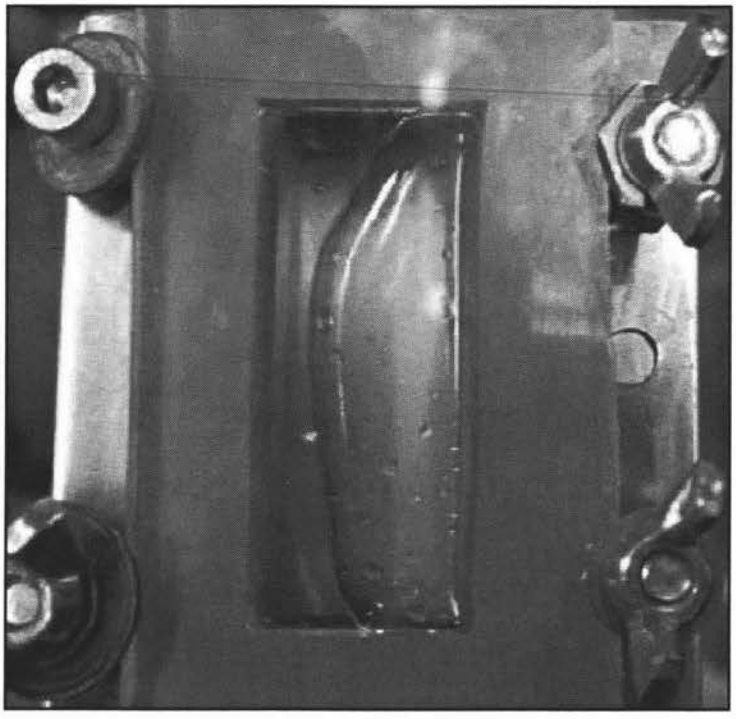

Figure 5.2 Miniature plate heat exchanger showing trapped air bubbles

The air trapped during start up has two major effects. It influences on both the OHTC trace and the fouling deposit. The effect of air on OHTC can be explained by the resistance equation:

$$R_t = R_{ss} + R_p + R_c + R_m + R_f \qquad \textbf{(3.5)}$$

The air adds an extra resistance term which will be called R_a:

$$R_t = R_{ss} + R_p + R_c + R_m + R_f + R_a \qquad \textbf{(5.1)}$$

Assuming thicknesses of resistance layers are constant, an estimation of thermal resistance can be made from the inverse of the thermal conductivity.

$$R \approx \frac{\chi}{\lambda} \qquad \textbf{(5.2)}$$

where: λ = thermal conductivity (W/mK)

χ = thickness of layer (m)

Table 5.1 gives the thermal conductivities and estimated thermal resistance calculated using Equation (5.2) of air, milk and stainless steel at 25°C.

Table 5.1 Physical properties of MPHE materials

Material	Thermal Conductivity (W/mK)	Estimated Thermal Resistance (m^2K/W)
Stainless Steel	150	0.00667
Air	0.0241	41.5
Milk	0.5	2

The thermal resistance of air is considerably larger than milk and stainless steel which means the total resistance was governed by the thermal resistance due to air. Since the air layer was not stable during the runs, the heat flux would fluctuate randomly resulting in the OHTC trace no longer recording only the thermal resistance due to fouling.

The second effect of trapped air was the loss of contact between the milk stream and the test plate. Milk components cannot deposit on the surface unless there is a physical contact. Figure 5.3 shows an example of a test plate fouled by a MPHE with the presence of air bubbles. The large clean patch to the right of the photograph represents a trapped air bubble. The fouling appears to develop around the edges of the bubble. Commonly, one air bubble covered the entire plate resulting in no fouling.

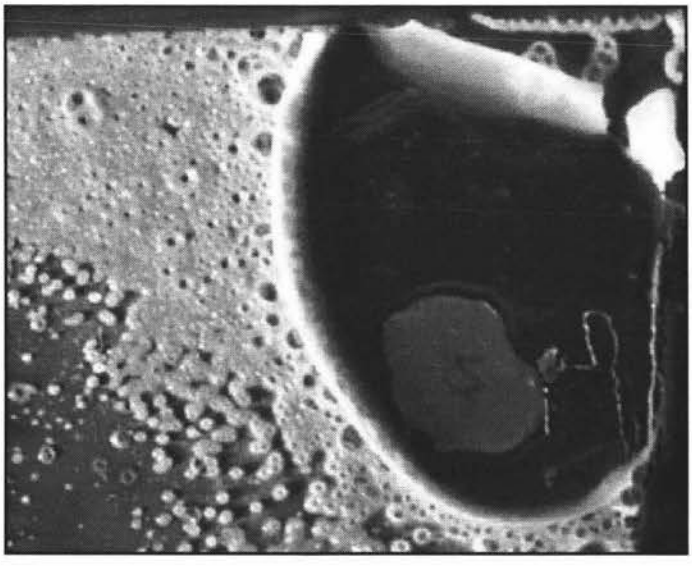

Figure 5.3 Effect of trapped air on fouling deposit

Obviously, the effect of trapped air was significant and required a solution before the MPHE could be used to study fouling. A number of potential solutions were investigated to reduce the effect of trapped air.

Air bleed from the modules:

The first potential solution investigated was the use of an air bleed to continuously remove the air from the MPHEs throughout the run. The MPHEs were individually inspected using the polycarbonate sheet (see Figure 5.2) to establish the location of the trapped air. A hypodermic needle (Becton Dickinson 20G1TW 0.9 X 25 mm, Biolab Scientific Ltd., Auckland, N.Z.) was inserted into the appropriate location of each MPHE as shown by Figure 5.4.

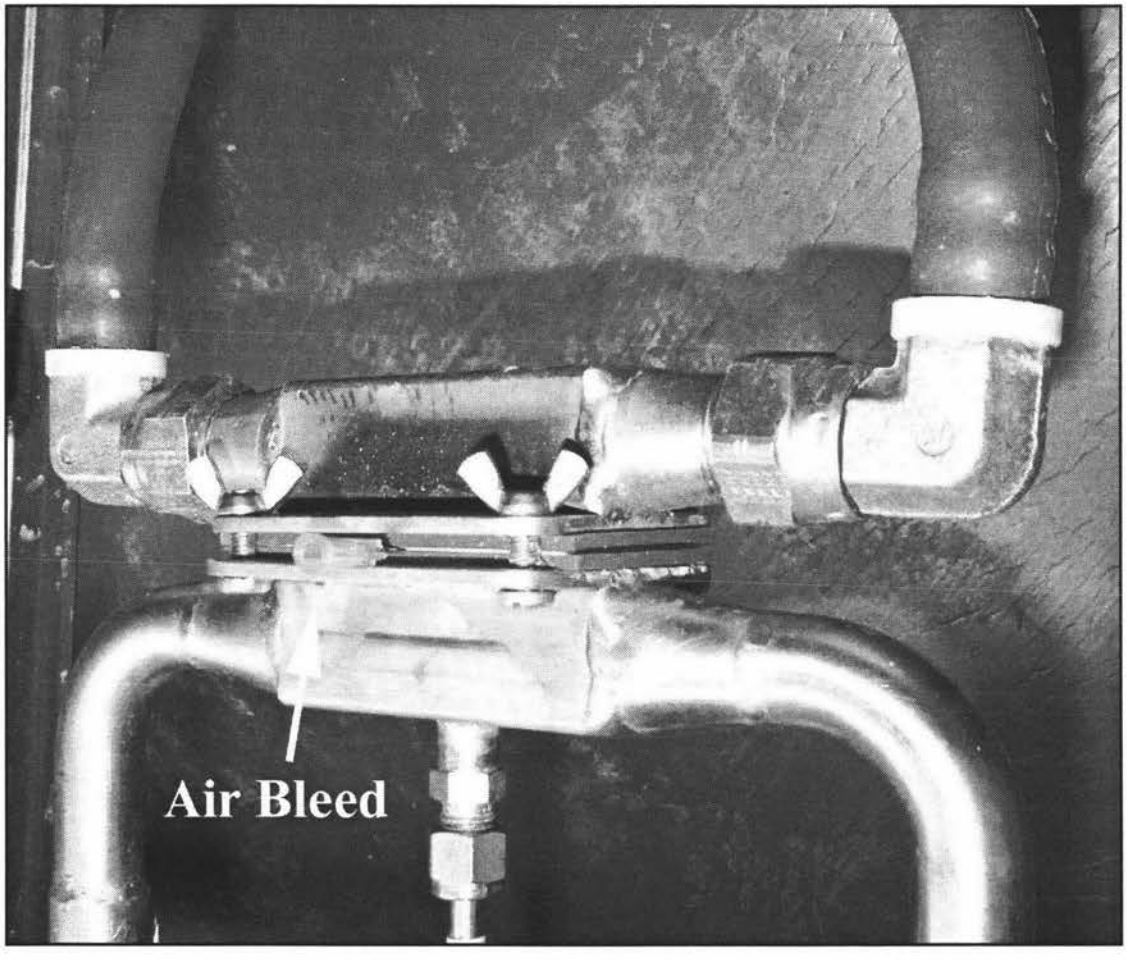

Figure 5.4 Installed air bleed in a miniature plate heat exchanger

The air bleed performed well with respect to removing the trapped air from the MPHEs (runs 7 and 8), but there were disadvantages to this technique. The flow

pattern of milk was modified by the bleed valve resulting in atypical fouling patterns. A foam layer developed on top of the fouling deposit (see Figure 5.5) which was undesirable and the bleed also performed inconsistently between the modules. These variations between modules were undesirable and therefore the bleed technique was abandoned.

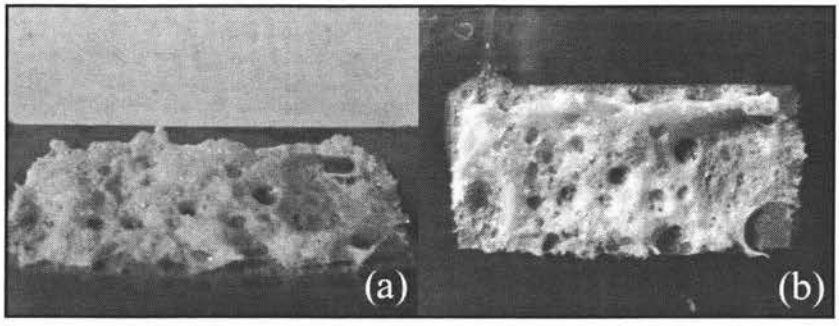

Figure 5.5 Test plate fouled using air bleed technique showing undesirable foam layer (a) side view MPHE 1 (b) plan view MPHE 1 [Run 7]

Inversion of fouling rig:

Another potential method to reduce the effect of trapped air on the fouling deposits and heat flux traces was to invert the rig so that the highest point in the milk line was no longer underneath the test plate. After inverting the rig, the start up air was trapped in the main flow line as indicated by Figure 5.6.

After start up, air was removed through appropriate placed sample ports in the main flow line. An example of a sample port is shown in Figure 5.6. A hypodermic needle and syringe were used to remove the air.

The inverted rig resulted in complete elimination of trapped air underneath the test plate. The rig inversion technique was adopted in all subsequent work.

It may be suggested that air would cause similar problems in the hot water circuit. This was not the case because the flowrate of hot water was relatively high which forced trapped air from the modules soon after start up. Using a high milk flowrate was undesirable because of the cost of milk.

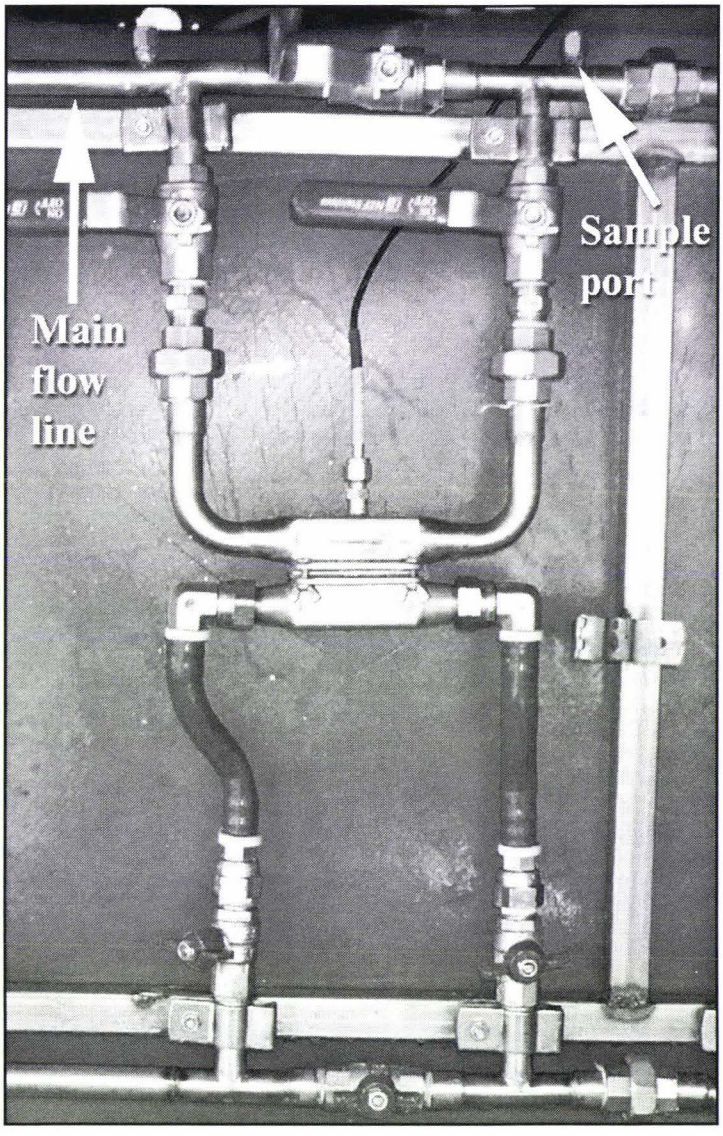

Figure 5.6 Section of inverted fouling rig showing high points (main flow line) and sample ports

5.2.2 Effect of Air Released from Heated Milk

Despite rig inversion air continued to cause problems. Although the trapped air problem had been resolved, air released from the milk during the run influenced the RTD measurements. Figure 5.7 gives the RTD traces installed in the six MPHEs of the fouling rig for run 16. Note that for the first two hours of the run the RTD traces are reasonably constant. Then a sudden decrease occurs in the trace of the RTD of the first module (indicated by (1) in Figure 5.7). Fifteen minutes later a similar decrease occurs in the trace of the second module (2). This change travels down successive modules in the rig at approximately 20 minute intervals.

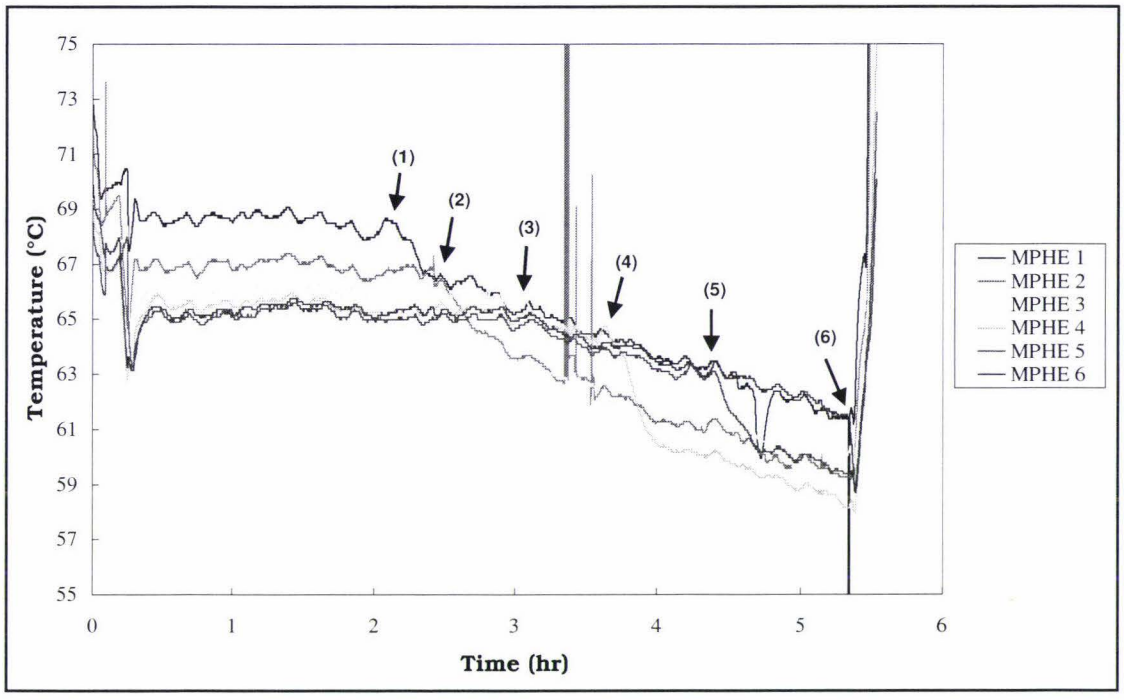

Figure 5.7 RTD trace showing effect of released air [Run 16]

A possible explanation for this trace is offered. When milk is held at 4°C, dissolved air is present within the milk. When the milk is heated, the air is released and travels to high points in the pilot plant. The first high point is situated at the entrance of the fouling rig. Air begins to accumulate at this location at the beginning of the run. This high point eventually fills completely with air released from the heated milk. As milk keeps entering the rig, released air eventually spills over from this location and travels to the next high point. After two hours the released air reaches the first module (point (1) in Figure 5.7). Hence the drop in the RTD trace because the air temperature reflects the temperature of the steel surface which is in contact with ambient air. Eventually the high point in the first module becomes saturated with air and the disturbance travels downstream (points (2)-(6) in Figure 5.7). Figure 5.8 and Figure 5.9 show a prediction of the movement of air through the rig. The influence of the stainless steel mass on the RTD measurements will be discussed in detail in Section 5.2.5.

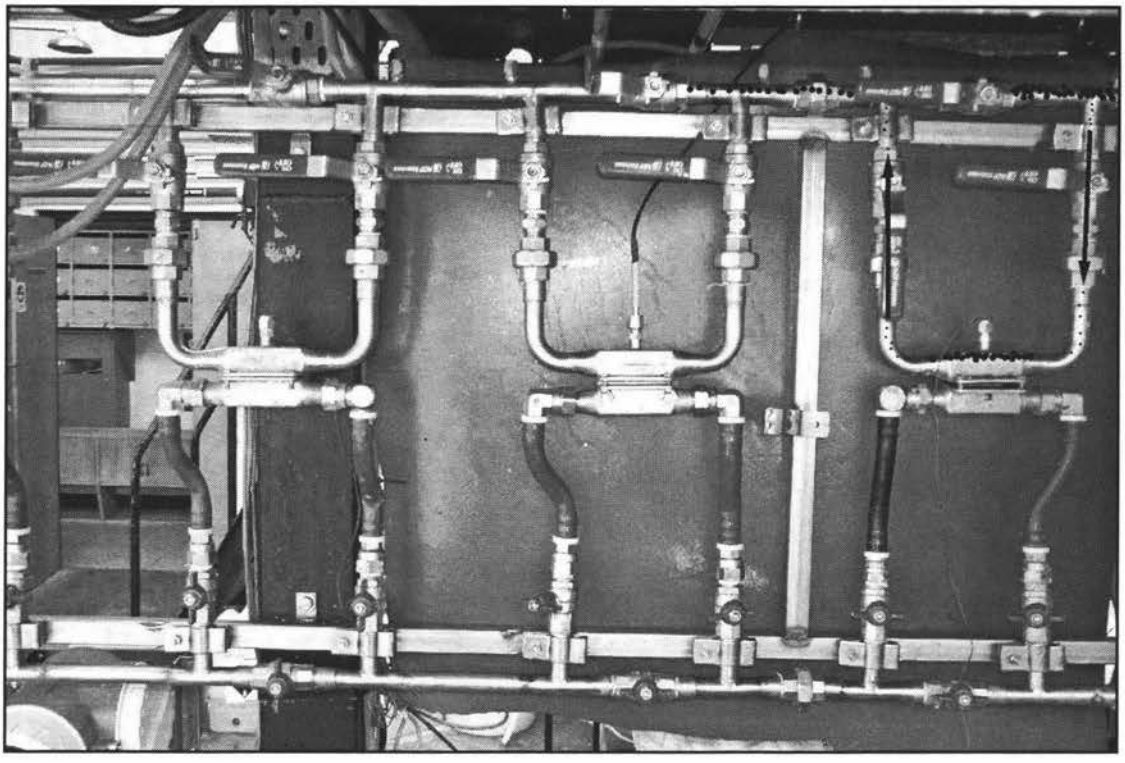

Figure 5.8 Inverted rig showing predicted movement of air (black dots and arrows). MPHE 1 has been saturated in air hence the RTD trace for MPHE 1 was influenced at this point in time. Air has started to collect in the circuit of MPHE 2.

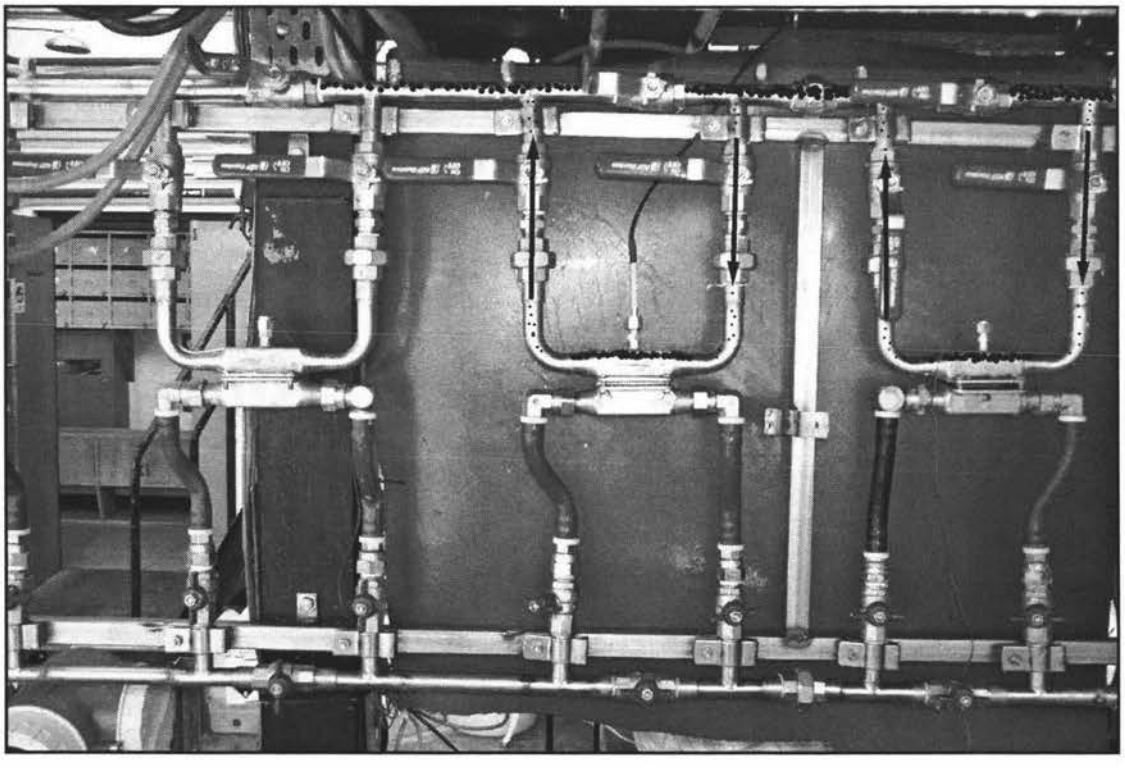

Figure 5.9 Inverted rig 20 minutes later showing predicted air movement (black dots and arrows). Both MPHEs 1 and 2 are now saturated in air hence both RTDs are influenced at this point in time.

To eliminate the problem of released air, a section of pipe was installed at the entrance of the fouling rig. The purpose of this section of pipe was to reduce the flow of air to the fouling rig by introducing a downward section. The downward section meant air could be removed through a sample point upstream from the first DSI. Periodically, a syringe and needle would be used to remove the air at this sample point. To ensure air was completely eliminated from the rig, the syringe and needle was also inserted into the sample ports along the main line periodically during the runs. This technique was adopted for all subsequent work.

5.2.3 Influence of Probe on Heat Flux and Fouling Pattern

The introduction of the probe into a system should not change the heat flux.

$$q = \frac{\Delta\theta}{R_t} \tag{5.3}$$

$$R_t = R_{ss} + R_p + R_c + R_m + R_f \tag{3.5}$$

Ideally, the thermal resistance of the probe and the attachment paste should be as small as possible.

$$R_t >> R_p + R_c \tag{5.4}$$

If the thermal resistance attributed to the probe is high, the fouling deposit directly above the probe may be influenced due to relatively small surface temperatures.

One important side effect of a heat flux probe was its possible interference with normal fouling patterns. It was found in sighter trials (runs 1-6) that both the thickness of the test plate and the mode of heating could lead to probe interference. The sighter trials used a prototype MPHE inserted in a simple recycle system (see Figure 5.10). These trials used thermocouples to measure the process fluid and hot water temperatures. Hot water and milk were pumped co-currently through the MPHE using two pumps. Two water baths were used to heat the hot water and milk separately.

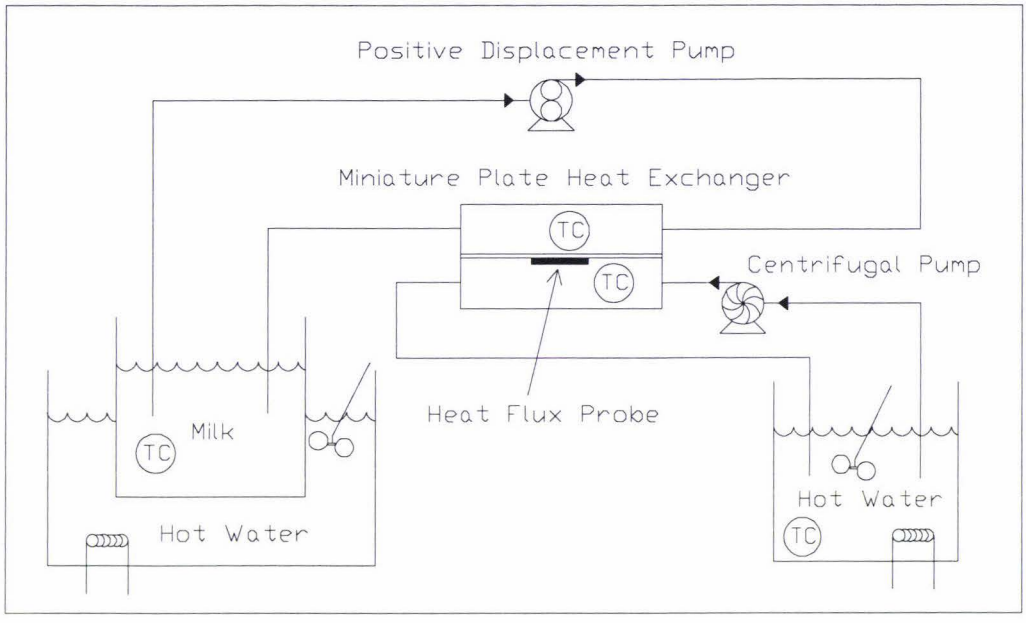

Figure 5.10 Experimental set up for sighter trials [Runs 1-6]

Table 5.2 shows a summary of operating conditions for runs 1-6. Surface fouling mode refers to the condition when the surface temperature is above the denaturation temperature of β-lactoglobulin (65°C), but the bulk liquid temperature is not. Bulk fouling mode refers to the condition when both surface and bulk temperatures are above 65°C as discussed in Section 2.3.3.

Table 5.2 Summary of the operating conditions for Runs 1-6

Run No.	Plate Thickness (mm)	Bulk Liquid Temperature (°C)	Surface Temperature (°C)	Fouling Mode
1	0.06 ± 0.01	61 ± 0.5	79 ± 0.5	Surface control
2	0.06 ± 0.01	63 ± 0.5	80 ± 0.5	Surface control
3	0.06 ± 0.01	62 ± 0.5	79.5 ± 0.5	Surface control
4	0.06 ± 0.01	67 ± 0.5	79 ± 0.5	Bulk control
5	0.06 ± 0.01	66.5 ± 0.5	79 ± 0.5	Bulk control
6	1.55 ± 0.01	58 ± 0.5	79 ± 0.5	Surface control

Figure 5.11 shows photos of the test plates from the six runs. The black rectangles in the photos represent the position of the probe attached to the heating medium side of the plate. Run 1 was a control trial and therefore a probe was not installed on the test plate.

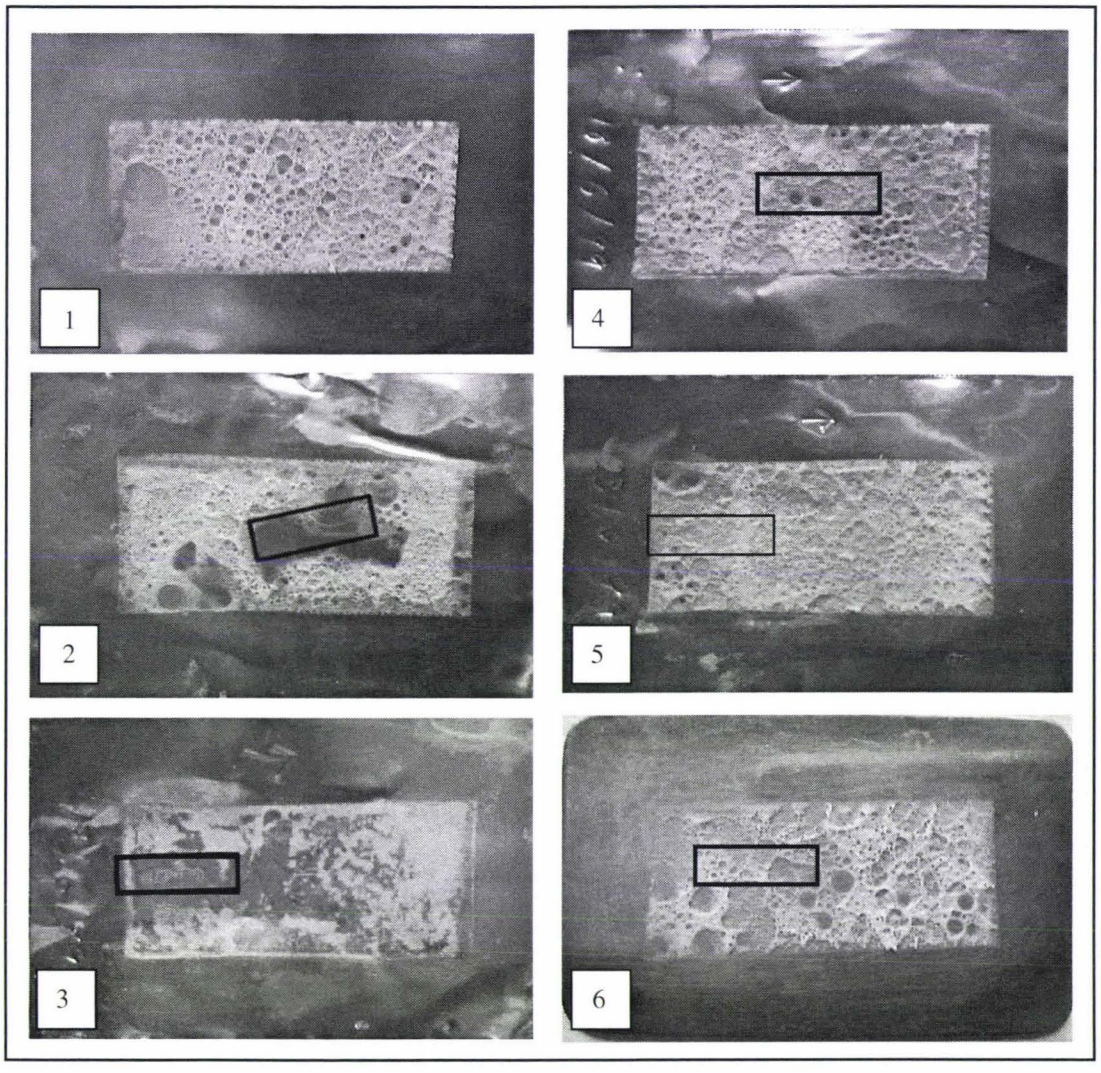

Figure 5.11 Six test plates demonstrating the probe's influence on fouling deposits [Runs 1-6]

The control experiment (run 1) using a 0.06 mm plate under surface fouling mode produced a uniform fouling layer over the entire plate. When the probe was installed using the same plate thickness and fouling mode (run 2), interference in fouling pattern was noted at the location directly above the probe. Repeating the run again (run 3) but moving the probe to the process fluid inlet, resulted in the clear patch also moving to the inlet. When repeating runs 2 and 3 under bulk fouling mode (runs 4 and 5), there was no noticeable interference from the probe. Repeating run 2 with a thick plate of 1.55mm (run 6), there was no apparent clear patch observed.

A thin test plate (0.06 mm) has a smaller thermal resistance than a thick test plate (1.55 mm). Therefore when the test plate is thin the resistance of the probe has a

greater influence on the total thermal resistance of the system. The total thermal resistance of a test plate installed in a MPHE without a heat flux probe is given by:

$$\left[\frac{1}{U_o}\right]_{NP} = R_{ss} + R_m \qquad \textbf{(5.5)}$$

where: $\left[\frac{1}{U_o}\right]_{NP}$ = inverse of overall heat transfer coefficient for a clean plate with no probe (m^2K/W)

The total thermal resistance of a test plate with heat flux probe installed in a MPHE is given by:

$$\left[\frac{1}{U_o}\right]_{P} = R_{ss} + R_m + R_p + R_c \qquad \textbf{(5.6)}$$

where: $\left[\frac{1}{U_o}\right]_{P}$ = inverse of overall heat transfer coefficient for a clean plate with probe (m^2K/W)

If the test plate is thin:

$$R_{ss} << R_p \qquad \textbf{(5.7)}$$

Then

$$\left[\frac{1}{U_o}\right]_{P} >> \left[\frac{1}{U_o}\right]_{NP} \qquad \textbf{(5.8)}$$

Hence

$$q_P << q_{NP} \qquad \textbf{(5.9)}$$

If the test plate is thick:

$$R_{ss} >> R_p \qquad \textbf{(5.10)}$$

Then

$$\left[\frac{1}{U_o}\right]_{P} \approx \left[\frac{1}{U_o}\right]_{NP} \qquad \textbf{(5.11)}$$

Hence

$$q_P \approx q_{NP} \qquad \textbf{(5.12)}$$

A thin film heat flux sensor was chosen to minimise the thermal resistance effect added by the probe but this disturbance cannot be eliminated altogether. It was originally planned to use thin stainless foils as the test plates so that the fouling samples could be left undisturbed on the plates that would then be thin sectioned for microscopic observation. The results of these sighter experiments showed that this is not possible, particularly if the milk temperature is relatively low. Throughout the remainder of the work 0.60 mm thick plates were used.

5.2.4 Influence of Probe Attachment on Fouling Pattern and Heat Flux

Changes in the heat transfer paste layer (R_c) during a run may also introduce error into the heat flux measurement. The method of probe attachment is discussed in Section 4.4.1. Figure 5.12 (a) shows a test plate with a probe installed. Figure 5.12 (b) shows a probe attached to a polycarbonate sheet. The heat transfer paste can be seen to form a uniform layer between the polycarbonate sheet and probe.

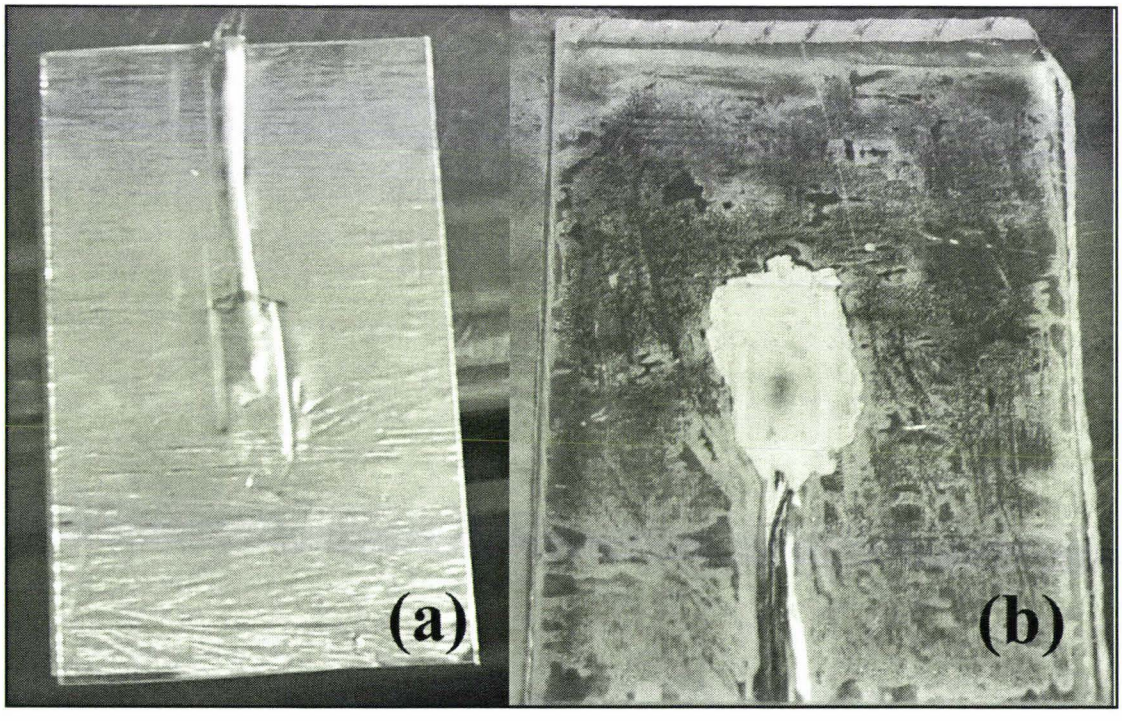

Figure 5.12 Probe attachment (a) heating medium side of test plate showing probe attached with aluminium tape (b) probe attached to polycarbonate sheet showing heat transfer paste layer

The first heat transfer paste used during installation of the heat flux probe was Electrolube non-silicone heat transfer compound (HTC). The paste had a thermal conductivity of 0.9 W/mK and a temperature range of –200°C to 130°C (Electrolube HTC Technical Data Sheet, 1997). The paste was used during initial trials. However, when the probe was removed from the test plate at the end of initial trials the paste had dried out. Therefore the thermal resistance of the paste had changed over the duration of the run. Since the thermal resistance was required to be stable throughout the run, this paste could not be used. A second Electrolube product (silicone heat transfer compound) was then tested for appropriateness.

Silicone heat transfer compound (HTS) had similar properties to HTC except HTS operated over a temperature range of –100°C to +200°C (Electrolube HTS Technical Data Sheet, 1997). Observations at the end of trials using HTS indicated that the paste had not dried out during the run. Therefore HTS was used for the remaining runs.

A second resistance to heat transfer associated with the probe attachment was the thermal resistance introduced by the aluminium tape. This resistance will only have an effect (if any) on the fouling deposit's pattern because the OHTC is calculated using the temperature reported by the thermocouple on the surface of the heat flux sensor not in direct contact with the test plate. Variations in thermal resistance of the aluminium tape are removed from the calculation of OHTC and therefore do not affect the probe's trace.

Initially, the heat flux probes were installed on the test plates using a square section of aluminium tape slightly larger than the probe. This method of attachment may have an effect on the fouling deposit pattern. Therefore, an experiment (run 22) was designed to investigate the effect the aluminium tape on the fouling pattern. Figure 5.13, (a) shows a test plate partially covered by aluminium tape on the heating medium side. The resulting fouling deposit is shown as Figure 5.13, (b). The fouling deposit located directly above the tape (indicated by the white lines) was made up of small islands whereas the deposit covering the rest of the plate had formed a canopy layer. The results of this experiment suggest the added thermal resistance introduced by the tape affects the pattern of fouling.

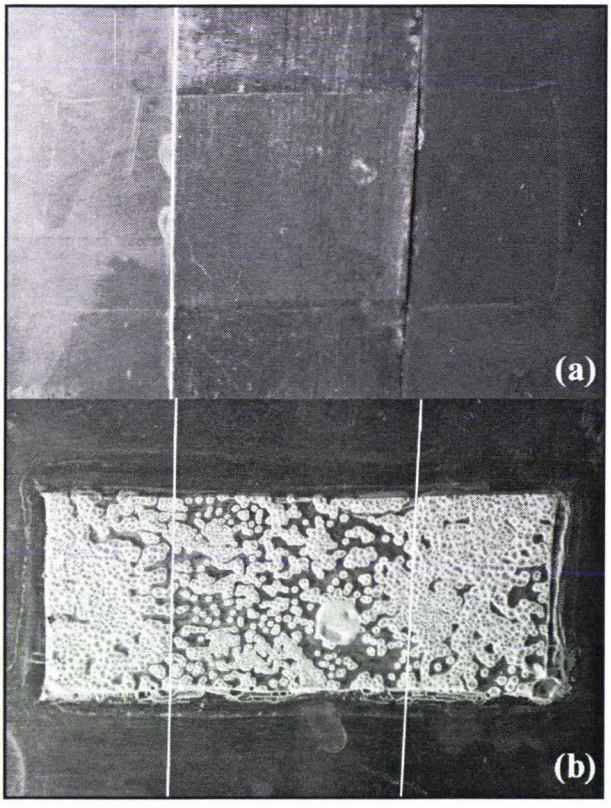

Figure 5.13 Effect of (a) tape attachment on (b) fouling pattern.

There was no other obvious temporary method to secure the probe to the plate. Therefore, to reduce the local effect of the aluminium tape the test plates were covered entirely with aluminium tape on the heating medium side of the plate (as described in Section 4.4.1). Any thermal resistance introduced by the aluminium tape would be constant over the entire area of the plate.

5.2.5 Influence of Temperature Sensor Design on Overall Heat Transfer Coefficient

Calculation of the OHTC requires a measurement of process stream temperature and heating medium temperature as shown in Equation (3.3).

$$U = \frac{q}{\theta_s - \theta_p} \qquad \textbf{(3.3)}$$

The process stream was measured by a RTD and the heating medium was measured by a type T thermocouple mounted on the heat flux surface exposed to the heating medium.

The RTD sensor was placed inside a stainless steel sheath and installed in the MPHE through a Swagelok fitting as shown by Figure 5.14.

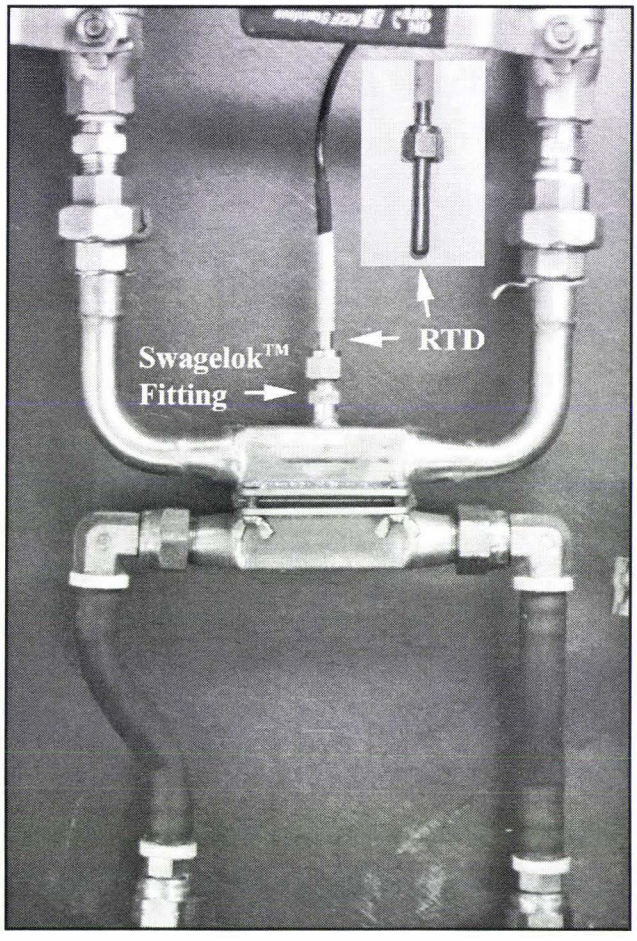

Figure 5.14 RTD installed in miniature plate heat exchanger. Once installed sealed end of RTD was approximately 5mm from the test plate.

Observations made over a period of 2 months suggested that the RTD measurement may not accurately reflect the process stream temperature. A possible explanation for this observation was that thermal conduction was influencing the RTD measurement. An experiment (run 16) was conducted to investigate the possibility of thermal conduction between the pipe steel mass and the RTD. A cloth saturated with cold water was placed on nearby piping downstream, behind the RTD (MPHE 1). The cloth was held in place for several minutes before being removed. This technique was repeated for MPHE 3. Figure 5.15 shows the temperature measurement made by the two RTDs. Clearly, introducing the cloth had an effect on the RTD measurement which indicates that the RTD was in direct contact with the piping mass a phenomenon called bridging.

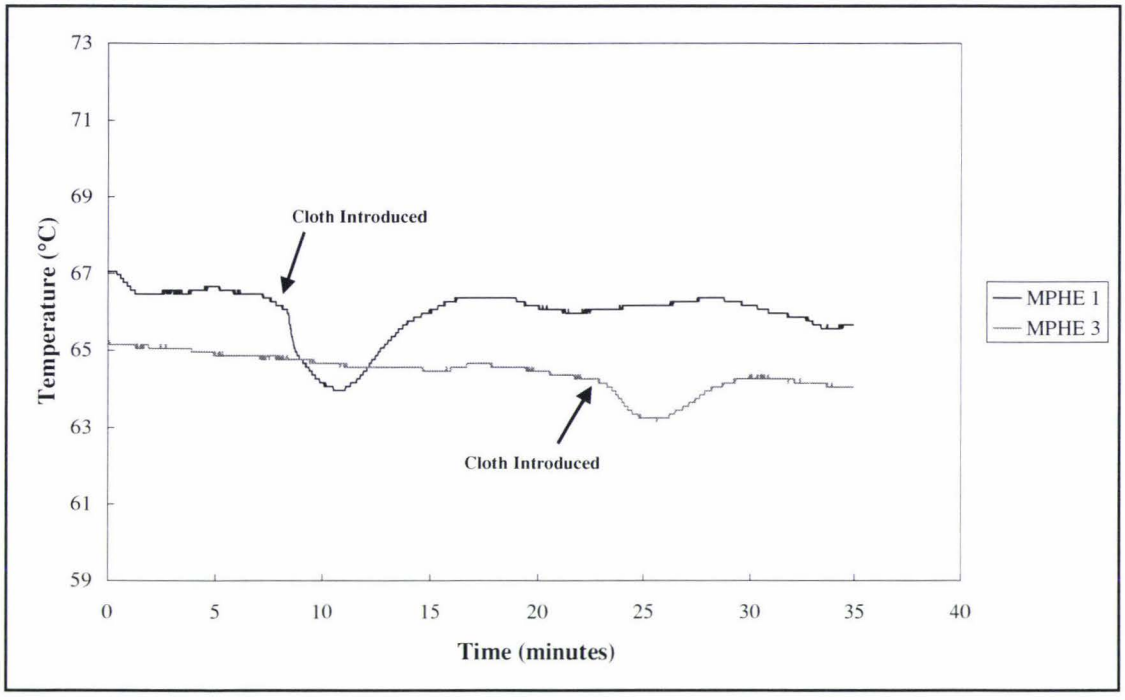

Figure 5.15 RTD trace showing effect of bridging [Run 16]

An o-ring was inserted into the Swagelok fitting to isolate the RTD sheath from the piping. However, the RTD's response still appeared sluggish. An experiment (run 17) was set up to compare the response time and accuracy of the RTDs with Type T thermocouple sensors. The thermocouples used were not housed in stainless steel sheaths and therefore had a smaller thermal mass compared with the RTDs. For this experiment, the RTDs were installed in the Swagelok fitting with o-ring as shown by Figure 5.14. The Type T thermocouple sensors were installed between the test plate and flange of the MPHEs on the process fluid side. Two silica gaskets were used to seal the gap around the thermocouple wire. The thermocouple sensors were therefore completely thermally insulated from the steel piping mass. In any one MPHE, the two temperature sensors were never more than 10 mm apart.

Figure 5.16 shows the trace of temperature measurement made by the RTD and thermocouple for MPHE 1. The thermocouple had a faster response time and measured temperatures, on average, 5-6°C higher than the RTD in this pilot plant. It was established that heat dissipation from the section of the sheath that protruded outside the pipe was responsible for this error.

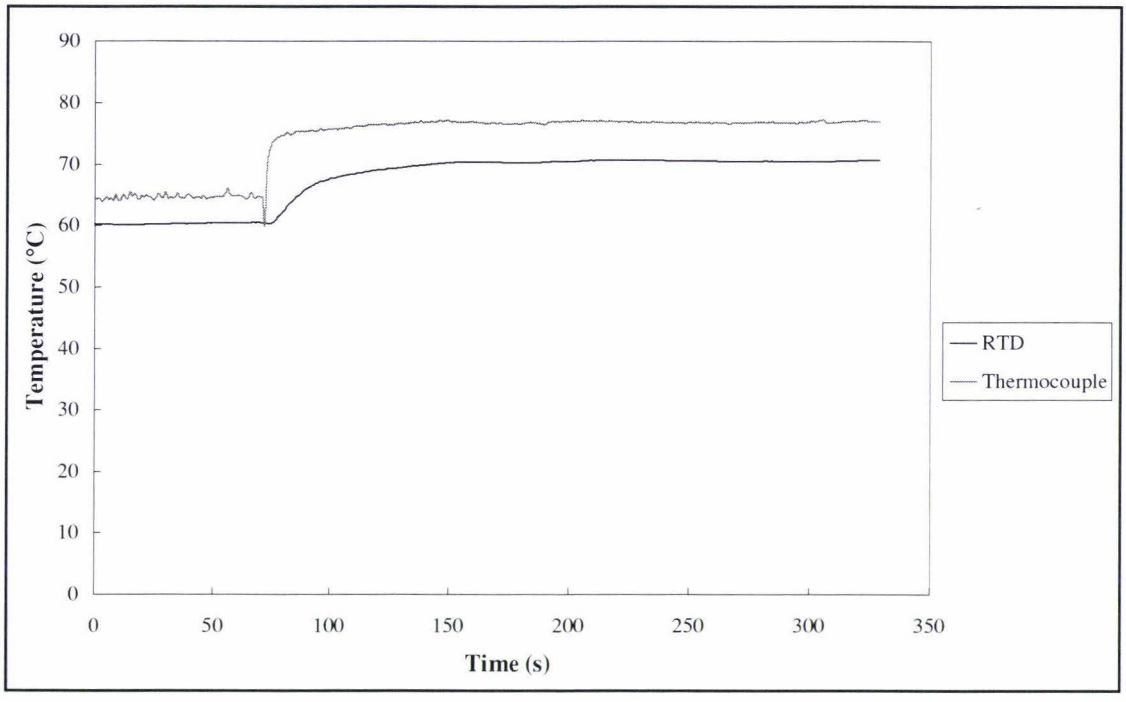

Figure 5.16 Comparison of process fluid temperature as measured by RTD and thermocouple for MPHE 1 [Run 17]

The difference in performance of the temperature sensors was reflected in the overall heat transfer trace. The heat flux measured by the probe for this experiment (run 17) was converted to OHTC using measurements from the two temperature sensors. Figure 5.17 shows the heat flux trace for MPHEs 1 and 2.

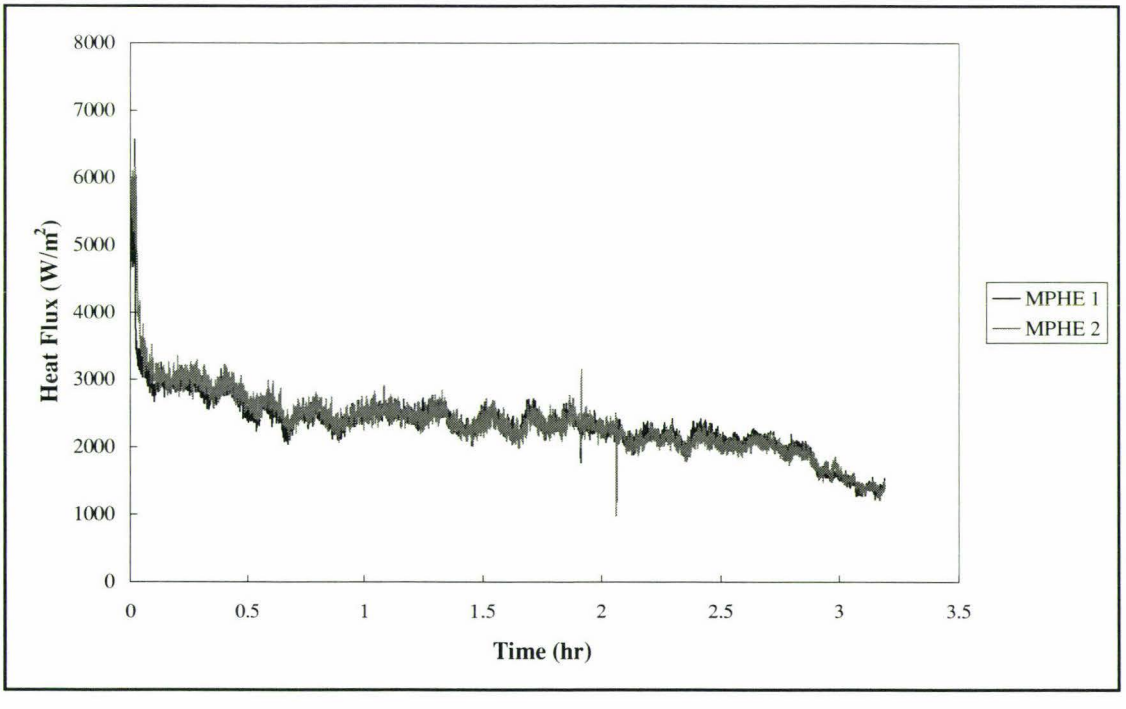

Figure 5.17 Heat flux trace for MPHEs 1 and 2 [Run 17]

Figure 5.18 and Figure 5.19 show the overall heat transfer coefficient traces for MPHEs 1 and 2.

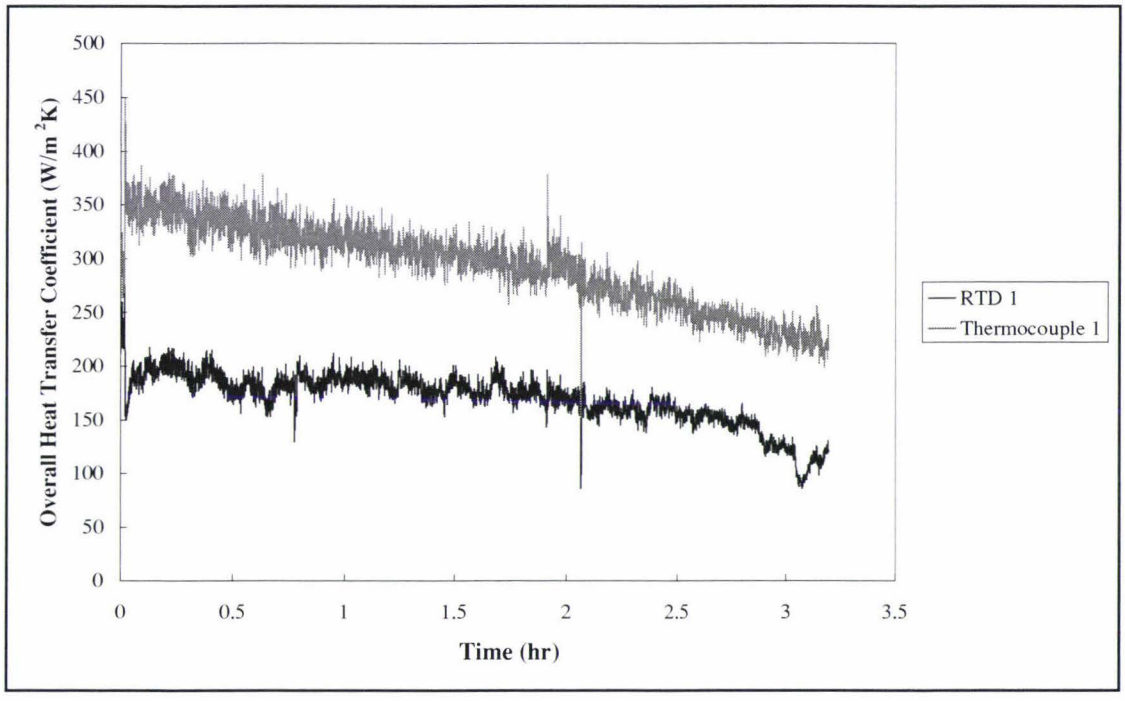

Figure 5.18 Overall heat transfer coefficient calculated by RTD and thermocouple sensor measurements for MPHE 1 [Run 17]

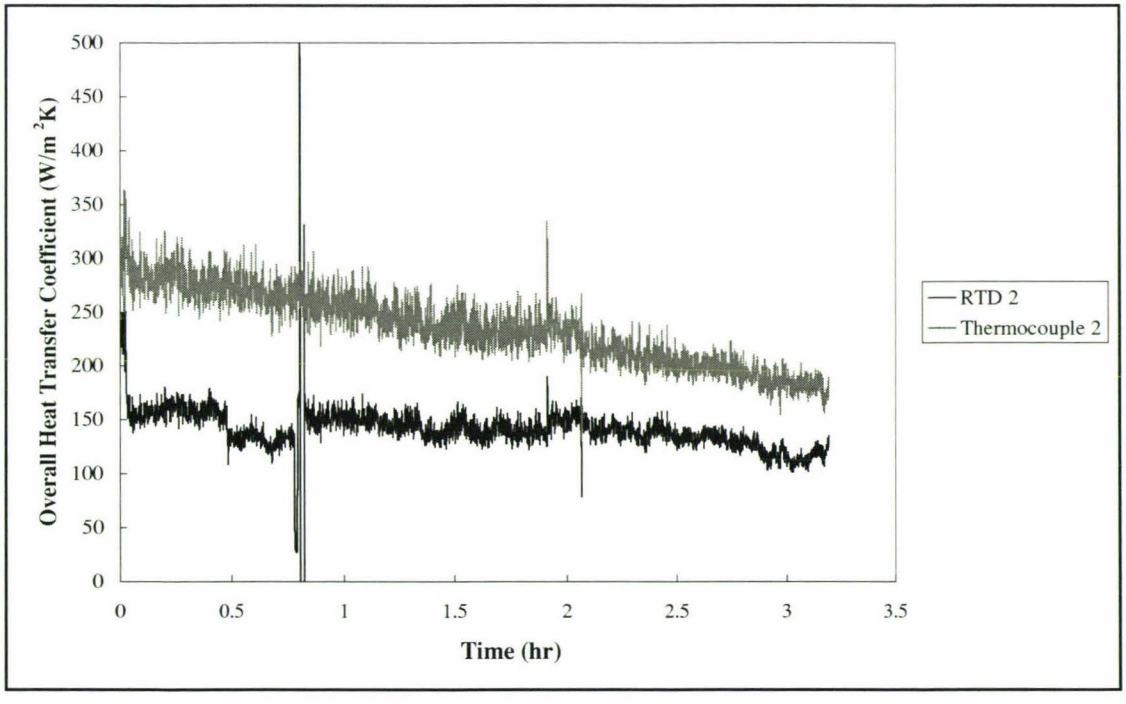

Figure 5.19 Overall heat transfer coefficient calculated by RTD and thermocouple sensor measurements for MPHE 2 [Run 17]

The OHTC was obtained by dividing the heat flux by the driving force. An example calculation is given in the Appendix (Section 9.3). There were several differences between the resulting OHTC traces.

1. The apparent value of the OHTC was higher when the milk temperature was measured with a thermocouple. This reflects the fact that the temperature recorded with the thermocouple was higher than that recorded by the RTD. Therefore the perceived temperature driving force was smaller.
2. The OHTC slope caused by the onset and build up of fouling was higher when calculated by thermocouple temperature measurements.
3. Fluctuations seen in raw heat flux data of Figure 5.17 were smoothed out in the OHTC trace calculated from the thermocouple temperature measurements. These fluctuations were still present in the OHTC trace calculated from the RTD temperature measurements. The wall heat flux is obtained by temperature measurements using a thermopile. The hot side temperature was obtained from the thermocouple attached to the wall heat flux probe. When both hot sides and process sides are measured with thermocouples, the temperature driving force and the measured heat flux are in phase and the OHTC trace is smoothed. When the process fluid is measured with a RTD, the trace lags the hot side temperature because of the slower response of the RTD as shown Figure 5.16. In this situation the measured temperature driving force and heat flux are out of phase and the fluctuations in the heat flux cannot be smoothed out in the OHTC trace.
4. The initial steep decrease was eliminated when calculating OHTC with thermocouple measurements. This may also be explained by the faster response time of the thermocouple. The sharp decrease indicated by the RTD trace is therefore not a true fouling effect but an effect due to slow response of the RTDs.

Clearly, the heat flux sensor operates more effectively when incorporated with a temperature sensor that has a similar response time. This observation was made late in the study, therefore time constraints did not allow previous experiments made with RTDs to be repeated with thermocouples.

Fortunately, although the numerical values of OHTC calculated from the RTD measurements are not reliable, the trend is still observable as shown in Figure 5.18 and Figure 5.19. The results of fouling studies under different operating conditions

could still be analysed with confidence. In addition there were also photographs and thickness measurements to corroborate the trends indicated by the OHTC trace.

5.2.6 Normalisation

Conditions such as process fluid temperature, flow pattern or probe attachment are not identical across modules. Therefore it was not possible to compare overall heat transfer coefficients directly. A solution was to normalise the OHTC by dividing by the original overall heat transfer coefficient U_o at the beginning of the run. This resulted in a normalised overall heat transfer coefficient (NOHTC) which allowed direct comparison between modules. The normalisation process was not perfect because it was difficult to pinpoint the exact start of fouling represented by U_0 because of noise associated with start up. The U_0 value was determined by the value of OHTC at time equal to zero.

$$U_n = \frac{U}{U_0} \tag{5.13}$$

where U_n = normalised overall heat transfer coefficient

U_0 = overall heat transfer coefficient at time equal to zero

To illustrate the effect of normalisation, the data from run 21 will be used. This experiment used three modules with different orientations in series. Thermocouples were used to measure the process fluid stream. Figure 5.20 shows the overall heat transfer coefficient for the three MPHEs used in the experiment. There is a clear difference between the raw values of OHTC for MPHE 3 and MPHE 1 and 2. When the heat transfer coefficient was divided by the original overall heat transfer coefficient value, the difference between the MPHEs was no longer apparent as shown in Figure 5.21.

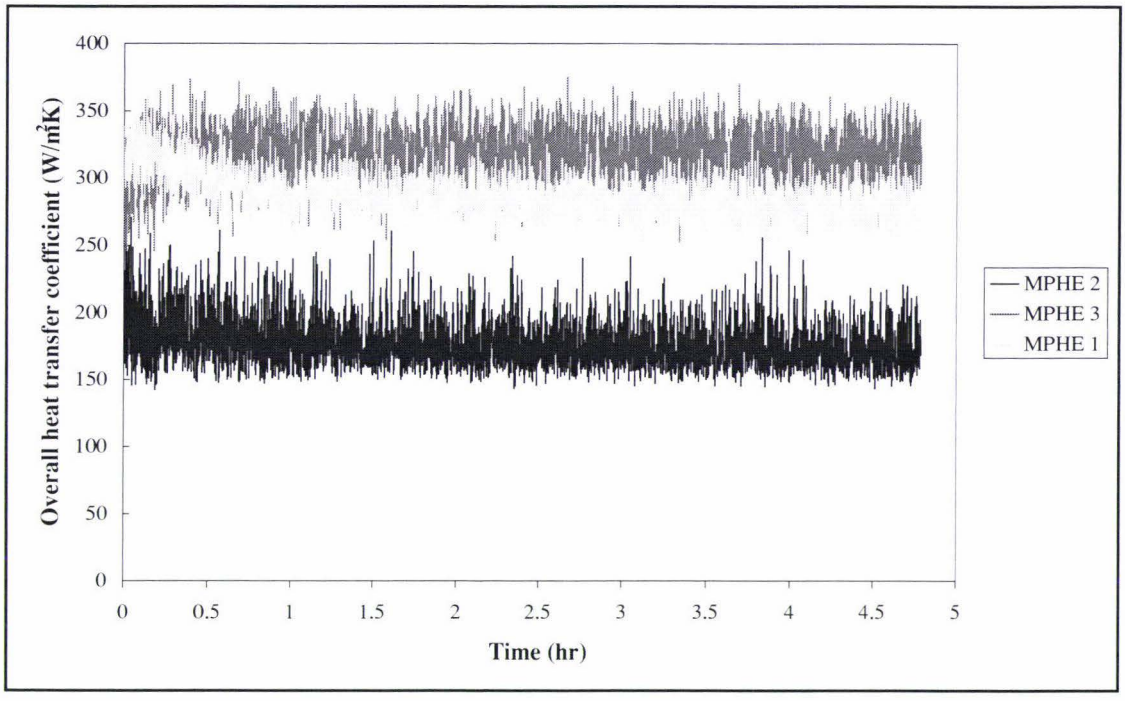

Figure 5.20 Overall heat transfer coefficient showing a difference between MPHE 3 and MPHE 1 and 2 [Run 21]

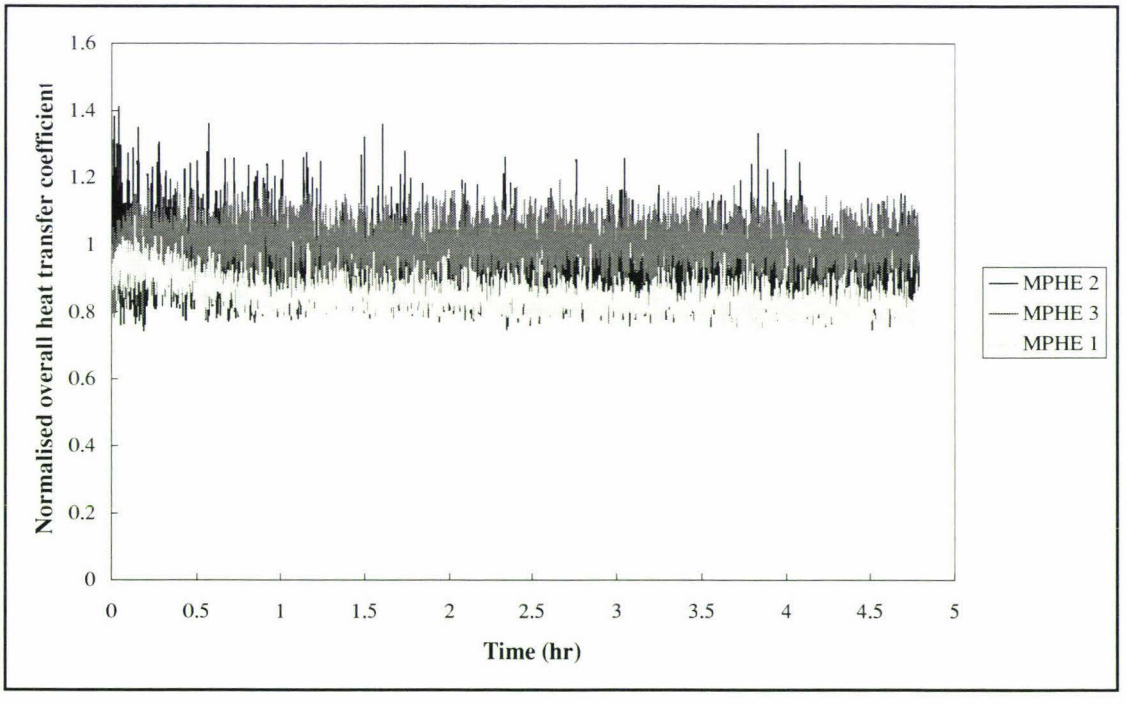

Figure 5.21 Normalised overall heat transfer coefficient showing reduction of difference originally observed between MPHE 3 and MPHE 1 and 2 [Run 21]

Figure 5.21 shows that fouling occurred at the same rate above the probe in all three MPHEs.

5.2.7 Fouling Deposit Thickness versus Probe Trace

An experiment (run 9) was designed that allowed the removal of whole milk fouling deposits on test plates of the MPHE at different stages of development. After a plate had been removed from the fouling rig, an average measurement of thickness was made using the method described in Section 4.6.1. Table 5.3 lists the average fouling deposit thickness measurements for an experiment using whole milk heated at a temperature of 75°C and heating medium at 90°C (run 9).

Table 5.3 Average fouling deposit thickness values [Run 9]

Module No.	Run time (min)	Average Thickness (mm)
6	10	0.150
5	30	0.172
4	68	0.385
3	130	0.801
2	180	0.855
1	253	0.887

Figure 5.22 shows a plot of average fouling deposit thickness over time for run 9.

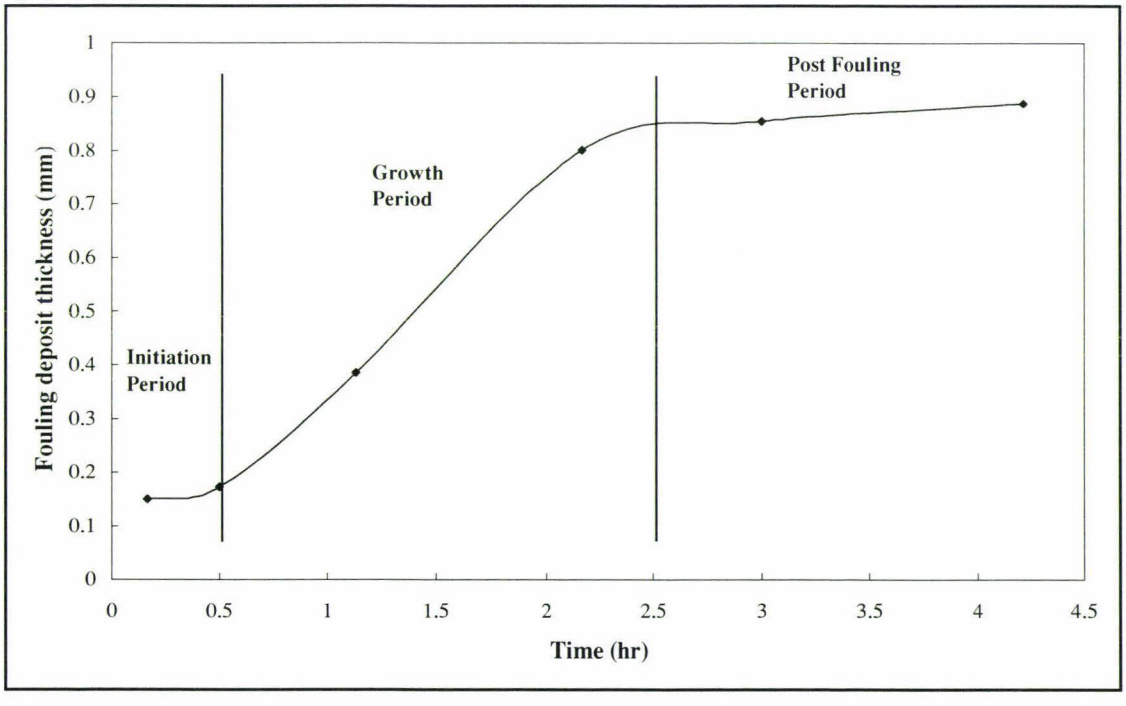

Figure 5.22 The development of a fouling layer with time for milk heated at 75°C [Run 9]

Many authors (Delplace *et al.*, 1994, Bott, 1989) have reported fouling resistance curves with three distinct phases. The authors reported initially, a conditioning or initiation phase where little fouling took place. This was followed by a growth phase where fouling developed at a steady rate. Finally, a post-fouling phase was reported where little change in fouling resistance was noted. The measurements of average thickness obtained here show three distinct phases (Figure 5.22) and corroborate deductions of Delplace *et al.* 1994, and Bott 1989 made for OHTC traces. Little growth occurred during the first 30 minutes, followed by a steady fouling thickness increase for two hours. Finally, the last two hours showed a relatively small change in thickness relating to the post-fouling time period.

Each test plate in Run 9 had a heat flux probe installed. Figure 5.23 shows the NOHTC trace for the six test plates used in the trial. The numbers on the plot indicate the point of test plate removal. Each trace shows a reduction in normalised heat transfer coefficient, indicative of fouling.

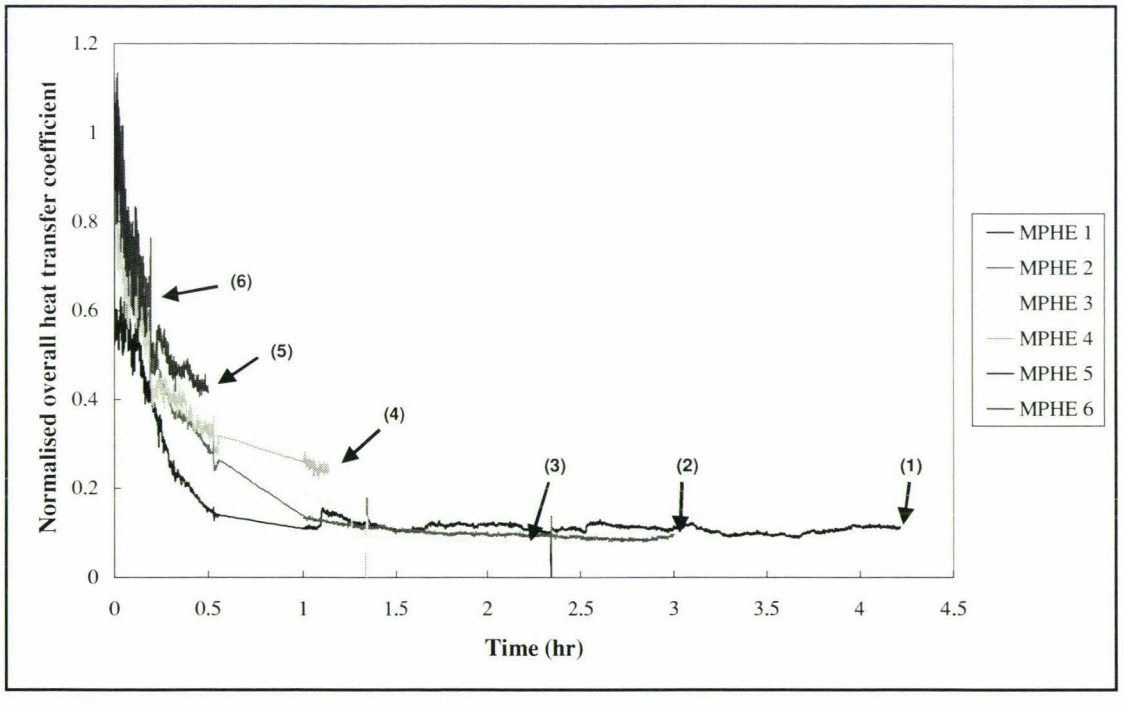

Figure 5.23 Normalised heat transfer coefficient showing times of test plate removal [Run 9]

An attempt was made to compare the magnitude of OHTC change with fouling deposit thickness. The thermal fouling resistance (R_f) value was calculated for each

test plate at time of removal. A sample calculation of R_f is provided in the Appendix (Section 9.4). Figure 5.24 shows the thermal fouling resistance (R_f) as calculated by Equation (3.7) versus the fouling deposit thickness. The results suggest a linear correlation between thermal fouling resistance and fouling deposit thickness.

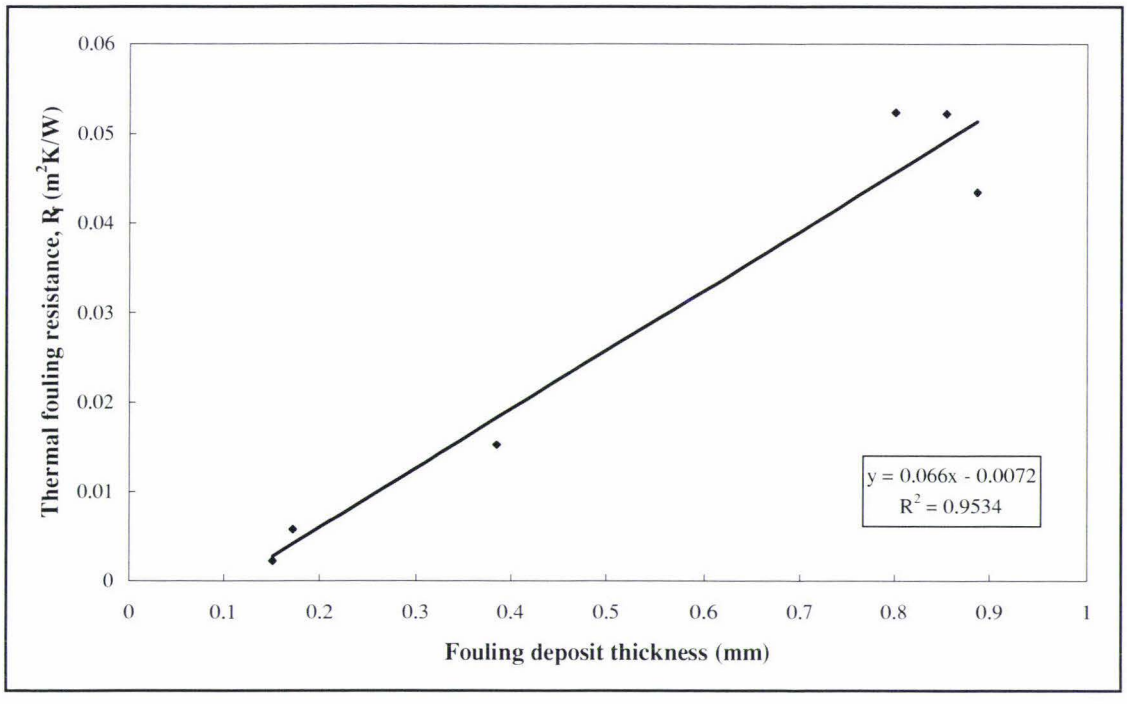

Figure 5.24 Thermal fouling resistance versus fouling deposit thickness of whole milk heated in a miniature plate heat exchanger at 90°C [Run 9]

In summary, the heat flux sensor appears to give clear indications of the rate and extent of the fouling process. Provided the sensor can be incorporated with a temperature sensor of similar sensitivity, the probe would be an ideal method of locally detecting the rate and presence of whole milk fouling in industry.

5.2.8 Types of Fouling Layers Obtained from the MPHEs

Before presenting the results from fouling studies conducted with the MPHEs, a summary of types of fouling deposits obtained using the MPHE is offered. It was possible to differentiate between two types of fouling layers in the deposit called here "bottom" and "top" layers. The bottom layer will not be called an initiation layer described in published literature (Delsing and Hiddink, 1983; Fryer, 1989; Foster and Green, 1990; Foster *et al.*, 1989; Belmar-Beiny and Fryer, 1993) because of uncertainties associated with the equivalence of the two layers. Time constraints did

not allow a composition analysis of the bottom layers to be conducted and therefore no comparison can be made between the bottom layers obtained in the current research and initiation layers mentioned in literature. The bottom layer is so named because it was directly in contact with the heated surface, while the top layer developed on top of the bottom layer. Figure 5.25 shows examples of a bottom fouling layer and a top fouling layer.

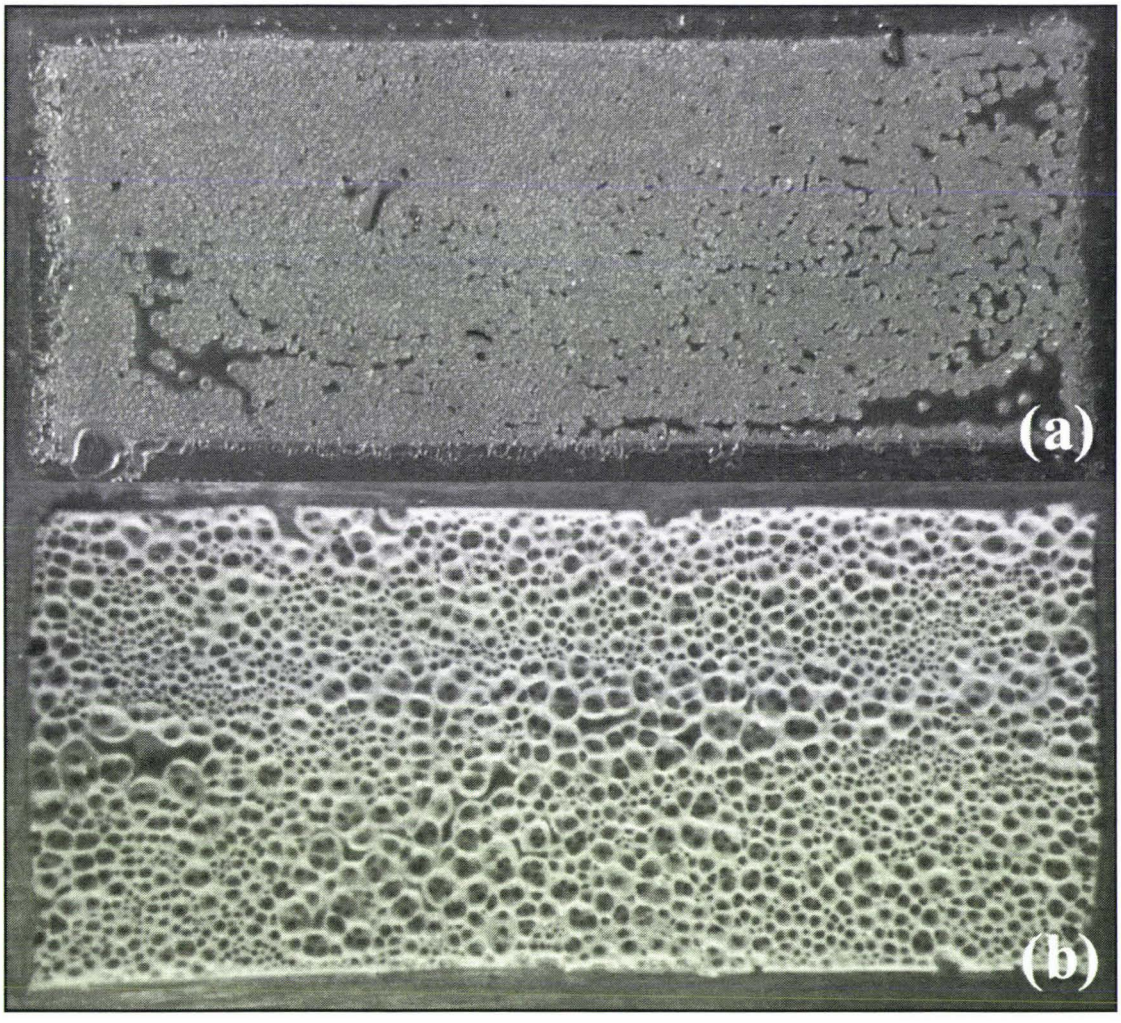

Figure 5.25 Types of fouling layers (a) bottom and (b) top

Two types of top layer fouling were observed, which will be called "canopy" and "island" fouling. An example of island fouling is shown as Figure 5.26. Figure 5.27 is an example of canopy fouling. The canopy pattern occurred when the entire fouling window was covered with deposited material while island fouling referred to a fouling pattern where distinct islands are observed.

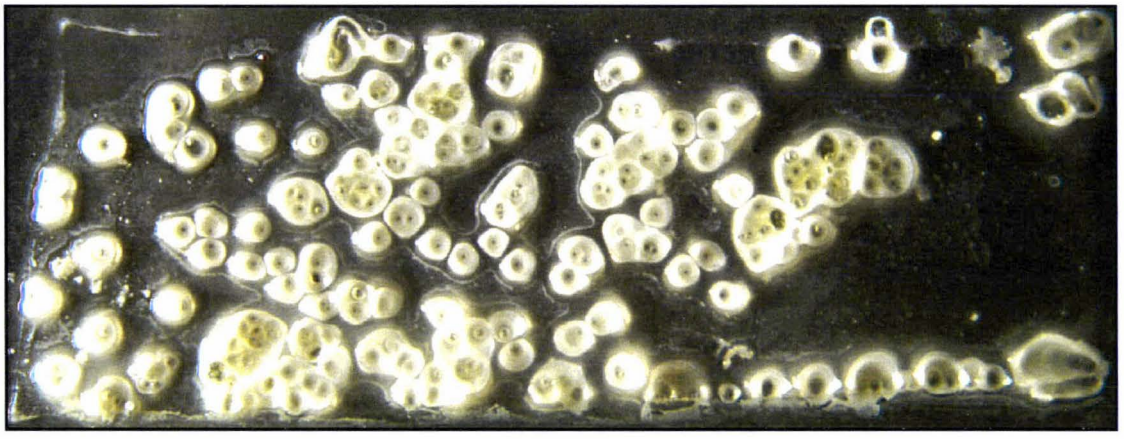

Figure 5.26 Island fouling pattern

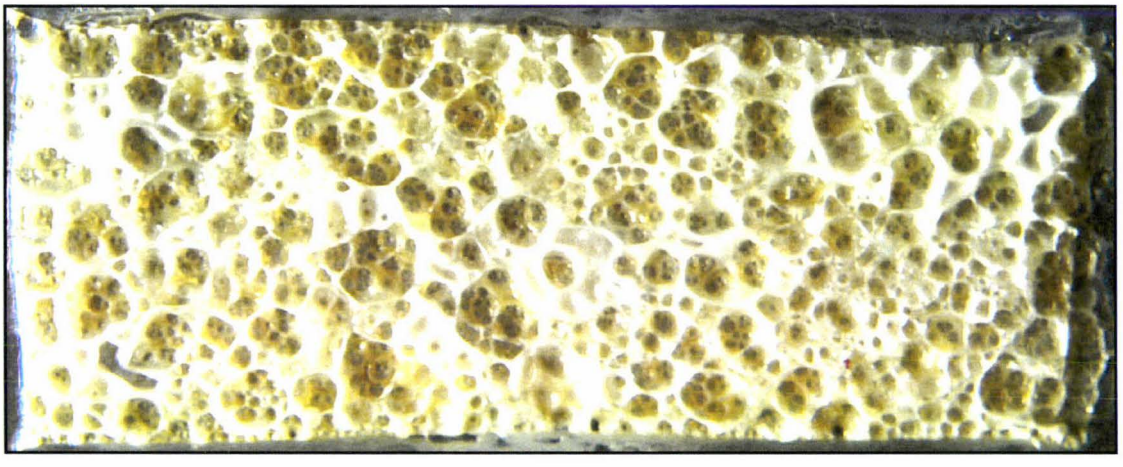

Figure 5.27 Canopy fouling pattern showing colour difference between top and bottom layers

Another visual observation made was differences in colour of the fouling layers. The bottom layer was usually a golden brown colour which may be attributed to the Maillard reaction. The bottom layer was closest to the heated surface and since it was deposited first, had a longer exposure time to hot temperatures. The longer exposure time may explain why the Maillard reaction was restricted to the bottom layer. The top layer was usually a creamy white colour. This layer was not in direct contact with the heated surface and thereby was less exposed to high temperatures. Therefore within the fouling run duration, the Maillard reaction may not have had enough time to act on the top layer. Figure 5.27 shows an example of a fouling deposit with top and bottom layers present.

5.3 Research Falling Film Evaporator

Commissioning experiments were carried out to ascertain the usefulness or otherwise of the research falling film evaporator. Trials were conducted to investigate the stability of resistances within the RFFE system discussed in Section 3.3. Time constraints precluded detailed studies of fouling kinetics.

Both visual observations and quantitative measurements were used during these runs. Digital photography was used to capture images of the fouling deposit at the conclusion of each run and heat flux sensors located on the steam side of the evaporator plate provided real-time measurements of fouling build-up.

5.3.1 Milk Fouling Deposit on Evaporative Surface

A control trial (run 14) was conducted with the absence of installed heat flux probes. The purpose of this trial was to refine techniques of camera work and lighting. Since, this trial was the first to be conducted, a secondary objective was to determine if fouling would develop on the evaporator plate. Milk entered the weir box at 85°C with a flowrate of 60 l/h. The pressure of the evaporator system was –0.35 bar. The trial duration was 15 minutes.

Figure 5.28 shows a photograph of the fouling deposit on the evaporative surface after run 14. A uniform deposit was present over the entire surface heated by the steam chamber. Fouling was not observed on the area of evaporator plate in front of the weir box. The structure of the RFFE fouling was more compact than that observed for the MPHE fouling (see Figure 5.27). The MPHE fouling tended to be soft and moist whereas the RFFE fouling was hard and compact. The bottom and top layers and two different colours observed with MPHE fouling (see Section 5.2.8) was not observed with fouling deposited on the evaporative surface of the RFFE.

Fouling started to develop immediately after the milk flowed over the evaporative surface. Hence, the research falling film evaporator readily allows induction of fouling on evaporative surfaces.

Figure 5.28 Section of evaporator plate of research falling film evaporator showing uniform fouling layer [Run 14]

5.3.2 Influence of Heat Flux Probe on Fouling Pattern

The heat flux probe when installed in the RFFE adds extra thermal resistance to the evaporator plate in the same way as was shown with the MPHE (see Section 5.2.3). Thus the total thermal resistance of the system:

$$R_t = R_{ss} + R_p + R_c + R_m + R_f \qquad \textbf{(3.5)}$$

where: R_{ss} = heat transfer resistance contributed by stainless steel plate (m^2K/W)

R_p = heat transfer resistance contributed by probe (m^2K/W)

R_c = heat transfer resistance contributed by cement (m^2K/W)

R_m = heat transfer resistance contributed b y milk (m^2K/W)

R_f = heat transfer resistance contributed by fouling (m^2K/W)

The added thermal resistance due to the probe is especially important in evaporator fouling studies because any reduction in surface temperature may cause atypical evaporator fouling patterns. Since it was shown that the RFFE fouls readily (see Section 5.3.1), any influence on the fouling pattern made by the introduction of the heat flux probe would be visibly recognisable.

Three experiments (runs 18, 19 and 20) were conducted with three installed heat flux probes. Probes were positioned on the back of the evaporative surface within the steam chamber heating area. The three probes were installed at the top, middle and bottom of the steam chamber using the method described in Section 4.4.1. The probes were not removed between these runs i.e. the probes remained in the identical location for all three runs. There was an RTD installed inside the milk weir (corresponding to the top probe) and an RTD installed at the milk outlet from the RFFE (corresponding to the bottom probe). There was no complementary temperature measurement of process fluid for the middle probe. For this reason, the output from the middle heat flux probe was not used to calculate NOHTC.

In practice RTDs could be used in the evaporator because they were not in contact with the metal mass of the pilot plant and therefore were not subject to heat loses by conduction as observed with the RTDs installed in the MPHEs (see Section 5.2.5).

Since the RTDs were installed in the evaporator's acetal covers, they were thermally insulated from the stainless steel evaporator casing. Figure 5.29 shows the temperature changes recorded by the RTDs and heat flux probes' thermocouples (TC) for run 19.

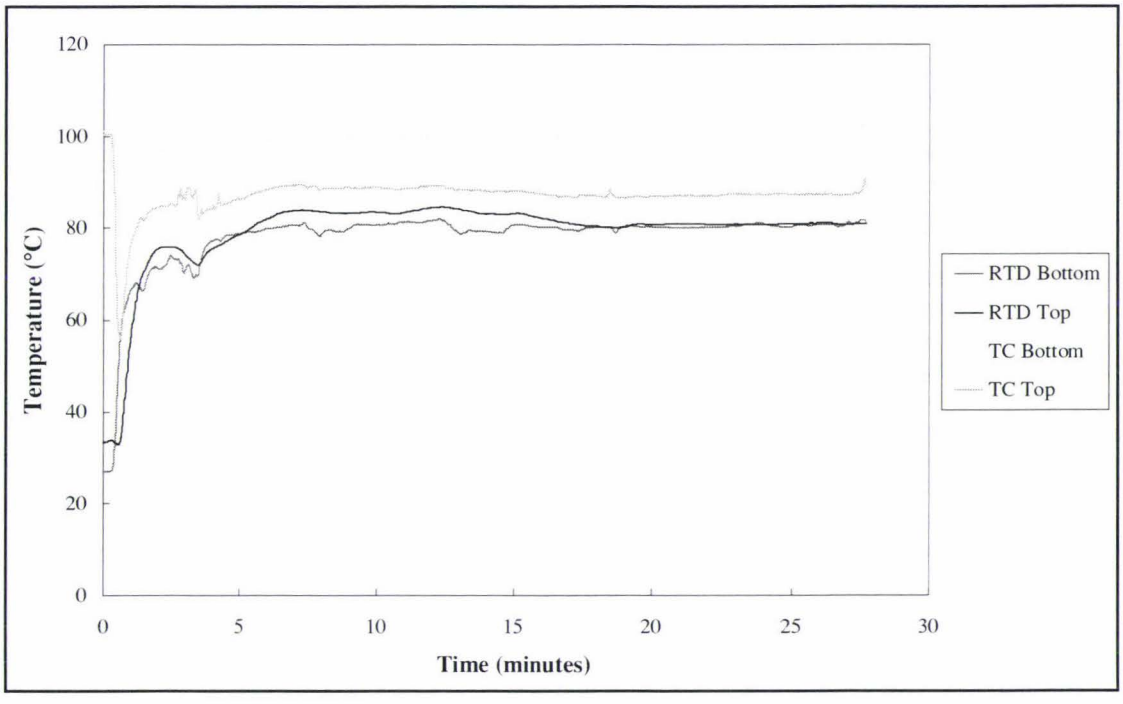

Figure 5.29 Changes in temperature during the operation of the RFFE [Run 19]

The RTD installed at the bottom of the RFFE recorded temperatures lower than those recorded by the RTD immersed in the milk weir (top RTD). The top RTD trace was smooth while RTD bottom trace fluctuated (Figure 5.29). These observations can be explained by the fact that the RTD installed at the bottom of the RFFE was not immersed completely in liquid during the entire run time whereas the top RTD was completely immersed for the entire run duration.

Initially, the heat flux probe's thermocouples recorded a temperature of 100°C before the milk flow was initiated for run 19 (Figure 5.29). Once milk flow commenced the top thermocouple stabilised at a temperature of 87°C while the temperature recorded by the bottom probe stabilised at a temperature of 100°C. This observation was not expected because the temperature of the steam was 100°C (the temperature the heat flux probe's thermocouples were recording). Two reasons are offered to account for these temperature discrepancies:

1. Poor distribution of steam within the steam chamber. The design of the steam inlet (see Section 4.3.11.1) may provide poor distribution of steam within the steam chamber. The thermocouple temperature recordings (Figure 5.29) suggest less steam was present at the top of the steam box compared with the bottom.
2. Influence of milk temperature on thermocouple readings. The milk enters the RFFE at a temperature of approximately 80°C, by the time it reaches the top thermocouple a small amount of heating has occurred. However when the milk reaches the bottom thermocouple, the milk has reached its maximum equilibrium temperature and therefore has no influence on the temperature measurement made by the thermocouple. This hypothesis is supported by the fact that the middle heat flux probe's thermocouple reading was between that of the top and bottom thermocouple readings as shown by Figure 5.30.

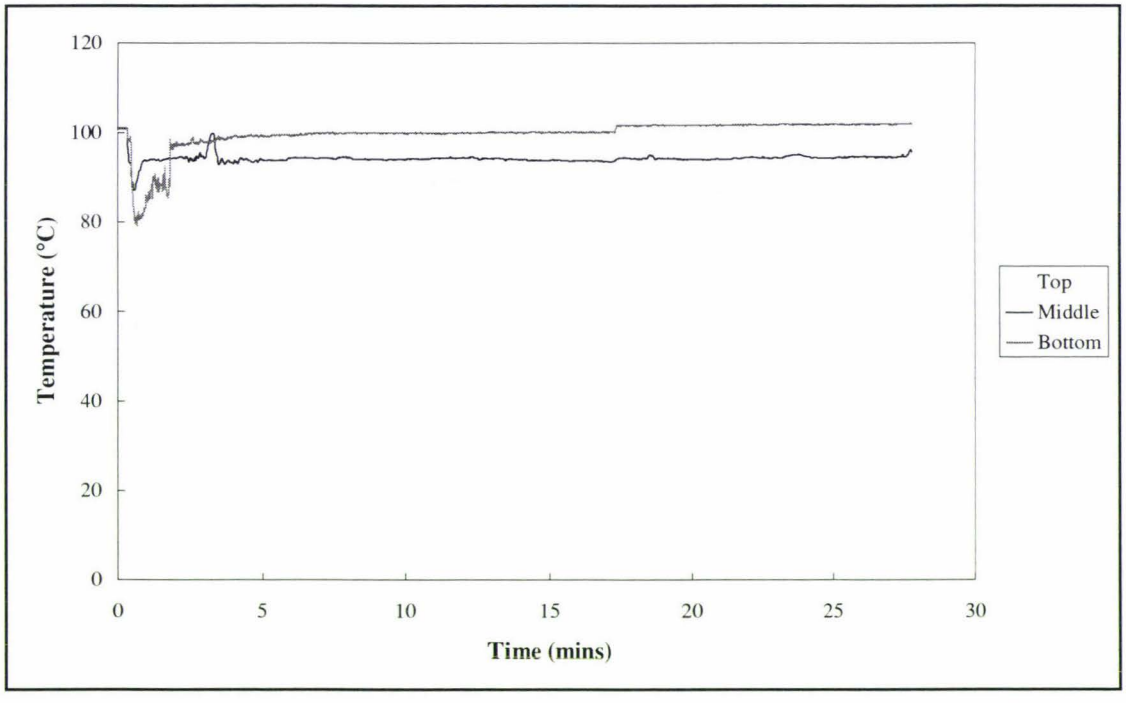

Figure 5.30 Temperature gradient over length of evaporator plate as recorded by thermocouples of the heat flux probes [Run 19]

Regardless of which reason caused the reduction in temperature at the top thermocouple, the temperature of surface at the location of the top heat flux probe's thermocouple was less than the rest of the plate. This temperature reduction will have an effect on fouling directly above the heat flux probe. Figure 5.31 shows the

surrounding area of the evaporator plate at the location of the top heat flux probe for runs 19 and 20.

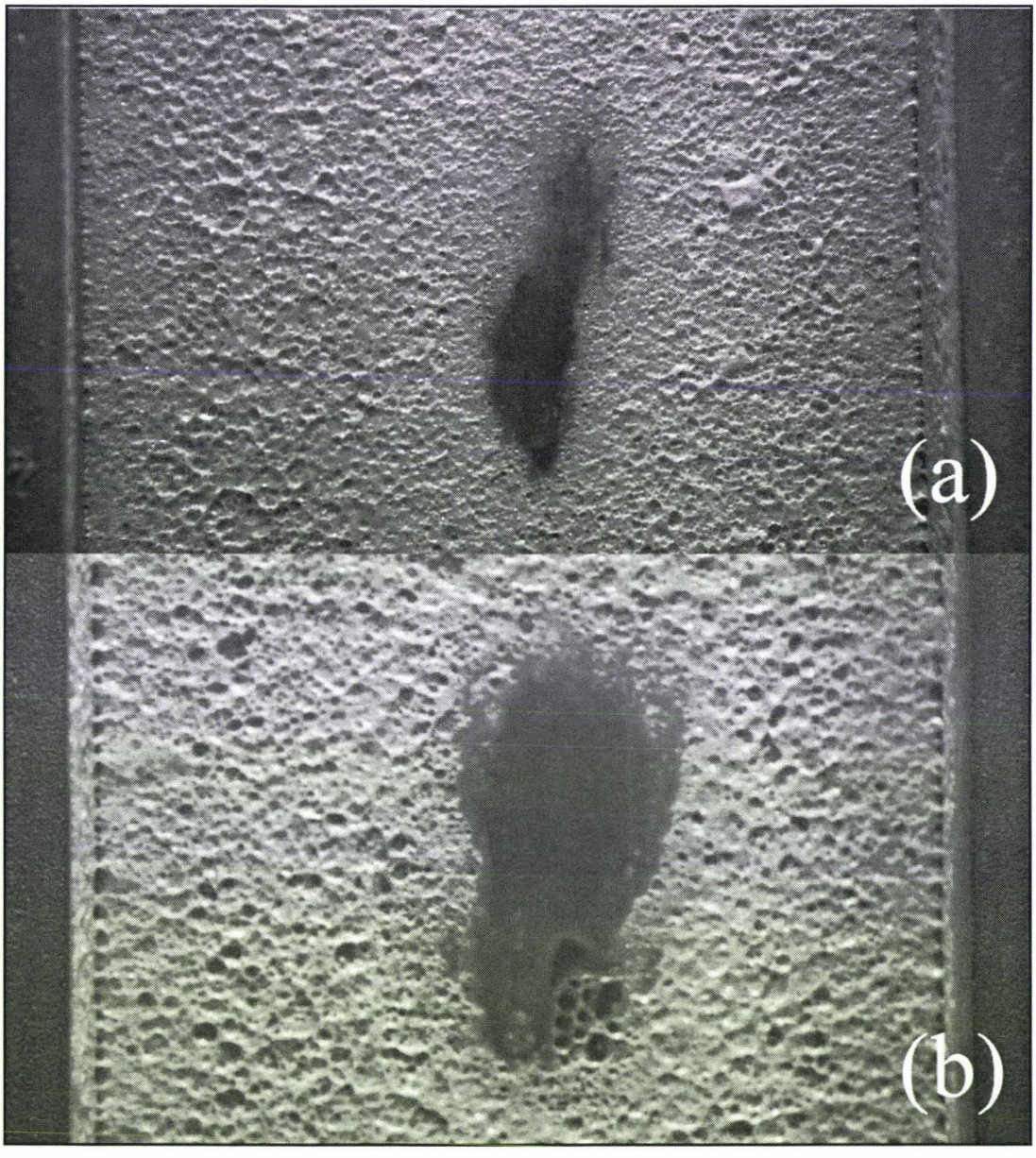

Figure 5.31 Influence of top heat flux probe on fouling pattern of research falling film evaporator plate for (a) run 19 (b) run 20

Both photos show a region of minimal fouling above the top heat flux probe installation sites. The placement of the probe was the same for both trials. The added thermal resistance associated with the probe has lowered the temperature to a point where the evaporative deposits no longer occur. However, fouling may occur eventually above the probe, it is likely that different fouling kinetics exist under these conditions.

5.3.3 Influence of Aluminium Tape on Fouling Pattern

The thermal resistance of the aluminium tape may also influence the fouling pattern in a similar manner to that of the heat flux probe. Since the evaporator plate has been shown to foul readily, any influence introduced by the aluminium tape would be visibly recognisable. Figure 5.32 shows the area of the evaporator plate surrounding the location of aluminium adhesive tape used to attach the probe to the plate for run 18. The aluminium tape was placed horizontally across the plate. The fouling free zone observed at the centre of Figure 5.32 coincides with the position of the aluminium tape. This trial indicates that at low enough temperatures, the aluminium adhesive tape influences the fouling pattern. The added thermal resistance associated with the aluminium tape reduces the evaporative surface temperature in a similar way to that of the heat flux probe.

Figure 5.32 Section of evaporator plate showing fouling free zone associated with added thermal resistance attributed to aluminium adhesive tape

5.3.4 Normalised Overall Heat Transfer Trace

Although the heat flux probe influenced the fouling pattern when the temperature recorded by the heat flux sensor was relatively low (e.g. top heat flux probe of run 19), the interference was eliminated when the temperature recorded was relatively high (e.g. bottom heat flux probe of run 19). Figure 5.33 shows sections of the evaporator plate where heat flux probes were installed for run 20. Figure 5.33, (a) shows the fouled area surrounding the top heat flux probe while Figure 5.33, (b) shows the fouled area surrounding the bottom heat flux probe. There is a region of minimal fouling above the top heat flux probe while full fouling coverage is observed above the bottom probe. The temperature recorded by the top heat flux probe thermocouple was 85 °C while the bottom was 100°C.

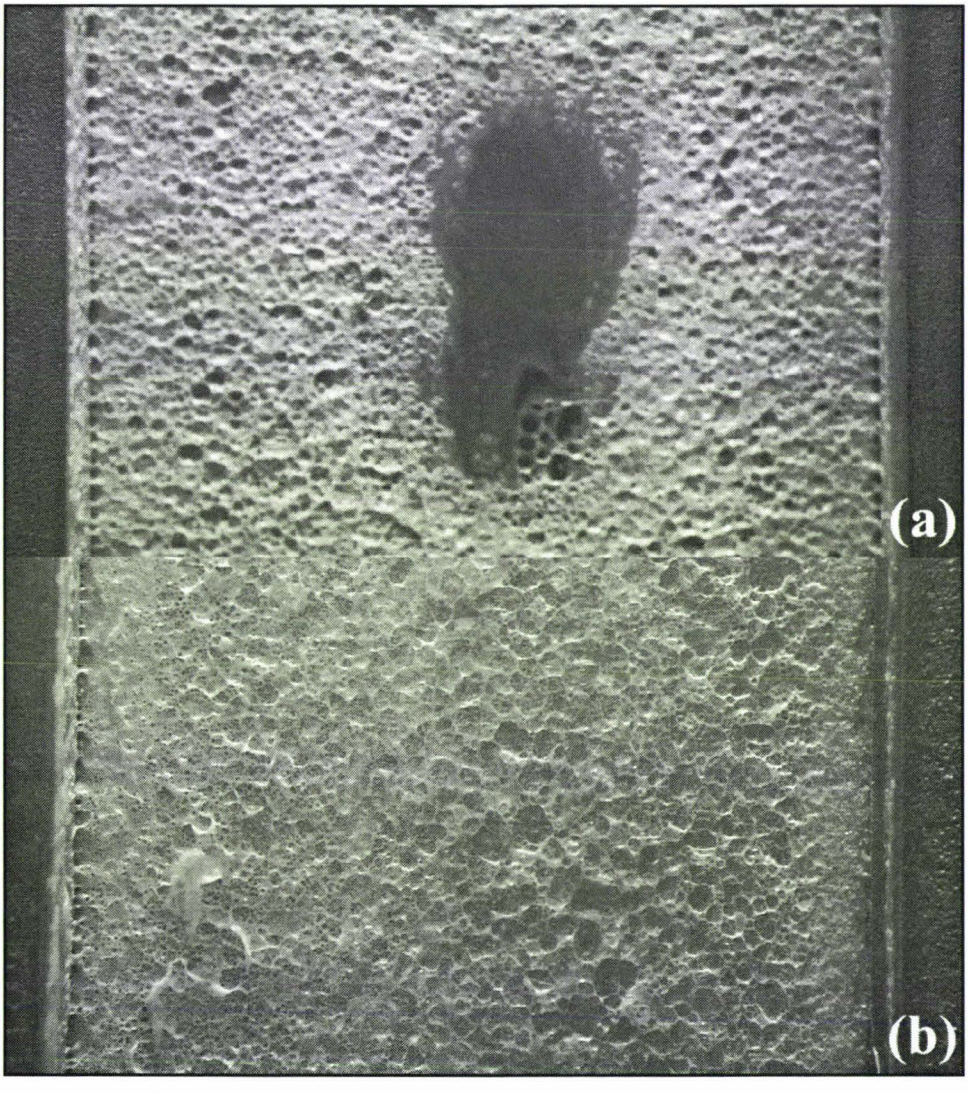

Figure 5.33 Sections of evaporator plate showing fouled area surrounding installed heat flux probes (a) top of plate (b) bottom of plate [Run 20]

Since there was a definite observed difference in fouling at the location of the two installed heat flux probes for run 20 (see Figure 5.33), the calculated NOHTC traces should reflect this difference. Figure 5.34 shows the NOHTC traces for the two heat flux probes installed in the RFFE for run 20.

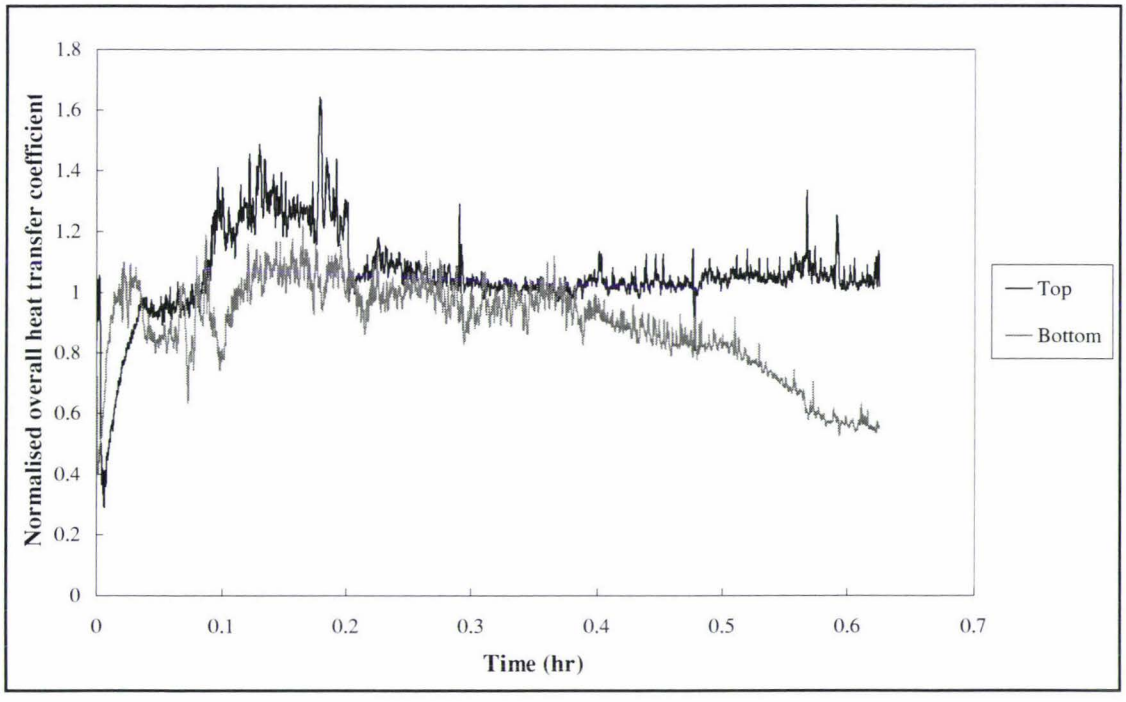

Figure 5.34 Normalised heat transfer coefficient calculated from heat flux probes detecting different extents of fouling on the evaporator plate [Run 20]

Although the NOHTC trace calculated from readings of the bottom heat flux probe showed a decrease (indicative of fouling), there were serious fluctuations in NOHTC during the first 12 minutes of the run. Similar fluctuations were observed in the NOHTC trace of the top probe. The OHTC was calculated from readings of RTDs not at the same location of heat flux probes i.e. installed in the milk weir and milk exit from the RFFE. Since it has been shown that lag time of the RTD has a large effect on the resulting NOHTC for the miniature plate heat exchangers (see Section 5.2.5), a similar effect may explain the observed fluctuations in NOHTC traces for this run. For the fouling probe to operate successfully within a falling film evaporator a synchronisation process will need to take place between the RTDs and heat flux probes. It is recommended that the development of a synchronisation process should take place in future work.

6 FOULING STUDIES

6.1 Milk Fouling on Heated and Unheated Surfaces

Fouling studies are often carried out on model dairy fluids, particularly whey solutions to simplify the analysis (Delplace *et al.*, 1994; Delplace and Leuliet, 1995; Belmar-Beiny and Fryer, 1993; Belmar-Beiny and Fryer, 1992; Gotham *et al.*, 1992; Fryer *et al.*, 1996; Fryer and Bird, 1994; Schreier *et al.*, 1994; Belmar-Beiny *et al.*, 1993). In most of these published studies, the process fluid passes over a heated surface. Fouling on unheated surfaces by whole milk has only been studied by Truong *et al.* (1998) in New Zealand. No previous studies comparing the rate and mode of fouling of whole milk on both heated and unheated surfaces have been reported. Therefore, an experiment was set up with the same batch of whole milk flowing through MPHEs with heated and unheated test plates (run 10). Hot water flowed through 3 MPHEs (heated surface) of the fouling rig at 90°C. Hot water did not flow through the remaining 3 MPHEs (unheated surface).

Figure 6.1 shows the heat flux traces for a heated and an unheated test plates in run 10. Figure 6.2 shows the corresponding NOHTC traces for each plate. There was a clear decrease in heat flux for the heated surface but no apparent decrease for the unheated surface (Figure 6.1) which was reflected in the corresponding NOHTC traces (Figure 6.2). The fluctuations observed in the NOHTC trace for the unheated surface over the first hour was attributed to the poor response of the RTD measuring the milk temperature which was discussed in Section 5.2.5. The poor response of the RTD introduced noise into the unheated surface's NOHTC trace which would be expected to be flat similar to the unheated heat flux trace of Figure 6.1.

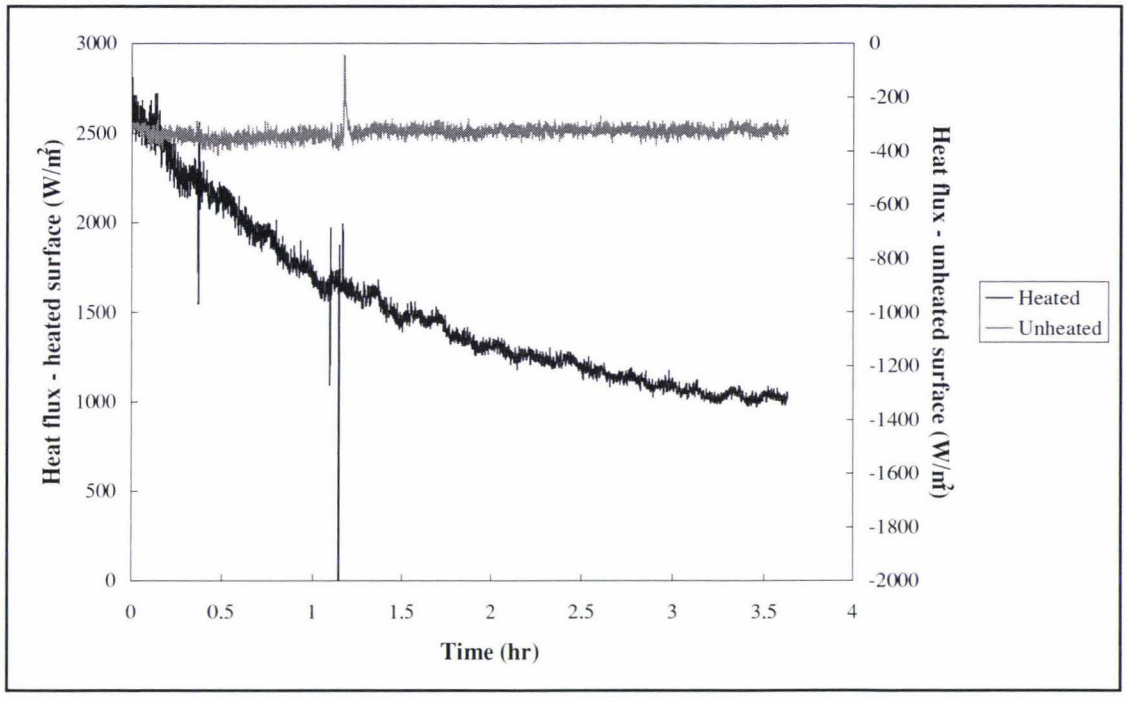

Figure 6.1 Raw heat flux trace for heated and unheated surfaces [Run 10]

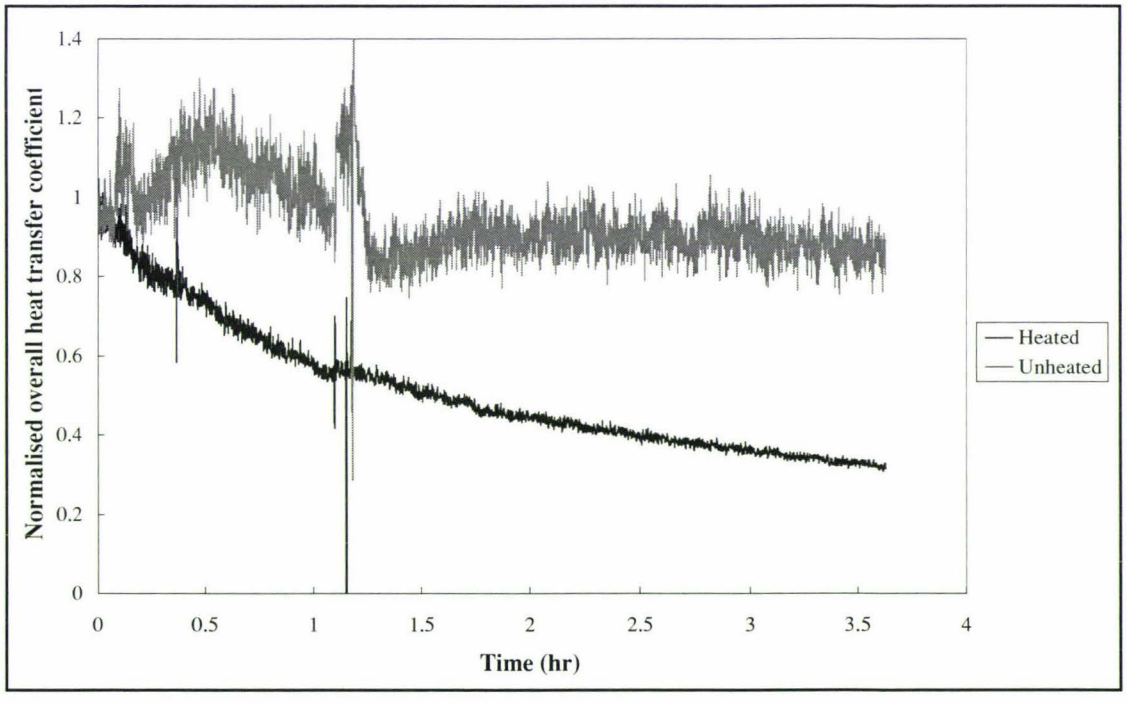

Figure 6.2 Normalised overall heat transfer coefficient for heated and unheated surfaces [Run 10]

Figure 6.3 shows photographs of the fouling deposits on the heated and unheated surfaces. After approximately 4 hours canopy fouling was seen on the heated surface (Figure 6.3, (a)) whereas there was no visible evidence of fouling on the unheated

surface (Figure 6.3, (b)). The calculated NOHTC for each condition (heated and unheated) agrees with the visual evidence.

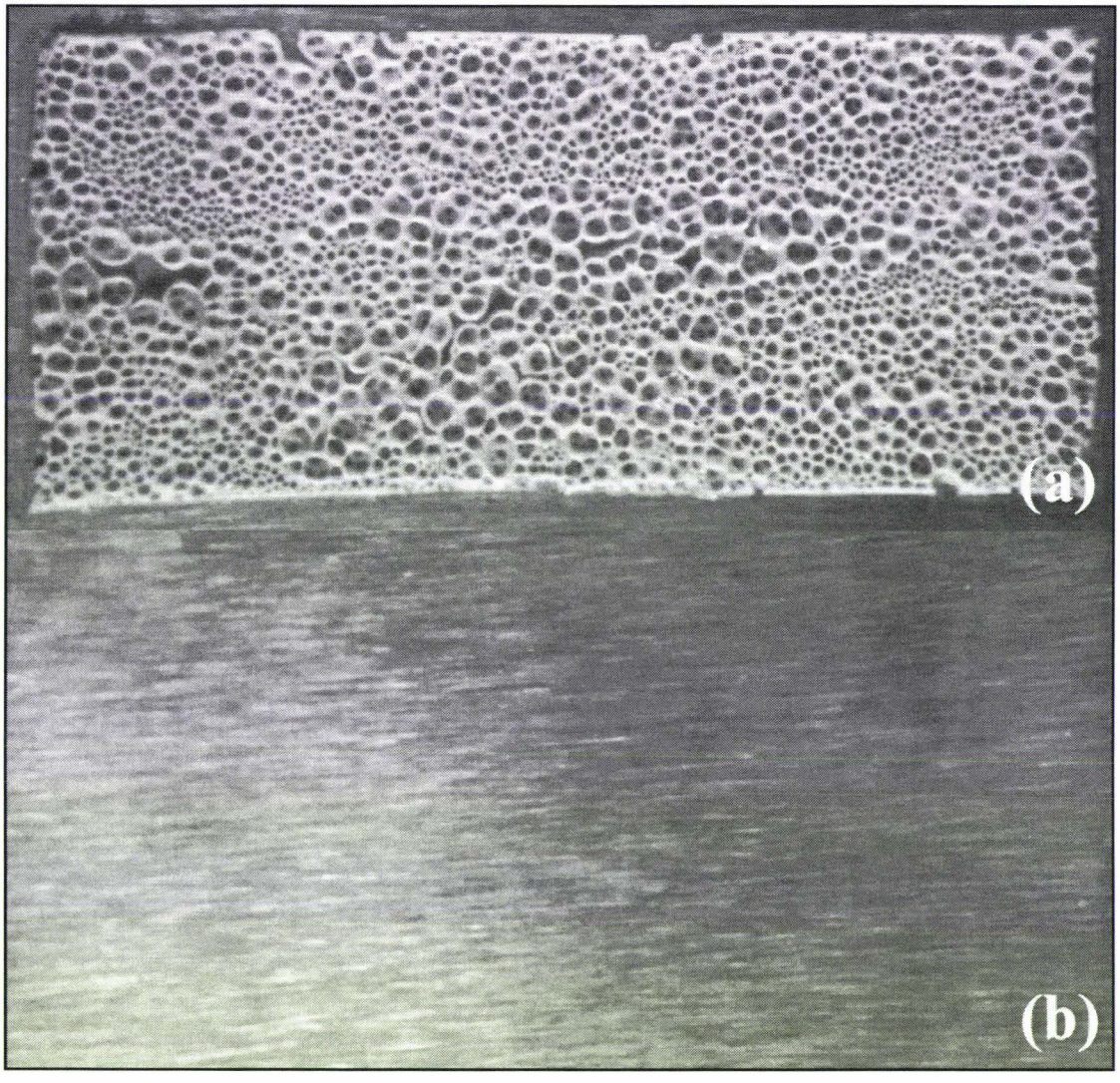

Figure 6.3 Test plates exposed to different operating procedures (a) heated surface and (b) unheated surface [Run 10]

Truong *et al.* (1998) reported on the build up of fouling on unheated surfaces. Their data were obtained from a commercial plant with probes installed directly after the DSI where the milk temperature was 95°C. Their data showed a marked decrease in OHTC after 6 hours.

The absence of fouling observed on the unheated plates (Figure 6.3, (b)) in the pilot plant used in this research project may be attributed to three possible causes:
(a) run time too short,

(b) inappropriate plate geometry to aid unheated fouling,

(c) plate position in pilot plant – less fouling occurs further away from heating source (Truong *et al.*, 1998).

It is suggested that any further work should use longer run times to obtain fouling on both heated and unheated surfaces. If no unheated plate fouling is observed with longer run times, the configuration of the fouling rig may need to be modified so that the distance from the DSI to the modules is reduced.

6.2 Air and Water Start Up

In early runs it was noted that fouling started almost immediately when the milk made contact with the MPHE heated surface, i.e. there appeared to be no initiation phase. This observation differed from results both abroad (Bott, 1989; Delplace *et al.*, 1994; de Jong, 1997; Jeurnink, 1996; Fryer, 1989) and in New Zealand (Fung, 1998; Ma and Trinh, 1999) who all reported an initiation phase.

The early trials conducted in the pilot plant began with the fouling rig filled with air. The incoming milk slowly pushed out this air and therefore the milk would hit a dry and heated plate which may result in a burn-on effect. It is suspected that this burn-on of milk solids upon first contact promotes immediate growth of canopy fouling. However, the proof of this hypothesis will require quite complex experiments using surface electron microanalysis to identify the chemicals deposited upon first contact. No attempt was made to gather evidence towards this hypothesis during this thesis. Runs conducted in this mode are referred to "air start up".

In industry, milk powder plants are usually filled with rinse water from a previous CIP run when the milk enters the plant. This mode of operation is referred to "water start up". An experiment (run 22) was conducted to compare the effects of an "air start up" and a "water start up" on the rate of fouling.

Figure 6.4 shows the calculated NOHTC for two MPHEs (one air start up and one liquid start up). There was a noticeable difference between the two experimental configurations. There was no decrease in NOHTC for the liquid start up procedure

while the air start up exhibited a strong decrease already observed in previous individual experiments.

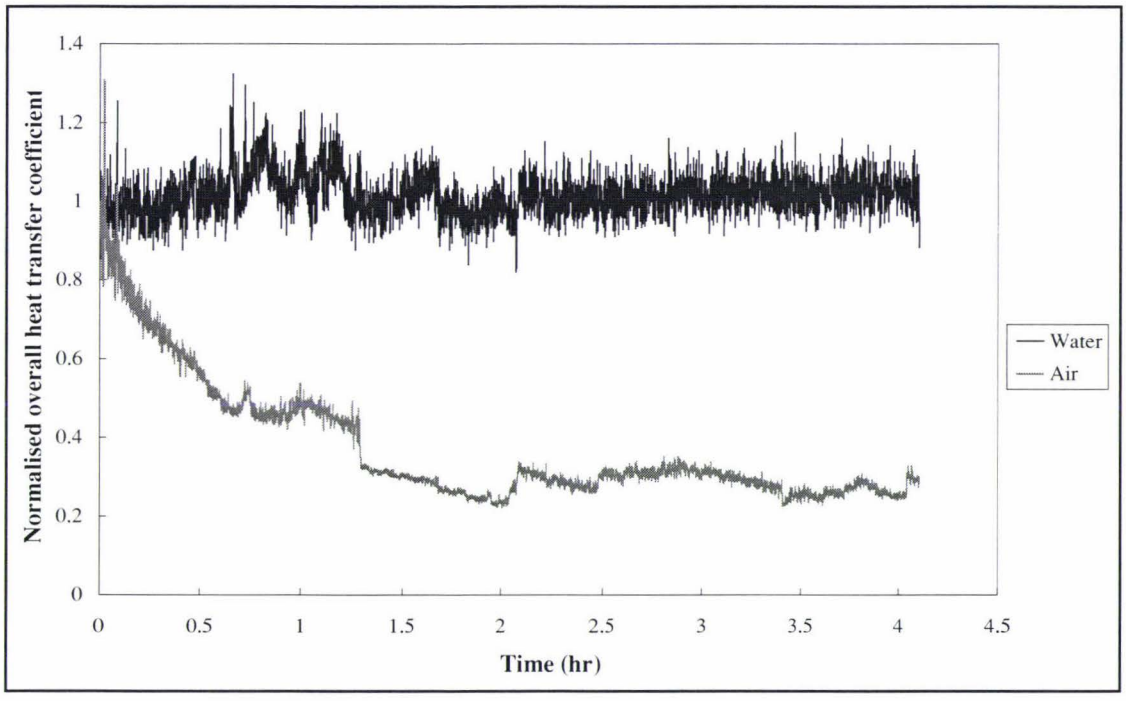

Figure 6.4 Normalised overall heat transfer coefficient for water and air start up [Run 22]

Figure 6.5 shows photographs of the fouling patterns that developed following air and liquid start ups. The water start up test plate (Figure 6.5, (a)) had a scattering of island deposits around the edges of the fouling window. No fouling was observed above the location of the heat flux probe. The air start up plate (Figure 6.5, (b)) clearly shows a uniform layer of fouling completely covering the plate including the probe region. Thus the visual evidence supports the proof of the heat flux probe that air start up leads to substantially more fouling than liquid start up.

The total amount of fouling in run 22 especially for the water start up configuration is smaller than previous runs (e.g. run 16). Although, the amount of fouling observed in other water start up trials was higher than observed in this trial (run 22), the quantity of fouling observed previously was not as high as that observed on the air start up test plates for this trial. Other researchers (Grandison, 1988; Burton, 1967) studying milk fouling in the Northern hemisphere have shown that the rate and weight of fouling varied throughout the milking season. A similar observation was made by a

researcher using the DTHE installed in the pilot plant used in this research project (Ma, 2000). Ma (2000) found that there was a decrease in fouling rate ($R_f U_o$) from 4 to 0.4 during the months February to March. Therefore the comparatively low fouling observed during this experiment (run 22), also conducted in March, was most likely due to seasonal variation. It is suggested that any further work should use milk processed prior to March (i.e. during the New Zealand milking season) for experiments investigating the effect of liquid and air start up procedures.

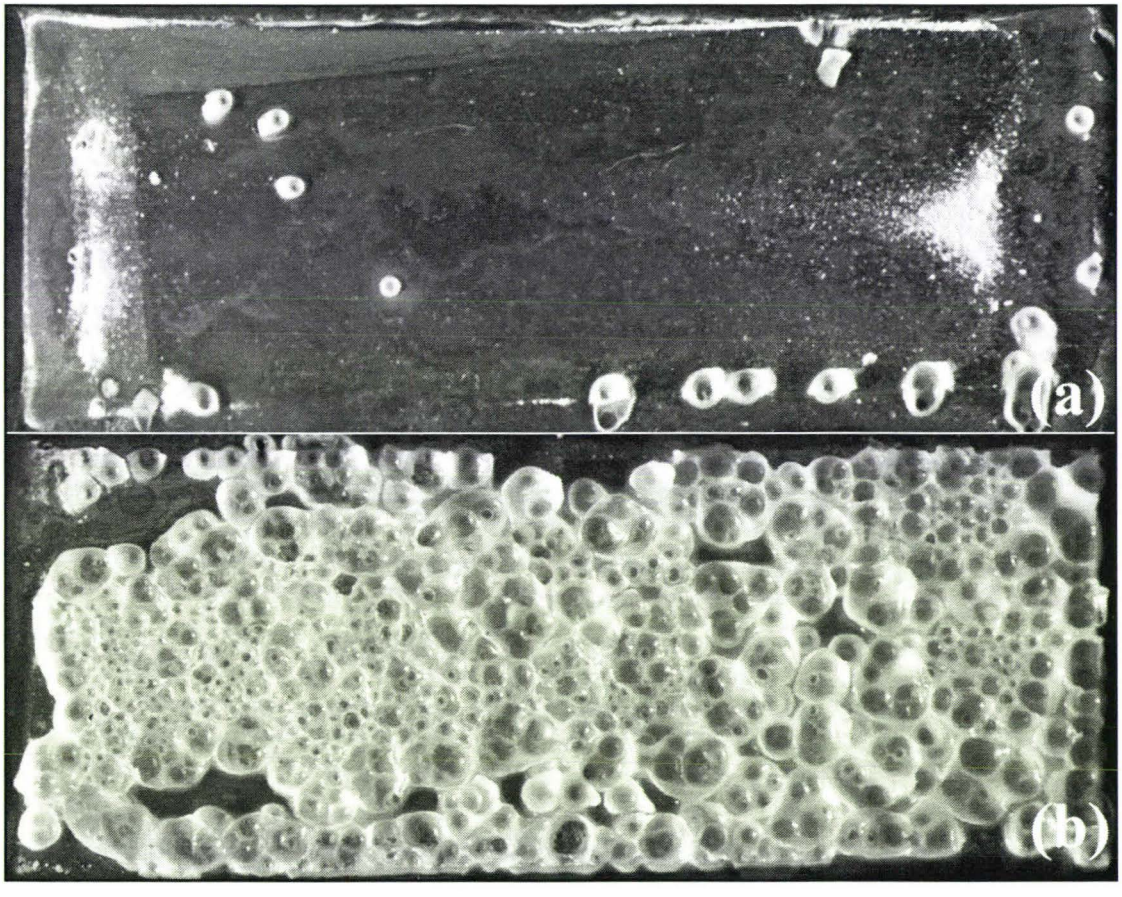

Figure 6.5 Test plates exposed to different start up procedures (a) water (b) a ir [Run 22]

6.3 Surface Conditioning by Operational Protocol (SCOP)

An experiment was designed to test the effect of delayed heating on fouling rate (run 13). Delayed heating refers to a situation where the heating medium was not flowing through the MPHE when the process fluid first entered the MPHE. Thus the test plate of the MPHE was originally at ambient temperature (25°C). The heating medium flow was initiated seven minutes after the milk entered the MPHE and was left on for the remainder of the run (Run 13). This technique was called "hot side unsteady state start up" (HSUSS).

An alternative operating procedure was called "hot side steady state start up" (HSSS), refers to a situation where the heating medium (90°C) was flowing in the MPHE before the milk initially entered the MPHE. Thus the surface of the test plate in the MPHE was approximately 90°C.

A trial (run 13) used six MPHEs in series with MPHEs 1, 2 and 3 HSSS and MPHEs 4, 5 and 6 HSUSS all using air start up mode. Two modules (one HSSS and one HSUSS) were isolated 30 minutes into the run to compare the bottom fouling layers that had developed in each of the two procedures. The remaining four modules were left running until the conclusion of the run approximately 9 hours later when the test plates were removed from the MPHEs and photographed.

Figure 6.6 shows the NOHTC traces of the four probes (the two short traces referred to samples taken of each start up procedure after 30 mins of plant operation) installed in the MPHEs. The trace suggests minimal fouling occurred in the HSUSS modules while extensive fouling took place in the HSSS modules. Furthermore, there was a clear difference in fouling between the two start up procedures (HSSS and HSUSS) after 30 minutes of operation.

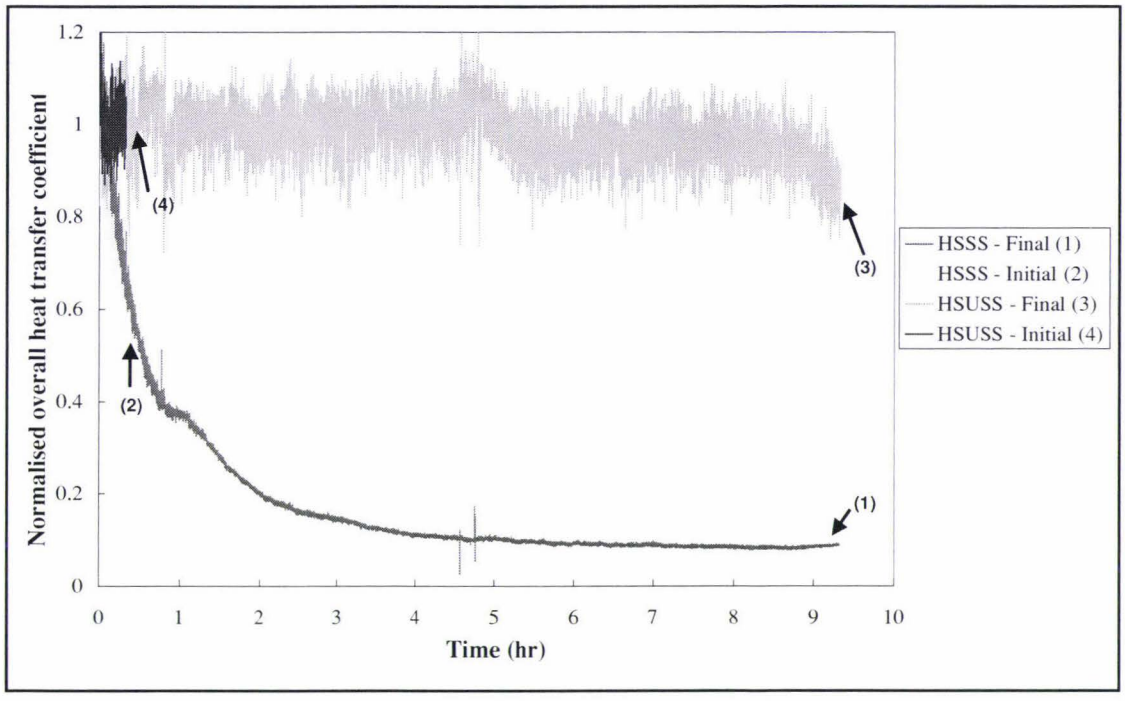

Figure 6.6 Normalised heat transfer coefficient for hot side steady and unsteady state start up [Run 13]

Figure 6.7 shows photographs of the fouling pattern for four plates used in this experiment (run 13). Figure 6.7 (b) and (d) show the bottom layers after 30 minutes of plant operation. The HSSS mode (b) had already produced canopy fouling while the HSUSS mode (d) only produced a sparse few islands. After 9 hours of operation the HSSS mode (a) produced a thick canopy layer but the HSUSS mode (c) produced a fouling layer similar to that observed for the HSSS mode after 30 minutes of operation (b). The photographs corroborate the evidence provided by the NOHTC traces.

The experiment has shown that the start up configuration on the heating medium side of the fouling rig has a definite effect on the kinetics of fouling by whole milk on heated surfaces. It appears that the temperature of the plate on first contact with the milk, has a substantial effect on the length of the initiation period. Surprisingly very little information exists on the mechanisms of the initiation period. Arguments by previous authors (Delsing and Hiddink, 1983; Fryer, 1989; Foster and Green, 1990; Foster *et al.*, 1989; Belmar-Beiny and Fryer, 1993) are inconclusive and contradictory. Mathematical modelling of the duration of the initiation period is almost non-existent.

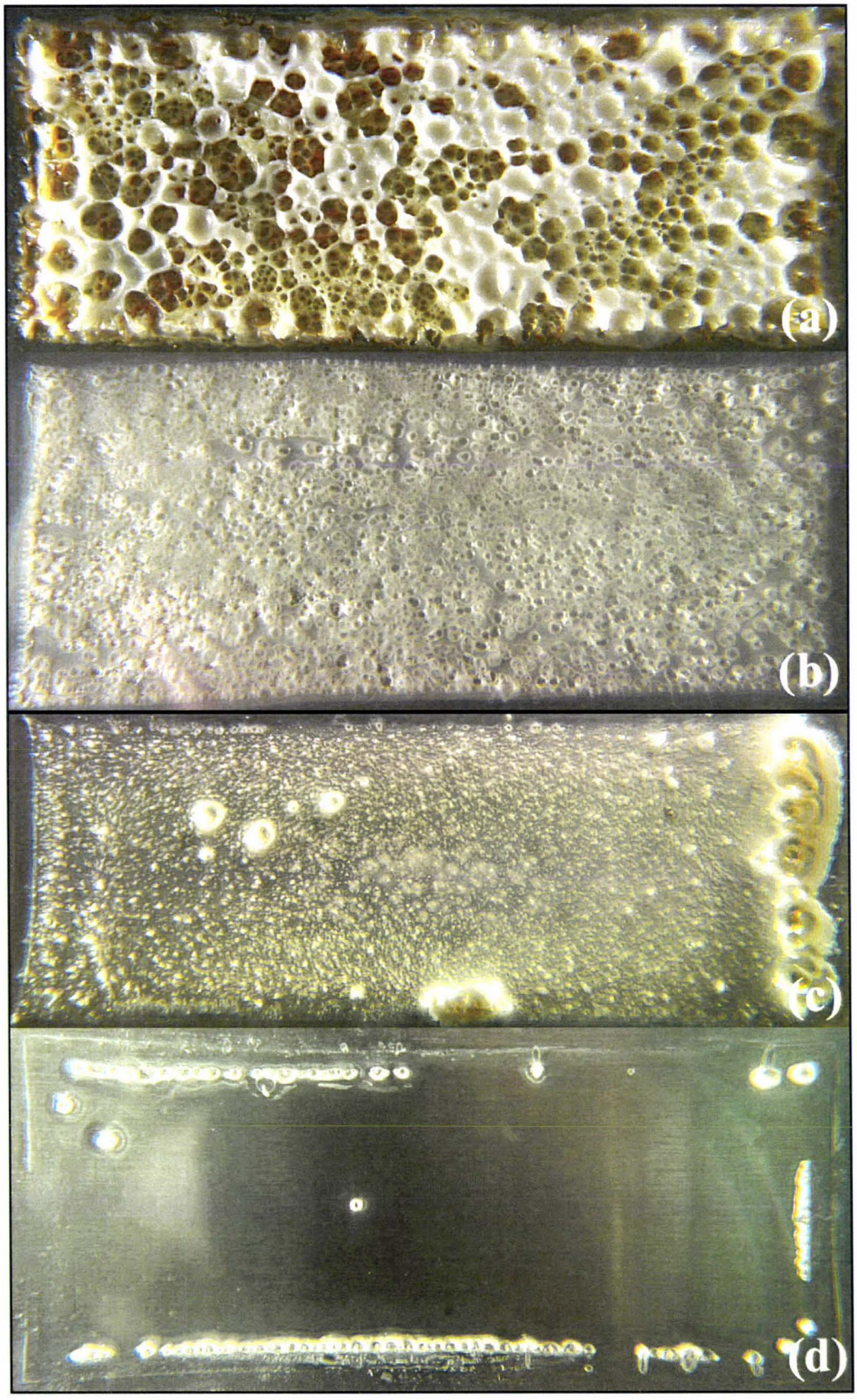

Figure 6.7 Test plates exposed to different start up procedures (a) hot side steady state – 9.5 hrs (b) hot side steady state – 0.5 hrs (c) hot side unsteady state – 9.5 hrs (d) hot side unsteady state – 0.5 hrs [Run 13]

The present experiment shows that manipulation of this initiation period may have an even stronger impact on industrial practice than manipulation of the slope of growth period observed in fouling curves. It is opportune here that in the previous section the start up of the milk side also has an effect on the length of the initiation period. The causes of the extension to the initiation period observed during these trials are unknown because of lack of information.

Manipulation of the SCOP run has induced the system of whole milk flowing past heated surfaces to act as though the surface was unheated even though the heating was initiated a few minutes into the run. Upon first contact milk solids deposit almost instantly on the surface. Previous authors (Foster and Green, 1990; Foster *et al.*, 1989; Belmar-Beiny and Fryer, 1993) suspect they are proteins but have not been able to state exactly which protein. Since most authors worked with model solutions, in particular whey solutions, their findings may not, in any case, apply to results of this work using whole milk.

Two possible reasons are offered to explain the lack of fouling seen on the unsteady state heated surface:

(a) there maybe a component that is crucial to the fast initiation of the fouling that was deposited in the HSUSS.

(b) there maybe a deposited component that actively inhibits the initiation phase.

However this work points out an important principle that has not been discussed in published literature of fouling by whole milk products. The principle of first contact. The condition under which the milk first contacts the equipment surfaces has a significant effect on the development of the fouling layers. Because of the importance of these findings a second experiment was conducted (run 23). The second experiment confirmed the results of run 13 in all aspects.

Before concrete recommendations are made to industry, the preliminary results obtained in this work must be further validated with a number of runs of the SCOP manipulation with both air and water start up. The test plates of the MPHE should be situated as close to the PHE as possible because this may have an effect on the results of the SCOP.

Serious work must be performed on the chemistry of first contact most probably at a PhD level. There is a need to derive models for the initiation period which will be undertaken by the current research group. The research group also intends to present a full model of growth and initiation period of whole milk fouling.

6.4 Orientation of Test Plate

Previous authors at Massey University (Fung, 1998; Ma and Trinh, 1999) have suggested that heat exchanger plate orientation plays a role in the structure of fouling of whole milk. Ma and Trinh (1999) observed a difference in fouling layers on the upper and lower sides of a horizontal heated tube. The fouling on the upper side was thinner, harder and more compact than the fouling on the lower side. They suggested that fat in whole milk tends to migrate towards the wall because of hydrophobic attraction. When the heated tube was horizontal, the creaming process reinforces the movement of fat to the underside of the pipe, especially when the milk velocity was low, but the upper side was shielded resulting in an upper layer richer in minerals and protein and hence harder and more compact (Ma and Trinh, 1999).

Ma and Trinh (1999) used a double tube heat exchanger for their investigation. An experiment (run 21) was designed to investigate the rate and structure of fouling on three different test plate orientations using the manipulated fouling rig (refer to Section 4.3.6).

The fouling rig configuration is shown in Figure 6.8 and allowed the following orientations:

- Milk flow horizontal and above the heating medium (MPHE 1).
- Milk flow vertical and flowing counter-current to flow of heating medium (MPHE 2).
- Milk flow horizontal and below the heating medium (MPHE 2).

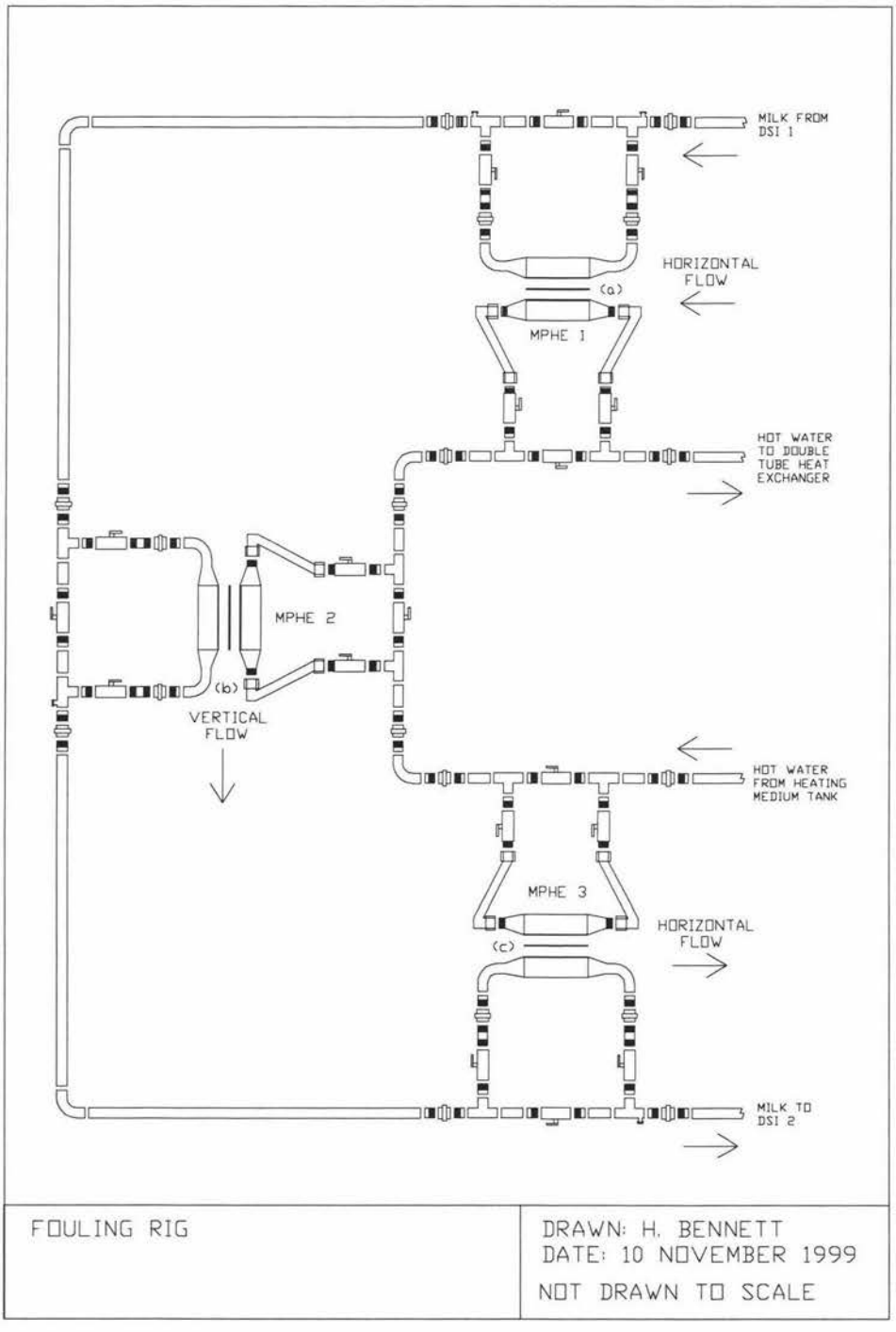

Figure 6.8 Fouling rig configuration with three different test plate orientations (a) horizontal and above the heating medium (b) vertical to the heating medium (c) horizontal and below the heating medium

Figure 6.9 shows the NOHTC trace based on the data obtained from the three heat flux probes installed in the miniature plate heat exchangers. The traces suggest no fouling deposited directly above the probes installed in MPHEs 2 and 3. There was a

slight decrease in NOHTC for MPHE 1. However the evidence from the NOHTC traces in this instance is not conclusive within experimental uncertainties.

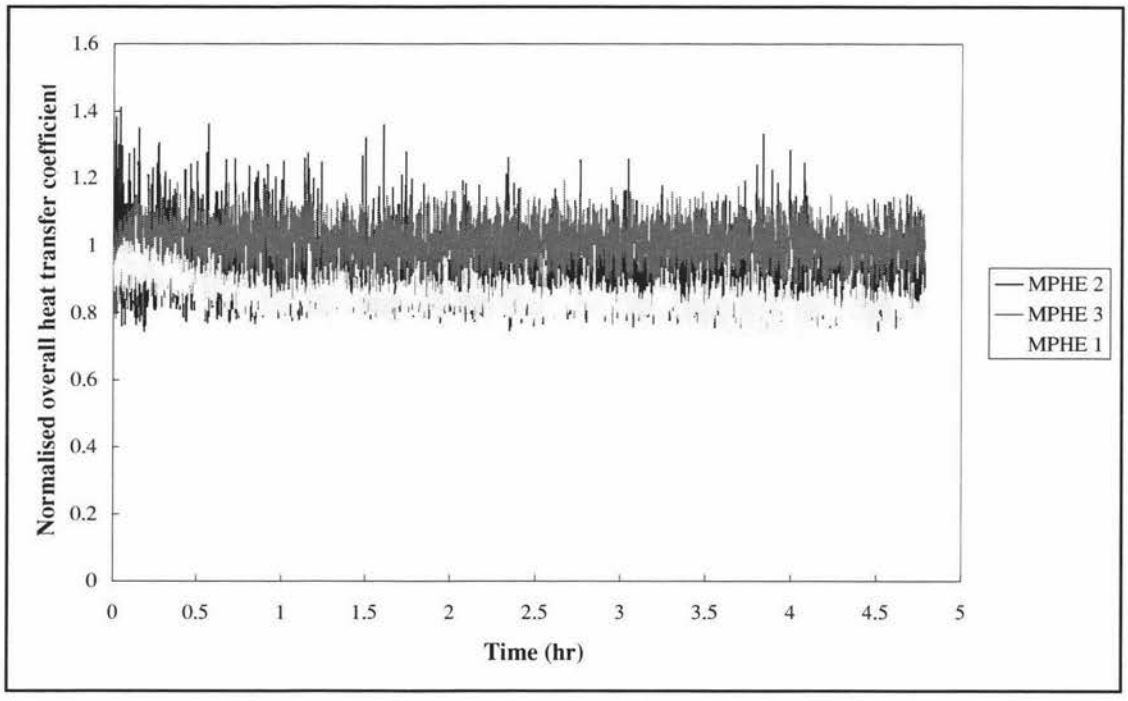

Figure 6.9 Normalised overall heat transfer coefficient for different test plate orientations: MPHE 1: horizontal and above the heating medium, MPHE 2: vertical to the heating medium, MPHE 3: horizontal and below the heating medium [Run 21]

Figure 6.10 shows photographs of the fouling deposits for the three orientations. Island fouling was noted on all test plates but the density of deposits is different between the three configurations.

There was a difference in the size of the islands between the test plates. When the milk flows above the heated plate, large thick islands covered approximately half the plate with some directly above the location of the heat flux probe. The vertical configuration produced very little fouling. Horizontal milk flowing below the plate showed evidence of air bubbles at corners (as discussed in Section 5.2.1) and small densely packed islands covering the majority of the plate.

There appears to be differences in the extent and pattern of fouling between the 3 orientations however, total amount of fouling in all cases was very small making quantitative comparisons difficult and this would explain the lack of variation in the

NOHTC traces. The experiment was conducted in March during times of reduced fouling as discussed in Section 6.2. Because of possible seasonal effects it is recommended that this work is repeated during the peak of the New Zealand milking season before firm conclusions are made.

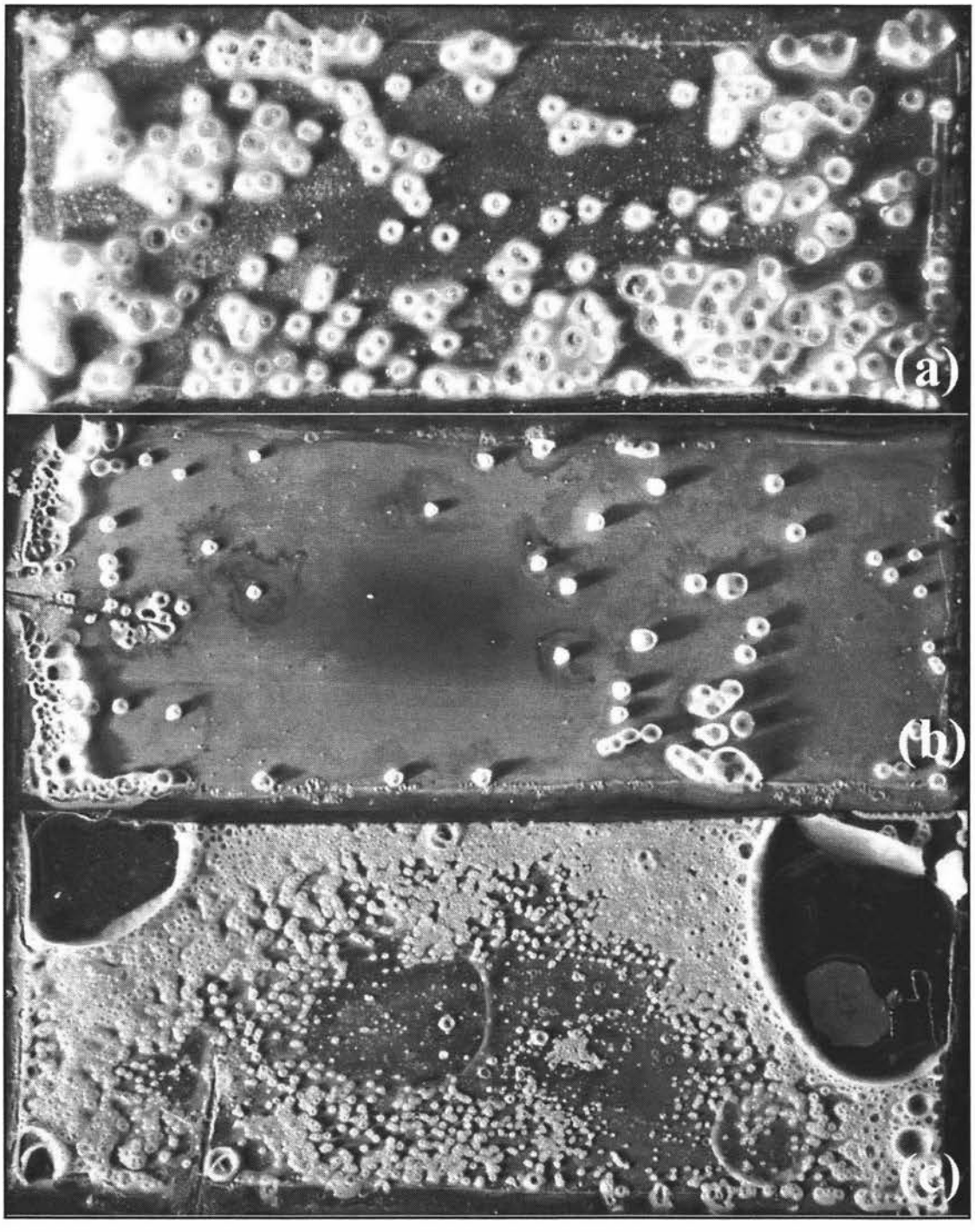

Figure 6.10 Photographs of heating plates taken from rig configuration shown in Figure 6.8. (a) horizontal and above the heating medium (MPHE 1) (b) vertical to the heating medium (MPHE 2) (c) horizontal and below the heating medium (MPHE 3) [Run 21]

There is little previous work on fouling by whole milk on heated and unheated surfaces. There is no existing mathematical model of fouling of whole milk. The current research group is conducting a substantial program of research on fouling by whole milk. Work completed by the group has identified a number of new variables that need to be included in the existing mathematical model. These variables are as follows:

- the fat content (C. Ma)
- effect of fat globule membrane damage (L. Fung)
- effect of start up procedures on the initiation period (H. Bennett)
- possible effect of orientation (H. Bennett)
- effect of enzymatic damage (C. Ma)

A fully developed mathematical model of fouling by whole milk including the above variables and traditional variables such as β-lactoglobulin denaturation will be presented in future publications.

7 CONCLUSIONS AND RECOMMENDATIONS

7.1 Conclusions

A commercial heat flux sensor has been successfully used to indicate the presence of whole milk fouling on heated surfaces installed in a miniature plate heat exchanger. It was found that the heat flux passing from the heating medium to the milk flowing on the other side of the heat exchanger plate could be used as a reliable indicator of fouling thickness provided all thermal resistances in the system, except for the resistance of the growing fouling layer, remained constant during the run.

The type of cement used to attach the sensor to the plate was important. Non-silicone heat transfer paste was chosen over a silicone based heat transfer paste because the latter dried out over the duration of a run.

Aluminium tape was used to press the probe against the test plate. The tape was situated on the outer surface of the on-board thermocouple on the heating medium side and therefore did not have an effect in the overall heat transfer coefficient calculated. However the presence of the tape did affect the fouling pattern. To eliminate this local effect, the aluminium tape was applied to the entire area of the test plate.

Although the resistance of the stainless steel plate stayed constant during a trial, the thickness of the plate influenced the pattern of fouling at the location directly above the installed heat flux probe. Similarly, the probe resistance stayed constant throughout a run, but influenced the fouling pattern especially when the system was operated under surface-controlled mode. This problem was solved by using relatively thick plates (0.6 mm).

Air was found on the milk side of the test plate during the commissioning runs of the pilot plant. Air present in the equipment before a run became trapped at high points in the plant, for example, under the test plates during low flowrates. When the milk

flowed under a test plate, an air cushion formed preventing contact between the milk and the test plates resulting in no fouling. A secondary effect of the presence of air was the instability associated with the thermal resistance during the run. The layer of air probably varied its volume and shape throughout the run and hence the thermal resistance associated with it also varied. The solution was to invert the fouling rig resulting in milk flowing above the test plates.

Dissolved air was released slowly from the milk during the heating process and accumulated in the high points of the pipe-work in the plant. Once a high point was filled with air any additional air would travel downstream towards the next high point. When the air reached an RTD it would isolate part of the probe from the milk giving an erroneous temperature measurement. These disturbances were seen on the control computer as characteristic waves of temperature disturbance travelling down the plant over the run. The operation was stabilised by removing the released air periodically from the first high point after the milk heater.

The fouling monitoring system consisted of two sensors: a heat flux sensor and a temperature sensor. For the system to give a true local measure of overall heat transfer coefficient, the two sensors were required to be accurate and in phase with each other. The original temperature sensor for milk were Resistance Temperature Devices (RTD) housed in a stainless steel sheath. They were found to be inaccurate and to have a response time that lagged the response time of the heat flux sensors by 40 seconds. Two reasons were found for this effect. The attachment of the sheath to the pipe in the early periods of commissioning gave direct contact between the sheath and the surrounding piping system. This so-called bridging effect meant that the RTD measured the temperature of the entire piping mass which responded very slowly to temperature changes. The piping mass was also at a different temperature to the milk because of heat loses to the surrounding air. Typically the measured temperature could be up to 10°C lower than the true temperature. After the RTD sheath was isolated from the pipe by the inclusion of a rubber o-ring, the temperature offset of 5°C was still observed. It was established that heat dissipation from the section of the sheath which protruded outside the pipe was responsible for this error. Thus in order to get a true temperature, a naked sensor was immersed into the milk stream. The use of a Type T thermocouple resolved this issue.

Measurements after incorporation of the heat flux probe system into the research falling film evaporator emphasised the necessity of having the two sensors in close proximity of each other. Due to variations in temperature over a length of metal, a measurement of temperature up or down stream from the heat flux sensor would not provide an accurate estimate of the temperature directly above the heat flux probe. This observation is important if the fouling monitoring system is to be used in industry because the location of the heat flux probe will be dictated by the location of the complementary temperature sensor. Other commissioning trials conducted with the research falling film evaporator supported findings made with the miniature plate heat exchangers concerning problems associated with the added thermal resistance due to the heat flux probe attachment technique used.

In the present series of studies of fouling behaviour of whole milk it was shown for the same bulk temperature, fouling occurred much faster on an unheated surface. This observation lead to a next series of experiments aimed at manipulating the start up condition of the plant. Flow on both the milk side and the heating medium side were manipulated. Air start up (on the milk side) produced much more fouling than water start up. Similarly HSSS produced much more fouling than HSUSS start up. These results point to an important principle, namely the principle of first contact, that the state of the stainless steel surface when the milk first makes contact has an important effect on the subsequent rate of fouling. The use of this principle to delay the onset of fouling is a completely new concept proposed in this thesis. The present work also highlights the fact that present mathematical models of fouling have not produced any predictions for the all-important initiation period which is influenced by the principle of first contact.

An attempt was made to study fouling deposits on miniature plate heat exchanger plates using different orientations. There was a visible difference between the size of the fouling islands according to different orientations however no firm conclusions were made regarding the effect of orientation on fouling. It is suggested that further fouling work use milk obtained from the peak of the New Zealand milking season.

7.2 Recommendations for Further Work

7.2.1 SCOP Manipulation

Further work is required to validate the conditioning of the surface by changing start up procedure (SCOP manipulations). Further work is also required to identify which components deposit first onto the surface and what influence they have on inhibiting or facilitating fouling.

7.2.2 Seasonal Variation

Results of trials conducted over a period of three months by several workers of the research group showed that milk in March fouled less than milk collected during previous months. Further work must be conducted to elucidate the effect of seasonal variation of fouling by whole milk.

7.2.3 Evaporator

It was projected that the mechanism of fouling on evaporator surfaces is completely different to that on heat exchanger surfaces. Preliminary work on the research falling film evaporator tends to support this hypothesis but never proceeded beyond commissioning stage because of time constraints. This work should proceed in future projects.

7.2.4 Use of the fouling monitoring system to identify the fouling pattern within a plant

The fouling monitoring system could be used to map the worst-case areas of fouling within a milk processing plant. Results obtained in this study suggest these areas will be located on heated surfaces. Therefore, it is recommended that a fouling monitoring system be installed on the heating medium side of a plate within a plate heat exchanger. A number of logistical difficulties are expected in this case.

7.2.5 Development of a synchronised and accurate temperature sensor

The performance of the monitoring system is limited by the synchronisation of the two sensors. If the monitoring system is to be installed in areas of the plant where the sensors cannot be in close proximity of each other (for example, evaporator), a synchronisation process will need to take place. Investigation is warranted here.

Another error incurred by the temperature sensor was the inaccurate temperature recordings. The main cause of this offset was heat loss to the surrounding pipe-work. A temperature sensor that is thermally isolated from both the pipe-work and the hygienic stainless steel casing should be developed.

8 REFERENCES

Belmar-Beiny, M.T. and Fryer, P.J. (1993) Preliminary stages of fouling from whey protein solutions. *Journal of Dairy Research,* **60** (4):467-483.

Belmar-Beiny, M.T., Gotham, S.M., Paterson, W.R., Fryer, P.J. and Pritchard, A.M. (1993) The effect of Reynolds number and fluid temperature in whey protein fouling. *Journal of Food Engineering,* **19** (2):119-139.

Bott, T.R. (1989) Fouling of heat exchangers: A review. In: *Process Engineering in the Food Industry: Developments and Opportunities*, (Edited by Field, R.W. and Howell, J.A.), 97-109, Elsevier Applied Science, London and New York.

Britten, M., Green, M.L., Boulet, M. and Paquin, P. (1988) Deposit formation on heated surfaces: effect of interface energetics. *Journal of Dairy Research,* **55** (4):551-562.

Burton, H. (1961) A laboratory method for the investigation of milk deposits on heat exchange surfaces. *Journal of Dairy Research,* **28** 255-263.

Burton, H. (1965) A method for studying the factors in milk which influence the deposition of milk solids on a heated surface. *Journal of Dairy Research,* **32** 65-78.

Burton, H. (1967) Seasonal variation in deposit formation from whole milk on a heated surface. *Journal of Dairy Research,* **34** 137-143.

Burton, H. (1968) Reviews of the Progress of Dairy Science. *Journal of Dairy Research,* **35** 317-330.

Calvo, M.M. and de Rafael, D. (1995) Deposit formation in a heat exchanger during pasteurization of CO2-acidified milk. *Journal of Dairy Research,* **62** (4):641-644.

Dam Madsen, K. (1994) Vibration Sensor. *Sanitation of Food Processing Plants,* 72-86.

Dannenberg, F. and Kessler, H.G. (1988) Reaction kinetics of the denaturation of whey proteins in milk. *Journal of Food Science,* **53** (1):258-263.

Davies, T.J., Henstridge, S.C., Gillham, C.R. and Wilson, D.I. (1997) Investigation of whey deposit properties using heat flux sensors. *Food and Bioproducts Processing,* **75** (Part C):106-110.

De Jong, P. (1997) Impact and control of fouling in milk processing. *Trends in Food Science & Technology.* **8** (12):401-405.

De Jong, P., Bouman, S. and van der Linden, H.J.L.J. (1992) Fouling of heat treatment equipment in relation to the denaturation of beta -lactoglobulin. *Journal of the Society of Dairy Technology.* **45** (1):3-8.

De Wit, J.N. (1990) Thermal stability and functionality of whey proteins. *Journal of Dairy Science,* **73** (12):3602-3612.

Delplace, F. and Leuliet, J.C. (1995) Modelling fouling of a plate heat exchanger with different flow arrangements by whey protein solutions. *Food & Bioproducts Processing,* **73** (C3):112-120.

Delplace, F., Leuliet, J.C. and Tissier, J.P. (1994) Fouling experiments of a plate heat exchanger by whey protein solutions. *Trans IChemE,* **72** 163-169.

Delsing, B.M.A. and Hiddink, J. (1983) Fouling of heat transfer surfaces by dairy liquids. *Netherlands Milk & Dairy Journal,* **37** (3):139-148.

Electrolube Non-Silicone Heat Transfer Compound Technical Data Sheet (1997) Electrolube, UK.

Electrolube Silicone Heat Transfer Compound Technical Data Sheet (1997) Electrolube, UK.

Foster, C.L., Britten, M. and Green, M.L. (1989) A model heat-exchange apparatus for the investigation of fouling of stainless steel surfaces by milk. I. Deposit formation at 100 deg C. *Journal of Dairy Research,* **56** (2):201-209.

Foster, C.L. and Green, M.L. (1990) A model heat exchange apparatus for the investigation of fouling of stainless steel surfaces by milk. II. Deposition of fouling material at 140 deg C, its adhesion and depth profiling. *Journal of Dairy Research.* **57** (3):339-348.

Fryer, P.J. (1989) The uses of fouling models in the design of food process plant. *Journal of the Society of Dairy Technology,* **42** (1):23-29.

Fryer, P.J., Belmar-Beiny, M.T. and Schreier, P.J.R. (1995) Fouling and cleaning in milk processing. In: *Heat-induced changes in milk,* (Edited by Fox, P.F.), Second Edition, International Dairy Federation, Belgium.

Fryer, P.J. and Bird, M.R. (1994) Factors which affect the kinetics of cleaning dairy soils. *Food Science & Technology Today,* **8** (1):36-42.

Fryer, P.J. and Pritchard, A.M. (1989) A comparison of two possible fouling monitors for the food processing industry. In: *Process Engineering in the Food Industry: Developments and Opportunities*, (Edited by Field, R.W. and Howell, J.A.), 131-141, Elsevier Applied Science, London and New York.

Fryer, P.J., Robbins, P.T., Green, C., Schreier, P.J.R., Pritchard, A.M., Hastings, A.P.M., Royston, D.G. and Richardson, J.F. (1996) A Statistical Model for Fouling of a Plate Heat Exchanger by Whey Protein Solution at UHT Conditions. *Trans IChemE,* **74** (C):189-199.

Fung, L. (1998) *The effect of fat globule membrane damage in the absence of air on fouling in heat exchangers*, MTech Thesis, Massey University, Palmerston North.

Gotham, S.M., Fryer, P.J. and Pritchard, A.M. (1992) Beta -Lactoglobulin denaturation and aggregation reactions and fouling deposit formation: a DSC study. *International Journal of Food Science & Technology,* **27** (3):313-327.

Grandison, A.S. (1988) UHT processing of milk: seasonal variation in deposit formation in heat exchangers. *Journal of the Society of Dairy Technology,* **41** (2):43-49.

Jeurnink, T.J.M. (1990) Effect of proteolysis in milk on fouling in heat exchangers. *Netherland Milk and Dairy Journal*, **45**: 23-32.

Jeurnink, T.J.M. (1995a) Fouling of heat exchangers by fresh and reconstituted milk and the influence of air bubbles. *Milchwissenschaft,* **50** (4):189-193.

Jeurnink, T.J.M. (1995b) Fouling of heat exchangers in relation to the serum protein concentration in milk. *Milchwissenschaft,* **5**: 257-260.

Jeurnink, T.J.M. (1996) *Milk fouling in heat exchangers*. Ph.D. Thesis, Wageningen Agricultural University, The Netherlands.

Jeurnink, T.J.M. and Brinkman, D.W. (1994) The cleaning of heat exchangers and evaporators after processing milk or whey. *International Dairy Journal,* **4** (4):347-368.

Jeurnink, T.J.M., Brinkman, D.W. and Stemerdink, A. D. (1989). Distribution and Composition of Deposit in Heat Exchangers. In: *Fouling and Cleaning in Food Processing*, (Edited by Kessler, H.G. and Lund, D.B.), University of Munich.

Jeurnink, T.J.M. and de Kruif, K.G. (1995) Calcium concentration in milk in relation to heat stability and fouling. *Netherlands Milk & Dairy Journal,* **49** (2):151-165.

Jeurnink, T.J.M., Walstra, P. and de Kruif, C.G. (1996) Mechanisms of fouling in dairy processing. *Netherlands Milk & Dairy Journal,* **50** (3):407-426.

Jones, A.D., Ward, N.J. and Fryer, P.J. (1994) The use of a heat flux sensor to monitor milk fluid fouling. In: *Fouling and Cleaning in Food Processing*, (Edited by Fryer, P.J., Hasting, A.P.M. and Jeurnink, T.J.M.) European Commission, Brussels.

Kessler, H.G. and Schraml, J.E. (1996) Effects of Concentration on Fouling at Hot Surfaces. In: *Fouling and Cleaning in Food Processing*, (Edited by Fryer, P.J., Hasting, A.P.M. and Jeurnink, T.J.M.) European Commission, Brussels.

Lalande, M. and Corrieu, G. (1981) Fouling of a plate heat exchanger by milk. In: *Fundamentals and Applications of Surface Phenomena Associated with Fouling and Cleaning in Food Processing*, (Edited by Hallstrom B., Lund, D.B. and Tragardh, A.C.), University of Lund, Sweden.

Lalande, M., Tissier, J.P. and Corrieu, G. (1984) Fouling of a plate heat exchanger used in ultra-high-temperature sterilization of milk. *Journal of Dairy Research,* **51** (4):557-568.

Lund, D.B. and Bixby, D. (1975) Fouling of heat exchange surfaces by milk. *Process Biochemistry.* **10** (9):52-55. 0032-9592.

Lyster, R.L.J. (1970) The denaturation of α–lactalbumin and β-lactoglobulin in heated milk. *Journal of Dairy Research,* **37** 233-243.

Ma, C. (2000) *Personal Communication*, Institute of Food Nutrition and Human Health, Massey University, Palmerston North.

Ma, C. and Trinh, K.T. (1999) The Role of Fat in Milk Fouling. In: *Milk Powders for the Future 4,* 99-105, Palmerston North.

Maas, R., Lalande, M. and Hiddink, J. (1985) Fouling of a plate heat exchanger by whipping cream. In: *Fouling and cleaning in food processing,* (Edited by Lund, D., Plett, E. and Sandu, C.), 217-225, University of Wisconsin, Madison.

Mikkelsen, H.O. (1994) Optical Sensor. *Sanitation of Food Processing Plants,* 54-70.

Paterson, A.H.C., Radford, G. and Campanella, O.H. (eds) (1996) *41.210 and 42.202 Second Year Engineering*, Massey University, Palmerston North.

Roefs, S.P.F.M. and de Kruif, K.G. (1994) A model for the denaturation and aggregation of beta -lactoglobulin. *European Journal of Biochemistry,* **226** (3):883-889.

Sandu, C., Lund, D., O'Neal, B., Singh, R. and Almas, K. (1984) A plate heat exchanger designed to study fouling in food processing. *Engineering sciences in the food industry,* **1** 199-207.

Schreier, P.J., Green, R.C.H., Pritchard, A.M. and Fryer, P.J. (1994) The use of a heat flux sensor to monitor milk fluid fouling. In: *Fouling and Cleaning in Food Processing*, (Edited by Fryer, P.J., Hasting, A.P.M. and Jeurnink, T.J.M.) European Commission, Brussels.

Skudder P. J and Bonsey A. D (1985) The effect of milk pH and citrate concentration on the formation of deposit during UHT processing. In: *Fouling and cleaning in food processing,* (Edited by Lund, D., Plett, E. and Sandu, C.), 226-234, University of Wisconsin, Madison.

Skudder, P.J., Brooker, B.E., Bonsey, A.D. and Alvarez-Guerrero, N.R. (1986) Effect of pH on the formation of deposit from milk on heated surfaces during ultra high temperature processing. *Journal of Dairy Research,* **53** (1):75-87.

Skudder, P.J., Thomas, E.L., Pavey, J.A. and Perkin, A.G. (1981) Effects of adding potassium iodate to milk before UHT treatment. I. Reduction in the amount of deposit on the heated surfaces. *Journal of Dairy Research,* **48** (1):99-113.

Steinhagen, R., Muller-Steinhagen, H. and Maani, K. (1990) *Heat exchanger applications fouling problems and fouling costs in New Zealand Industries.*, Auckland: University of Auckland.

Swartzel, K.R. (1983) Tubular heat exchanger fouling by milk during ultra high temperature processing. *Journal of Food Science,* **48** (5):1507-1511.

Tissier, J.P. and Lalande, M. (1986) Experimental Device and Methods for Studying Milk Deposit Formation on Heat Exchange Surfaces. *Biotechnology Progress,* **2** (4):218-229.

Truong, H.T., Anema, S., Kirkpatrick, K. and Trinh, K. T. (1998) In-line measurements of fouling and CIP in milk powder plants. In: *Fouling and Cleaning in Food Processing*, (Edited by Fryer, P.J., Hasting, A.P.M. and Jeurnink, T.J.M.) European Commission, Brussels.

Truong, H.T., Trinh, K.T. and Mackereth, A.R. (1996) Structural Change of Fouling Deposits from Whole Milk in Heat Treatment Equipment. In: *IPENZ Annual Conference 1996 "Engineering Providing the Foundations for Society"*, IPENZ, Auckland.

Visser, H., Jeurnink, T.J.M., Schraml, J.E., Fryer, P. and Delplace, F. (1997) Fouling of heat treatment equipment. *Bulletin of the International Dairy Federation,* **328** 7-31.

Withers, P.M. (1994) Ultrasonic sensor for the detection of fouling in UHT processing plants. *Food Control,* **5** (2):67-72.

Withers, P.M. (1996) Ultrasonic, acoustic and optical techniques for the non-invasive detection of fouling in food processing equipment. *Trends in Food Science & Technology,* **7** (9):293-298.

Yoon, J. and Lund, D.B. (1989) Effect of operating conditions, surface coatings and pretreatment on milk fouling in a plate heat exchanger. In: *Fouling and Cleaning in Food Processing*, (Edited by Kessler, H.G. and Lund, D.B.), University of Munich.

Yoon, J. and Lund, D.B. (1994) Comparison of two operating methods of a plate heat exchanger under constant heat flux condition and their effect on the temperature profile during milk fouling. *Journal of Food Process Engineering,* **17** 243-262.

9 APPENDIX

9.1 Temperature Sensor Calibration Data

Table 9.1 Temperature Sensor Calibration Data

Temperature Sensor No.	Average Reported Temp at 0°C	Average Reported Temp at 100°C	Regression Coefficients	
			a	b
5	-0.04	99.8	1.002	0.0432
5*	0.2	100.3	1.000	-0.2323
6	1.1	100.7	1.004	-1.133
7	0.06	99.8	1.002	-0.06
7*	0.1	100.4	0.997	-0.1333
8	1.4	100.7	1.006	-1.362
9	-0.111	99.6	1.002	0.112
9*	-0.3	99.9	0.997	0.3275
10	1.1	100.8	1.004	-1.139
11	0.02	99.9	1.001	-0.024
11*	-0.3	99.9	0.998	0.3004
12	1.0	100.6	1.003	-0.963
13	-0.09	99.8	1.002	0.091
13*	-0.1	99.7	1.001	0.145
14	0.8	100.5	1.002	-0.757
15	0.02	99.6	1.004	-0.018
15*	-0.1	100.5	0.994	0.0994
16	0.8	100.6	1.002	-0.791

* Type T thermocouple

Example Calculation:

For sensor No. 5:

$$a = \frac{100}{\theta_{100} - \theta_0} = \frac{100}{99.8 - (-0.04)} = 1.002$$

$$b = -a\theta_0 = -1.002(-0.04) = 0.0432$$

If a read temperature from sensor No. 5 was 75°C then the calibrated value would be:

$$\theta_c = a\theta_r + b = 1.002(75) + 0.0432 = 75.2°C$$

9.2 Summary of Experimental Trials

Table 9.2 Description and Operating Conditions of Trials Conducted

Run No.	Date	Description	Plate thickness (mm)	Milk flowrate (l/h)	Milk temperature entering unit operation (°C)	Heating medium temperature entering unit operation (°C)
1	11-06-99	Effect of probe – control (no probe installed), surface control.	0.06	120	61	79
2	16-06-99	Effect of probe – centre of plate, surface control.	0.06	120	63	80
3	17-06-99	Effect of probe – milk inlet end of plate, surface control.	0.06	120	62	80
4	18-06-99	Effect of probe – centre of plate, bulk control.	0.06	120	67	79
5	23-06-99	Effect of probe – milk inlet end of plate, bulk control.	0.06	120	67	79
6	08-07-99	Effect of probe – centre of plate, surface control.	1.55	120	58	79
7	15-12-99	Commissioning of pilot plant.	0.6	45	75	85
8	17-12-99	Effect of air on fouling deposit.	0.6	45	72	85
9	25-01-00	Deposit thickness.	0.6	45	75	90
10	26-01-00	Heated and unheated surfaces.	0.6	45	76	90
11	27-01-00	Reproducibility between MPHEs.	0.6	45	75	90
12	28-01-00	SCOP – enzyme laced whole milk.	0.6	46	77	87

Table 9.2 Description and Operating Conditions of Trials Conducted (Cont.)

Run No.	Date	Description	Plate thickness (mm)	Milk Flowrate (l/h)	Milk temperature entering unit operation (°C)	Heating medium temperature entering unit operation (°C)
13	31-01-00	SCOP – fresh whole milk.	0.6	45	75	90
14	07-02-00	Evaporator – lighting, camera work and sealing of evaporator.	0.6	45	85	100
15	08-02-00	Heated and unheated surfaces.	0.6	60	82	90
16	10-02-00	Effect of air released from milk. Heated and unheated water start-up. RTD bridging.	0.6	45	72	87
17	28-02-00	Comparison of RTDs and thermocouples for milk temperature measure.	0.6	45	80	88
18	01-03-00	Evaporator trial	0.6	60	82	100
19	01-03-00	Evaporator trial	0.6	120	85	100
20	02-03-00	Evaporator trial	0.6	60	85	100
21	10-03-00	Fouling plate orientation.	0.6	45	80	88
22	14-03-00	Water and air start-up. Effect of aluminium tape.	0.6	47	75	89
23	16-03-00	SCOP – air start-up.	0.6	45	75	90

9.3 Example Calculation of Normalised Overall Heat Transfer Coefficient

Table 9.3 Results from Run 16

	A	B	C	D	E	F	G	H	I	J	K
1	Date	Time	Time (s)	Time (hr)	FIX:HF0.F	FIX:HF1.F	FIX:HF2.F	Heat Flux I	Heat Flux I	Heat Flux I	FIX:MILK_
2	3/10/2000	10:43:52	0	0	817	776	1646	2979.639	2895.863	6142.513	0.71
3	3/10/2000	10:43:56	4	0.001111	792	798	1457	2888.463	2977.962	5437.206	0.72
4	3/10/2000	10:44:00	8	0.002222	775	702	1410	2826.463	2619.711	5261.813	0.71
5	3/10/2000	10:44:04	12	0.003333	750	673	1519	2735.287	2511.489	5668.577	0.72
6	3/10/2000	10:44:08	16	0.004444	769	709	1515	2804.581	2645.833	5653.65	0.7
7	3/10/2000	10:44:12	20	0.005556	752	781	1347	2742.581	2914.522	5026.71	0.72

	L	M	N	O	P	Q	R	S	T	U	V
1	FIX:TC0.F	FIX:TC1.F	FIX:TC2.F	FIX:TC3.F	FIX:TC4.F	FIX:TC5.F	TCR0	TCR1	TCR2	Process flu	Process flu
2	88.6	87.7	86.7	79.3	72.1	66.2	87.83198	86.87264	85.88141	79.04057	71.76774
3	88.6	88.5	87.3	79.4	72.7	66.2	87.83198	87.67752	86.48363	79.14054	72.36608
4	88.5	88.5	87.2	79.3	72.7	66.3	87.73157	87.67752	86.38326	79.04057	72.36608
5	88.7	88.7	87.3	79.4	72.9	66.4	87.93239	87.87874	86.48363	79.14054	72.56553
6	88.7	88.4	87.2	79.4	73.4	66.4	87.93239	87.57691	86.38326	79.14054	73.06415
7	88.7	88.5	87.6	79.3	73.5	66.6	87.93239	87.67752	86.78474	79.04057	73.16388

	W	X	Y	Z	AA	AB	AC	AD	AE	AF
1	Process flu	UA Module	UA Module	UA Module	TD0	TD1	TD2	Milk Upper	Milk Vertica	Milk Lower
2	66.32789	338.9262	191.7168	314.1385	8.79141	15.1049	19.55352	1	1	1
3	66.32789	332.334	194.4927	269.7597	8.691444	15.31143	20.15574	0.98055	1.014479	0.858729
4	66.42759	325.2173	171.0951	263.675	8.690998	15.31143	19.95567	0.959552	0.892437	0.839359
5	66.52729	311.116	164.0081	284.0489	8.791856	15.3132	19.95634	0.917946	0.855471	0.904215
6	66.52729	318.9976	182.3109	284.7329	8.791856	14.51275	19.85597	0.941201	0.950939	0.906393
7	66.72669	308.4386	200.8126	250.6081	8.891821	14.51364	20.05806	0.910046	1.047444	0.797763

Example Calculation:

Calculating the overall heat transfer coefficient for MPHE 1 (the shaded row):

$$U = \frac{q}{\theta_s - \theta_p}$$

$$U = \frac{H2}{R2 - U2}$$

$$U = \frac{2979.639}{87.832 - 79.041}$$

$$U = 338.93 = X2$$

Calculating the normalised overall heat transfer coefficient for MPHE 1 (the shaded row):

$$U_n = \frac{U}{U_0}$$

$$U_n = \frac{X2}{X2}$$

$$U_n = \frac{338.93}{338.93}$$

$$U_n = 1 = AD$$

9.4 Example Calculation of Thermal Fouling Resistance

Table 9.4 Results from Run 9

	A	B	C	D	E	F	G	H	I
35	MPHE No	Time (s)	Time (hr)	Thickness (mm)	U	1/U	U_0	$1/U_0$	R_f
36	6	600	0.17	0.1504	181.61	0.005506	309.79	0.003228	0.0023
37	5	1800	0.50	0.1722	101.92	0.009812	246.51	0.004057	0.0058
38	4	4080	1.13	0.3852	50.27	0.019893	213.63	0.004681	0.0152
39	3	7800	2.17	0.8008	17.67	0.056593	235.19	0.004252	0.0523
40	2	10800	3.00	0.8548	17.33	0.057703	181.62	0.005506	0.0522
41	1	15180	4.22	0.8872	20.4	0.04902	180.54	0.005539	0.0435

Example Calculation:

Calculating the thermal fouling resistance for MPHE 6 (the shaded row):

$$R_f = \frac{1}{U} - \frac{1}{U_0}$$

$$R_f = \frac{1}{E36} - \frac{1}{G36}$$

$$R_f = \frac{1}{181.61} - \frac{1}{309.79}$$

$$R_f = 0.00551 - 0.00323 = F36 - H36$$

$$R_f = 0.0023 = I36$$

9.5 Contents of CD-ROM

A CD-ROM containing the remaining Appendix information is provided. The contents of the CD-ROM is as follows:

- Raw and manipulated data for all trials in Microsoft Excel 97 SR-2 format.
- Readme.txt files for each trial.
- All plotted graphs in Microsoft Excel 97 SR-2 format.
- Digital photographs of all test plates and evaporator plates produced in the trials.
- An electronic copy of the thesis, including figures, in postscript format.
- Details of the CD-ROM in a Readme.txt file.

The structure of the CD-ROM is as follows: The root directory of the CD-ROM has a folder named "CD" and a Readme.txt file. The Readme.txt file gives details of the CD-ROM. Within the CD directory are separate folders for each run (23 in total). For the miniature plate heat exchanger trials there are eight folders within a run folder. The eight folders are titled "MPHE 1-6", "MSExcel" and "Readme". Digital photos of each test plate are located in the corresponding MPHE folder. A Microsoft Excel 97 workbook giving raw data, manipulated data, and plots of the data is located in the MSExcel folder. Trial notes are located in the Readme folder in *.txt format. The research falling film evaporator run folders only have three folders: "Plate", "MSExcel" and "Readme". Digital photos of the evaporator plate are given in the Plate folder.

A folder name "Thesis" located in the CD folder has an electronic copy of the thesis in PostScript format. The file can be viewed by any PostScript viewer.